

A NEURAL ORIGIN FOR CENTRAL NERVOUS SYSTEM GERM CELL TUMOURS

**Christopher Callum Lee Tan,
BSc.**

**Thesis submitted to the
University of Nottingham for
the degree of Doctor of
Philosophy**

July 2013

Abstract

Germ cell tumour (GCT) is the collective term for several subtypes of tumour. GCTs most commonly occur in the testis or ovary around puberty, but they also occur at several non-gonadal locations in the human body. These so-called “extra-gonadal” GCTs have the same histology and protein markers as those that arise at gonadal locations. This observation prompted several hypotheses to explain where these tumours come from. Extragenadal locations include the base of the spine (sacrococcygeal region), the abdomen (retroperitoneum), the chest cavity (mediastinum), and the brain (intracranial). The origin of central nervous system (CNS) GCTs is the main focus of this thesis.

The most widely accepted hypothesis for extragonadal GCTs was originally proposed by Gunnar Teilum in 1965. Teilum proposed that all GCTs that arise in the human body have a common cell of origin. Teilum’s experiments showed that a germ cell progenitor could give rise to a GCT. This was one piece of evidence that led him to suggest that since GCTs in the testis and ovary arise from a germ cell progenitor, perhaps GCTs in other locations also arise from these progenitors. For extra-gonadal GCTs, these progenitors are thought to mismigrate and become trapped at several locations around the body. The regions where GCTs occur are suggested to be those regions where these progenitors have become trapped, such as the brain. However, research into pluripotency has revealed a mechanism of generating a GCT from an endogenous population of cells isolated from the brain, neural stem cells, using the upregulation of only a single gene, Oct4.

In this thesis I test the hypothesis that CNS GCTs may arise from a neural progenitor, and not just from a germ-cell progenitor. I will use several strategies to test this hypothesis with different methodologies. Published literature is first used to review and re-analyse the case for a neural cell of origin for CNS GCTs. This hypothesis is then experimentally tested in subsequent chapters, culminating in a unifying hypothesis for how CNS GCTs may arise.

Acknowledgements

I would like to acknowledge and thank those who have given me academic support and challenged me to develop as a scientist, including: Paul Scotting, Jane Hewitt, Andreas Leidenroth, Jennie Jeyapalan, Robin Grant, Ruman Rahman and those in the Children's Brain Tumour Research Centre, Valerie Wilson, Anestis Tsakiridis, and past and present members of D13.

I have received a generous amount of funding from the scientific community, especially from: MRC, Children with Cancer UK, Disease Models and Mechanisms, British Society of Cell Biology, British Society of Developmental Biology, and Genetics Society.

Finally, I would like to acknowledge the love and support my grandparents, mother, brother, and girlfriend, have given me.

Declaration

Except where acknowledged in the text, I declare that this thesis is my own work and is based on research that was undertaken by me in the School of Life Sciences, University of Nottingham, during the period September 2009 to October 2013.

Chris Tan

18.10.2013

Table of Contents

Chapter 1: Introduction	1
1.1. Germ cell tumours.....	1
1.2. Clinical review of CNS GCTs.....	5
Geographical variation in occurrence	7
Location of GCTs and age distribution for occurrence.....	7
1.3. The germ-cell progenitor hypothesis for CNS GCTs.....	9
History of GCTs	9
The currently accepted hypothesis for the origins of GCTs	10
The currently accepted mechanism for the mismigration of germ-cell progenitors	13
GCTs exhibit similar histology and markers regardless of location	14
Experiments in transgenic mice confirm that germ cells can mismigrate to extragonadal locations	15
Gonadal and extragonadal tumours exhibit loss of imprinting.....	16
Gain of isochromosome 12p is a marker for GCTs in all locations.....	19
1.4. Hypothesis for the aetiology of CNS GCTs	21
Evidence against germ-cell progenitors as the cell of origin for CNS GCTs ...	22
Evidence for pluripotency as a mechanism for CNS GCT formation.....	24
Oct4 gene structure and Oct4 isoforms	24
Mechanisms that regulate OCT4	27
Processes regulated by OCT4	30
OCT4 function in pluripotency	30
Neural stem cells can be readily activated to form teratomas by activation of the pluripotency gene Oct4.....	32
Expression of pluripotency genes in GCTs.....	35

Extragenital GCT subtypes share a common lineage	36
Mechanisms by which NSCs might be transformed to form GCTs	36
Demethylation as a mechanism for GCT formation	39
Diseases associated with GCTs and their relationship to OCT4	40
1.5. Aims of project	41
Chapter 2: Materials and methods	43
Chapter 3: A meta-analysis of the location and biology of GCTs in the brain	61
3.1 Introduction	61
3.2 Results:	63
Teratomas can invade any region of the brain	63
Evidence for a cell of origin in the lateral regions of the brain	67
CNS GCTs can recur as almost any of the other GCT subtypes	67
CNS GCTs can be mixed with other GCT or non-GCT subtypes	69
3.3 Discussion	73
All GCTs in the CNS can form from a common cell of origin – resection and recurrence	73
All GCTs in the CNS have a common cell of origin – mixed GCTs	75
Why GCTs are sometimes mixed with non-GCTs	77
3.4 Conclusion:	79
Chapter 4: An <i>in vivo</i> study of teratoma formation in the brain	81
4.1 Introduction	81
4.2 Aims	83
4.3. Results:	84
Detection of luminescence in ES-Luc cells	86
In vitro validation of pluripotency of the ES-Luc cell population: pluripotency markers	86

In vivo validation of ES-Luc cells for teratoma formation and luminescence	87
Optimisation of stereotaxic cell-transplantation into the brain	90
Injection of ES-Luc cells into the ventral midline and lateral hemispheres ...	94
Injection of approximately 5,000 ES-Luc cells into the ventral midline and lateral hemispheres	103
4.4 Discussion	107
4.5 Conclusion	109
Chapter 5 Neural stem cells and activation of OCT4	111
5.1 Introduction	111
5.2 Aims.....	112
5.3 Results	117
OCT4 activation localised to Nestin-expressing cells in a transgenic mouse model.....	117
Establishing and maintaining a transgenic-mouse colony	118
Isolation and characterisation of neural stem cells	119
Time delay between doxycycline addition and OCT4 and NANOG activation	121
Time delay between removal of doxycycline and silencing of Oct4	121
Activation of OCT4 in E8.5 ex-vivo brain tissue forms pluripotent colonies	124
Activation of OCT4 triggers cells in E8.5 ex vivo brain tissue to form a teratoma in a mouse kidney.....	127
Induction of OCT4 in mouse embryos from E8.5-E10.5 causes minimal embryologic disruption	128
Induction of OCT4 in mouse embryos from E13.5 to birth causes minimal disruption to development.....	130
Induction of OCT4 from E11.5-E14.5 causes spontaneous embryo reabsorption	134

Induction of OCT4 from E13.5-E16.5 caused minimal effects on later development	134
5.4 Discussion.....	135
OCT4 induction in mouse brain tissue and teratoma formation	135
OCT4 induction in vivo.....	136
Chapter 6: <i>KIT</i> and <i>ETV1</i> expression in the CNS as a mechanism for germinoma formation	139
6.1 Introduction	139
6.2 Hypothesis.....	142
6.3 Aims.....	143
6.4 Results	143
RNA-expression plasmid construction	143
Etv1 in situ hybridisation on E15.5 and adult mouse brains.....	144
Etv1 in situ hybridisation on a postnatal day 7 mouse brain	146
Allen Brain Atlas expression	148
Kit and Etv1 expression in the medulla oblongata and medullary spine region	161
6.5. Discussion:.....	170
Overlap of Kit and Etv1 expression correlates with germinoma formation	170
Expression of only Etv1 or Kit does not correlate with germinoma formation	171
Kit and Etv1 as part of the brain-cell hypothesis.....	172
GCTs may share KIT activation of ETV1 as a common mechanism regardless of location.....	173
Clinical cases support KIT activation of ETV1 as a mechanism for GCT formation.....	174
6.6 Conclusion	175

Chapter 7: Discussion.....	177
7.1. Introduction	177
CNS GCT subtypes have a lineage relationship	177
Challenges for the germ-cell progenitor hypothesis.....	178
7.1.1 Hypothesis.....	178
Plasticity and the incidence of CNS GCTs in children	181
7.1.2 CNS GCTs are not restricted to the midline	181
GCTs are in the midline and PGCs migrate in the midline	181
GCTs occur in locations other than the CNS and gonads	182
7.1.3 The role of methylation in CNS GCTs	183
Do progenitors for CNS GCTs lack imprinting?.....	183
7.2. Chemoresistance and OCT4	184
7.3. 12p and pluripotency	186
7.4. The KIT-ETV1 axis	187
Imprinting and the KIT-ETV1 axis	188
The KIT-ETV1 axis and germinoma incidence.....	188
7.5. Factors influencing CNS GCT incidence.....	191
Geographical variation in the incidence of CNS GCTs.....	191
The relationship between Klinefelter syndrome and CNS GCTs	191
7.6. Conclusion	192
References	195
Appendix I – Genotyping transgenic mice	207
Appendix II - <i>in situ</i> hybridisations.....	209
Appendix III - Publications arising from this thesis.....	225

Table of Figures

Figure 1.1. The germ-cell progenitor hypothesis.....	2
Figure 1.2. GCT categorisation, locations, and incidence.....	4
Figure 1.3. Germ cell tumour classifications.	6
Figure 1.4. Germ-cell model schematics.	12
Figure 1.5. Schematics of models relating to the germ-cell theory.	18
Figure 1.6. OCT4 transcripts and interaction pathways	26
Figure 1.7. Three mechanisms known to be able to form a pluripotent cell.	34
Figure 1.8. The brain-cell theory for intracranial germ cell tumours	38
Table 3.1 A – Locations of CNS teratomas in the ventral midline	64
Table 3.1 B – Locations of CNS teratomas in non-midline regions.....	65
Figure 3.1 – Overlapping regions of where teratomas can grow in the central nervous system.....	66
Figure 3.2 - The relationship between the different subtypes of germ cell tumour.	68
Table 3.2 – Resection and recurrence of GCTs.....	69
Table 3.3 – Germ cell tumour subtypes mixed with other GCT subtypes..	71
Table 3.4 – Germ cell tumour subtypes mixed with non-GCTs.	72
Figure 3.3 - A summary of two different hypotheses of how germ cell tumour progenitors could form a GCT after it has been resected.....	76
Figure 4.1. Optimisation and stable transfection of a heterogeneous ES cell population with a luciferase plasmid.....	85
Figure 4.2. A teratoma assay using ES-Luc cells in mice testis or kidney. ...	89
Figure 4.3. Optimisation of stereotaxic mouse brain injection	91

Figure 4.4. Optimisation of injection site based on the adult mouse brain vasculature.....	93
Figure 4.5. Visualisation of luminescence in adult mice 6 days after being injected with ES-Luc cells.....	95
Figure 4.6. The light intensity recorded for six separate mice over 12 days following injection of ES-Luc cells.....	96
Figure 4.7. Dorsal view of adult mice brains 12 days after injection of ES-Luc cells.....	98
Figure 4.8. Ventral view of adult mice brains 12 days after injection of ES-Luc cells.....	99
Figure 4.9. Histology of the midline mouse, M3.....	101
Figure 4.10. Histology of the lateral mouse, L3.....	101
Figure 4.11. Histology of a teratoma in an adult mouse brain injected with ES-Luc cells.....	102
Figure 4.12. Histology of normal and tumour tissue in an adult mouse brain injected with ES-Luc cells.....	102
Figure 4.13. Detection of luminescence emitted from ES-Luc/teratoma cells.....	104
Figure 4.14. Teratoma formation in mice brains using low concentrations of ES-Luc cells.....	106
Figure 5.1. A breeding scheme showing the production of mice that express Oct4 in NESTIN-expressing cells upon doxycycline treatment....	114
Figure 5.2. OCT4-inducible transgenic mice.....	115
Figure 5.3. Validation of neural stem cell derived from Oct4 mice.....	120
Figure 5.4. The effect of addition and removal of doxycycline on Oct4 and <i>Nanog</i> expression.....	123
Figure 5.5. E8.5 brain tissue with activated OCT4 can form pluripotent cells and teratomas, but older tissue loses this ability.....	126

Figure 5.6. In vivo activation of OCT4 in mouse embryos.	129
Figure 5.7. Induction of Oct4 from E13.5-birth has minor effects on embryogenesis.....	132
Figure 6.1. In vitro optimisation of Kit and Etv1 probes.....	141
Figure 6.2. Optimisation of Etv1 probe on sagittal E15.5 embryos and adult mouse brain tissue.....	145
Figure 6.3. Postnatal day 7 mouse transverse sections of a brain hybridised with anti-sense Etv1 for in situ hybridisation.	147
Figure 6.4. A comparison between sections of respective ages from the Allen Brain atlas compared to my results.....	149
Figure 6.5-6.23. In situ hybridisation using a Kit or Etv1 anti-sense probe on various ages and views of mouse brain taken from the Allen Brain atlas or EMAGE database.	152
Figure 6.5-6.11. All regions that show positive staining have been identified except those in the medulla or hindbrain regions.	153
Figure 6.12-6.16. In situ hybridisation on whole-mount or whole-embryo sections for Kit and Etv1.	160
Figure 6.17-6.23. All positive staining in the spine, hindbrain or medulla oblongata regions are indicated.	162
Figure 6.24. Images from either a transverse or sagittal view of a germinoma in the medulla oblongata region.....	167
Figure 6.25. Sagittal or transverse images of germinomas in the spine. .	168
Table 6.1 Germinomas in the medulla oblongata or medullary spine	169
Figure 7.1. A schematic of the potential mechanisms involved in forming different subtypes of GCT from a brain cell.....	180
Figure 7.2. The proposed differences between teratoma and germinoma formation over development.	190

Abbreviations

<u>Abbreviation</u>	<u>Full name</u>
5-Aza	5-deoxyazacytidine
A	Anterior
p	Posterior
l	lateral
A	Amygdaloid area
AC	Anterior commissure
AHEC	Alveus of the hippocampus and external capsule
AFP	Alpha fetoprotein
APN	Anterior pretectal nucleus
AR	Amygdalohippocampal region
AP	Anterior-posterior
BAN	Basolateral amygdaloid nucleus
BNS	Bed nucleus of stria terminalis
C	Cerebellum
CAN	Central amygdaloid nucleus
CC	Corpus callosum
CIS	Carcinoma in situ
CLOT	Cortical plate to lateral olfactory tract
CNS	Central nervous system
CP	Cerebral peduncle
CpG	Cytosine phosphate-guanine
CT	Computerised tomography
Cx	Cortex
CTN	Centromedian thalamic nucleus
DBB	Diagonal band of broca
DG	Dentate gyrus
DHC	Dorsal hippocampal commissure
DMTN	Dorso medial thalamic nucleus
DNMT	DNA methyltransferase
DS	Dorsal subiculum
DV	Dorsal-ventral
E	Epiphysis
EC	Embryonal carcinoma
EGF	Epidermal growth factor
ES/ESC	Embryonic stem cell
Fb	Forebrain
FCH	Field CA1 of the hippocampus
FBS	Fetal bovine serum
FGF	Fibroblast growth factor
FR	Fasciculus retroflexus
GCT	Germ cell tumours
GFAP	Glial fibrillary acidic protein
GP	Globus pallidus

GRN	Gigantocellular reticular nucleus
H&E	Haematoxylin and eosin
H	Hippocampus
Hb	Hindbrain
HCG	Human chorionic gonadotrophin
HDAC	Histone deacetylase
HF	Hippocampal fissure
IC	Internal capsule
ICR	Imprinting control region
IGF	Insulin growth factor
IGCNU	Intratubular germ cell neoplasia unclassified
IMOT	Intermediate zone to medial olfactory tract anterior
INPC	Interstitial nucleus of posterior commissure
IO	Inferior olive
LAN	Lateral amygdaloid nucleus
LH	Lateral habenula
LM	Lacunosum moleculare
LPN	Lateral preoptic nucleus
Luc	Luciferase
LV	Lateral ventricle
MAP2	Microtubule-associated protein
MAN	Medial amygdaloid nucleus
MEF	Mouse embryonic fibroblasts
MFB	Medial forebrain bundle
MH	Medial habenula
MHN	Medial habenula nucleus
ML	Medial lemniscus
MIAN	Mediolateral amygdaloid nucleus
MLF	Medial longitudinal fasciculus
MMN	Medial mammillary nucleus
MO	Medulla oblongata
MOT	Medial olfactory tract
MRI	Magnetic resonance imagine
MPN	Median preoptic nucleus
MRN	Magnocellular red nucleus
MTN	Mediodorsal thalamic nucleus
NRO	Nucleus raphe obscurus
NRP	Nucleus raphe pallidus
NSC	Neural stem cells
NTB	Nucleus of trapzioid body
OB	Olfactory bulb
OGT	O-linked N-acetylglucosamine transferase
ON	Optic nerve
OT	Optic tract
P	Pons
PA	Preoptic area
PAG	Periaqueductal gray

PBS	Phosphate buffered saline
PBPN	Parabrachial pigmented nucleus
PCO	Pre-clinical oncology
PCN	Precommissural nucleus
PGC	Primordial germ cell
PF	Prerubral field
PFA	Paraformaldehyde
PfTN	Parafascicular thalamic nucleus
PGN	Pregenulate nucleus
PH	Pyramidal cell layer of the hippocampus
PN	Pontine nucleus
POU5F1	Pit-Oct-Unc domain class 5 transcription factor 1
PPN	Prepositus nucleus
preTN	Pretectal nucleus
PRN	Pontine reticular nucleus
PS	Posterior subiculum
PTN	Periventricular thalamic nucleus
PvTN	Paraventricular thalamic nucleus
P1RF	P1 reticular formation
RFN	Retroparafascicular nucleus
RIN	Rostral interstitial nucleus
RLH	Radiatum layer of the hippocampus
RMN	Raphe magnus nucleus
RN	Reuniens nucleus
rtTA	Reverse transcription transactivator
RT-PCR	Reverse transcriptase polymerase chain reaction
RTN	Reticular thalamic nucleus
S	Subiculum
SAC	Superior anterior colliculus
SCID	Severely combined immune-deficient
SCP	Superior cerebellar penduncle
SI	Substantia innominata
SIN	Subincertal nucleus
SLH	Statum lucidum hippocampus
SMN	Supramammillary nucleus
SN	Subthalamic nucleus
SO	Subcommissural organ
Sp	Spine
T	Tectum
TN	Tuberomammillary nucleus
VITN	Ventrolateral thalamic nucleus
VLTN	Ventral linear thalamic nucleus region
VML	Ventral midline
VP	Ventral pallidum
VS	Ventral subiculum
YST	Yolk sac tumour
VTN	Ventromedial thalamic nucleus

VZ	Ventricular zone
ZI	Zona incerta

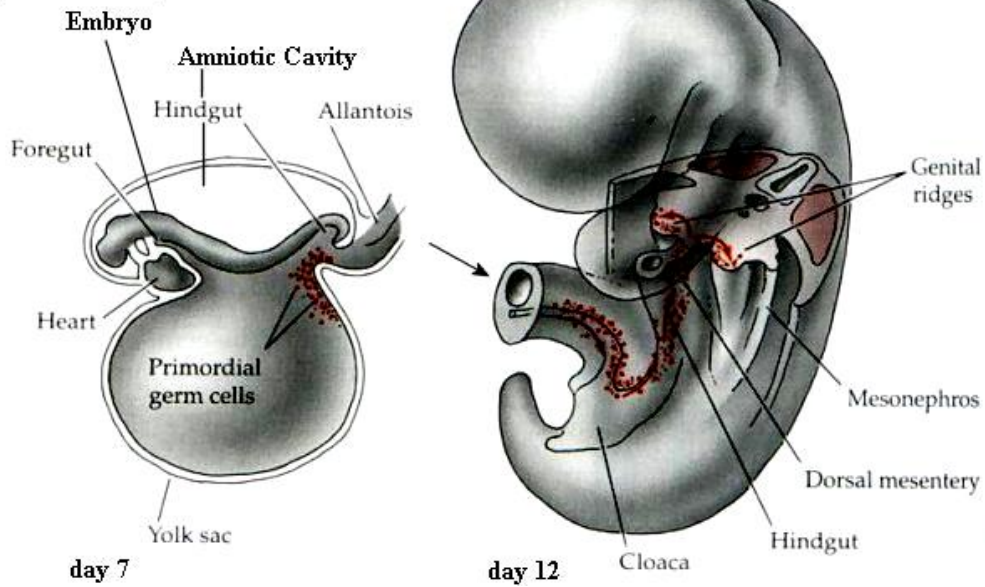
Chapter 1: Introduction

1.1. Germ cell tumours

Germ cell tumours (GCTs) are a diverse group of tumours that can occur at multiple sites around the body. Regardless of where GCTs arise, they are all thought, by most, to originate from germ-cell progenitors, which have a specific migratory pattern (Figure 1.1 A).

GCTs include polyembryomas, yolk sac tumours (endodermal sinus tumours), seminomas/dysgerminoma/germinoma (together known as 'germinomatous'), teratomas, embryonal carcinomas, and choriocarcinomas. GCTs mainly occur in the gonads (testis and ovary) but can form at extragonadal locations. Outside of the gonads, GCTs generally occur in the midline of the body, in the mediastinum (chest cavity), the retroperitoneum (abdomen), the sacrococcygeal symphysis region (base of the spine), or in the brain (Figure 1.1 B).

(A) **Migration of mammalian primordial germ cells**



(B)

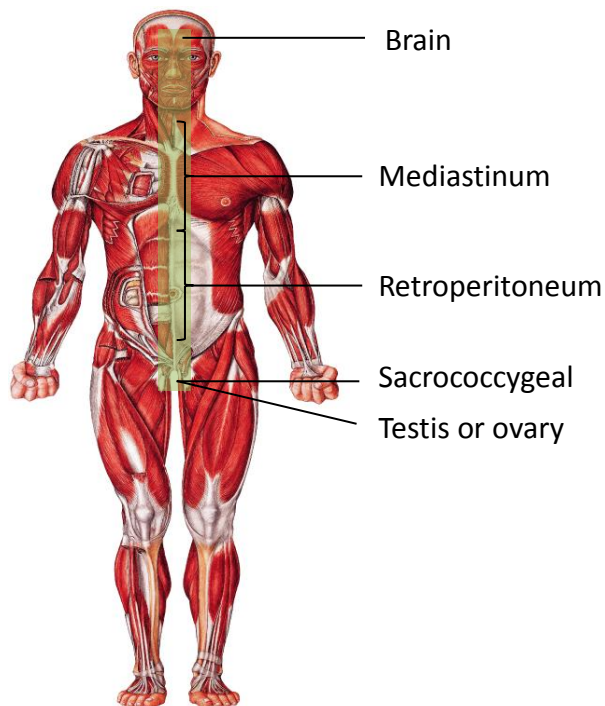


Figure 1.1. The germ-cell progenitor hypothesis. (A) Schematic of the migration of primordial germ cells. PGCs originate in the yolk sac at approximately 3-4 weeks after conception in humans. These PGCs migrate from the endodermal epithelium to dorsal mesentery of the hindgut then towards the genital ridges. Taken from [1] (B) Germ cell tumours have been documented to mainly occur in the midline of the body highlighted in green.

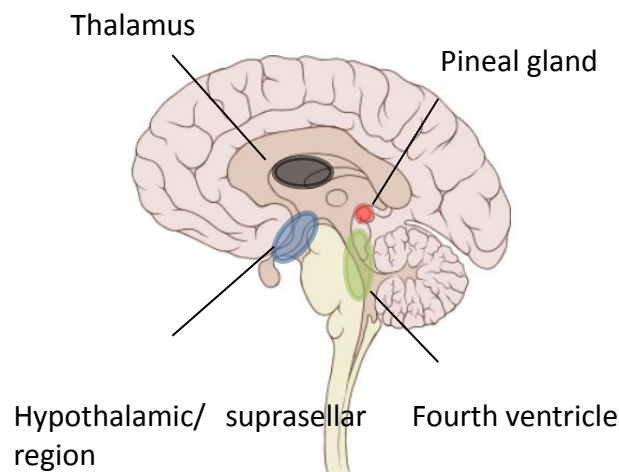
Terminology can be confusing, with each tumour type being referred to by the same name regardless of the location except for germinomatous (or seminomatous) tumours. In the brain, these are referred to as germinomas; in the testis, these are seminomas; and in the ovary, they are called dysgerminomas [2] (Figure 1.2 A). In the brain, GCTs mainly occur in the pineal and suprasellar regions (near the hypothalamus), but have been found in the 4th ventricle and thalamus regions (Figure 1.2 B). Embryologically, all these sites can be classed as being in the ventral midline [3]. As an added complication, GCTs have often been found with mixed subtypes; for example, a germinoma mixed with a teratoma.

Teratomas also have contentious terminology. These can be benign tumours, often called mature teratomas, or teratomas with an embryonal component, also called immature teratomas or teratocarcinomas [4]. Teratomas are graded on the percentage of embryonal or neuroepithelium component [5]. This begins with grade 0, a mature teratoma; grade 1 contains <10% immature component; and grade 3 contains >50%. The immature component has been used as a marker for potential metastasis, but it is only considered metastatic when it has spread. Since GCTs can vary widely before becoming metastatic, it is often better to grade a tumour based on protein markers and other prognostic factors to determine the probable outcome, rather than whether it has metastasised. For the purposes of simplicity in this thesis these will all be referred to as teratomas.

(A)

Germinomatous	Non-germinomatous
Germinoma (brain)	Embryonal carcinoma
Dysgerminoma (ovary)	Teratoma
Seminoma (testis)	Yolk sac tumour/ endodermal sinus tumour
	Choriocarcinoma

(B)



(C)

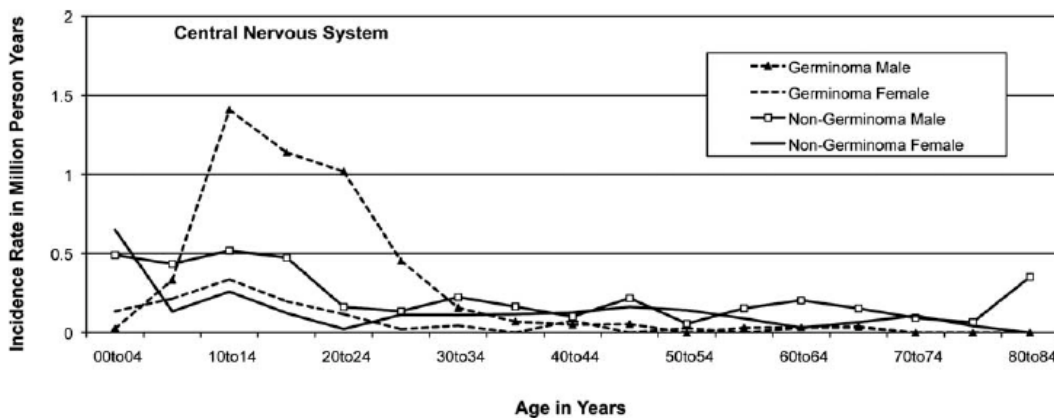


Figure 1.2. GCT categorisation, locations, and incidence (A) A table of the subcategories of GCT; either germinomatous or non-germinomatous. Note that germinomatous tumours are histologically identical regardless of location but the terminology varies if it is in the brain, ovary, or testis. (B) Sagittal view of a brain with the most common locations for GCTs; the pineal region, the suprasellar/hypothalamic region, the thalamus, and the fourth ventricle. (C) Incidence rate in million person years compared to age in years in the CNS for male/female, and germinomas/non-germinomas. The dotted lines signify germinoma, and black lines signify non-germinoma [taken from Arora, 2012]

1.2. Clinical review of CNS GCTs

This section briefly outlines the major clinical features of CNS GCTs; including, geographical variation, locations of GCTs, and age of incidence. This section will begin with a brief introduction to GCTs.

GCTs are classed as a single group of tumours but each GCT subtype (see Figure 1.2 A and Figure 1.3) varies significantly in its clinical behaviour. Teratomas are generally benign, and germinomatous tumours are malignant but highly curable; in contrast, yolk sac tumours and choriocarcinomas are often malignant and less responsive to standard therapies [6]. Despite being benign, teratoma has a far worse prognosis in all locations when diagnosed prenatally. Excluding those which arise intracranially, the survival rates for pre- and perinatal teratomas range from 23% to 100% depending upon the location [7]. However, intracranial teratomas, the second most common location for teratoma in neonates, are almost invariably fatal when diagnosed at birth [8, 9]. This poor prognosis is largely due to their size and growth at the expense of normal brain tissue. Also, as discussed in Chapter 3, surgical removal of a relatively benign form of GCT can be followed by the recurrence of a higher-grade tumour of the same or a different malignant subtype at the same site.

Extragonadal GCTs are most common in children and young people. In particular, intracranial tumours are the most common form of extragonadal GCT in young males [10]. Unlike neonatal teratomas, most GCTs (such as germinomas) are regarded as highly curable. However, because of the young age of the patients, the side-effects of chemotherapy and radiotherapy are particularly problematic. In addition to effects on the hormonal development of those young people, treatment at such an early age leads to a particularly high rate of late sequelae - primarily cardiovascular disease and secondary malignancies - increasing the probability of these occurring by approximately twofold [11, 12].

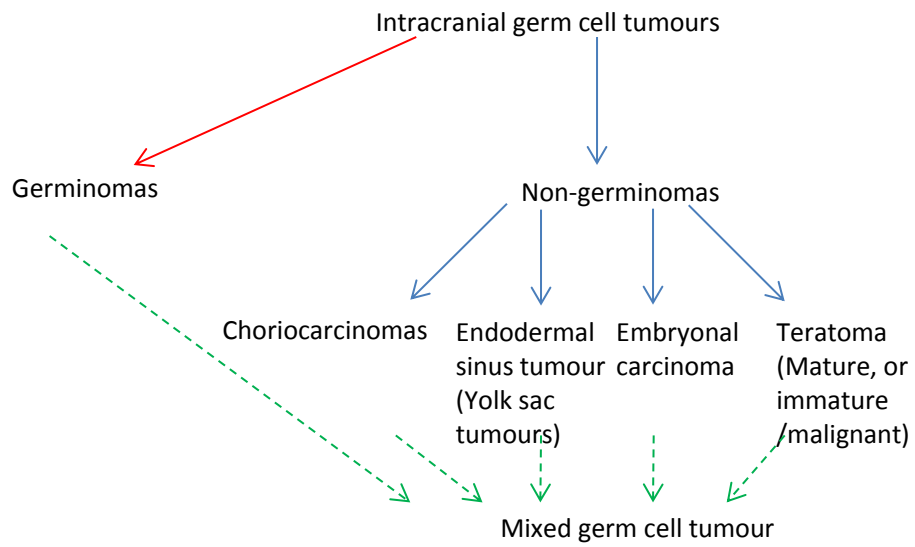


Figure 1.3. Germ cell tumour classifications. A hierarchy of how the World Health Organisation classifies germ cell tumours [Kleihues, 1993][13] Germinomas and non-germinomas are segregated, but all can contribute to a mixed tumour.

Late sequelae are mainly caused by the non-specific methods of action used to treat CNS GCTs. A better understanding of the biology of these tumours might lead to alternative treatments that are equally or more effective but carry less severe side effects.

CNS GCT varies both in incidences between different countries, and in their locations in the CNS. These features, along with the age that these tumours arise, are important in understanding the aetiology of CNS GCTs. Therefore, these will be the next topic for discussion.

Geographical variation in occurrence

CNS GCTs are rare compared to other GCT locations, but incidence varies geographically. In the Far East, the incidence is 2-3% of all primary intracranial neoplasms and 8-16% of paediatric cases, compared with 0.3-0.6% and 3-4% respectively in the West [14-16]. This percentage equates to an approximate incidence of 1 child per 1 million [17]. The differences found between the East and the West vary widely between studies – in fact, some reports dispute that there is a difference at all [18].

Location of GCTs and age distribution for occurrence

Each of the subtypes of GCT in specific anatomical locations has a distinctive age distribution. Since GCTs can arise at several locations in the body, the statistics below are separated into GCTs in general, and then those that arise in the brain.

Epidemiological studies have revealed that when all ages are included, over 90% of GCTs are testicular. These testicular GCTs most frequently occur in young men. Although much less common, ovarian tumours span a similar, but slightly younger age range [19]. In comparison, sacrococcygeal tumours are predominantly perinatal; CNS GCTs occur predominantly before the age of 3; and mediastinal GCTs occur between the ages of 15-40. GCTs in neonates are one of

the most common tumours of this age, and approximately 95% of these tumours are teratomas.

In the brain, each histological subtype has a particular age distribution, with germinomas arising in patients between 7 and 30 years of age. In contrast, the peak age of occurrence for non-germinomas is from birth to 20 years, after which their occurrence remains low but approximately constant into old age (Figure 1.2 C). Teratomas are particularly unusual as they are most frequently diagnosed at birth. Indeed, a very notable feature is that GCTs account for only ~3% of brain tumours in children or adults, few of which are teratomas, but over 50% of brain tumours diagnosed pre- and peri-natally are teratomas [7]. The male to female incidence of CNS GCTs is approximately 3:1, with the majority in the pineal region in males, and an excess of suprasellar tumours in females. This has been disputed when CNS GCTs have been stratified by location: pineal region tumours appear to show gender differences but non-pineal CNS GCTs do not [20].

One of the largest studies examined Japanese and American registries and found that 40% of CNS GCTs were located in the pineal region, with the remaining 60% in non-pineal regions of the brain. The overwhelming majority of CNS GCTs, 82%, were diagnosed as germinomas [18].

The true incidence of prenatal CNS GCTs is difficult to determine. Between 20-30% of all pregnancies are spontaneously aborted before term [21]; since teratomas can be well-formed by the end of the first trimester, it is plausible that CNS GCTs could cause miscarriage. Autopsies on these aborted fetuses are only carried out if there is a specific reason to do so, so the studies required to determine if teratomas might have been present and even caused the miscarriage are rarely performed.

1.3. The germ-cell progenitor hypothesis for CNS GCTs

GCTs have been introduced from a clinical perspective, but how do these tumours arise? This thesis proposes a hypothesis that contradicts the currently accepted model to explain the aetiology of GCTs. In order to understand how these two hypotheses differ, both are explained in the next two sections. The currently accepted hypothesis of how GCTs develop will be described by introducing the history of GCTs, the mechanism that has been proposed to explain their origin, and the observations that have been used as evidence to support the argument.

History of GCTs

All GCTs are proposed to derive from the progenitors of the male and female germ line. For extragonadal GCTs, Teilum's 'germ-cell hypothesis' proposes that germ-cell progenitors mismigrate during early embryogenesis, become trapped in midline locations at various points along the body's anteroposterior axis, and emerge as tumours when local events allow or promote reactivation of their proliferation (Teilum [22] referenced by Oosterhuis [2]) (Figure 1.1 A). In short, the normal process of germ-cell migration is disrupted.

This hypothesis therefore arose because GCTs that form in the brain and other sites along the body's midline share several features in common with gonadal GCTs, such as chromosomal alterations and marker secretion. Investigations into specific gene expression, DNA-methylation, and mutations (such as activating mutations of the *KIT* oncogene [23]) of these tumours were later used to support Teilum's model. These arguments in favour of the germ cell hypothesis were recently reviewed by Oosterhuis *et al.* (2007) [2], and will each be discussed in this section. While markers and histology are undeniably similar regardless of location, I propose that the mismigration of germ-cells is not the only possible explanation for extragonadal GCT formation. In section 1.4 I will

outline the arguments to suggest that an alternative model for GCT formation at extragonadal locations is more likely.

Before explaining the currently accepted hypothesis for extragonadal GCT formation, it is important to mention an alternative hypothesis. This alternative to both Teilum or our hypotheses is the “embryonic cell theory” [24]. This hypothesis suggests that these tumours may arise from embryonic stem-cell (ESC) progenitors in the brain. However, this hypothesis also relies on misplacement of these progenitors. Since this is neither the consensus, nor relevant to my proposed hypothesis, it will not be discussed further.

The currently accepted hypothesis for the origins of GCTs

In 1965, Teilum proposed that germ-cell tumours that arose outside of the gonads had a germ-cell progenitor as the cell of origin. Since then, clinicians have accepted the assumption that all GCTs originated from a germ-cell progenitor, regardless of location [25]. The arguments to support this hypothesis are outlined below.

Primordial or progenitor germ-cells (PGCs), or their derivatives, have been proposed to be the cells of origin for all GCTs. PGCs originate outside of the embryo in the extraembryonic mesoderm of the yolk sac around 7 days post coitum (dpc) in mice or 3-4 weeks after conception in humans [26, 27]. During development, PGCs migrate from the dorsal mesentery of the hindgut towards the gonads [20] (Figure 1.1 A). The normal migration of PGCs is in the ‘midline’ plane of the embryo.

It has been proposed that extragonadal GCTs arise from mismigration of PGCs along the midline of the embryo instead of towards the gonadal ridge. GCTs have been well documented to arise in midline locations of the brain, such as the pineal region. The formation of tumours in a specific pattern, such as in the midline, has not been found for any other type of tumour; indeed, the closest known observation is a metastasis, but primary CNS GCTs are not

classified as metastases. Before exploring the proposed mechanism for mismigration of PGCs that leads to the development of extragonadal GCTs, it is important to understand the aetiology of gonadal GCTs.

Chaganti *et al.* (2000) have suggested that since GCTs often contain chromosomal aberrations, the cell of origin “may be one with replicated chromosomes that expresses wild-type p53, harbours DNA breaks, and may be prone to apoptosis” [28]. This cell has been proposed as the zygotene-pachtyene spermatocyte (figure 1.4 A; approximately 9 days) because of the recombination checkpoint it operates [29]. Aberrations in this mechanism would hypothetically allow an increased 12p, expression of cyclin D2, and p53 expression. All of these features are found in at least some gonadal and non-gonadal GCTs.

Chaganti’s explanation is relevant to gonadal GCTs but occurs after PGCs have migrated. Since extragonadal locations do not provide the correct environment to form spermatogonia, it seems unlikely that PGCs could migrate and form spermatogonia, acquire mutations or chromosomal aberrations, and then form a GCT. Equally, it seems unlikely that developed zygotene-pachtyene spermatocytes could leave the gonads and migrate to the brain.

In contrast, Schneider *et al.* (2006) [30] proposed that CNS GCTs arise from mismigration of germ-cell progenitors. According to this theory, these PGCs become trapped in distinct extragonadal locations before forming a tumour by proliferating and differentiating in an aberrant environment. It is important to compare the undifferentiated forms of germ cell progenitors with undifferentiated GCTs in order to understand their relationship.

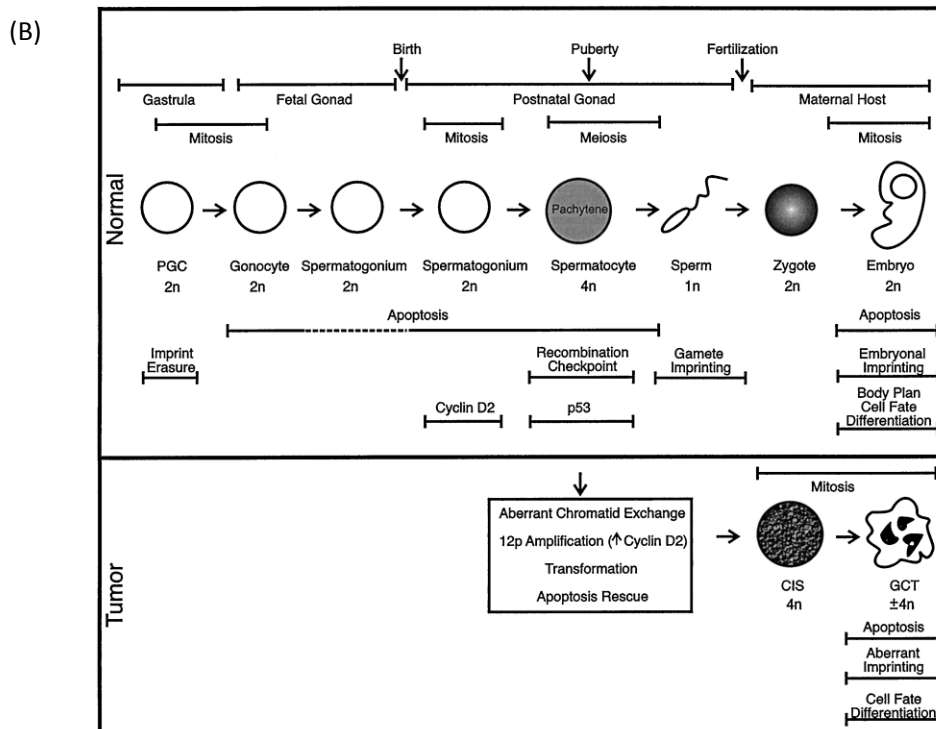
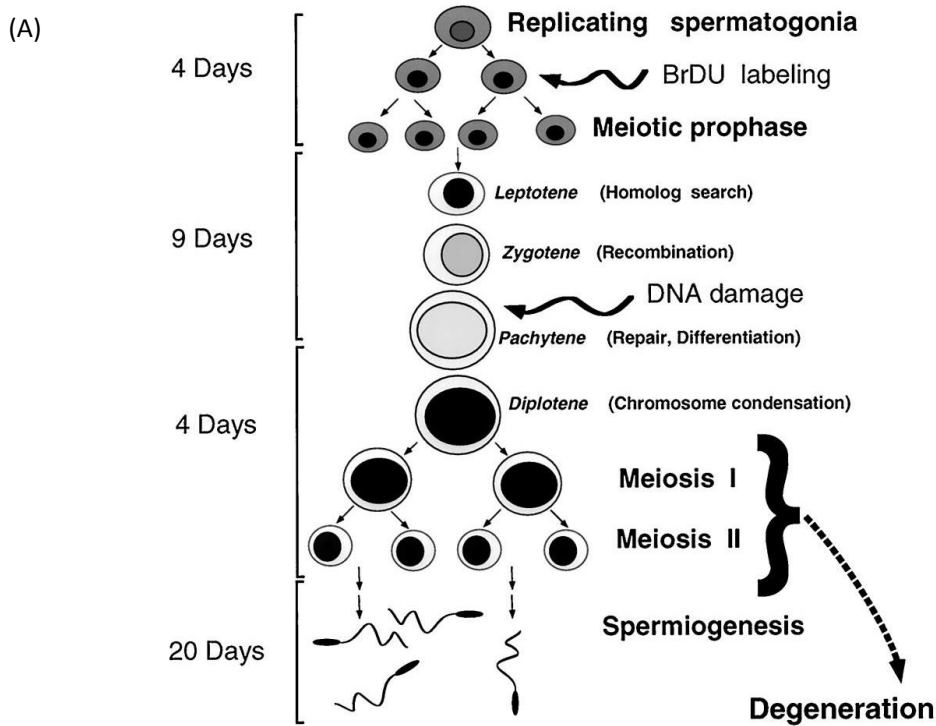


Figure 1.4. Germ-cell model schematics. (A) A schematic showing the hierarchy of development from spermatogonia to spermatogenesis. Spermatogonia are found in the developed testis so this process occurs after puberty [Schwartz, 1999]. (B) A diagram showing the comparison between normal development from PGCs to an embryo, and a proposed mechanism for tumour formation. Spermatogonia or spermatocytes acquire mutations such as 12p gain and form CIS, which can lead to any type of GCT depending on additional mutations [Chaganti, 2000].

Primordial germ cells (PGCs), or gonocytes, are cells that are normally responsible for gametogenesis. PGCs have the potential to form intratubular germ cell neoplasia unclassified (IGCNU), also known as carcinoma *in situ* (CIS). PGCs are accepted to be the progenitors of testicular GCTs, and are an undifferentiated progenitor cell type. Skakkebaek *et al.* (1998) suggested that germinoma/seminoma is a proliferative form of CIS, and that non-germinomatous GCTs developed from CIS cells that have acquired additional stem cell properties (Figure 1.4 A). Non-germinomatous tumours are seen early in human development and germinomatous tumours more frequently occur later in development. Skakkebaek *et al.* (1998) proposes this relationship between various subtypes and age as evidence that CIS is an intermediate form of progenitor. Teratomas often occur at birth, and germinomatous and non-germinomatous GCTs can be found during teenage years; however, germinomatous tumours are the most common GCT subtype found in older patients.

In summary, Skakkebaek *et al.* (1998) suggests that germinoma/seminoma is simply a PGC/CIS/ITGCNU that has proliferated, in comparison to non-germinomatous GCTs, which have acquired stem-like properties [31]. The origins of GCTs in the gonads have been widely accepted and will be uncontested in this thesis. However, how do these PGCs arrive at extragonadal sites? The currently accepted mechanism – the dysregulation of PGC pathway tracking – is the next topic of discussion.

The currently accepted mechanism for the mismigration of germ-cell progenitors

PGC migration is controlled by the protein KIT and its ligand, STEEL. Local tissue releases STEEL and this determines the route for PGCs to travel (the migration route of PGCs is illustrated in red in Figure 1.1A.). When STEEL is absent, PGCs undergo apoptosis [32, 33]. One mechanism that might circumvent the need for STEEL to activate KIT receptor would be a mutation in the *KIT* gene

that abrogates KIT's need for a ligand. Indeed, these mutations are found in many germinomas, which may support the germ-cell hypothesis. However, some germinomas, and most non-germinoma GCT subtypes lack *KIT* mutations, which argues against this hypothesis.

The occurrence of sacrococcygeal GCTs has been used to strengthen the argument that extragonadal GCTs arise from PGCs that have mismigrated. PGCs arise close to the coccyx, and teratomas occur in a similar region around birth [34-36]. Since PGCs originate close to the tissue that forms the coccyx, non-migrating PGCs may give rise to these tumours in this location. Since proponents of a PGC origin for GCTs suggest coccygeal GCTs arise from PGCs that have not migrated, they also propose that PGCs also initiate GCTs in other non-gonadal locations [37]. This evidence is contentious, and Chapter 1.4 explains why GCTs are found in this region.

This section examined the mechanism that is currently accepted for PGC migration from the hindgut to various locations in the body, and how they eventually form GCTs. The next sections will examine the evidence that has been used to support this hypothesis.

GCTs exhibit similar histology and markers regardless of location

GCTs that have arisen in non-gonadal locations have very similar histology to those in the gonads. This includes the secretion of alpha-fetoprotein (AFP) in yolk sac tumours and human chorionic gonadotropin (HCG) for choriocarcinomas. The tumour cells also have similar morphology; for example, germinomas and seminomas both display undifferentiated germinal epithelium regardless of the location. Equally, germinomatous tumours in all locations express high levels of the protein KIT [25].

The incidence of the different GCT subtypes varies in different ages and locations (Figure 1.2 C). Schneider *et al.* (2006) [30] suggested stratifying GCTs by age rather than by tumour site or histology. They based their hypothesis on a

genetic analysis of isochromosome 12p and other gains. Specifically, the tumours that were analysed had the same histology/morphology regardless of age but had different molecular biology i.e. chromosomal aberrations [37]. These differences in chromosome copy number are discussed later. First, a different type of marker that supports a primordial germ cell origin will be discussed.

Experiments in transgenic mice confirm that germ cells can mismigrate to extragonadal locations

Gonadal GCT formation and mismigration of PGCs have been studied in several mouse models. Cook *et al.* (2011) [38] developed a population of mice that could consistently form teratomas in the gonads. These mice had mutations in *Dnd1* and *Bax* genes, which control PGC migration and survival. These mutations prevented PGCs from downregulating pluripotent genes such as *Nanog* and *Oct4*. In summary, pluripotent abilities of PGCs were maintained in these mice and these progenitors formed teratomas in the gonads. However, no GCTs formed outside of the gonads.

To test if PGCs or germ cells could, in principle, survive in non-gonadal locations, Runyan *et al.* (2008) [39] utilised *Bax*-null mice crossed with GFP-OCT4 mice. Briefly, *BAX* controls apoptosis of PGCs, so PGCs that migrate outside of the normal route to the gonads would now survive. In GFP-OCT4 mice, GFP expression was found where OCT4 was expressed. OCT4 was used as a marker for PGCs, therefore, GFP expression was used to visualise the migration of PGCs. This study found that PGCs do migrate near the coccyx, where teratomas have been known to arise, suggesting that PGCs that did not undergo apoptosis could perhaps form sacrococcygeal teratomas. Since PGCs appeared to be able to form one type of extragonadal GCT, this was extended as a potential mechanism to form all extragonadal GCTs. Criticisms of this study and mechanism are discussed later in Chapter 1.4.

Gonadal and extragonadal tumours exhibit loss of imprinting

Lack of imprinting in extragonadal GCTs suggests that GCTs arise from germ-cell progenitors. To understand this, it is first important to discuss the process of DNA silencing through methylation, and imprinting.

DNA methylation is a process whereby methyl groups are attached to a DNA base; specifically, a cytosine group. These methyl groups have been hypothesised to block the transcriptional machinery from binding to DNA; therefore, DNA methylation is a process to silence transcription. The sites to which methyl groups attach are known as 'CpG sites' because methyl groups are only attached to a cytosine (C) base when it is 5' to a guanine (G) base [40]. DNA methylation is complex and not fully understood. Hypermethylation of a region of DNA in the promoter region will often silence a gene, but it is unknown what level of methylation in a region will allow transcription: is 40% methylation of the CpG sites in a gene promoter enough to silence transcription? The current consensus is that the regulation of each gene by methylation is different and some CpGs are more important than other. Later, DNA methylation and its role in silencing the gene that transcribed the transcription factor OCT4 will be discussed (Chapter 1.4). For now, the importance of methylation in silencing genes will be used to describe imprinting.

Imprinting occurs during embryogenesis, and results in the exclusive expression of either the maternal allele or the paternal allele. For this parental-specific expression to occur, the allele that is not transcribed is silenced by methylation. An example of an imprinted gene is IGF2, which is expressed from the non-imprinted paternal allele. In comparison, H19 is expressed exclusively from the non-imprinted maternal allele (reviewed by [41]).

Imprinting can occur in many cell types of the body, and many loci in the genome. High resolution analysis of embryonic and adult mouse brains revealed that over 1300 loci are influenced by parent-of-origin effects [42]. Different regions and ages of the brain were regulated by either maternal or paternal influences. Specifically, maternal alleles were activated during embryogenesis,

while paternal alleles were silenced. This process reverses during later brain development, with paternal alleles becoming activated, and maternal alleles being silenced. Indeed, sex-specific differences in genes apparently control hypothalamic region function, i.e. imprinted genes were more commonly shown in females [43]. In summary, imprinting is a complex process that influences a wide range of genes and in a variety of tissues. However, erasure of imprinting is thought to normally occur exclusively in germ cells.

Imprinted genes in primary gonocytes have their methylation marks and histone modifications erased at 10.5-12.5 dpc in mice. Imprinting is then re-established between 10-25 dpc in developing oocytes and 14.5-18.5 dpc for spermatogonia (Figure 1.5)[44]. Therefore, the cell of origin of GCTs has been suggested to be a germ-cell progenitor because of the similarity in imprinting status between GCTs and PGCs that have had their imprinting erased; furthermore, extragonadal GCTs also lack imprinting.

The erasing of imprinting enables the selective methylation of genes depending on the gender of the gametes. This erasure of imprinting, or lack of imprinting, is a phenomenon that is only thought to occur in germ cell progenitors, at specific times. Since GCTs often exhibit lack of imprinting, this has been used as evidence of GCT aetiology.

GCTs that arise in the testis or ovary have been examined for imprinted genes and several studies found a significant lack of imprinting [45]. This pattern of imprinting is also seen in GCTs that arise in the brain. The commonality between lack of imprinting in both gonadal and non-gonadal GCT supports their analogous cell of origin. SNRPN is one gene that has been examined for the lack of imprinting. The imprinting pattern for SNRPN has not been seen in other cancers and does not appear to have a role in oncogenesis [37]. Therefore SNRPN was proposed as a good marker for imprinting since it should only inform about the cell of origin, rather than a protein that could cause cancer.

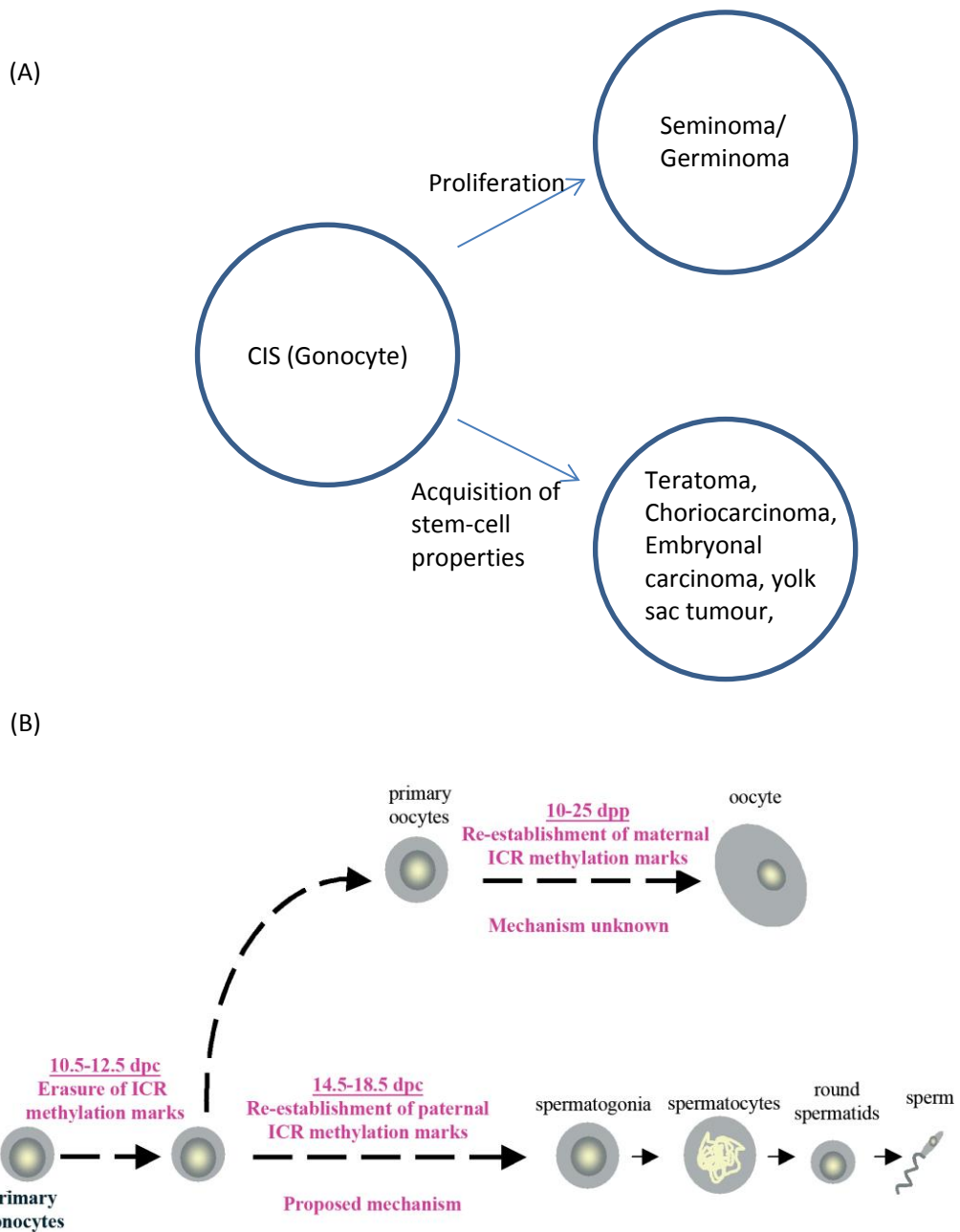


Figure 1.5. Schematics of models relating to the germ-cell theory. (A) CIS and gonocytes are presumed to be similar entities. CIS has been proposed to either proliferate to form germinoma, or undergo acquisition of stem-like properties to form the other subtypes of GCT. Adapted from [Skakkebaek, 1998][31] (B) The erasure and re-establishment of imprinting in mice. Methylation is erased between 10.5-12.5 dpc, before being re-established for normal spermatogonia or oocyte function [Jelinic, 2007][44].

When IGF2 is maternally imprinted, H19 is paternally imprinted and vice versa. However, analysis of both gonadal and non-gonadal GCTs revealed monoallelic expression of IGF2 but biallelic H19 expression, indicating a lack of imprinting of the maternal alleles. This erasure of methylation occurs during the development of female gametes, suggesting that this methylation pattern is a signature of where the cell of origin came from i.e. a PGC [37]. There also appears to be a difference in the IGF2 and H19 imprinting pattern in paediatric patients compared to adults, which has prompted the suggestion that the PGC was at a different stage of maturation in younger patients than in older ones.

Gain of isochromosome 12p is a marker for GCTs in all locations

Chromosomal gain studies examining gonadal GCTs revealed an increase of chromosome 12p copy number [46]. Other studies found other gains such as 1q, 3p, and 20q, or deletions such as 1p, 6q, and 18q, but these will not be discussed in detail [47]. Instead, in this section I will discuss 12p or i(12p) because these have been suggested markers of germ-cell progenitor as the cell of origin for all GCTs [5]. To allow an understanding of this argument, I will describe the progression of GCTs in the gonads and the link of i(12p) to invasiveness, before exploring the relevance of i(12p) or 12p gain in the CNS.

Nearly all gonadal GCTs have one or more copies of isochromosome 12p (i(12p)), or a partial gain of 12p at one of several locations in the genome [28]. This gain has been suggested to be an aberration which occurred early in the oncogenesis pathway and has been retained. Indeed, the frequency of 12p or i(12p) gain suggests that it is required for GCT formation or progression in the gonads.

Carcinoma *in situ* (CIS), or intratubular germ cell neoplasm unclassified (ITGCNU), is the equivalent to gonocytes (Figure 1.5 A). As previously mentioned, ITGCNU is histologically similar to germinoma, and germinoma may be an undifferentiated form of CIS. For gonadal GCTs, the cell of origin has been proposed to be either CIS/ITGCNU or the differentiated cell type spermatocytes

[48]. Chiganti *et al.* (2000) suggested that i(12p) is gained by aberrant recombination of a spermatocyte during meiosis [28](Figure 1.5 B). In order to understand the origins of CNS GCTs, it is important to first understand how gonadal GCTs are believed to form with respect to i(12p).

The gain of i(12p) has been associated with ITGCNUs that were invasive, but non-invasive ITGCNU do not appear to exhibit i(12p) gain. Diagnoses of non-invasive ITGCNU are rare but have been documented. This indicates that the acquisition of i(12p) can be an event occurring after the germ cells reach the gonads [49]. Equally, embryonal carcinoma-like cells have only been detected after the invasive stage i.e. when they have acquired i(12p) gain. Embryonal carcinoma cells are very similar to embryonic stem cells, and are thought to be a CIS cell that has acquired other stem-like or invasive properties. The consensus is that i(12p) is a marker for invasiveness, not necessarily GCT initiation [48]. This is important because if these aberrations can occur in GCTs which have been formed after successful germ-cell progenitor migration, i(12p) gain cannot be used as a marker or an event that is exclusively acquired during PGC migration.

Most CNS GCTs also exhibit chromosomal aberrations, which can include the i(12p) or partial 12p gain, suggesting that extragonadal GCTs arise from the same progenitor as gonadal GCTs [30]. It has been suggested that the gain occurs between the gonadocyte and the spermatocyte stage when germ cell progenitors are proposed to undergo mismigration and travel with this aberration to the brain. In summary, the gain of i(12p) or parts of 12p have been found in all gonadal GCTs and the majority of CNS GCTs, which has been used to suggest that gain of 12p is a marker for a GCT cell of origin.

Gain of 12p in CNS GCTs have been examined in several studies [50]. These studies suggested that since 12p was not ubiquitous in all CNS GCTs, 12p did not have an integral role in their initiation or maintenance.

Indeed, GCTs arising before puberty may be genetically distinct from those that arise later, allowing them to be stratified by age rather than location [37]. Extragonadal GCTs that arise in children between prenatal and infant stages lack

gain of 12p, instead having a range of different chromosomal aberrations including 1q gain or 1p loss [47]. Isochrome 12p gain is much more common in adolescent boys, approximately 80%; in the brain, however, there are examples for each of the subtypes of GCT that either possess or do not possess the 12p gain [51-55].

Proponents of the currently accepted hypothesis for extragonadal GCTs have argued that the 12p gain is found in both gonadal and extragonadal locations, and therefore they have a common cell of origin. Schneider *et al.* (2006) [30] believe that the 12p gain is likely to occur during the early stages of migration of primordial germ cells and this either forms gonadal GCTs or extragonadal tumours.

Studies examining other types of brain tumours, such as medulloblastomas, have revealed that two histologically-identical tumours can have a different cell of origin and mechanism of formation [56]. Identifying the cell of origin for extragonadal GCTs is clearly complicated; it seems counter-intuitive that 12p has been suggested as a marker for germ cell tumour formation as an early event because this gain is not required to form a GCT. A gain that is found in two histologically similar tumours is not necessarily indicative of their common cell of origin, but it may be informative about the mechanism of forming that tumour. In summary, 12p gain may be an aberration that can initiate an event that leads to the formation of a GCT, but the cell of origin is not necessarily of PGC origin.

This section has examined the data and 12p, or i(12p), is not necessarily gained in all CNS GCTs. Chromosomal gains are discussed in Chapter 1.4 as a possible mechanism for formation or invasiveness, but they do not appear to be strong evidence of a PGC lineage.

1.4. Hypothesis for the aetiology of CNS GCTs

In this section I will argue against the currently accepted hypothesis for the origins of extragonadal GCTs, specifically in the CNS. First, the arguments that

have been used in section 1.3 will be contended using relevant literature, and then the arguments in favour of an alternative mechanism will be discussed, i.e. the activation of OCT4 in neural progenitors.

Evidence against germ-cell progenitors as the cell of origin for CNS GCTs

The main arguments against the currently accepted hypothesis have been reviewed before [24], so this section will update the evidence against a germ-cell as the cell of origin for extragonadal GCTs.

SNRPN has been implicated as a reliable marker for lack of imprinting, a phenomenon that has been suggested to only occur in germ cells. However, Lee *et al.* (2010) [57] provided evidence that SNRPN exhibits variable methylation in neural stem cells in the brains of mice and humans. Therefore, germ-cells are not the only cells that lack methylation or imprinting.

It appears plausible that a brain tumour arises from a population of cells endogenous to the brain, rather than from migration of cells that originate outside of the embryo. Therefore, our hypothesis suggests that lack of imprinting is intrinsic to cancer formation and progression. Further, Jelinic *et al.* (2007) [44] showed that loss of imprinting has been documented in a range of other cancers. More importantly, lack of imprinting has been determined in gliomas, a type of brain tumour that originates from neural progenitors [58]. Here, Uyeno *et al.* (1996) proved that it is possible for a cancer that lacks imprinting to develop from a population of cells endogenous to the brain. Therefore, a CNS GCT would not be unique in exhibiting a lack of imprinting, and lack of imprinting is more likely to be a mechanism to form a cancer instead of being a marker for germ-cell progenitor migration.

The other arguments to support a germ-cell progenitor as the cell of origin for CNS GCTs include i(12p) gain and experiments to disrupt germ-cell migration that form GCTs. Gain of copy number has already been discussed - briefly, it

appeared to be a marker for invasiveness and progression, rather than an early event in germ-cell migration.

The evidence for PGC mismigration by Runyan *et al.* (2008) [39] presented in Chapter 1.3 requires further discussion. Runyan's study suggested that PGCs could migrate near the sacrum or coccyx when *BAX* had been mutated. The authors suggested that this observation was evidence that PGCs may form sacrococcygeal GCTs, and therefore extragonadal GCTs. However, there are several arguments against extrapolating extragonadal GCTs to include CNS GCTs. Firstly, no PGCs migrated to the brain, or even near the brain. Second, no GCT formation was observed in the brain. Even though there was a much higher number of PGCs that migrated to extragonadal locations, due to apoptotic disruption, PGCs still did not form tumours. Indeed, in a normal embryo, it is likely that the number of mismigrated PGC would be far fewer without the additional mutations used in the *BAX* model. Therefore, if a higher number of PGCs could not form a GCT, it is unlikely that this is a mechanism for initiating GCTs in the sacrococcygeal region.

Proponents for the PGCs hypothesis would argue that perhaps additional mutations are required to form GCTs, such as mismigratory mutations. However, if an apoptotic mechanism is required in order to promote PGC survival it may be unlikely that another mutation to dysregulate migration would also occur in a human patient. Tumours in children often have very few mutations since they do not have a long time in order to acquire multiple somatic mutations. Therefore, it seems unlikely that a mutation in apoptosis and mismigration would both occur in a single cell that migrates to the brain.

We will propose an alternative mechanism for sacrococcygeal teratoma formation at the end of this chapter. Since the arguments for germ-cell progenitors forming CNS GCTs have been reviewed, our alternative hypothesis for CNS GCTs will be the next topic for discussion.

Evidence for pluripotency as a mechanism for CNS GCT formation

In recent years, many studies have used the ability of cells to generate a teratoma, one subtype of GCT, as an assay of that cell's ability to produce all cell types of the body i.e. pluripotency [4]. These studies have provided new support for the hypothesis that teratomas could be derived from cell types in the body other than germ-cell progenitors. Furthermore, there is good evidence that the other GCT subtypes are 'lineage related' to teratomas. Therefore, if teratomas could arise from non-germ cell lineages the same could be true of the other subtypes. The evidence for both propositions will be analysed: that teratomas could readily arise from somatic cells with no relationship to the germ-cell lineage; and that other GCTs are directly related to teratomas and could therefore have the same non-germ cell origins. These considerations suggest that all CNS GCTs are likely to be caused by transformation of endogenous brain cell progenitors. One reason that they share features in common with gonadal germ-cell-derived GCTs may be that they share the same molecular defects, and in turn these cause shared biological features. In order to dispute the arguments in favour of a germ-cell progenitor as the cell of origin for extragonadal GCTs, it is necessary to understand what makes a cell pluripotent.

One of the most important genes is Oct4 (also known as Pou5f1) and this encodes the transcription factor OCT4, so this will be discussed at length. This section will first examine the gene structure for Oct4 before detailing the mechanisms that regulate OCT4, and the processes that OCT4 regulates. The final topic of this section will describe the role of OCT4 in pluripotency and explain the relevance to this thesis, i.e. as a potential mechanism for neural progenitors to form GCTs.

Oct4 gene structure and Oct4 isoforms

Oct4, also known as Oct3, OTF3, or OTF4, is an octamer-binding transcription factor that is crucial for development and pluripotency. OCT4 is transcribed from the Pou5f1 (POU domain, class 5, transcription factor 1) gene on chromosome 17

in mice or chromosome 6 in humans. POU (or Pit/Oct/Unc) domain-containing proteins have the ability to bind DNA. For consistency, this thesis will use Oct4 as the gene name synonymous to Pou5f1. Oct4 can generate 3 different transcripts known as OCT4A, OCT4B, and OCT4B1 (Figure 1.6 A). These transcripts can form 4 isoforms; OCT4A, OCT4B-190, OCT4B-265, and OCT4B-164, due to alternative stop and start codons or alternative splicing. Only OCT4A is known to be important in embryonic stem cell self-renewal and pluripotency. Although the functions of other isoforms are not fully characterised, it is known that they cannot sustain ESC self-renewal and are not thought to have similar functions to OCT4A [59, 60]. OCT4 in this thesis refers to the pluripotency-related protein translated from the OCT4A transcript.

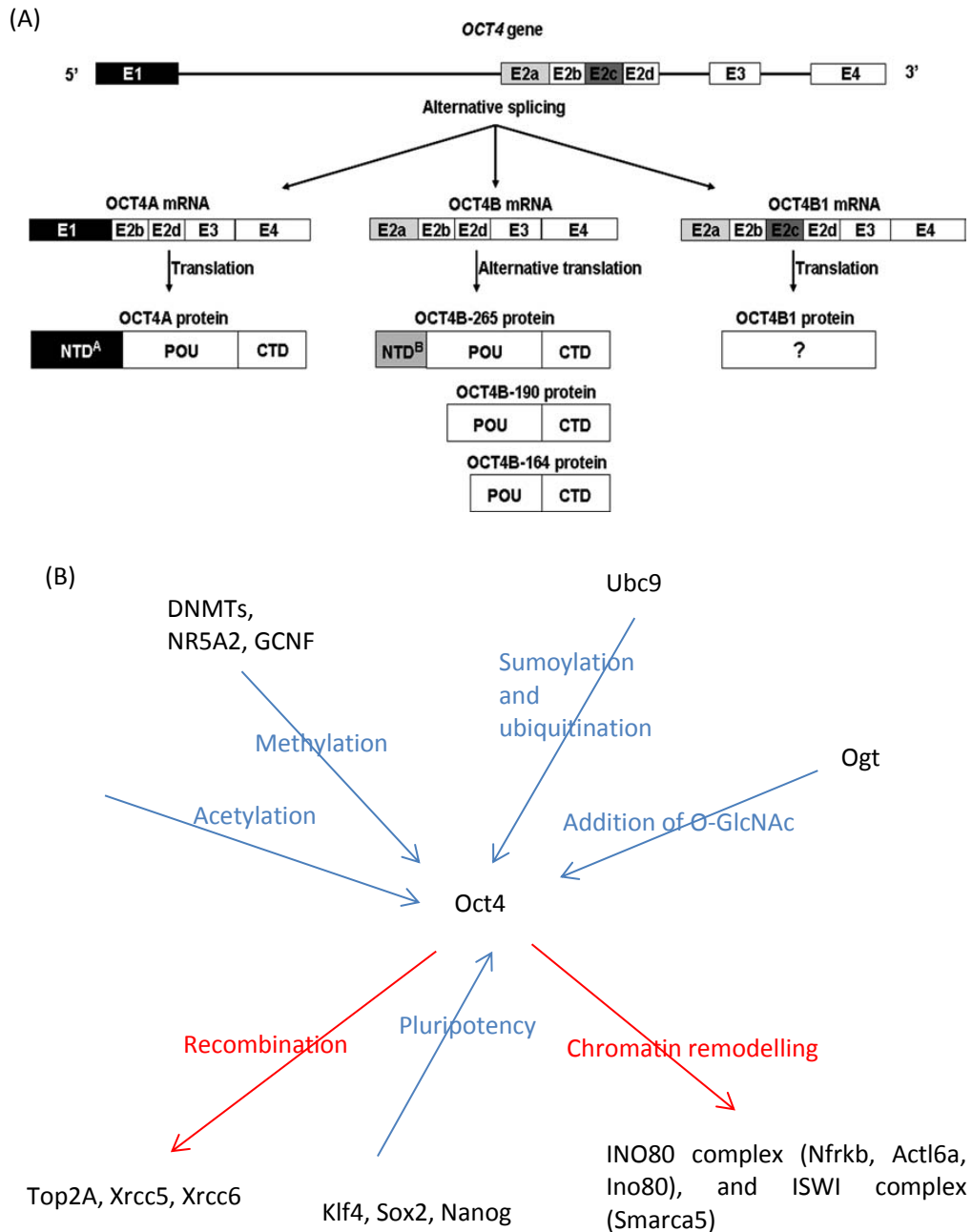


Figure 1.6. OCT4 transcripts and interaction pathways. (A) Diagram of the Oct4 gene's alternative splicing and isoforms for Oct4. Each exon is labelled E1-E4 with exon 2 divided into E2a-E2d. Alternative splicing produces three mRNA transcripts of Oct4A, Oct4B, and Oct4B1. These transcripts produce a total of 4 isoforms but only Oct4A protein is found to be important in pluripotency. Diagram from [Wang, 2010][59] (B) A summary of the important interactions that Oct4 is regulated by (in blue) or interacts with (in red). Oct4 is part of a vast regulatory network.

Oct4 contains two POU domains: an amino-terminal specific POU domain (POUs), and a carboxyl-terminal homeodomain (POUh) [61]. Both of these domains use a helix-loop-helix conformation to bind DNA for OCT4s various functions - the most noteworthy of which is its role as a transcription factor.

The Oct4 gene is conserved across diverse species from mammals such as *Homo sapiens* (humans), *Pan troglodytes* (chimpanzee), and *Mus musculus* (house mouse), to *Danio rerio* (zebrafish) suggesting its importance across evolution. The importance of OCT4 is reinforced by the extensive network of proteins that OCT4 interacts with.

Mechanisms that regulate OCT4

OCT4 itself is regulated by several mechanisms (Figure 1.6 B). The first is related to a protein called UBC9, which is an E2 Ubiquitin conjugating enzyme for SUMO modification. UBC9 is thought to stabilise OCT4 as one mechanism to regulate the levels of protein in the cell [62]. This is significant because OCT4 regulates stem cell renewal and pluripotency in a concentration-dependent manner.

OCT4 expression is a complex process that is controlled by a multitude of factors that interact with the promoter, and the distal- and proximal- enhancers. Retinoic acid has been shown to dissociate the factors involved in all three of these areas, which leads to a decrease in OCT4 mRNA levels [63]. However, when the complexes that interact with only one of these regulatory elements (promoter, distal, or proximal enhancer) are removed, there is little effect on OCT4 mRNA levels. This suggests a complex regulatory pathway for the regulation of Oct4 expression. One mechanism to regulate whether these proteins can bind to either the promoter, proximal, or distal enhancers is DNA methylation. DNA methylation is arguably the most important mechanism to regulate Oct4 expression.

The Oct4 gene has multiple regions of dense CpG sites called islands. When a high percentage of the CpG sites in islands become methylated the transcription of Oct4 is silenced [64]. 5-Aza-2-Deoxycytidine (5-Aza) is a drug that has been experimentally shown to globally demethylate the genome, which includes the promoter region of Oct4 to allow Oct4 expression. 5-Aza inhibits methylation by binding DNA methyltransferases (DNMTs) covalently to the DNA and disrupting interactions between DNMTs and transcriptional repressors. This leads to inhibition of methylation and dissociation of histone deacetylases (HDACs), which can in turn remodel the chromatin in order for genes to be expressed [65].

Oct4 transcription is silenced by methylation of the distal enhancer, proximal enhancer, and promoter region of Oct4. The mechanism by which Oct4 is transcriptionally silenced by methylation is outlined by Deb-Rinker *et al.* (2005) [66]. This process of methylation and maintenance is one that may have a role in tumour formation. If DNA methylation is not properly established the result may be aberrant gene expression. In fact, aberrant DNA methylation is a hallmark of many cancers [40]. Indeed, cancer is not the only disease with underlying DNA methylation dysfunction, highlighting the importance of this silencing mechanism [67].

Aberrant DNA methylation has been documented as a cause for several developmental diseases. Spina bifida is one such disease, which is caused by lack of methyl groups or metabolites [67, 68]. The fact that methylation has been known to cause both developmental diseases and cancer is important for this thesis. Dysregulation of methylation has been established as a mechanism for forming tumours, therefore it may be relevant for GCTs in the CNS.

Demethylation is associated with activation of a gene, and therefore this may be one mechanism of activating Oct4. Undifferentiated ESCs have predominately unmethylated promoter- and enhancer-regions, which supports this theory. Demethylation appears to be a prerequisite to expression but there are other factors that are required. For example, the promoter region of Oct4

can be acetylated at lysine 9 and 14 to allow the gene to be transcriptionally active [69]. This modification is one of several that are not fully understood.

Oct4 expression requires a complex network of proteins. LRH-1 (liver receptor homolog-1), also known as NR5A2, binds to the proximal enhancer and promoter regions to activate and maintain Oct4 expression; however the mechanism for this activation is unknown.

GCNF expression is thought to inversely correlate with Oct4 expression due to a complex network of interactions [70]. GCNF differentially recruits methylated CpG binding domain (MPD) factors to the Oct4 promoter for DNA methylation and silencing. Knockout of GCNF caused the Oct4 promoter to be less methylated and allowed expression of Oct4; however, the level of expression was lower than normal, suggesting redundancy in the regulation of Oct4 expression.

Embryonic stem cells (ESCs) highlight the balance between Oct4 expression and silencing. Once the promoter or other regulatory elements in Oct4 are methylated, transcription is normally permanently silenced. The most obvious question is how ESCs maintain Oct4 expression after it has been activated. In ESCs where Oct4 is active, the promoter, distal, and proximal enhancers are complexed by DNA binding proteins and transcription factors, which prevent methylation. The complexes that bind DNA allow continuous expression of Oct4 until differentiation signals remove these factors. During differentiation these factors are removed and transiently replaced by repressors that are thought to ensure long term silencing of the gene. Soon after these repressors bind, sequential DNA methylation occurs, which silences Oct4 [66]. Silencing of Oct4 in mice occurs by E8.5 and correlates strongly with increased expression of GCNF [71]. However, some studies have shown that neural stem cells still express Oct4 as late as E13.5 [64]. Notably, expression of Oct4 in NSCs at E13.5 was much lower than ESCs.

Processes regulated by OCT4

OCT4 interacts with a wide range of proteins (as reviewed by Pardo *et al* (2010) [72], summarised in Figure 1.6 B), which control several processes including recombination and chromatin remodelling. OCT4 interacts with the topoisomerase TOP2A, and helicases XRCC 5 and XRCC 6, which are all associated with recombination. OCT4 is also known to have a role in chromatin remodelling by binding to NANOG [73] and interacts with the chromatin remodelling proteins NFRKB (Nuclear factor related to kappa-B-binding protein), ACTL6A (Actin-like protein 6A), and INO80. OCT4 binds to subunits at the ISWI Chromatin Remodelling Complex such as SMARCA5 indicating OCT4's diverse roles in chromatin remodelling. While the mechanism for OCT4's regulation of chromatin remodelling through such factors is unclear, dysregulation of OCT4 may have disruptive effects on chromatin structure.

Pardo *et al.*(2010) [72] showed OCT4 interaction with several enzymes including OGT (O-linked N-acetylglucosamine transferase). OGT links O-linked N-acetylglucosamine to OCT4 to regulate apoptosis and epiboly movements. OCT4 in ESCs has been shown to be modified by O-GlcNAc by Webster *et al* [74]; however, the exact effect of this modification is not known.

OCT4 is also known to bind to several key pluripotency factors including KLF4, SOX2, and NANOG [72]. Clearly, OCT4 is regulated in a complex manner with several redundant mechanisms. This implies that OCT4 is an important transcription factor, and evolution has selected for mechanisms that tightly control Oct4 expression. The role of OCT4 in pluripotency and as a master regulator is the most relevant process to this thesis and therefore will be examined more closely.

OCT4 function in pluripotency

OCT4 is a transcription factor that has been well-documented for its role in pluripotency and stemness: stemness is a feature that separates a stem cell

from a somatic cell. Pluripotency will be discussed first, and the role of OCT4 will be highlighted after.

A pluripotent cell is one that can self-renew, and has the capability to differentiate into all of the cell lineages in the embryo and adult. ESCs from the inner cell mass of an embryo are a good example of a pluripotent cell type. Four key genes are required for the induction of a pluripotent cell from a somatic cell: KLF4, SOX2, OCT4, and MYC [75]. Regulation of the levels of OCT4 is a tightly controlled balance because downregulation of OCT4 causes differentiation into mesoderm and endoderm, but overexpression causes differentiation into ectoderm. In this respect, OCT4 is different from many other transcription factors because OCT4 level needs to be carefully maintained in order to either activate or repress transcription. Sterneckert *et al.* (2012) [76] have suggested that OCT4 does not simply activate pluripotency; rather, they suggest that OCT4 is a “gatekeeper into and out of the reprogramming expressway that can be directed by altering the experimental conditions”. Pluripotency appears to rely on several factors, and crucially OCT4 is required for reprogramming.

OCT4 has been suggested as a gatekeeper/master regulator, and transdifferentiation has been used as evidence for this. Activation of OCT4 in the presence of signals such as fibroblast growth factor (Fgf) and epidermal growth factor (Egf) have been used to induce somatic cells directly into neural progenitors instead of pluripotent ones [77]. In summary, OCT4 is integral to initiating pluripotency and stemness.

In addition to initiation of pluripotency, OCT4 is also important in self-renewal. OCT4 cooperates with two transcription factors: SOX2 and NANOG. Both SOX2 and NANOG are integral to self-renewal; however, it is important to note that NANOG is not necessary for induction of pluripotency. NANOG, OCT4, and SOX2 can activate or repress expression of each other. Aside from modulating the expression of these genes, OCT4 and NANOG can bind to MYC-N, which is known to promote self-renewal and proliferation [78]. Within the genome, OCT4 and NANOG were shown to have 1083 or 3006 DNA binding sites

respectively [78]. This suggests that these pluripotency regulators interact with a wide range of sites, and maintain pluripotency through a complex network. It is likely that there are several feedback mechanisms to regulate pluripotency instead of a binary system to activate and maintain pluripotency; for example, the regulation of NANOG, OCT4, and SOX2 modulating each other's expression levels [79].

The OCT4-SOX2-NANOG regulatory network is clearly crucial for the maintenance of pluripotency in stem cells. Each of these proteins can maintain its own expression by combining into complexes with other pluripotent factors; for example, OCT4 and SOX2 can form a heterodimer, which feedback to maintain their own expression [80]. Equally, OCT4 can repress its own expression, presumably to regulate the fine balance between over- and under-expression [79]. This illustrates the intricate regulation of each of these genes. The complexity of this process provides several mechanisms that may be a cause for dysregulation. This thesis tests the hypothesis that dysregulation of one of these mechanisms may lead to the aberrant expression of genes such as OCT4.

In summary, OCT4 is a master regulator of both induction of pluripotency and self-renewal. While it is integral to these processes, several other pathways modulate the behaviour of the pluripotency of the cell, such as SOX2, NANOG, MYC, and KLF4. This complex and vast network is finely balanced and may be a weakness that allows tumour formation through activation of OCT4.

Neural stem cells can be readily activated to form teratomas by activation of the pluripotency gene Oct4

Teratomas are very unusual because they include cell types derived from all of the three germ layers that make up the developing embryo. As such, they can contain many of the differentiated cell types of the body, such as skin, bone, muscle and hair, but in a disorganized form. Despite their size, and sometimes very rapid growth, teratomas rarely metastasise and so are considered benign.

Since teratomas contain all three germ layers, the ability of a cell to form a teratoma is used as an assay of that cell's pluripotency. In particular, teratoma formation has recently been used to determine if specific treatments can cause a cell to acquire such pluripotency, a key goal of studies to generate stem cells from somatic cells in regenerative medicine.

In 2006, Takahashi *et al.* [75] found that the overexpression of just four genes was sufficient to trigger a process in somatic cells, such as fibroblasts, that led some of them to become pluripotent. This technique parallels other methods of forming pluripotent cells such as somatic cell nuclear transfer, and cell fusion (Figure 1.7). Pluripotent cells produced by overexpression of these four genes (also known as 'induction') were then able to form teratomas when transplanted into immune deficient mice [75]. More strikingly, in 2009, Kim *et al.* found that overexpression of a single gene, Oct4, was sufficient to initiate a process in neural stem cells (NSCs) that eventually induces pluripotent cells to form [81].

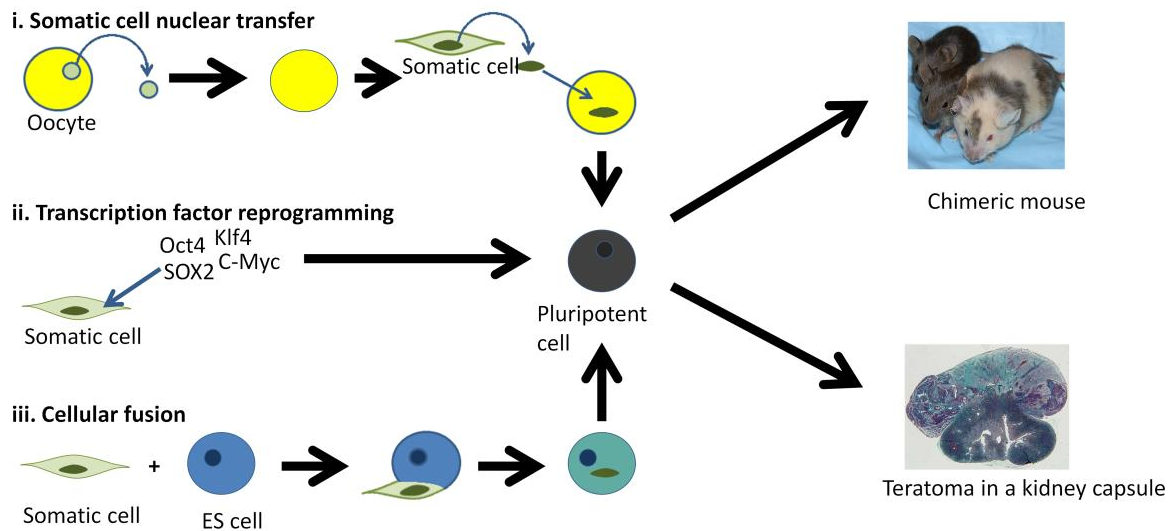


Figure 1.7. Three mechanisms known to be able to form a pluripotent cell. Three methods for generating pluripotent cells are illustrated. (i) Somatic cell nuclear transfer: an enucleated oocyte is injected with a somatic nucleus. *In vitro*, these cells can be cultured to produce embryonic stem (ES) cells. (ii) Transcription factor reprogramming: a specific combination of several genes expressed in combination can reprogram a somatic cell to form a pluripotent cell. The original four factors are *OCT4*, *KLF4*, *C-MYC*, and *SOX2*; however, each of these can be replaced by a different gene illustrating the redundancy in reprogramming [Greenow,2012] [82]. (iii) Cellular fusion: ES cells and somatic cells can be fused to form a cell that exhibits pluripotent features. Each one of these methods generates a pluripotent cell that can contribute either to a chimeric mouse or to a teratoma if transplanted.

In fact, NSCs may be the only somatic cell type that is so easily encouraged to become pluripotent - in other words, to acquire the ability to form a teratoma. For many years, Oct4 has been regarded as one of the key genes necessary for the pluripotent capability of an embryonic stem cell (ES cell). But what do we know of OCT4 in the cells of the developing brain?

Dividing cells in the early developing brain of foetal mice maintain a low level of expression of Oct4, but by this stage of development the cells are clearly no longer pluripotent [64]. In fact, these cells express a dramatically reduced level of OCT4 compared with the embryonic stem cells that are found much earlier in embryonic development. This reduced expression seems to be due to methylation of the regulatory region of the gene, which becomes even more pronounced as brain development proceeds, such that the Oct4 gene is effectively silenced by two thirds of the way through gestation. However, Oct4 expression can be readily reactivated by treatment with the demethylating agent, 5-azacytidine [83-85]. If the same is true in humans, then disruption to the methylation of this gene in just one cell during the early period when this methylation is incomplete, and therefore potentially more plastic, could recapitulate the pluripotency experiments described above. This could lead to inappropriate expression of Oct4 resulting in the formation of a teratoma. The activation of OCT4 in neural progenitors provides a plausible mechanism to explain why this type of tumour can appear in the brain by the point of birth and occur at a much lower frequency later in life.

Expression of pluripotency genes in GCTs

So is there any evidence that OCT4 is reactivated in human teratomas or other GCTs seen in the brains of patients? Recent studies of GCTs, including those using global gene expression analyses, have demonstrated substantial expression of Oct4 in germinomatous tumours, including those in the brain [86-88]. Oct4 expression is not, however, a notable feature of teratomas or yolk sac tumours. This can be explained by the complex nature of these tumours.

In fact it would be surprising if Oct4 did feature highly on the list of genes seen in pure teratomas or yolk sac tumours; the majority of cells in such tumours are differentiated, and OCT4 is a feature of the proliferating stem cell proposed to be responsible for growth of the tumour.

In summary, Oct4 overexpression in NSCs can trigger teratoma formation, and Oct4 expression is a significant feature of cells from several subtypes of GCT. Since Oct4 expression correlates closely with the methylation status of its promoter and can be activated experimentally by demethylation, loss of methylation of the Oct4 gene in NSCs during embryogenesis would be predicted to allow these cells to form teratomas. This leads us to hypothesise that Oct4 is more readily activated by demethylation in early embryogenesis and that this leads to one or more cells to become pluripotent. These cells then form a teratoma that can grow to a significant size by birth.

Extragenadal GCT subtypes share a common lineage

Activation of Oct4 expression in NSCs can lead to the formation of teratomas, although this has not been shown in the brain. This is significant and Chapter 4 tests the hypothesis that OCT4 can initiate the formation of a CNS GCT. But what of the other subtypes of GCT? The most direct line of evidence in support of the hypothesis that Oct4 expression can result in the formation of all subtypes of CNS GCT is the direct lineage relationship these other subtypes have to teratomas. Since there is strong evidence that little needs to go wrong for NSCs to form teratomas, this relationship implies that the other CNS GCTs could also be NSC-derived. This topic will be discussed in greater depth in Chapter 3.

Mechanisms by which NSCs might be transformed to form GCTs

We propose that CNS GCTs are likely to originate from neural progenitors rather than germ-cell progenitors that have mismigrated. We hypothesise that Oct4 expression may be the mechanism by which neural progenitors retain or

acquire pluripotent properties leading to the formation of teratomas and perhaps other types of GCT. It seems likely that other subtypes of GCT arise when additional events also occur in GCT progenitor cells. In addition to expressing high levels of OCT4, germinomatous tumours often exhibit mutations in the tyrosine kinase receptor oncogene, KIT, regardless of their location [23]. These mutations may therefore drive the tumour to develop as this class of GCT. Other common molecular events that are highly restricted to specific subtypes of GCT remain to be elucidated.

One striking feature of non-germinomatous tumours is a high level of gene-specific methylation [89, 90], which could therefore play a role in determining the GCT subtype. Hence, disrupted methylation might cause activation of Oct4, but silence other genes, thus providing a unifying mechanism for this group of tumours. A schematic containing our NSC hypothesis can be found in Figure 1.8.

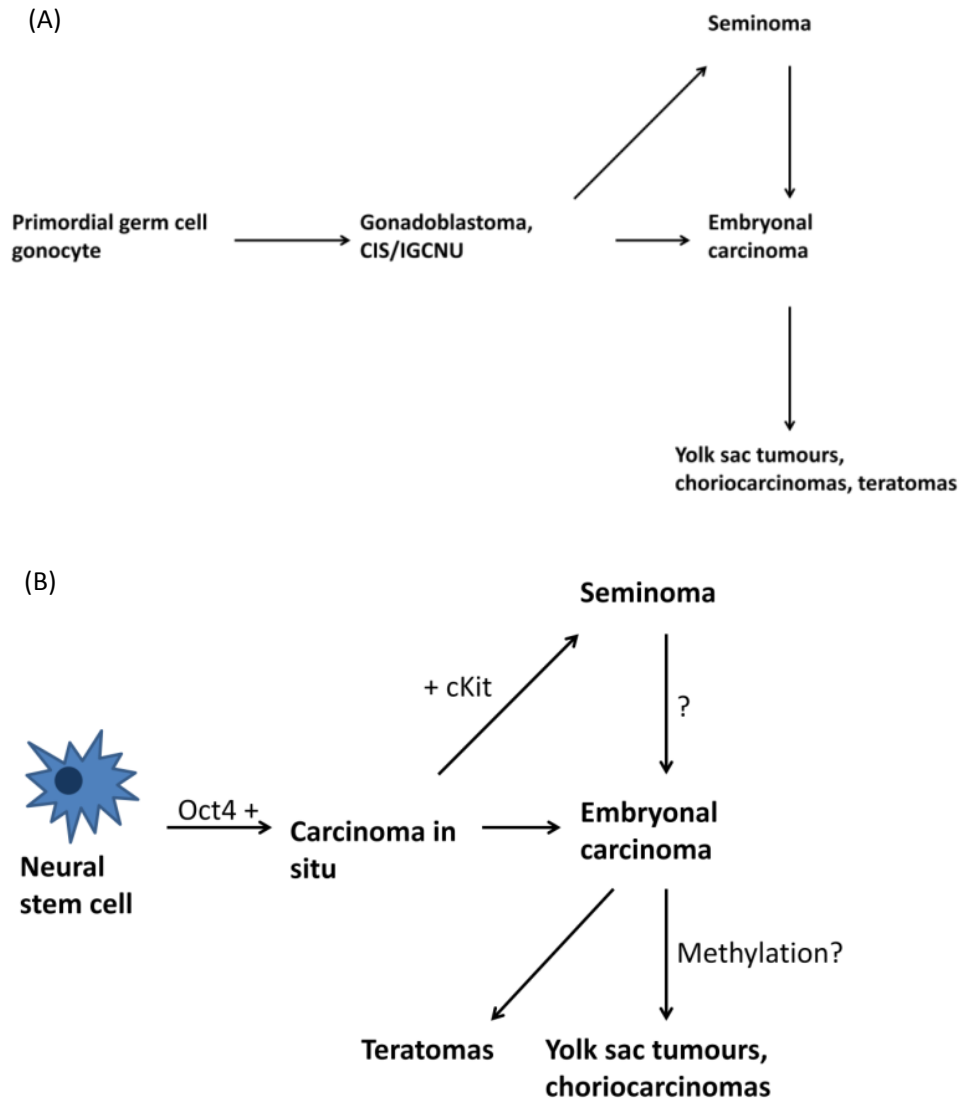


Figure 1.8. The brain-cell theory for intracranial germ cell tumours. (A) Model for the aetiology of different histological subtypes of GCT. Activation of OCT4 may lead to aberrant cell growth and pluripotency to form something equivalent to CIS. This will go on to form an immature embryonal carcinoma and progress to a teratoma. (B) Model for the aetiology of neural stem cell-derived intracranial GCT. Neural stem cells acquire or maintain Oct4 expression to form a cell with pluripotent features. This cell can form any type of germ cell tumour found in the CNS. If these cells are in an environment that supports tumour formation, these cells can simply differentiate into teratoma and embryonal carcinoma. Yolk sac tumours and choriocarcinomas may require an additional event to allow differentiation into this lineage, possibly involving aberrant methylation. Since germinomas robustly express KIT that often carries an activating mutation, this may be the event that biases the cells towards this type of tumour.

Demethylation as a mechanism for GCT formation

The carcinogenic model of cancer development, which is accepted for adult cancers, seems unlikely to explain the earliest tumours seen in children. The reason that cancer is generally a disease of old age is the time it takes for sequential carcinogenic damage to accumulate in the genome of a single cell. Given the early age of occurrence in children, especially teratomas that are found at birth, a faster alternative mechanism is needed to explain children's tumours (Reviewed in [91]). Methylation changes are a prime candidate for a single event that could disrupt the expression of many genes, producing cells with all of the features necessary to form a cancer. Indeed, aberrant methylation has been shown to occur in a range of other types of paediatric brain tumours [92-94].

Our model suggests that demethylation of Oct4 either activates or maintains its expression inappropriately. If demethylation of Oct4 is a pivotal event in GCT aetiology, this could have a direct bearing on therapeutic strategies since levels of DNA methylation can be directly affected by drugs such as 5-azacytidine. By better understanding the role of methylation in the aetiology of these different classes of GCT, evidence-based strategies targeting methylation could be developed. In particular, if the molecular machinery that specifically regulates Oct4 methylation can be determined, then this could be targeted by a more directed therapy instead of using drugs that alter DNA methylation globally.

The Oct4 gene has been examined for promoter methylation as a mechanism for silencing expression. However, little is known about the role of OCT4 protein and methylation of other regions of DNA. OCT4 has been shown to have a role in demethylating specific regions of DNA, although this mechanism has not been elucidated [95]. This may eventually provide a mechanism by which OCT4 self regulates its own methylation - by methylating and silencing other genes. In short, the gene that encodes Oct4 expression, and OCT4 itself, are both

part of a complex regulatory system that involves DNA methylation, and disruption of this system may lead to the formation of a GCT.

Diseases associated with GCTs and their relationship to OCT4

A striking observation is that Down's syndrome (caused by the presence of an extra chromosome 21) and Klinefelter's syndrome (caused by the presence of an extra X chromosome) are associated with an increased prevalence of CNS GCTs [96-98]. Why these very different disorders result in this particular type of brain tumour is not yet known, but it does imply that overexpression of a complex set of genes produces a particular bias towards extragonadal GCTs. This presumably overrides any deficiency in brain cell proliferation that might exist in people with Down's syndrome. Given that these disorders involve different chromosomes, it seems possible that any mechanism that causes overexpression of a large set of genes might also bias towards extragonadal GCT development. Deregulation of epigenetic gene control (such as DNA methylation) represents one such potential mechanism and an alternative to a model that relies simply on activation of OCT4.

Similar arguments may apply to the origins of GCTs in other extragonadal regions, such as mediastinal and sacrococcygeal tumours. This requires that a likely progenitor be identified in these locations. In the case of the sacrococcygeal tumours there is indeed evidence of such a progenitor. In Chapter 1.3 the argument in favour of a germ-cell progenitor suggested that sacrococcygeal tumours arose from mismigration of germ-cells. This was partially due to the proximity of the normal germ-cell progenitor migratory route. However, recent studies of mouse embryos, Cambray and Wilson (2007,2002) [99, 100] have shown that pluripotent progenitor cells remain present at the base of the spine as late as mid-gestation in mice. Given that sacrococcygeal tumours are generally seen by birth, when they can already be very large, it is plausible that these tumours are initiated at a time during foetal development when such pluripotent progenitor cells might still be present. To date, no similar

progenitor has been identified in the mediastinal region, though there have been few studies that had the potential to identify such cells. In summary, at least one extragonadal location appears to contain a pluripotent GCT-progenitor, which weakens the argument that all GCTs arise from mismigrating PGCs.

1.5. Aims of project

This project aims to test an alternative to the hypothesis that all GCTs arise from PGCs that have mismigrated. One of the main aims is to determine if there is an alternative cellular origin for intracranial GCTs along with a potential mechanism: the activation of Oct4 by demethylation of its promoter region. Our model provides a testable hypothesis; that activation of OCT4 in NSCs of the developing brain could trigger formation of a GCT, most likely a teratoma. If this proves to be true, it will then provide a starting point to establish the full aetiology of these tumours. Published clinical reports support a model in which the various histological subtypes of GCT are largely inter-convertible; therefore, it should also be possible to use a mouse model to analyse potential mechanisms that underlie these transitions, such as *KIT* mutations in germinomatous tumours.

The topics discussed in this thesis examine several features related to CNS GCTs. The first section examines phenomena specific to GCTs, such as the frequent occurrence in the midline instead of the lateral regions of the brain. The second section examines Oct4 expression as a mechanism for CNS GCT formation using *in vitro* and *in vivo* techniques. The final section proposes a mechanism to form one of the subtypes of CNS GCT: germinomas.

Chapter 2: Materials and methods

Literature review criteria

There were several criteria for the literature review examining teratomas in the intracranial region. The intracranial region was defined as the CNS, excluding the spinal cord. There are several types of teratoma near the CNS that were not included; for example, epignathus (teratoma of the palate) and intraocular teratomas. Equally, cases where teratomas were mixed with other subtypes were not included in the results.

There were no restrictions on the age of the patient, language of the publication, or access to publication. For inclusion in the results, there must have been a diagnostic scan, (for example MRI or CT), and only cases published after 1990 were included.

The main sources of peer-reviewed cases were Pubmed (www.ncbi.nlm.nih.gov/pubmed), and Web of Knowledge (<http://apps.webofknowledge.com>). Search terms included 'teratoma', 'intracranial', 'central nervous system', 'germ cell tumour', 'brain', and 'head' in various combinations.

Each of the cases that matched the criteria was assessed for references to other papers; for example, if a paper mentioned other cases of CNS teratoma, these were also included as long as they matched the criteria. Over 500 papers were reviewed, and all those papers that matched the criteria were included in the results.

Transgenic Mice

Nestin-rtTA, TetO-Oct4 mice

Nestin-rtTA mice (FVB-Tg (Nes-rtTA) 306Rvs/J, The Jackson Laboratory) were crossed with TetO-OCT4 mice (B6;129-Gt(ROSA)26Sor^{tm1(rtTA*M2)Jae} Col1a1^{tm2(tetO-Pou5f1)Jae}/J, The Jackson Laboratory). This produced mice that were homozygous for the Nestin-rtTA transgene, and homozygous for TetO-OCT4.

Col1a1::TetOP-OCT4 mice

All mice were homozygous for the Rosa26-rtTA-nls cassette. Adult male mice (B6;129-Gt(ROSA)26Sor^{tm1(rtTA*M2)Jae} Col1a1^{tm2(tetO-Pou5f1)Jae}/J, The Jackson Laboratory) that were heterozygous for the Col1a1::TetOP-OCT4 cassette were crossed with homozygous females to set up a colony of mice. The genotype for each mouse in the breeding program was confirmed to be either homozygous, heterozygous, or wild-type for the Col1a1::TetOP-OCT4 cassette.

In vivo induction of OCT4 in Col1a1::TetOP-OCT4 mice with doxycycline

OCT4 was induced *in vivo* by administering 100µl of 2.4mg/ml doxycycline (Fluka) in sterile water per day by gavage.

Genotyping

Ear punches from Col1a1::TetOP-OCT4 mice were digested in DirectPCR lysis reagent (Tail) (Viagen) and 0.5mg/ml proteinase K (Roche) in a rotating oven at 55°C for 18 hours. Lysates were then heated to 85°C for 45 minutes.

PCR reactions (for primers see Table 6.1) were carried out using the following reagents: Biomix Red (Bioline) (1x), primers (250nM of each), water, and DNA lysate.

PCR was used to amplify regions of DNA using a thermo cycler (Techne-312 or G-Storm-GS1) with the following conditions: 96°C for 2 minutes, 30 cycles at 96°C for 30 seconds /59°C for 30 seconds/72°C for 30 seconds, and a final extension of 72°C for 2 minutes. The PCR mixture was loaded directly into a 1.2% agarose gel and electrophoresed for 25 minutes at 150V.

Tissue culture and cell culture assays

Fibroblast culture

Mouse embryonic fibroblasts (MEFs) (American Type Culture Collection – STO cells, CRL-1503) were cultured in medium (DMEM, 10% FBS) and placed in 0.1% gelatin (Sigma-Aldrich G1393)-coated flasks. MEFs were passaged when 80-90% confluent and the medium was changed at least every 3 days.

MEFs were prepared for passage by removing medium and washing with PBS. Warm 1x trypsin (Invitrogen) was added to the flask and left for 6 minutes at 37°C. PBS was added to the cell suspension and centrifuged at 200 G for 5 minutes. The supernatant was aspirated, leaving the cell pellet. The pellet was either plated at a concentration of 5×10^6 cells per T75 flask, or frozen. When the cells required freezing 1×10^7 cells were suspended in cold freezing medium (20% DMSO, 80% FBS) placed directly into a -80°C freezer.

To culture MEFs from frozen, one vial was placed directly from -80°C to a 37°C water bath and left to thaw for approximately 2 minutes. The cells were washed with PBS and centrifuged at 200 G for 5 minutes. The supernatant was removed and the cell pellet was resuspended in warm culture medium. These cells were cultured in a 0.1% gelatin-coated T75 flask.

Mitotic inactivation of MEFs

MEFs were mitotically inactivated using mitomycin C (Sigma Aldrich). MEFs were cultured until 70-80% confluent before being treated with 10µg/ml

mitomycin C for 24 hours. After treatment, the cells were washed with PBS; which was subsequently replaced with culture medium.

Culturing of primary mouse neural stem cells

Mouse brain tissue of various ages (E11.5, E13.5, P7) was dissected from the lateral ventricular region, ventral midline, or mixed brain. The dissected tissue was homogenised using a scalpel in 1x PBS and the partially homogenised suspension was liquidised further. After allowing the solid clusters of tissue settle to the bottom of the tube the PBS was aspirated off (and kept for direct culture) and Accutase (Patricell) was added to the remaining pellet. Tubes were incubated at 37°C for 20 minutes with periodic agitation. The cell solution was pipetted and the tubes were filled with PBS. The supernatant was transferred to clean tubes and centrifuged for 5 minutes at 200 G. Accutase was added to the remaining solid tissue pellet for a second homogenisation step then PBS was added and centrifuged. The supernatant from these two sets of tubes was discarded and pellet resuspended in warm neural stem cell medium (NSC medium) [Neurobasal medium 1x (Gibco), 1:1 DMEM F-12 1x (Gibco), B27 (0.1x)(Invitrogen), N2 final (0.1x)(Invitrogen), FGF (20ng/ml)(Invitrogen), and EGF (20ng/ml)(Sigma)]. Pen/strep (0.05U/ml penicillin and 50ng/ml streptomycin in 0.9% NaCl)(Sigma) were added when contamination was a risk. Each cell type was plated into a different well in a 6-well plate in neural stem cell medium and incubated at 37°C in 5% CO₂.

Neural stem cells were split by first centrifuging the liquid medium containing the floating neurospheres. The supernatant was removed and accutase was used to resuspend the pellet before being left for 20 minutes at 37°C. Accutase was diluted with PBS (5x) (phosphate buffered saline) and centrifuged at 200 G. The supernatant was aspirated and the cells were resuspended in warm medium. This single cell solution was plated at a cell density of between 1×10^4 and 1×10^5 per well in a 6-well plate.

Neurospheres were prepared for freezing by dissociating with accutase (as above). Single cells were frozen using 10% DMSO in DMEM F-12 at a minimum cell concentration of 1×10^5 cells.

Self-renewal assay

Cultured neurospheres were rinsed, centrifuged, and dissociated using the method previously stated. The single cell suspension was washed with DMEM and centrifuged at 200 G for 5 minutes. Pelleted cells were resuspended in neural stem cell medium including growth factors. The number of cells was calculated using a haemocytometer and trypan blue (Sigma). The volume required for 1/3 neural stem cell was calculated and volume was added to one well of a 24 well plate. A minimum of 3 wells were plated and a final well which contained approximately 1×10^3 cells functioned as a cell stock. An appropriate amount of warm medium was added and then incubated at 37°C in 5% CO₂.

Single cells were monitored for growth into neurospheres over 3 days. Wells that contained neurospheres had the medium carefully removed and replaced with accutase, then incubated at 37°C in 5% CO₂ for 8 minutes. Single cell suspensions were washed with PBS and centrifuged at 200 G for 5 minutes. The cell pellet was resuspended in neural stem cell medium and plated into a single well of a 24-well plate at a dilution of 1/3 cell per well.

This process of plating a single neural stem cell into a well of a 24-well plate, culturing, dissociating, washing, centrifuging, and replating constituted a single passage. Each original neural stem cell underwent 3 consecutive passages to confirm its ability to self-renew.

Differentiation assay

Coverslips were coated with 15µg/ml laminin (Sigma) suspended in DMEM for 4 hours. Neural stem cells were cultured on laminin-coverslips and cultured as a monolayer until 50% confluent. The medium coating the coverslip was aspirated and changed to: Neurobasal medium 1x (Gibco), 1:1 DMEM F-12 1x (Gibco), pen/strep (0.05U/ml penicillin and 50ng/ml streptomycin in 0.9% NaCl)(Sigma), B27 (0.1x)(Invitrogen), N2 final (0.1x)(Invitrogen), and 10µM

retinoic acid (Sigma). After 24 hours this medium was replaced with neural stem cell medium without growth factors i.e. Neurobasal medium 1x, 1:1 DMEM F-12 1x, pen/strep (0.05U/ml penicillin and 50ng/ml streptomycin in 0.9% NaCl), B27 (0.1x), and N2 final (0.1x). The monolayer of differentiated neural stem cells was allowed to grow for 3 days before being prepared for immunofluorescence.

Doxycycline treatment of neural stem cells

Neural stem cells that required doxycycline for activation of the transgene were treated with 1µg/ml of doxycycline (Fluka) added to normal neural stem cell medium. Neural stem cells were sustained under doxycycline once treatment began and the medium was changed a minimum of once every 3 days.

Culturing mouse embryonic stem cells

Mouse embryonic stem cells (E14TG2A) were provided by Val Wilson and The Institute for Stem Cell Research, Edinburgh. T75 flasks were coated with 0.1% gelatin (Sigma) for 1 hour. The gelatin was aspirated and flasks were left to dry for 20 minutes. Frozen ES cells were thawed quickly at 37°C and added to 10ml warm embryonic stem cell medium [GMEM (Sigma), 10% foetal calf serum (Gibco), 1x non-essential amino acids (Invitrogen), 2mmols/L glutamine (Invitrogen), 1mmols/L sodium pyruvate (Invitrogen), 0.1mols/L 2-mercaptoethanol (Sigma), 100units/ml Lif (donated by Val Wilson)]. This cell solution was centrifuged at 200 G for 5 minutes. The medium was aspirated and the cell pellet was resuspended in warm ES medium, before being transferred to a gelatin-coated T75 flask.

ES cells were prepared for passage by removing the medium and rinsing twice with PBS. Trypsin was added to the cells and incubated at 37°C for 6 minutes. Trypsinised cells were transferred into ES medium then centrifuged at 200 G for 5 minutes. The cell pellet was resuspended in ES medium and the cells were counted using a hemocytometer. Dissociated cells were either plated in T75 flasks or frozen. Approximately 5×10^6 cells were plated in ES medium per

gelatin-coated T75. If in excess, 1×10^7 cells were frozen in ES medium with DMSO (Sigma) at a final concentration of 10% per vial and stored in a -80 freezer.

Zeocin kill curve

ES cells were plated at 1×10^5 ES cells per well in a 0.1% gelatin-coated 6-well plate. After 24 hours, the medium in each well was aspirated and replaced with 3ml of ES medium including Zeocin (Invivogen) at final concentrations of 0 μ g/ml, 5 μ g/ml, 10 μ g/ml, 20 μ g/ml, 35 μ g/ml, and 50 μ g/ml. Four wells for each concentration were tested. Every 2 days one well was counted using a hemocytometer whilst the others were passaged with fresh medium and Zeocin.

Bacterial plasmid cloning

ETV1 RNA probe plasmid

PCR was used to amplify the full-length coding sequence of *ETV1* to produce a 1kb product (see table 1 for primer list). A pBluescriptII SK+ plasmid (Stratagene) was cut using restriction enzymes; Xba1 (NEB) and Xho1 (NEB). This cut pBluescriptII SK+ plasmid was ligated to the 1kb *ETV1* insert using 400U of T4 ligase (New England BioLabs, M0202) per 20ul reaction. A molar ratio of insert to vector ratio of 3:1 was used. This ligation was incubated at 37°C for 1 hour.

Transformation

α -select chemically competent cells (Bronze efficiency)(Bioline) were thawed slowly on ice. Plasmid DNA [250ng pEGFP (Clontech) or 200ng pORF (InvivoGen)] was added separately to competent cells and incubated on ice for 30minutes. Bacterial cells were heat shocked at 42°C for 40 seconds and then placed on ice for 2 minutes. SOC medium was added to the transformation reactions, and the mixture was incubated for 1hr at 37°C whilst being shaken.

Transformation mix was plated onto LB agar containing ampicillin (100 μ g/ml) or kanamycin (100 μ g/ml), for pORF and pEGFP respectively. Plates were incubated overnight at 37°C. Single colonies from transformed bacteria

grown on LB plates with appropriate selection were selected and cultured in Mu medium overnight shaking at 200 RPM (New Brunswick Scientific C25 Incubated Shaker) at 37°C.

Plasmid DNA purification

5ml of bacterial culture was centrifuged at 16000 G for 1 minute. The supernatant was discarded and the pellet was resuspended by vortexing with resuspension solution (GenElute Plasmid Miniprep kit, Sigma). Lysis buffer was added (GenElute Plasmid Miniprep kit, Sigma), followed by neutralisation buffer (GenElute Plasmid Miniprep kit, Sigma), and then the tubes were centrifuged at 16000 G for 10 minutes. The cleared lysate was mixed with isopropanol and centrifuged at 16000 G for 5 minutes. The supernatant was discarded and 70% ethanol was added before being centrifuged again at 16000 G for 2 minutes. The supernatant was removed and the pellet was air-dried before resuspending the DNA pellet in sterile distilled water.

For larger plasmid concentrations plasmid maxi kit (Qiagen) was used following the manufacturers protocol.

Where clones were confirmed as having the correct insert, 5ml bacterial culture was mini-prepped using GenElute HP Plasmid Miniprep Kit (Sigma) following the recommended protocol.

Plasmid DNA restriction digest

Plasmid DNA (200ng) was digested using 2U/μl of the appropriate restriction enzyme (New England Biolabs) and 1x buffer before being incubated for 1-2 hours at 37°C (see Table X.2 for enzymes).

To digest and verify ligation in pJet vector (CloneJET PCR Cloning Kit) (Fermentas), DNA (200ng) was digested using BglII (2U/μl) (New England Biolabs), and BglII buffer (1x)(New England Biolabs) before leaving for 1-2 hours at 37°C.

Transfection and stable selection of eukaryotic cells

Transfection of Embryonic stem cells

ES cells were seeded at 1×10^6 in each of 3 T75 flasks. Two tubes were prepared; 20 μ l DharmaFECT3 (Thermo Scientific) in 500 μ l OptiMEM, and 10 μ g DNA (GFP, pORF, or equivalent volume of water) in 500 μ l OptiMEM. Each pair of tubes (GFP, pORF, and control) was mixed and left for 20 minutes at room temperature. Each solution was added drop wise to a separate T75 and placed in a 37°C incubator. Medium was changed the next day to include Zeocin at final concentration 10 μ g/ml. Cells were then cultured using the above mouse embryonic stem cell protocol.

Immunostaining

ES or neural stem cells at a cell concentration of 1×10^4 were cultured as a monolayer on gelatin-coated (0.1%) or laminin-coated (15 μ g/ml) coverslips respectively. Each coverslip was washed twice with PBS then fixed with 0.4% paraformaldehyde (PFA) for 15 minutes. The coverslips were rinsed twice with PBS for 5 minutes. The PBS was aspirated and replaced with 0.2% Triton X (Sigma) in PBS for 15 minutes, then washed twice with PBS for 5 minutes each. The coverslips were blocked for 1 hour 30 minutes using 3% BSA (Sigma) dissolved in 0.1% Triton X/PBS for OCT4 (Santa Cruz)(see Table 6.3). For NANOG (Abcam), 10% sheep serum in PBS was used to block coverslips for 2 hours at room temperature. The cells were incubated with 5 μ g/ml primary antibody in blocking solution for overnight at 4°C. Each coverslip was washed twice with PBS for 5 minutes. This was followed by two PBS washes for 30 minutes each whilst slowly shaking. Secondary antibodies (see Table 6.3 for antibodies) were added and left at room temperature for 1 hour. Each coverslip was again washed with PBS twice for 5 minutes, then twice for 30 minutes. PBS was removed and mounted with Dapi solution (Vectashield).

Polymerase chain reaction (PCR)

PCR reactions were carried out using the following reagents: buffer (1x), dNTP (0.8mM), primer (250nM of each), and a high fidelity *pfx* DNA polymerase Platinum Taq (0.1u/μl – requires 1.5mM MgCl₂) (Invitrogen). PCR was used to amplify regions of DNA or cDNA using a thermo cycler (Techne-312 or G-Storm-GS1) with the following conditions: 95°C for 5 minutes, 35-40 cycles of 94°C 1 minute /58°C 1 minute/72°C 45 seconds, and a final extension of 72°C for 2 minutes.

PCR purification

Amplified PCR products were purified using a PCR purification kit (Qiagen) according to the manufacturer's protocol. The DNA was eluted using sterile distilled water.

Sequencing

DNA samples were prepared for sequencing using the following reaction: 100-200ng purified DNA, 0.5μl/5μl reaction of BigDye (Applied Biosystems), 1x buffer, 1pmol/μl primer (Fermentas), and if necessary 0.5M Betaine (Sigma). Sequencing conditions were 96°C for 1 minute, 99 cycles of 96°C 20sec/50°C 20sec/60°C 1min, hold at 4°C. DNA was precipitated using adding 30μM sodium acetate, 100ng/μl glycogen, and ethanol. The mixture was incubated at -20°C for 15 minutes then centrifuged at 16000 G for 15 minutes. The supernatant was aspirated and the pellet was washed with 75% ethanol then centrifuged at 16000 G for 5 minutes. The supernatant was again aspirated and the pellet was left to air dry. The pellet was resuspended in sterile distilled water before being sent to Geneservice, Nottingham for sequencing.

RNA extraction

TRI reagent (Sigma) was added to each ES or NSC cell pellet and incubated at room temperature for 5 minutes. Chloroform was added and incubated at room temperature for 10 minutes then centrifuged at 16000 G for 15 minutes at 4°C. The aqueous layer removed and mixed with isopropanol then left at room temperature for 5 minutes. The mixture was centrifuged at 16000 G for 15 minutes at 4°C. Isopropanol was removed and washed with 70% ethanol before being centrifuged for 5 minutes at 16000 G. Ethanol was removed and the pellet was air dried before resuspending in DEPC water. The RNA was quantified using a Nanodrop spectrophotometer (Thermo Scientific). DNase 1 Amp grade (New England Biolabs) (0.05U/μl) and reaction buffer (1x) were added to the RNA and incubated for 10 minutes. Tubes were heated at 65°C for 10 minutes and stored at -80°C if necessary.

cDNA synthesis

For each reaction, 2μg RNA, 25ng/μl oligoDTs (Fermentas), 25ng/μl random primers (Promega), dNTP (10μM), and RNase free water were combined. The reactions were heated to 65°C for 5 minutes before being placed on ice for 1 minute. A final concentration of 1x first strand buffer (Invitrogen), 50mM DTT (Invitrogen) and 0.5U/μl Superscript III (Invitrogen) were added to each tube and placed in the thermocycler (Techne) for 5 minutes at 25°C, 45minutes at 50°C, then 15 minutes at 70°C. cDNA was stored in a -20°C freezer or used directly for PCR. Each reverse transcriptase reaction had a separate reaction with exactly the same contents except without Superscript III as a control.

Luciferase assay

Twelve wells of a 96-well plate were coated with 0.1% gelatin. ES cells were plated at a concentration of 2×10^4 in 6 of these wells and another 6 with ES-Luc cells (2 at 1×10^4 , 2 at 2×10^4 , and 2 at 4×10^4). A luciferase assay was performed using a Glomax 96 microplate illuminator (Promega) following the manufacturers protocol including cell lysis for 2 minutes with Bright-Glo Reagent.

Wax embedding

Embryos or brains from various transgenic rtTA-OCT4 mice were dissected and placed in 4% PFA for 24 hours at 4°C. The tissue was then serially dehydrated by changing the solution to 70% IMS for 24 hours, 80% IMS for 1 hour, 90% IMS for 1 hour, 95% IMS for 1 hour, and finally 100% EtOH for 1 hour. This solution was replaced with xylene for 10-30 minutes until the tissue became translucent. The xylene was removed and the tissue was transferred to hot wax for 1 hour. This wax was replaced with fresh wax and left for a further hour. The wax was replaced for the final time and the mould was left to set at room temperature.

Tissue transplantations into immune-deficient mice

Teratoma formation assay

ES-Luc cells and control ES cells were diluted to a total of 5×10^6 cells in 100µl PBS, and 20µl of each injected into the kidney capsule of SCID mice at pre-clinical oncology (PCO, Queen's Medical Centre, Nottingham). The mice were terminated 3 weeks after injection and the tumours were processed. A similar anaesthetic procedure was used to the intracranial injections below.

ES-Luc cell transplant into mouse brains

Mice were anaesthetised using ketamine/metoprolol, and a small incision through the skin was made along the midline of the skull. The mouse was secured onto an electronic Stereotaxic frame using a nose clamp. A small burr-hole was drilled through the skull using a 0.7mm diameter surgical drill bit.

The specific location of injection varied depending on whether the site was midline or lateral. The bregma is the point where the cranial bone sutures meet and can be viewed from the external anterior skull. Therefore, the bregma was used as a reference point for midline coordinates (AP -1.6mm, ML 1mm, DV 5mm), or lateral coordinates (AP -1.6mm, ML 3mm, DV 1mm).

ES-Luc cells were diluted to either 100,000 or 5,000 cells in 5µl of PBS and were loaded into a sterile Hamilton syringe with a 26g needle. The needle was slowly inserted through the burr hole to various depths and the cell suspension was slowly injected over a period of 1 minute. The needle was left *in situ* for a further minute before being slowly withdrawn over a period of 2 minutes. The burr hole was plugged with bone wax and the skin sutured.

The mice were given analgesia (Rimadyl 4mg/kg) before recovery, with further doses administered daily as required.

Luminescence imaging

Mice were anaesthetised and images were captured using a Xenogen biophotonic Spectrum and IVIS100 Imaging Systems. The light was detected in several different planes of view, which allowed for the construction of a three-dimensional image. This work was carried out by the division of pre-clinical oncology (PCO) at QMC.

Dissection, sectioning, and staining of brains

In all cases of Schedule 1, mice were terminated by cervical dislocation. The brain was dissected and placed into a fixative solution – 4% PFA.

Mice brains injected with ES-Luc cells were stored in fixative and processed (wax embedded and sectioned) by the Translational Research & Biobank in QMC. Haematoxylin and eosin staining was performed on at least one section from every processed brain.

In situ hybridisation

RNA probe synthesis

1µg of linearised DNA was added to transcription buffer (1x) (Promega), DTT (6mM) (Promega), rATP (6mM) (Promega), rGTP (6mM) (Promega), rCTP (6mM) (Promega), rUTP (6mM) (Promega), DIG-UTP (6mM) (Roche), RNasin (40U) (Promega), RNA polymerase (20U of either T7, or T3) (Promega). This mixture was left for 6 hours at 37°C. The probe solution was cleaned using the standard protocol for Illustra MicroSpin G-50 Columns (GE healthcare).

In situ hybridisation

N.B. PBST is PBS with 0.1% Tween 20 (Sigma); Hybridisation buffer is 50% formamide (Fisher), 5x SSC (pH4.5 with citric acid), 50µg/mL yeast tRNA (Roche), 1% SDS, and 50µg/mL heparin (Sigma); 20x SSC is 0.3M NaCl and 0.3M sodium citrate; 10x TBS is 135mM NaCl and 250mM Tris-HCl; 1x TBST is 10x TBST diluted 1 in 10 and 0.1% Tween-20; Alkaline phosphatase buffer is 100mM NaCl, 50mM MgCl₂, 100mM Tris-HCl pH9.5, 1% Tween-20, and 2mM levamisole (Sigma).

Wax-embedded embryos or brains were sectioned using a sectioning block (Anglia Scientific) set to 8µM, and attached to Superfrost Plus charged slides (Fisher). Sections were placed in histolene twice for 10 minutes. Histolene was replaced with 100% methanol for 1 minute, 75% methanol/25% PBST for 1 minute, 50% methanol/50% PBST for 1 minute, 25% methanol/75% PBST for 1

minute, and 100% PBST for 5 minutes. Proteinase K (10µg/ml) (Roche) at 37°C was used to overlay the slides for 15 minutes at room temperature. Slides were washed with PBST three times for 3 minutes each, and then immersed in ice-cold 4% paraformaldehyde in PBS for 20 minutes. Slides were washed three times for 5 minutes each. Approximately 200ng was added to hybridisation mix pre-warmed to 70°C. The mixture was overlaid on the slides and covered with Hybri-Slips (Sigma) then incubated in a sealed container at 70°C for 18 hours.

Slides were submerged in 50% formamide, 5xSSC, 1% SDS for 30 minutes at 65°C, and coverslips were removed. The solution was changed to 50% formamide, 2xSSC at 65°C for 30 minutes; this step was then repeated. The slides were washed three times for 5 minutes at room temperature. They were then placed in TBST with 10% FBS for 30 minutes. The solution was removed, and TBST with 1% FBS and 1/5,000 alkaline-phosphatase anti-DIG fragments (Roche) were added. The slides in this solution were left at 4°C for 18 hours.

The slides were washed three times for 20 minutes in TBST, then two times for 5 minutes in alkaline phosphatase buffer. The slides were incubated in alkaline phosphatase solution with 7.5mg/mL NBT (Roche) and 5mg/mL BCIP (Roche).

RNA Whole-mount in situ hybridisation

Whole E13.5 mouse embryos were fixed in 4% PFA in PBS for 24 hours. Embryos were sliced in half and dehydrated in methanol using a graded methanol/PBST series 25%, 50%, 75%, and 100% methanol for 5 minutes each. The methanol was replaced with fresh methanol and the sections were stored at -20°C.

Embryos were rehydrated in a 75%, 50%, 25% methanol/PBST series for 5 minutes each wash, followed by four 5 minute washes in PBST. PBST was replaced with 10µg/ml proteinase K in PBST for 20-60 minutes. The embryos were washed three times for 15 minutes in 2mg/ml glycine in PBST, then two times for 5 minutes in PBST. The embryos were post-fixed with 4% PFA for 20 minutes, before being washed 5 times for 5 minutes each in PBST. The samples were equilibrated slowly firstly for 10 minutes in 1:1 hybridisation solution/PBST,

then 10 minutes in hybridisation solution at 72°C. Incubation at 70°C in fresh hybridisation solution was left for 1 hour before being replaced with fresh hybridisation solution containing the RNA probe and left at 70°C for 24-72 hours.

The hybridisation solution containing the RNA probe can be stored at -20°C and re-used. The embryos were washed three times in 50% formamide, 5xSSC, 1% SDS at 65°C for 30 minutes each. This solution was replaced by 50% formamide, 2xSSC and again washed three times for 30 minutes each at 65°C. The embryos were left in 2% blocking reagent (Roche) in MABT for 60-90 minutes, before being left overnight at 4°C in 1/5000 anti-DIG AP antibody in MAB.

Post-antibody washes included eight in MAB for 15 minutes each, and three times in alkaline phosphatase buffer for 10 minutes each. The embryos were left to develop by adding 3.75mg/mL NBT (Roche) and 2.5mg/mL BCIP (Roche) in alkaline phosphatase solution. After 1-72hours of colour development, the embryos were washed with PBST and fixed in 4% PFA for 20 minutes before being washed again in PBST.

RNA probe binding specificity assay

Between 1-5ng of digested or undigested plasmid used to generate an RNA probe was baked onto a positively charged nylon membrane (Roche) for 2 hours at 80°C. Probe was diluted in 300ul of hybridisation buffer and rotated in a 1.5ml tube with the membrane. The membrane solution was changed to 2xSSC for 30 minutes at 65°C, then 0.1xSSC for 30 minutes at 65°C. The membrane was washed twice for 3 minutes in TBST at room temperature before being blocked with 10% serum in TBST for 30 minutes. The membrane was left at 4°C for 18 hours in 1 in 10,000 anti-dig fragments in TBST.

The membrane was washed in TBST three times for 10 minutes each. This was replaced by alkaline phosphatase buffer for 5 minutes before being incubated in alkaline phosphatase solution with 7.5mg/mL NBT (Roche) and 5mg/mL BCIP (Roche).

Name of gene	Primer 5'>3'	Size of product
Clathrin	TTT GTG CTT CTG GAG GAA AGA A GAC AGT GCC ATC ATG AAT CC	567bp
Nestin	CGC TGG AAC AGA GAT TGG AAG G GTC TCA GGG TAT TAG GGC AAG	257bp
Sox2	CCG CGA TTG TTG TGA TTA GT AGG GCT GGG AGA AAG AAG AG	94bp
Oct4	CTC GAA CCA CAT CCT TCT CT TAG GTG AGC CGT CTT TCC AC	856bp
Oct4-Nested	TGA TTG GCG ATG TGA GTG AT CAC GAG TGG AAA GCA ACT CA	470bp
Etv1	ATG GAT GGA TTT TAT GAC CAG TTA GTA CAC GTA TCC TTC GTT	1434BP
Col1a1 (Common)	CCC TCC ATG TGT GAC CAA GG	
Col1a1 (WT F)	GCA CAG CAT TGC GGA CAT GC	331bp
Col1a1 (Mut F)	GCA GAA GCG CGG CCG TCT GG	551bp
Rosa26 (Common)	AAA GTC GCT CTG AGT TGT TAT	
Rosa26 (WT R)	GGA GCG GGA GAA ATG GAT ATG	340bp
Rosa26 (Mut R)	GCG AAG AGT TTG TCC TCA ACC	650bp

Table 2.1. Primer sequences for mouse genes. Oct4-Nested amplifies part of the Oct4 coding sequence within the sequence that is amplified by Oct4 primers. All three genotyping primers are mixed together for either Col1a1 or Rosa26 amplification; common amplified either wild-type or mutant DNA. The larger amplified product indicates the presence of the transgene, while the smaller one lacks the transgene. A combination of a large band and a small band indicates heterogeneity. Primers were supplied by Fisher.

Name of enzyme	Restriction site sequence	Company
Apa1	GGGCC C	New England Biolabs
Xba1	T CTAGA	New England Biolabs
Xho1	C TCGAG	New England Biolabs
Not1	GC GGCCGC	New England Biolabs
BamH1	G GATCC	New England Biolabs
BglII	A GATCT	New England Biolabs

Table 2.2. Restriction enzymes used to digest plasmids. The restriction cutting site is labelled within the enzyme-specific sequence.

Antibody name	Raised in	Concentration	Mono- or polyclonal	Company	Code
MAP2	Chicken	1 in 250	Poly	Abcam	ab5392
GFAP	Mouse	1 in 250	Mono	Abcam	ab4648
NANOG	Rabbit	1 in 100	Poly	Abcam	ab21603
OCT4	Mouse	1 in 100	Mono	Santa cruz	sc5279 (C-10)
Anti-mouse 488	Chicken	1 in 500	Mono	Alexa	A-21200
Anti-rabbit 488	Goat	1 in 500	Mono	Alexa	A-11008
Anti-Chicken FITC IgY	Goat	1 in 500	Polyclonal	Abcam	ab46969

Table 2.3. Primary and secondary antibodies used in immunohistochemistry.

Chapter 3: A meta-analysis of the location and biology of GCTs in the brain

3.1 Introduction

GCTs are thought to arise from germ cells that migrate along the midline during embryogenesis. Contrary to this, we have proposed that GCTs that have arisen in the CNS had a neural or brain-cell progenitor instead of a germ-cell progenitor (see Chapter 1).

The generally accepted aetiology of CNS GCTs states that germ-cell progenitors migrate through the sagittal plane of the body, which is based on the observation that GCTs have been found at several locations that were considered midline. However, this does not necessarily mean that germ-cell progenitors were the cells of origin.

GCTs are a diverse group of tumours with large differences in gene expression and morphology. In order to limit the variables while studying this phenomenon, it is important to focus on only one of these tumours to begin with. Teratomas, one type of GCT, are easily formed using embryonic stem cells, which have been extensively studied and well characterised. The aetiology of the other GCT types is unknown, so the only known way to form a germinoma, for example, would be to use a cell line derived from a human tumour. For this reason, teratomas are an ideal candidate to study.

Teratomas are the most easily studied subtype of GCT because they are easily formed by several established methods, including embryonic stem-cell (ESC) transplantation. Teratomas do not require any activating mutations such as mutation of the oncogene MYC, and are easily identified by histopathology, as previously described. To understand GCTs as a group, teratomas can provide an initial insight into testing the current consensus of their aetiology i.e. Teilum's

theory of a germ-cell progenitor, compared to the proposed theory of a neural cell of origin.

Teratomas have been diagnosed during the prenatal period. Since they are well-formed by birth, we can infer that the cell of origin is also prenatal. In fact, since ultrasound has become more advanced, several papers have shown that teratomas can form as early as 11 or 13 weeks i.e. at the end of the first trimester [101, 102]. As stated in Chapter 1, the cell of origin for teratomas must therefore have existed between conception and the first trimester.

There are several questions to be answered: can teratomas/GCTs form in non-midline regions? Is there a growth advantage or disadvantage for the lateral regions? Are certain regions adverse to GCT survival? Or are GCTs that arise in certain regions detrimental to a child's survival?

These questions are each addressed over the next two chapters. This chapter discusses the observations of these tumours using a literature review to re-evaluate the locations that CNS teratomas can grow in, and why CNS GCTs are found mainly in the midline of the brain. The strategy includes a literature search for which GCT subtypes arise after resection, and which tumours can be mixed with GCT subtypes. The next chapter then uses these observations to test our hypothesis *in vivo* using ES cells to examine the potential for teratomas to form outside of the midline.

3.2 Results:

Teratomas can invade any region of the brain

The main strategy for this chapter used relevant literature to analyse the locations of intracranial teratomas. Several criteria were set before acquiring suitable papers, for example, only papers published 1990-2012 were used. Clinical cases that had an uncertain diagnosis or cases where teratomas were mixed with other subtypes were not included. Epignathus is a type of teratoma that develops in the mouth, so in order to simplify the study, epignathus were not included.

The majority of teratomas are known to occur in the perinatal range, and most germinomas occur in the teenage years. Since CNS GCTs are relatively rare, it is important to acknowledge that there may be a large amount of publication bias. Therefore, statistical analysis is not heavily relied on when analysing the regions where these tumours occur.

Data on a total of 96 CNS teratomas were collated from the literature and separated into two groups. These two groups were the ventral midline and non-midline locations (Table 3.1). Teratomas in the ventral midline group represent teratomas that occur in locations where GCTs have traditionally been associated i.e. the suprasellar region, the pineal region, and the basal ganglia. These data show that the majority of the teratomas analysed occurred in the midline (56 out of 96), mainly in the suprasellar and pineal regions, but 40 out of 96 occur in non-midline locations. Since there are only a limited number of CNS teratomas, it was inappropriate to test statistical significance of how frequent teratomas occur in the midline compared to the lateral hemispheres.

This study mainly focussed on teratomas that occur in the perinatal range and some in the teenage years. In addition, there were several studies that found teratomas in adulthood and these could be found in both midline and lateral locations [103, 104]. These case reports have clearly shown that teratomas have the ability to grow in all regions of the brain.

If the brain is separated into four lobes (frontal, parietal, occipital, and temporal) teratomas can be found contained in each one of these areas (Figure 3.1). Indeed, teratomas have even been found to arise in the cerebellum [103-105]. As expected there is an abundance of teratomas found in the classic locations for GCTs in the brain, with particularly frequency of occurrence in the pineal region (40 out of 96) and suprasellar (15 out of 96).

Location of tumour (Midline)	Age of patient	Survival	Treatment	Reference
Pineal region	9	Yes	TR	[106]
Pineal region	9	Yes	PR + C	[107]
Pineal region	27	Yes	TR	[108]
Pineal region	16	No	TR + R + C	[14]
Pineal region	9	Yes	TR + R	[109]
Pineal	14	Yes	TR + R	[110]
Pineal	6	Yes	TR	[110]
Pineal	Neo	Yes	TR	[110]
Pineal	Neo	No	ST	[111]
Pineal	Neo	No	ST	[112]
Pineal	2	Yes	TR + R + C	[50]
Pineal	5	Yes	PR + R	[113]
Pineal	16	Yes	PR + R	[113]
Pineal	12	Yes	PR + R	[113]
Pineal	18	Yes	PR	[113]
8x pineal				[114]
17x pineal				[115]
Suprasellar	12	No	TR	[110]
Suprasellar	Neo	No	ST	[116]
Suprasellar	6	Yes	PR	[117]
Sella turcica		No	ST	[118]
Suprasellar	Neo	No	N	[119]
Suprasellar	Neo	No	N	[120]
3x suprasellar				[114]
6x suprasellar				[115]
1x Basal ganglia				[114]

Table 3.1 A – Locations of CNS teratomas in the ventral midline

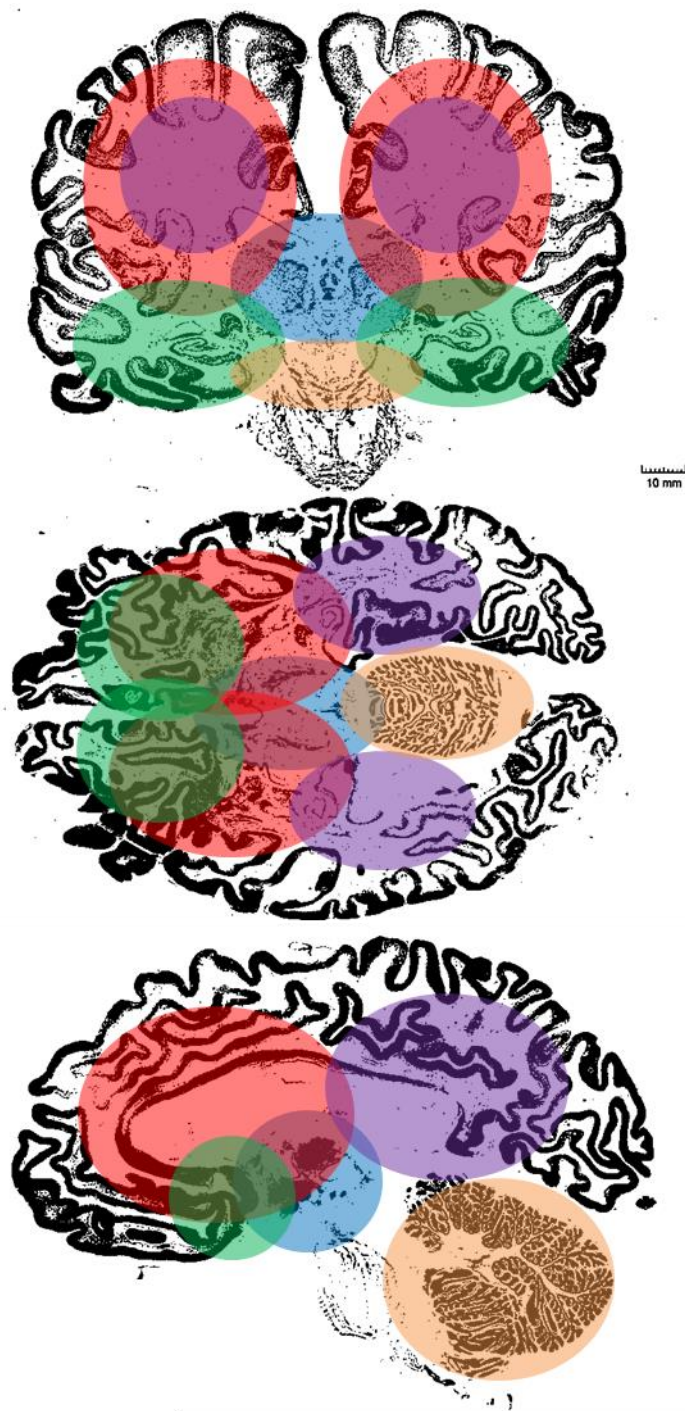
Neo = neonate, only a few days; 2nd T = second trimester; TR = total resection; PR = partial resection; NA = none; ST = stillborn or terminated; C – chemotherapy; R = radiotherapy.

Location of tumour (Non-midline)	Age of patient	Survival	Treatment	Reference
Right frontal lobe	2nd T	No	ST	[102]
Midline of the posterior fossa	6	Yes	TR	[121]
Left supratentorial region	Neo	No	N	[122]
Mid cranial fossa/ right frontal lobe	Neo	Yes	TR	[123]
Left anterior and middle cranial fossa	Neo	Yes	PR	[107]
Right lateral ventricle	Neo	No	TR	[124]
Cavernous sinus, i.e. Left frontal lobe	>1	Yes	TR	[125]
Left ventricle	>1	Yes	TR	[126]
Left cerebellar hemisphere	>1		TR	[127]
Third ventricle	1	Yes	TR	[128]
Right lateral ventricle	8	Yes	TR	[129]
Bi-Lateral ventricle and third ventricle	>1	Yes	TR	[129]
Both lateral and 3rd ventricle	5	Yes	TR	[130]
Right frontal lobe	10	Yes	TR	[130]
Left cerebral hemisphere	Neo	No	N	[131]
Choroid plexus of lateral ventricle	Neo	No	N	[132]
Left frontal lobe	Neo	No	PR	[133]
Pineal into right lateral ventricle	Neo	No	ST	[134]
Posterior fossa				[134]
Right temporal area (sylvian)				[134]
Lateral and 4th ventricle				[134]
Posterior regions				[134]
Cavernous sinus.				[134]
Midline and left lateral hemisphere	Neo	Yes	TR	[134]
Skull base	Neo	No	N	[135]
Left lateral ventricle	Neo	No	N	[136]
Centrally located and third ventricle	Neo	No	N	[137]
Temporal fossa	Neo	Yes		[138]
Anterior cranial fossa	Neo	No	ST	[139]
Right lateral ventricle	Neo	No	N	[140]
4th ventricle				[115]
Right temporal area (sylvian)				[115]
Posterior fossa				[115]
Cavernous sinus				[115]

Table 3.1 B – Locations of CNS teratomas in non-midline regions

Neo = neonate, only a few days; 2nd T = second trimester; TR = total resection; PR = partial resection; NA = none; ST = stillborn or terminated; C – chemotherapy; R = radiotherapy.

Table 3.1 A and B. The approximate location of the tumour reported in each paper is listed together with the age of the patient, the type of treatment, and whether the patient survived while part of each study. Locations are arranged by traditional ventral midline structures in the table A, followed by non-midline locations in table B. Sections left empty are due to unknown or ambiguous data.



Cerebellum [Coulibaly, 2012][141], Pineal region [Lee, 2009][115], Lateral ventricle [Smirniotopoulos, 1992][142], Right suprasellar [Kochi, 2003][14], Cavernous sinus [Pikus, 1995][125]

Figure 3.1 – Overlapping regions of where teratomas can grow in the central nervous system. Three views of an adult human brain (coronal, horizontal, and sagittal) with approximate teratoma formation transposed onto them. Importantly, a single reference was assumed to be able to form on either hemisphere, so each colour has two circles representing possible locations for teratomas. Brain scans modified from <http://brainmuseum.org>: Coronal Level 2240, Horizontal Level 1640, Sagittal Level 0212

Evidence for a cell of origin in the lateral regions of the brain

Patients were often diagnosed after they presented with significant symptoms, by which time the CNS teratomas in this study were at least several centimetres in diameter. Therefore the exact location of the cell of origin is difficult to determine. In some circumstances, radiological images have appeared to suggest that the cell of origin may not be midline; for example, Canan *et al.* (2000) published a clinical case of a neonate with a lateral teratoma exclusively in the left side of the brain [133]. However, other cases show ambiguity such as the case report by Selcuki *et al.* (1998). Selcuki reported a teratoma in the lateral ventricle but when examining the images it is unclear whether the origin was midline [129].

CNS GCTs can recur as almost any of the other GCT subtypes

GCTs are classified as a single group of tumours unified by the hypothesis that they have the same cell of origin, a germ cell progenitor. But what is the relationship between each of these distinct subgroups? Can one be transformed into another?

In order to investigate this, the literature was analysed for the resection of a GCT (embryonal carcinoma, teratoma, yolk sac tumour, or germinoma) followed by recurrence of a different one of these four subtypes. The search was unbiased in the first instance: only papers where the subtype that recurred was different to the original tumour after surgical resection were included; the patient could be any age; and only a single subtype of tumour could be present before and after resection. After this unbiased search, specific combinations of recurrence after surgery were examined.

Embryonal carcinomas were not separated from teratomas since they were assumed to be the undifferentiated version of a teratoma. Studies have shown

that it is quite common to find a pure, differentiated teratoma mixed with an undifferentiated embryonal carcinoma i.e. a teratocarcinoma.

Table 3.2 is an amalgamation of the included literature showing that it is possible for any of the GCT subtypes to recur after resection of one of the other GCT subtypes in the brain, illustrated in Figure 3.2. The only tumour that this situation was not found was the resection of a yolk-sac tumour recurring as a germinoma. Even with a search for this combination there were no cases in the literature.

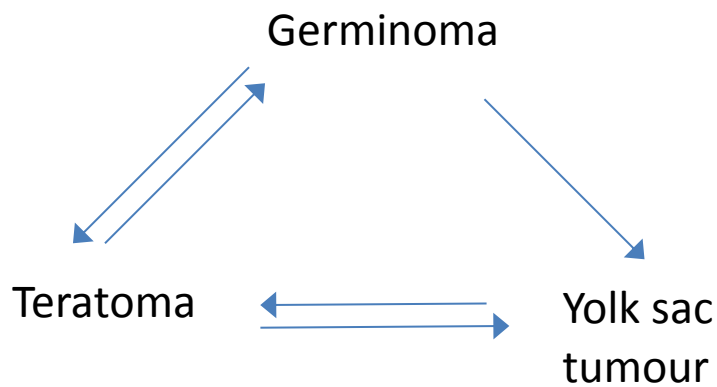


Figure 3.2 - The relationship between the different subtypes of germ cell tumour. When one of the subtypes is resected it is possible for any of the other subtypes to recur.

Original tumour	Location	Recurrent tumour	Location	Reference
Teratoma	Pineal	Germinoma	Basal ganglia	[143]
Teratoma	Pineal	Germinoma	Suprasellar	[144]
Teratoma	Pineal	Germinoma	Pineal	[145]
Epidermoid cyst/teratoma	Pineal	Germinoma	Pineal	[146]
Teratoma	Sellar	Germinoma	Third ventricle	[147]
Teratoma	Sacrococcygeal	Yolk sac tumour	Sacrococcygeal	[148]
Germinoma	Corpus callosum	Teratoma	Corpus callosum	[149]
Germinoma	Suprasellar and pineal	Yolk sac tumour	Mediastinum	[150]
Yolk sac tumour	Diencephalon/suprasellar	Teratoma	Suprasellar	[151]

Table 3.2 – Resection and recurrence of GCTs. Each row shows a report of a germ cell tumour recurring as a different subtype of germ cell tumour. The original tumour was resected and in some cases treated with chemotherapy before the recurrence of a different tumour. Teratomas, yolk sac tumours, embryonal carcinomas, and germinomas are all found to recur as each of the subtypes of GCTs. Choriocarcinoma was not included in this search, and to-date there are no papers showing the resection of a yolk sac tumour recurring as a germinoma.

CNS GCTs can be mixed with other GCT or non-GCT subtypes

CNS GCTs are frequently diagnosed with multiple subtypes of GCT present. These mixed GCT subtypes may seem counter-intuitive because the GCT subtypes differ greatly in their behaviour and gene expression. The current explanation for the presence of different GCT subtypes is that the proposed cell of origin for GCTs can give rise to all the different subtypes i.e. a germ-cell progenitor. The topic of GCTs mixed with a different type of cancer raises two questions: is there a pattern by which GCT subtypes are mixed with other GCT subtypes; and are GCT subtypes mixed with non-GCT cancers?

The method used to answer these questions was a review of published literature on GCT subtypes mixed with either another GCT subtype, or a non-GCT cancer. The initial search was initially limited to the brain and testis in order to determine which combinations of GCT subtype could be mixed. This was extended to include a case of all subtypes present in a tumour in the mediastinum and nearly all subtypes present in a single tumour in the ovary - these searches were specifically for occurrences of all subtypes of GCT present in a single tumour. Here, examples of each GCT subtype being mixed with each of the other subtypes of GCT were found (Table 3.3).

When examining a GCT subtype mixed with a non-GCT cancer, the search was not limited to a specific location in the body or the type of cancer the GCT subtype was mixed with. Table 3.4 shows that a range of non-GCT types have been found mixed with GCTs. A frequent observation was that GCTs contained a sarcomatous component. The most relevant observation is a choriocarcinoma and yolk sac tumour mixed with an astrocytoma and glioblastoma (Table 3.4). In fact, this case study reported that the mixed GCT was partially removed and irradiated before astrocytomas and glioblastomas arose. This subject is examined in more detail in the discussion.

Location	Teratoma	Embryonal Carcinoma	Germinoma/ seminoma	Yolk sac tumour	Chorio-carcinoma	Reference
Mediastinum	X	X	X	X	X	[152]
Ovary	X		X	X	X	[153]
Testis	X	X				[154]
Testis	X		X			[154]
Testis	X			X		[154]
Testis	X				X	[154]
Testis		X	X			[154]
Testis		X		X		[154]
Testis		X			X	[154]
Testis			X	X		[154]
Testis			X		X	[154]
Testis				X	X	[154]
Brain	X	X	X	X		[155]
Brain	X	X	X			[155]
Brain	X	X		X		[155]
Brain	X	X		X		[105]
Brain	X	X		X		[156]
Brain		X	X	X		[156]
Brain	X		X	X		[157]
Brain	X		X			[156]
Brain	X		X			[158]
Brain	X		X			[159]
Brain	X		X			[160]
Brain			X	X		[161]
Brain			X	X		[162]

Table 3.3 – Germ cell tumour subtypes mixed with other GCT subtypes. Each row constitutes a single tumour and whether it contained teratomas, embryonal carcinoma, germinoma/seminoma, yolk sac tumour, or choriocarcinoma. Both teratomas and embryonal carcinoma were identified as positive when the histological report indicated teratocarcinoma. Choriocarcinoma was not found in the brain but was found in the mediastinum. Ovary and mediastinum are included to illustrate the occurrence of mixed subtypes at non-testicular and non-brain locations.

Region of GCT	Primary GCT	Tumour mixed with GCTs	Reference
Brain	C + Y	astrocytoma or glioblastoma	[163]
Cerebellum	T + C + GS	hemangioblastoma	[164]
Para-aortic lymph node	Mixed	epithelioid trophoblastic tumour	[165]
Thyroid	T	Primitive neuroectodermal tumour	[166]
Mediastinum	G + T	Ganglioneuroma	[167]
Mediastinum	T + E	neuroblastoma	[168]
Mediastinum	T	angiosarcoma	[169]
Mediastinum	GS	angiosarcoma	[169]
Mediastinum	Y	angiosarcoma	[169]
Mediastinum	E	angiosarcoma	[169]
Mediastinum	C	angiosarcoma	[169]
Lung	T + Y	blastoma	[170]
Retroperitoneal	T	Papillary renal cell-like carcinoma	[171]
Liver	Y + T	Sarcoma	[172]
Colon	Y + C	Adenocarcinoma	[173]
Sacrum	T	Oligodendroglioma	[174]
Sacrum	T	Anaplastic ependymoma	[175]
Testis	T + Y	rhabdomyosarcoma	[176]
Testis	GS + T + Y	angiosarcoma in mediastinum	[177]
Testis	E + T + Y	sarcoma	[178]
Testis	Mixed	Neuroblastoma	[179]
Testis	T	nephroblastoma and rhabdomyosarcoma	[180]
Testis	T + E + GS	Meningioma	[181]
Ovary	T + Y	Rhabdomyosarcoma	[182]

Key: T - Teratoma, E - Embryonal carcinoma, G/S - Germinoma/seminoma, Y- Yolk sac tumour, C – Choriocarcinoma

Table 3.4 – Germ cell tumour subtypes mixed with non-GCTs. Each row highlights a paper showing the region and type of germ cell tumour mixed with a non-germ cell tumour type. The studies are ordered approximately by location beginning with the brain and ending at the sacrum for extra-gonadal GCTs, and gonadal GCTs at the bottom of the table.

3.3 Discussion

This chapter examined where GCTs can arise in the CNS, and the types of cancer that GCTs can be mixed with. There were two questions that this chapter aimed to address: are teratomas confined to the midline of the brain; and what is the relationship between the GCT subtypes and either GCT or non-GCT tumour subtypes.

There were several interesting treatment features that need to be discussed from the data; for example, why resection and therapy of one subtype of GCT could result in the formation of any of the other subtypes of GCT. The lines of evidence are used to argue that CNS GCTs originate from a brain-cell progenitor. Furthermore, we examine why teratomas seem able to arise anywhere in the CNS but are rarely diagnosed in lateral locations.

All GCTs in the CNS can form from a common cell of origin – resection and recurrence

There are several questions about the relationship between GCT masses and either their cell of origin or other subtypes of GCT. In an attempt to address these, the literature was assessed for examples of resection of a CNS GCT followed by the recurrence of a different GCT. This strategy examines which progenitors are present after the bulk of the tumour has been removed.

There were several assumptions and alternatives for this strategy; for example, the resected tumour and the recurred tumour were both assumed to arise from the same progenitor. Alternatively, chemotherapy or radiotherapy may have altered the original tumour.

After the resection of a CNS GCT subtype, any other GCT can recur; for example, the resection of a germinoma recurring as a teratoma. This suggests that when the tumour mass was removed, a progenitor cell remained and formed a different type of GCT. The original tumour was assumed to arise from

similar progenitors. This can be assumed because it is unlikely that several different progenitor types would be present in the same location at the same time. Resection and recurrence of a different subtype suggests that all GCTs have a common cell of origin.

It is important to acknowledge that this has not given us an insight into whether the cell of origin is from the brain or from germ cell progenitors. Proponents of PGCs forming CNS tumours would have perhaps suggested that one or more PGCs mis-migrated to a location where they were not eradicated and had the potential to grow; for example in the pineal region. This cell may have proliferated without differentiating, leaving some PGC progenitors to proliferate and differentiate when the tumour is resected. Although this data could not be used to distinguish between the germ-cell hypothesis and the brain-cell hypothesis, it can be used to understand the relationship between each of the subtypes of GCT in the CNS.

There has been some ambiguity in categorising the different subtypes of GCT. Each subtype has significantly different morphology, gene expression, and methylation status to the others, which has prompted the subcategories of germinomatous/seminomatous and non-germinomatous tumours, with teratomas/teratocarcinomas sometimes being classed as a separate entity [183]. A teratoma can recur as either a yolk sac tumour or a germinoma, which suggests the same progenitors that can form a teratoma can form a germinoma. This observation shows that teratomas are a tumour type that is representative of all GCT subtypes, since the progenitors that can form a teratoma are also capable of forming any other type of GCT. The relationship of teratomas to the other subtypes is important to bear in mind because this thesis uses teratoma formation as a surrogate assay for the potential to form a GCT.

There were no occurrences of germinomas arising after the resection of a yolk sac tumour. One possible explanation for this is that YSTs have a more aggressive chemotherapy and radiotherapy regime, so any progenitors to germinomas (which are very chemotherapy- and radiotherapy-sensitive) would

be eradicated. The lack of germinomas occurring after yolk sac tumours does not diminish the argument that each subtype is linked by their common aetiology because all other combinations of resection and recurrence of subtypes have been documented; for example, germinoma occurring after a teratoma, or teratoma after a yolk sac tumour.

All GCTs in the CNS have a common cell of origin – mixed GCTs

The types of tumour that were mixed in CNS GCTs were analysed in order to reinforce the evidence that all GCTs had a common cell of origin. In short, each subtype of GCT could be found mixed with each of the other subtypes of GCT. This suggests that all subtypes of GCT can arise from a single cell or group of progenitors. Whether these subpopulations form a hierarchy in which they represent increased differentiation, or whether they can all arise from a single population is debatable (Figure 3.3).

It would seem more likely that each subtype can arise from a common progenitor because it is possible to find each subtype with only one other subtype; for example, a mixed tumour of teratoma and germinoma does not always contain yolk sac tumour. Further, there may be a case for transforming one type of GCT into another; however this will be the discussion of another chapter. This heterogeneity and clonal evolution occurs in other types of cancers, even brain tumours.

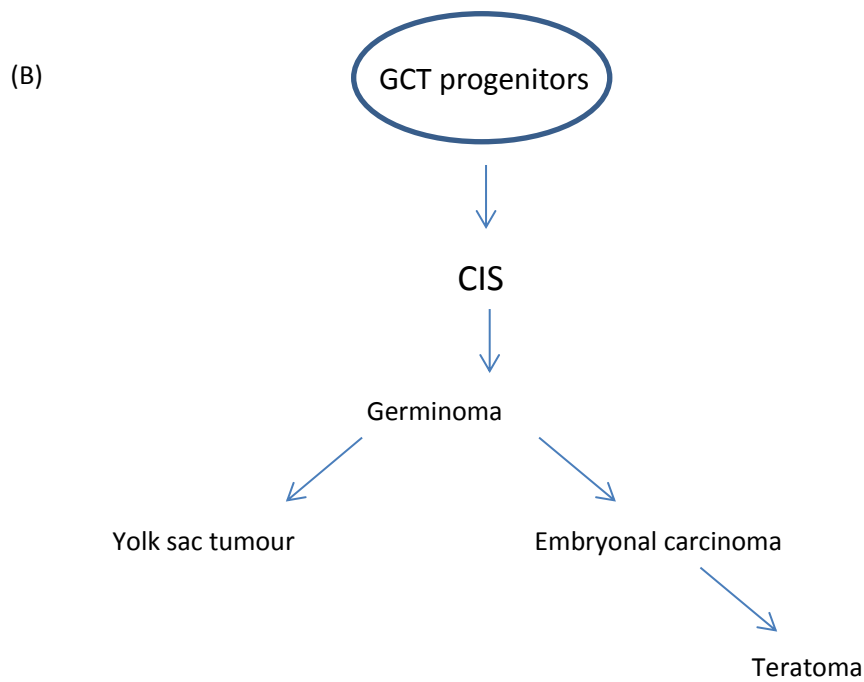
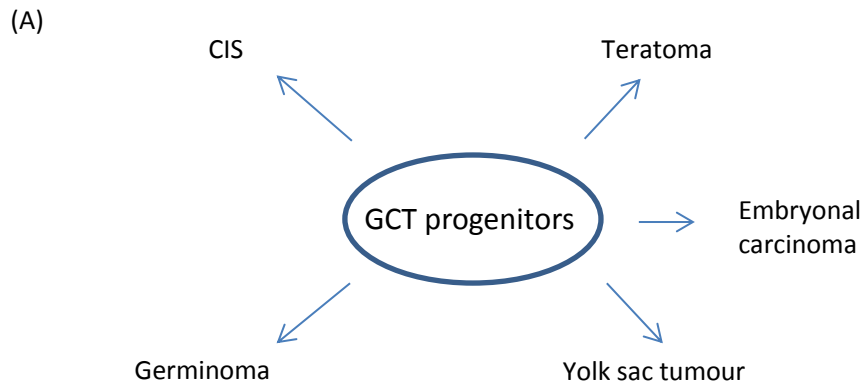


Figure 3.3 - A summary of two different hypotheses of how germ cell tumour progenitors could form a GCT after it has been resected. Either (A) all subtypes of GCT can arise from the same progenitor and it is the environment that dictates the subtype or (B) there is a hierarchy of formation based on how differentiated the subtype is.

Regardless of whether CNS GCTs are derived from PGCs or from brain cells these data provide evidence that all CNS GCTs can arise from the same cell of origin. The germ-cell hypothesis states that mismigrated cells have become trapped in distinct locations. However, patients are rarely diagnosed with GCTs in several locations throughout the body. Metachronous germinomas in the pineal and suprasellar regions are an exception. However, no patients have been documented with several GCTs in different locations at the same time; for example, in the gonads, retroperitoneum, sacrococcygeal, mediastinum, and brain. If there were patients with GCTs in several of these locations, it would be strong evidence of the route that PGCs have migrated and eventually formed GCTs. Therefore, proponents of a PGC of origin for extragonadal GCTs must concede that if their hypothesis is correct, only a few PGCs capable of forming GCTs reach extragonadal locations.

In summary, if the current germ-cell hypothesis is correct, only a few cells capable of forming a GCT would reach the CNS. This implies that the different subtypes can arise from a single cell instead of different progenitors forming several different subtypes of GCT. This unifies all GCT subtypes as having a common cell of origin regardless of the region that cell originated from. The arguments for a PGC or a neural-cell of origin have been examined in Chapter 1, and will be tested throughout this thesis.

Why GCTs are sometimes mixed with non-GCTs

The analyses in this chapter have revealed some unexpected findings. Brain tumours that have a known aetiology from endogenous brain cells have been found mixed with GCTs in non-CNS locations; for example a meningioma in the testis. While this may seem counter-intuitive, it is perhaps evidence of the pluripotent nature of these tumours, rather than aetiology linked to a specific location in the body. To clarify, it seems unlikely that two rare cancers would form independently in the same locations – it seems more intuitive that a single dysregulated mechanism has initiated both.

Many brain tumours require stem-cell features and mutations in order to cause oncogenesis; for example, mutations in the Wnt or sonic-hedgehog pathways. Both the brain-cell and germ-cell hypotheses have predicted that the cell of origin for all GCTs is pluripotent or has pluripotent features. Therefore, given the correct mutations, any type of tumour/cancer could form from the pluripotent progenitors that form GCTs. In fact, a study by Swartling showed that a mutation in MYCN gave rise to different tumours when engineered in different locations [184]. This suggests that the environment plays an important role in the type of tumour that forms from a progenitor. This may explain the strange combinations of GCTs with a different type of cancer, such as a GCT mixed with a meningioma.

Examples of CNS GCTs mixed with non-GCTs such as glioblastomas were very limited. Makidono *et al.* 2009 presented an interesting case of a child with a metachronous yolk-sac tumour and choriocarcinoma in the suprasellar and pineal regions [163]. These tumours are rare when they occur on their own, and metachronous GCTs are even more infrequent. This occurrence of two rare tumours suggests an underlying mechanism for their formation; perhaps disruption to methylation in the ventral midline. More strikingly, these two tumours recurred as two different types of brain tumour: astrocytoma and glioblastoma. Again, this observation suggests that there is an underlying mechanism for cancer formation in the ventral midline.

Mixed tumours in this study could not be used to definitively answer whether the cell of origin of CNS GCTs was a germ-cell or brain-cell. However, I propose that these mixed GCTs and non-GCTs have arisen from similar molecular defects.

Molecular characterisation of GCTs mixed with somatic-type malignancy showed that teratomas and non-GCTs often shared gain in i(12p) or 12p chromosomes [185]. The gain of 12p or i(12p) may therefore be an oncogenic mechanism that is capable of causing a range of tumour types to form, including

GCTs. Alternatively, disruption to a mechanism such as methylation may allow initiation of various types of cancer.

The hypothesis for gain of i(12p)/12p is not tested in this thesis but there are several experiments that could be used to test this; for example, manipulation of the i(12p)/12p copy number in embryonic stem cells and *in vivo* transplantation studies. Briefly, since ES cells appear to gain i(12p) after long term passage, it should be possible to select a cell line of ES cells that contains this chromosomal gain. This i(12p) cell line could then be used to differentiate any lineage since it is pluripotent. Additional aberrations such as a mutated form of Kit would allow this cell line to be used to test the ability of these cells to form a germinoma.

So why have GCTs been frequently reported as midline tumours? One possibility is that teratomas that have occurred in lateral regions are more likely to result in termination of the pregnancy. These tumours would therefore have been less likely to appear in the literature. Testing this hypothesis would be very difficult since these tumours are incredibly rare, and relies on assaying the tumours at a very early stage of development. This topic will be discussed further in Chapter 3.

3.4 Conclusion:

This chapter has outlined the argument for teratomas as representative of all GCT subtypes when analysing the cell of origin. Each GCT subtype seems to have the same cell of origin despite their distinct expression profiles and morphological differences. There appeared to be no restriction in teratoma growth regardless of location in the brain. This suggests that there was an event in the cells of the midline that preferentially allowed them to form, rather than an environment in the lateral regions that protects against GCT formation. However, it was difficult to determine the exact location for the cell of origin of these teratomas. Therefore, the ability of pluripotent cells to develop into GCTs in different regions of the brain is examined in the next chapter.

This meta-analysis set out to test whether non-midline regions can support growth of teratomas. Several non-midline regions of the brain allowed teratoma growth, so the next chapter tests whether teratomas can be initiated from a low number of progenitor cells.

Chapter 4: An *in vivo* study of teratoma formation in the brain

4.1 Introduction

Our hypothesis that GCTs in the brain have a neural cell of origin raises a number of questions. In particular, if the progenitors of CNS GCTs are neural, then the higher prevalence of GCTs in the midline regions must be explained. If neural stem cells are the cell of origin for CNS GCTs, it seems surprising that GCTs are rarely associated with the lateral ventricles where NSCs are most abundant. I propose two models to explain this bias in location.

It may be that there are specific features of the cells of the ventral midline that makes them intrinsically more susceptible to GCT formation. In the ventral midline, where GCTs are most often found, several genes are differentially expressed compared with the lateral hemispheres, of which *NR-CAM* and *VEMA* are two examples [186, 187]. More importantly, the imprinted genes *H19* and *IGF2* are differentially expressed in the ventral midline. Unlike other brain regions, where they are robustly imprinted and so expressed from only one allele, these genes are biallelically expressed in cells of the ventral midline [188]. Not only does this mean that levels of *IGF2* transcript are higher, but it also reveals a difference in the methylation of the genome in these cells, a feature also seen in the analysis of the imprinted gene, *Snrpn* [57]. Given our hypothesis that activation of Oct4 by demethylation could be a key event in the aetiology of these tumours, this lower level of genomic methylation in the ventral midline provides both support for this model and a possible reason why the tumours occur more often in this location.

An alternative explanation for the midline locations of GCTs is that the unique microenvironment of the ventral midline allows or promotes GCT formation. In particular, the ventral midline of the brain is a region of high hormonal activity such that the local concentration of factors such as IGFs and

GnRH could play a significant role in both the transformation of cells in this region and/or the type of tumour that a transformed cell becomes. A mutational event in a neural stem cell (NSC) that initiates the formation of a more typical type of brain tumour, such as glioma or ependymoma, might result in a GCT in the ventral midline because of local cues that promote pluripotency in those same cells. Indeed, a recent study showed that over-expression of oncogenic *N-MYC* protein in neural stem cells resulted in dramatically different tumour types depending on the brain region from which those cells were isolated [184].

Embryonic stem (ES) cells consistently develop into teratomas, a type of GCT, when transplanted into mice. Therefore, ES cell transplantation can be utilised as an assay for how susceptible an area in the brain is to forming a teratoma. This tests the hypothesis that the different regions of the brain permit or restrict teratoma formation due to their different microenvironments. In Chapter 3, teratomas were shown to be able to grow anywhere in the human brain, but most often occur in the midline. However, these observations cannot determine whether the different locations of the brain vary in their permissiveness for teratoma formation, and this is addressed in this chapter.

In this chapter I set out to assess our hypothesis by testing whether teratoma formation or growth is influenced by different regions of the brain.

4.2 Aims

The main objective of the experiments detailed in this chapter was to test for the differences in the ability of pluripotent cells to form teratomas in two regions of the brain: the ventral midline and the lateral hemispheres. The pluripotent cells used were mouse embryonic stem (ES) cells.

The first aim was to establish a heterogeneous ES cell population that stably expressed a protein that could be detected when these cells were grown as teratomas *in vivo*. In this case, luciferase was used. Furthermore, validation was required to show that the selection of a luciferase-expressing sub-clone of these ES cells had not diminished their ability to form teratomas or change vital pluripotent gene expression.

Luciferase activity was chosen because it was integral to imaging the location of cells when transplanted into mice. There were both ethical and practical reasons for this. Ethically, the tumour growth needed to be monitored in order to terminate the mice if the tumour grew beyond a certain size. Tumours in the brain require scans to visualise them because they cannot be palpated. Therefore, we did not know how fast the cells would grow into a tumour, and luciferase was an effective way of tracking growth. From a practical point of view, luminescence shows the location of the tumour, which was important in confirming that the tumour formed at the predicted injection site.

The second aim involved optimising the stereotaxic injection of these ES cells into discrete locations of the brain (a technique also utilised in later chapters).

The third and final aim was to control the cell number implanted in order to directly compare the tumour volume over time using luminescence as a measure *in vivo*.

4.3. Results:

Establishing an embryonic stem cell population that stably expresses luciferase

The luciferase plasmid, pORF-LucSh, (Invivogen) (Figure 4.1 A) confers resistance to the antibiotic Zeocin. At high concentrations, antibiotics can also kill cells that have some resistance; therefore, the first experiment was to test the toxicity of Zeocin to untransfected cells. Various concentrations of Zeocin were used on untransfected ES cells over several days (Figure 4.1 B) to establish the concentration required to eliminate all cells that did not express Zeocin stably by 4 days.

Cells cultured in concentrations higher than 10µg/ml proliferated very slowly over two or four days. Therefore, the data informed the decision to use 10µg/ml of Zeocin for subsequent experiments.

ES cells were transfected and selected for stable expression of the luciferase plasmid using 10µg/ml of Zeocin determined from the toxicity data (Figure 4.1 B). Figure 4.1 C details a schematic for this process of transfection, selection, and repopulation. Embryonic stem (ES) cells expressing luciferase are designated 'ES-Luc cells'.

The final population termed ES-Luc cells were only selected using Zeocin i.e. we did not derive a clonal line. A heterogeneous population of ES-Luc cells ensured that the majority of the cells would express luciferase and the luminescence could be used directly to estimate tumour size. In a cloned cell-line the luciferase gene could have been inserted into a locus that was silenced upon tumour formation or putative cell differentiation.

The heterogeneous population of ES-Luc cells was stably selected i.e. ES-Luc cells could proliferate in medium containing Zeocin at a rate similar to ES cells that were untransfected and growing in normal medium.

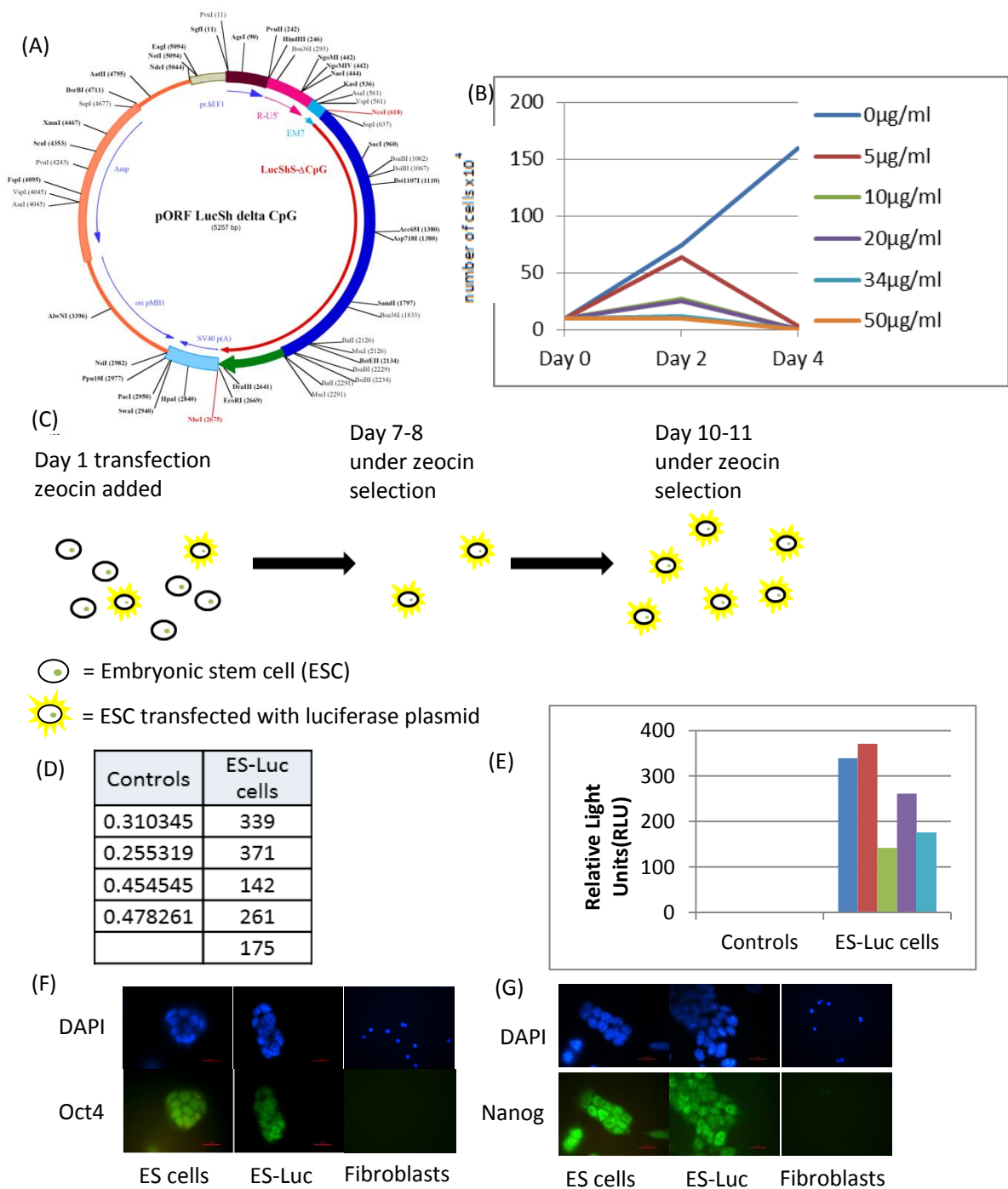


Figure 4.1. Optimisation and stable transfection of a heterogeneous ES cell population with a luciferase plasmid (A) The pORF LucSh delta CpG plasmid used to transfect embryonic stem cells. This plasmid contains no CpG sites in order to prevent methylation. EM7 confers resistance to the antibiotic Zeocin. (B) Ability of embryonic stem cells to survive in different concentrations of Zeocin. Each colour represents a different concentration over a 4-day period. (C) A schematic of the stable-transfection process, which took approximately 10 days. The protocol included transfection of the luciferase plasmid, selection of ES cells that had integrated the plasmid into their genome under Zeocin selection, and culturing of a heterogeneous population. (D) Ratios between firefly and *renilla* luminescence. This ratio internally controls the number of cells with the amount of luminescence for ES-Luc cells or untransfected ES cells. (E) Bar chart representing the relative light units for transfected embryonic stem cells compared to controls. (F-G) Immunofluorescence on untransfected ES cells (as a positive control), ES-Luc cells, and fibroblasts for a negative control. Green fluorescence is OCT4 in (F) and NANOG in (G). DAPI is blue staining in both.

Detection of luminescence in ES-Luc cells

The luminescence from ES-Luc cells was detected using a Glomax 96 microplate illuminator. The cells were cultured in wells of a 96-well plate, Dual-Glo Luciferase Substrate was added, and the Glomax machine assayed each well for luminescence. The addition of Dual-Glo Stop & Glo allowed for the detection of *Renilla* in order to form a normalised ratio of luminescence. One of the limitations of the Glomax was the detection of low-level luminescence in an empty well when adjacent to a well that contained luminescent cells. Therefore, when control- or ES-Luc-cells were placed into a given well in the 96-well plate, adjacent wells surrounding the tested well were left empty.

Five wells of the same heterogeneous ES-Luc population and 4 wells of untransfected ES cells were plated into the 96-well plate. Each well was plated to contain approximately the same number of cells. The emission readings (data not shown) were converted to a ratio using a *Renilla* control; during detection, Firefly luciferase is quenched and any *Renilla* luminescence is detected. The *Renilla* luminescence can be used to normalise the Firefly luminescence to find a ratio, and this ratio is shown in Figure 4.1 D. Figure 4.1 E summarises the results of this luminescence assay and clearly shows that each of the ES-Luc wells luminesced, confirming that the cells in the ES-Luc population stably expressed luciferase.

In vitro validation of pluripotency of the ES-Luc cell population: pluripotency markers

Completing the overall experiment depended on the ES-Luc population being undifferentiated, and capable of forming teratomas. The ES-Luc cells had been confirmed to stably express luciferase and the next experiment tested whether the ES-Luc population retained its pluripotent properties. Complete ES medium had been used to culture the ES-Luc cells, which should have prevented non-ES cells from proliferating. However, transfection can be a disruptive

process and the ES-Luc cells needed to be validated for pluripotency. Therefore, the first step was to assay markers of pluripotency using immunohistochemistry.

ES-Luc cells were tested for the expression of *OCT4* and *NANOG* proteins using immunohistochemistry. Untransfected ES cells were used as a positive control, and mouse fibroblasts were used as a negative control. ES-Luc cells and untransfected ES cells were both positive for *OCT4* and *NANOG* proteins, and mouse fibroblasts were negative for both proteins (Figure 4.1 F and G). Overlap between *OCT4* and *NANOG* proteins with DAPI staining confirmed that 100% of the cells were positive for *OCT4* and *NANOG*. This suggests that no differentiated cells were present.

In vivo validation of ES-Luc cells for teratoma formation and luminescence

Next, the potential of these ES-Luc cells to form teratomas and luminesce *in vivo* needed to be tested. For this, ES-Luc cells were injected into mice kidney capsules.

The kidney capsule is a highly vascularised organ in a mouse, which has been shown to support growth of pluripotent cells towards teratoma formation. Since there are two kidneys, even if an injected kidney loses function the mouse will normally continue to thrive. Both of these reasons informed the decision to use the kidney capsule for a preliminary experiment. This first experiment was designed to evaluate the potential of ES-Luc cells to luminesce *in vivo* and form a teratoma, which also tested whether the ES-Luc cells retained their pluripotent properties.

ES and ES-Luc cells were transplanted into the kidney capsule of 3 mice each. After 6 weeks, each one of these kidneys contained a large tumour. Each tumour was sectioned and stained with Masson's trichrome, the standard approved stain to highlight complex regions of the tumour. Figure 4.2 A-D presents four different fields of a tumour formed by ES-Luc cells. These four panels are representative of findings in the other tumours and show tissue from each of the

three germ layers; mesoderm, endoderm, and ectoderm. This confirmed that the ES-Luc cell population had the capability of forming teratomas.

The final preparatory step was to test our ability to detect luminescence of these ES-Luc cells *in vivo*. ES-Luc cells were injected into both the testis (Figure 4.2 E and F) and kidney (Figure 4.2 G), and all produced teratomas. Figures 4.2 E-G show both the position and approximate size of the tumour. The tumour images were captured by a machine that detected the intensity of light that was emitted from the cells in the tumour (Xenogen biophotonic Spectrum and IVIS100 Imaging Systems). The light intensity was detected in several different planes of view, which allowed for the construction of a three-dimensional image seen in Figure 4.2 G. This experiment confirmed that the ES-Luc population luminesced *in vivo* at a level that allowed detection.

There was some variability in the size of teratomas when comparing kidney with testis, and this has been documented previously [189]. Testicular teratomas had a fairly large mass of approximately 0.5cm^3 , but the kidney allowed for much greater growth. The two testicular tumours varied in the amount of light emitted, and this was reflected in the size of the tumours since one was much smaller than the other. This analysis confirmed that the luminescence from the ES-Luc cells was approximately proportional to the size of teratomas formed. This was important because it meant that detection of luminescence *in vivo* could be used as a marker for size for the ethical and practical reasons already discussed.

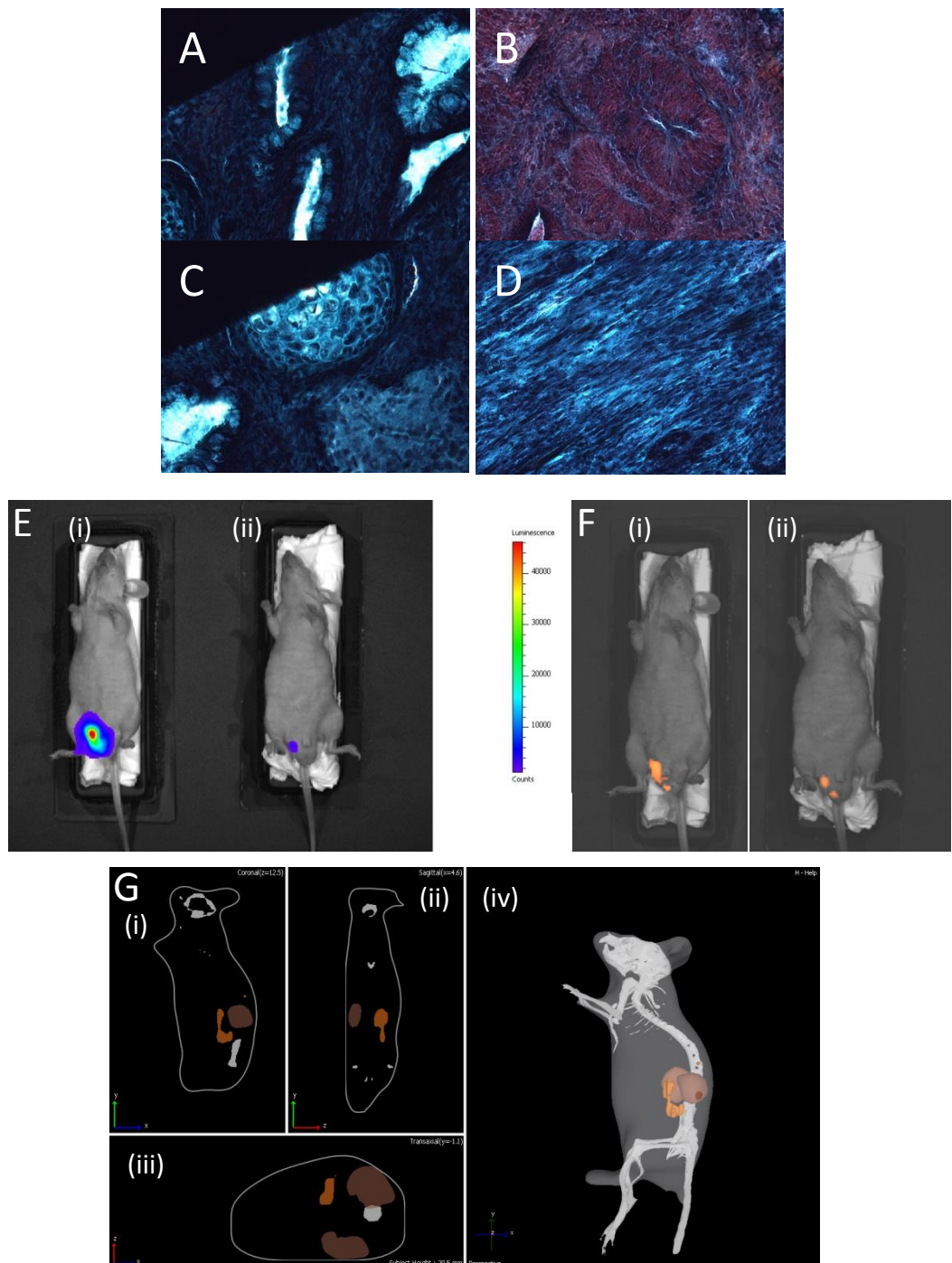


Figure 4.2. A teratoma assay using ES-Luc cells in mice testis or kidney. (A-D) Masson's trichrome staining on a teratoma formed from ES-Luc cells. (A) Endoderm. (B) Red rosettes representing immature nervous system i.e. ectoderm. (C) Circular light blue region indicates cartilage i.e. mesoderm. (D) Uniform lines of cells suggests smooth muscle i.e. mesoderm. (E) IVIS imaging showed hotspots of light produced by luminescent ES-Luc cells. Red indicates high levels of light and therefore a high concentration of cells, and blue is lower levels of light. (F) Spectral unmixing used to remove reflected light. The mouse on the right (ii) has an amplified signal in order to determine the location of the tumour, so the intensity of the signal is not comparable to (i). (G) (i-iii) Two dimensional or (iv) three-dimensional views of a kidney and tumour formed by ES-Luc cells. Light brown areas represent the kidney(s), and orange represents the tumour.

Optimisation of stereotaxic cell-transplantation into the brain

The ultimate goal of this chapter involved injecting ES-Luc cells into different regions of the brain to test where pluripotent cells had the ability to form a teratoma. The two different regions chosen were the ventral midline, where GCTs are known to occur; and a lateral region, where GCTs occur much less frequently. These two different regions are illustrated by Figure 4.3 A from a ventral view.

Figure 4.3 B (modified from Paxinos [190]) shows the locations of each of the injections - highlighted by green circles. Adult mouse brains are very small – approximately 10mm across – so stereotaxic equipment was required to achieve these precise injections. Stereotaxic equipment immobilised an anaesthetised mouse into a specific position. The equipment used reference points on the mouse skull to inject into a specific, replicable, three-dimensional position in the mouse brain. Injecting cells through the jaw would have been technically challenging and the literature showed that it was best to approach the regions of interest by drilling dorsally, i.e. through the top of the skull.

Once the skin had been removed from the dorsal skull it was possible to use the bregma (the convergence of the bone sutures) as a reference point for coordinates in three-dimensions. Figure 4.3 C shows the first attempt with coordinates: AP -1.6m (anterior-posterior), ML 0.3mm (medial-lateral), DV 5mm (dorsal-ventral) relative to the bregma. First, a small hole that a fine needle could pass into was drilled. For the preliminary experiments, dead mice and red dye were used in order to track the location of injection and the accuracy of the needle.

This initial attempt highlighted two issues: even using a dead mouse, there was significant bleeding as the drill entered; and the dye was not all localised specifically to the intended area. Figure 4.3 C (iv) highlights the inaccuracy of the injection: the actual position was rather lateral compared to the intended coordinates. Using Figure 4.3 B it was possible to estimate the coordinates of where the dye was placed: AP -1.6mm, ML 1.5mm, DV 4mm.

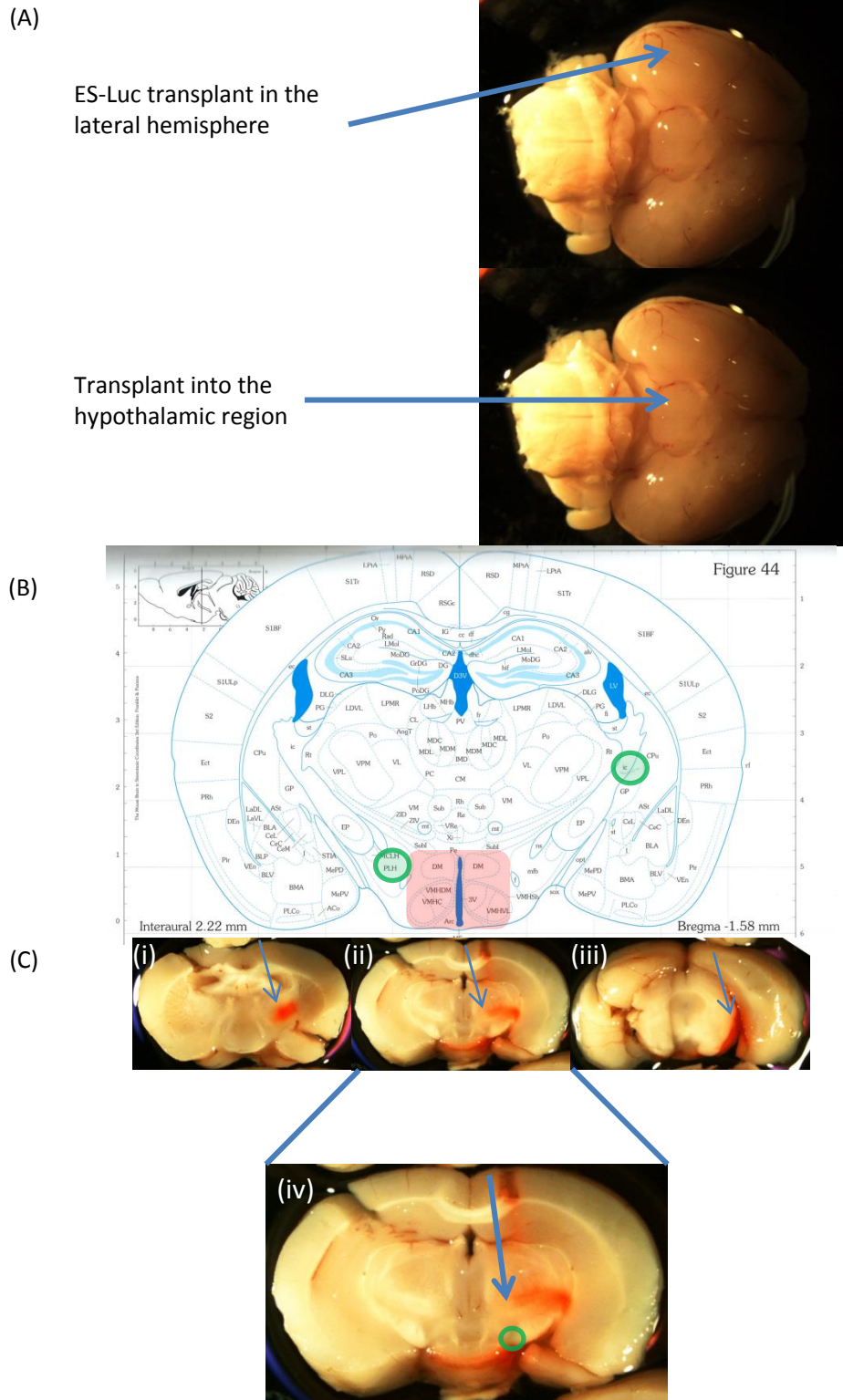


Figure 4.3. Optimisation of stereotaxic mouse brain injection. (A) Illustration of two locations where cells should be injected from a ventral view. (B) Schematic of an adult mouse brain from a coronal view. Green circles indicate the approximate coordinates of the lateral and midline locations targeted in injections. The red square represents the ventral midline and the hypothalamic region [190] (C) Validation of the coordinates following injection of a red dye. Three sections were taken to show the approximate position of the majority of the dye. (i) the track where the needle went in (ii), and leakage of dye (iii). (iv) shows that although the needle was placed in straight, the dye location is lateral to the target coordinates (highlighted by a green circle).

The first issue was to correct the bleeding caused by the drill because a live mouse would probably not survive such trauma to a large blood vessel. Figure 4.4 A shows the vascular network in an adult mouse, and the blood vessel which caused the bleeding was most likely the superior sagittal sinus [191]. Ideally the stereotaxic injection equipment would have allowed for rotation through the coronal plane in order to circumvent the vessel; however, the equipment used did not have this capability. Therefore, the original coordinates were altered to AP -1.6mm, ML 1mm, DV 5mm for the midline injections, and AP -1.6mm, ML 2.75mm, DV 3.5mm for lateral. These coordinates did not cause severe bleeding when a terminated mouse had a hole drilled and dye injected, and the dye appeared to be closer to the midline (Figure 4.4 B). The depth of injection was increased slightly for the main experiment in order to target the hypothalamic region instead of the thalamus.

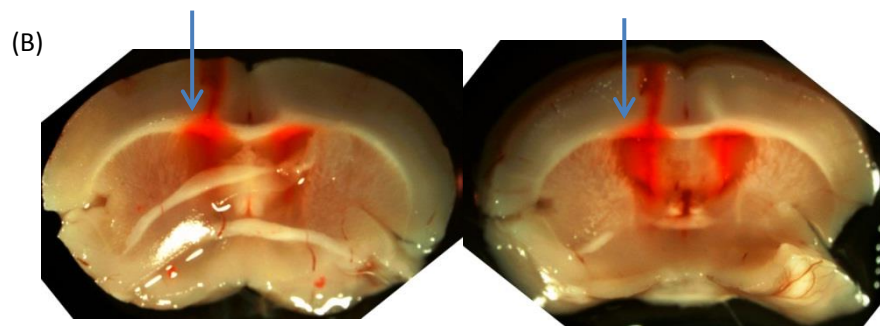
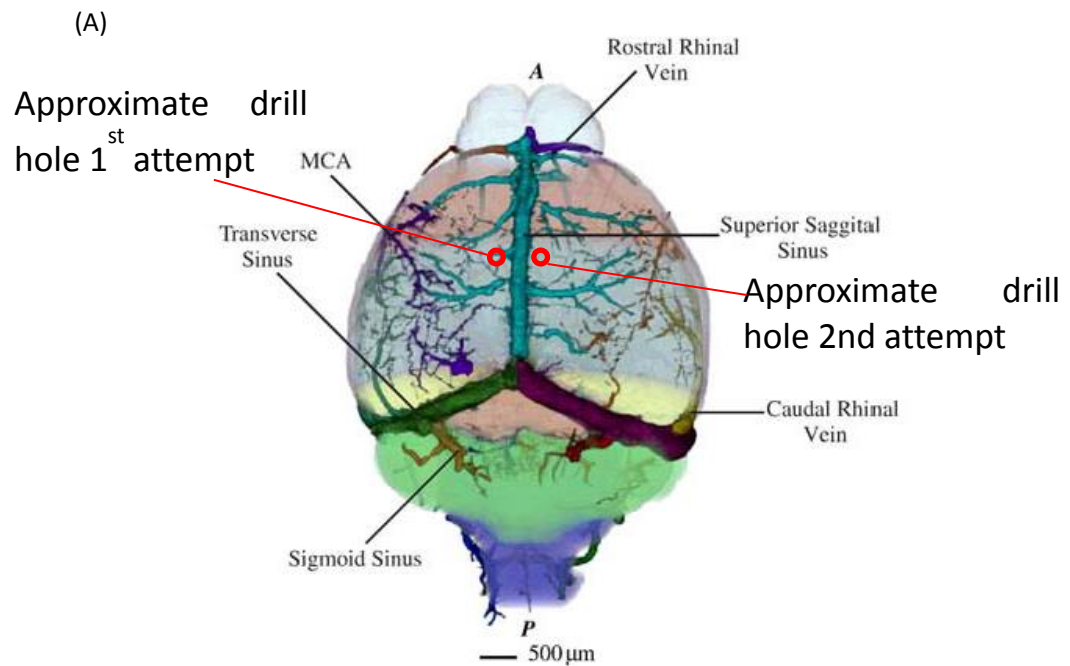


Figure 4.4. Optimisation of injection site based on the adult mouse brain vasculature. (A) Adult mouse brain viewed from the dorsal side highlighting the main vasculature . The darkened line in the centre of the brain is the superior sagittal sinus, and this branches laterally into the transverse sinus. The two small red circles indicate the approximate positions during the first attempts of injecting dye (Image taken from Dorr et al. (2007) [191]). (B) A coronal view of an adult mouse brain injected with red dye (indicated by a blue arrow) that did not cause bleeding during drilling.

Injection of ES-Luc cells into the ventral midline and lateral hemispheres

Drilling into the optimised coordinates caused only minor bleeding, and the injection of 100,000 ES-Luc cells into each of seven mice gave rise to no complications. Luminescence was not clearly detectable within the first few days of injection so the first visualisation was recorded 6 days after injection (Figure 4.5 A and B).

The intensity of light emitted from each of the seven mice varied widely. The location of injection of ES-Luc cells did not seem to correlate with the differences seen in luminescence. Midline mice were labelled M1-M4 and mice injected in the lateral region were labelled L1-L3. The two mice that showed the least luminescence were from separate groups (Figure 4.5 A mouse M2, and Figure 4.5 B mouse L3). In contrast, the two strongest signals (M4 from group 1 and L2 from group 2) were also from different groups (Figure 4.5 A and B). The same tube of ES-Luc cells was used for all injections so the concentration of cells should have been equal.

The preliminary experiment showed that luminescence correlated with the size of a teratoma. By day 12, one of the mice (M4) showed luminescent signal indicative of a very large teratoma. Therefore, this mouse was terminated and the brain was dissected and kept in fixative.

Luminescence was detected in all the remaining mice by 12 days summarised by Figure 4.6, although the signal was very weak in one of the midline-group mice (M2). There was no clear correlation between the region that ES-Luc cells were transplanted and the rate of growth; in fact, the mouse with the most, and the mouse with the least luminescence were both in the midline group (Figure 4.6 B).

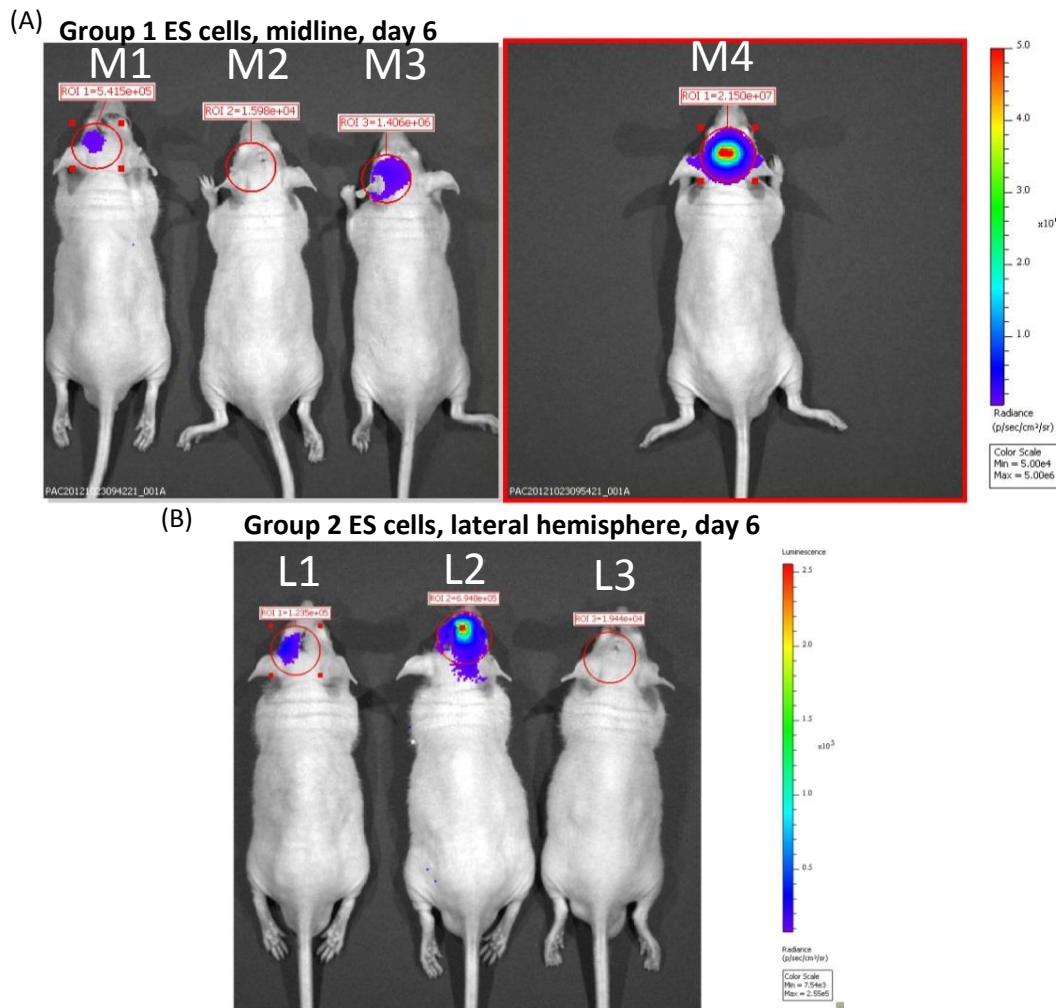
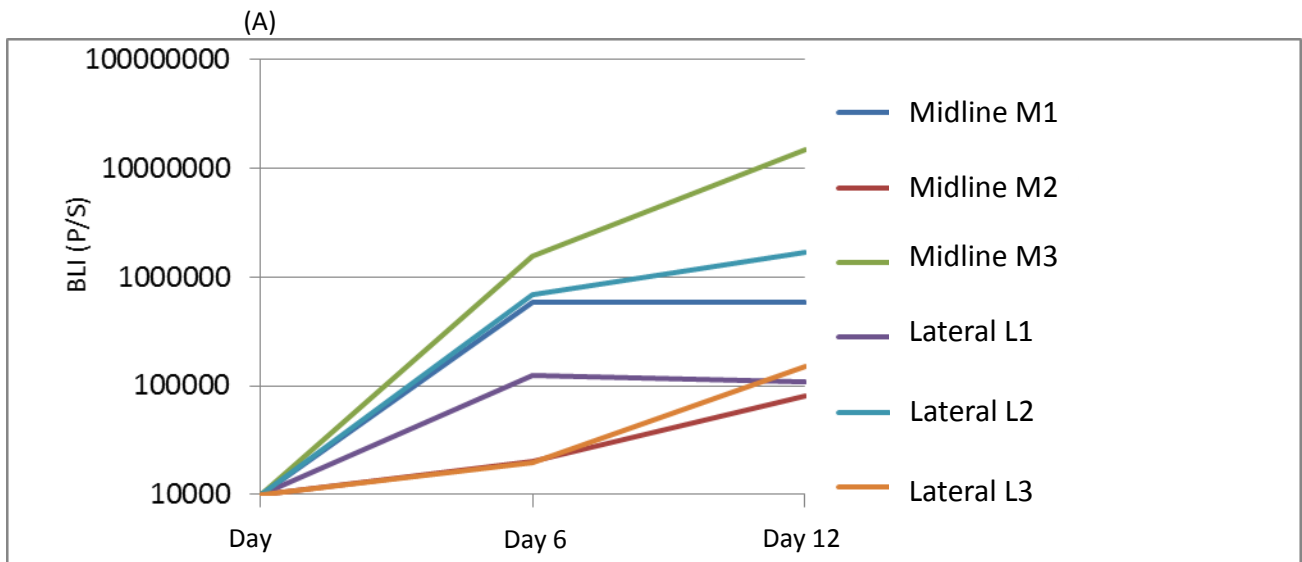


Figure 4.5. Visualisation of luminescence in adult mice 6 days after being injected with ES-Luc cells. (A) IVIS imaging of luminescence in the midline group, or (B) in the lateral group. (C) A bar chart of each mouse on the X-axis, with bioluminescent intensity (BLI) on the y-axis; note the y-axis log scale.



(B) **Group 1 ES cells, midline, day 12**



(C) **Group 2 ES cells, lateral hemisphere, day 12**

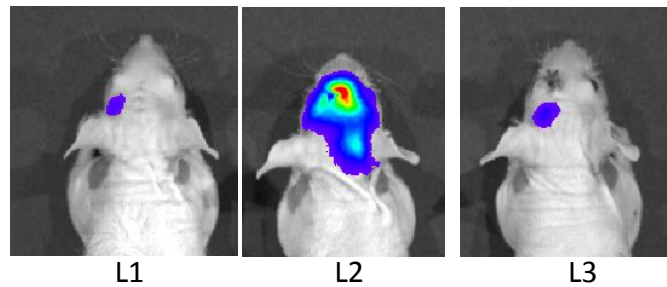


Figure 4.6. The light intensity recorded for six separate mice over 12 days following injection of ES-Luc cells. (A) Line graph of light intensity recorded over 12 days. Each colour represents a different mouse in either the midline- or lateral injected group. Note the light intensity on the y-axis log scale (Bioluminescent intensity). (B) IVIS imaging of luminescence in the midline group, or (C) in the lateral group from a dorsal view.

At 12 days the images showed that each of these mice had probably developed a teratoma so all remaining mice were terminated and their brains were dissected. Each brain showed substantial morphological differences when compared with a control brain that was only injected with dye. From the dorsal side, the effects were more subtle (Figure 4.7), with damage probably caused by necrosis (Figure 4.7 E) and swelling in the hemispheres of several of the brains (Figure 4.7 B, C, D, F and G). In contrast, the ventral view of these brains revealed considerable discolouring and damage. Although some of the brains were damaged in the process of removing them (Figure 4.8 A and E), it appeared that each brain had a large tumour when compared with the control brain (Figure 3.8 H). Using the relatively normal cerebellum and olfactory bulb as reference structures, the ventral midline appeared misshapen (Figure 4.8 A), or necrotic (Figure 4.8 B-D). None of the injected brains appeared symmetrical when compared to the control, especially those shown in Figure 4.8 B and G.

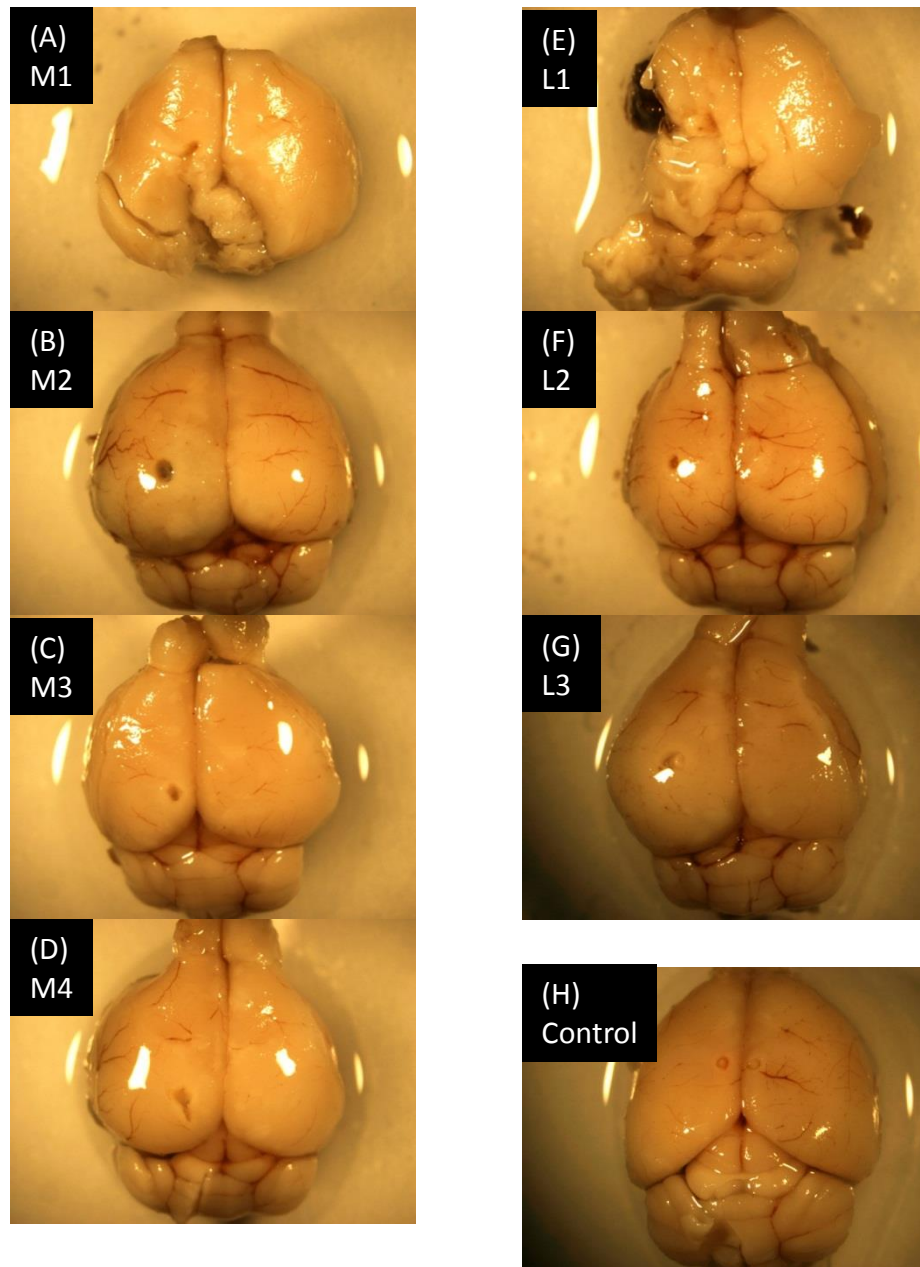


Figure 4.7. Dorsal view of adult mice brains 12 days after injection of ES-Luc cells. Injection of ES-Luc cells was into either (A-D) the midline, (E-G) lateral region, or (H) a dead mouse injected with dye used as a control. The injection site for each brain can be seen to the left of where the two hemispheres join. The anterior of the brain (olfactory bulb) is at the top of the images and posterior (cerebellum) is at the bottom.

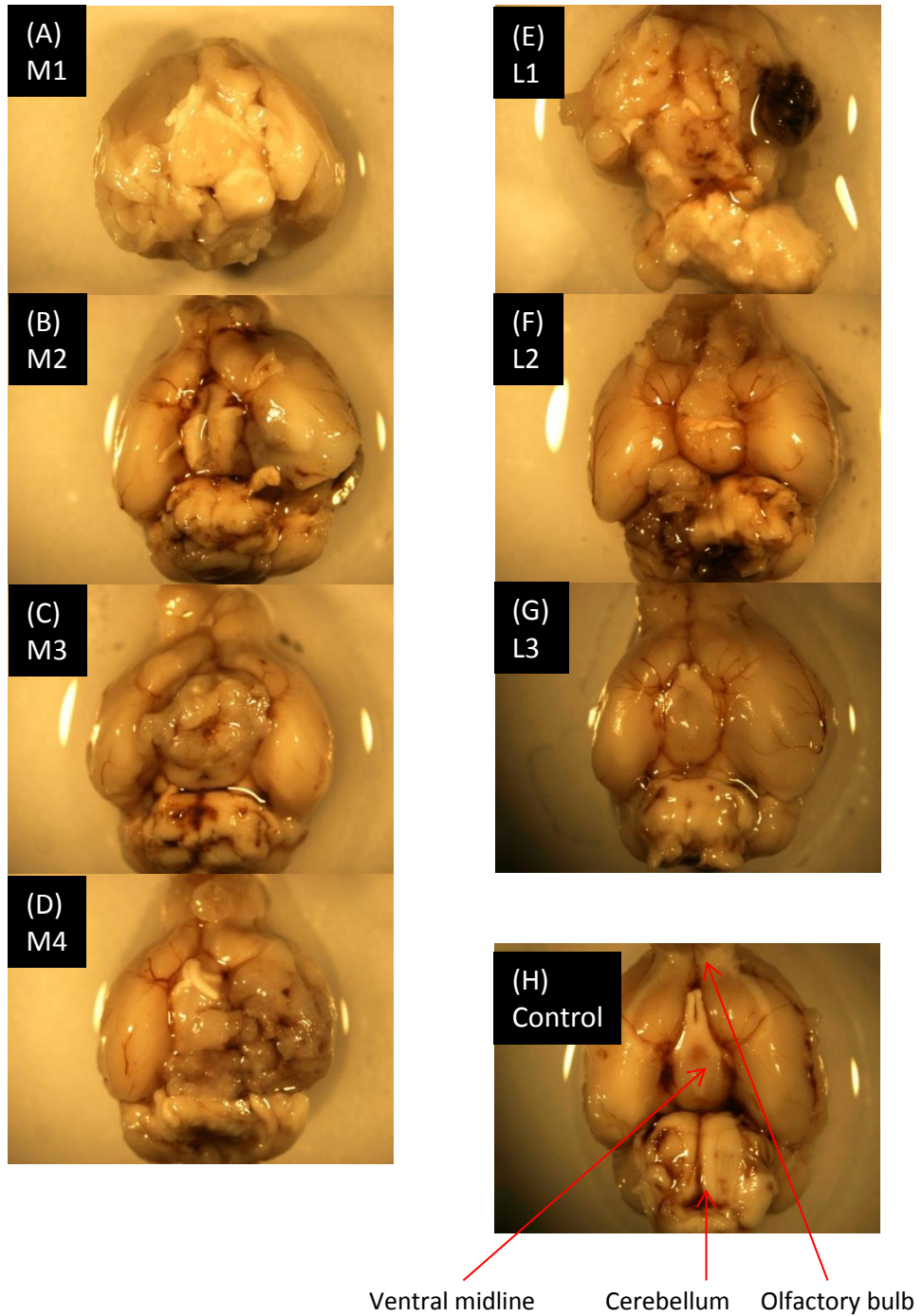


Figure 4.8. Ventral view of adult mice brains 12 days after injection of ES-Luc cells. Injection of ES-Luc cells was into either (A-D) the midline, (E-G) lateral region, or (H) a dead mouse injected with dye used as a control. The anterior of the brain (olfactory bulb) is at the top of the images and posterior (cerebellum) is at the bottom. (H) The control has the region in the centre highlighted as the ventral midline, the cerebellum at the bottom of the image, and the olfactory bulb at the top of the image to indicate where these structures would normally be found as a comparison to the injected brains.

Each of the dissected mouse brains was sectioned and one section from each brain was stained with haematoxylin and eosin (H&E). The sections were examined for regions of tissue that were representative of each of the three germ layers – mesoderm, endoderm, and ectoderm. Using this germ-layer criterion, all of the mouse brains injected with ES-Luc cells were histologically confirmed as being teratomas. Figures 4.9 and 4.10 represent a brain from the midline or lateral region respectively. Each figure shows the gross morphology of the brain containing the tumour, two sections of the brain stained with H&E, and detailed regions of the section to illustrate the three germ layers.

The three regions of teratoma that represented the germ layers included: high density endodermal cells similar to those in the gastrointestinal lining (Figure 4.9 C (i) and 4.10 C (i)); immature cartilage derived from the mesoderm (Figure 4.9 C (ii) and 4.10 C (ii)); and characteristic ‘neural rosettes’ which represent ectoderm (Figure 4.9 C (iii) and 4.10 C (iii)). An example of these three regions and their locations in a tumour can be found in Figure 4.11, and highlights the heterogeneous nature of a teratoma. With some brain tumours it can be difficult to distinguish normal brain from tumour; however, this was not the case with teratomas in the brain, which were well circumscribed and had a defined edge where the brain stopped and the tumour began (illustrated in Figure 4.12).

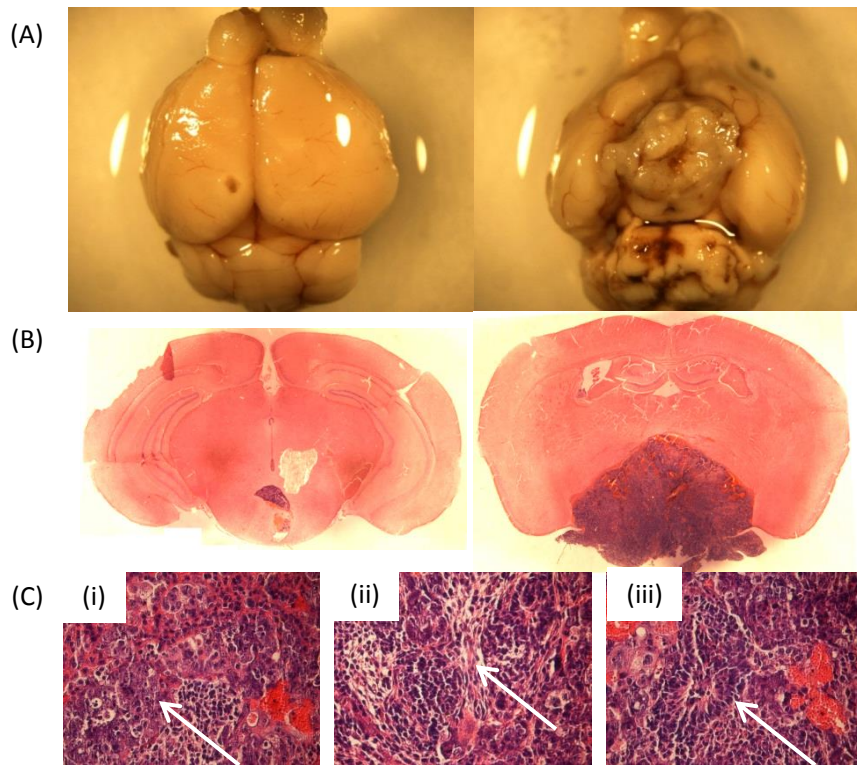


Figure 4.9. Histology of the midline mouse, M3. (A) An example of an adult mouse brain injected with ES-Luc cells into the midline – M3. (B) Two sections of (A) with haematoxylin and eosin stain. (C) 40x magnification of regions of (B) that represent the three germ layers; endoderm (i), cartilage/smooth muscle (ii), and rosettes characteristic of neural tissue (iii).

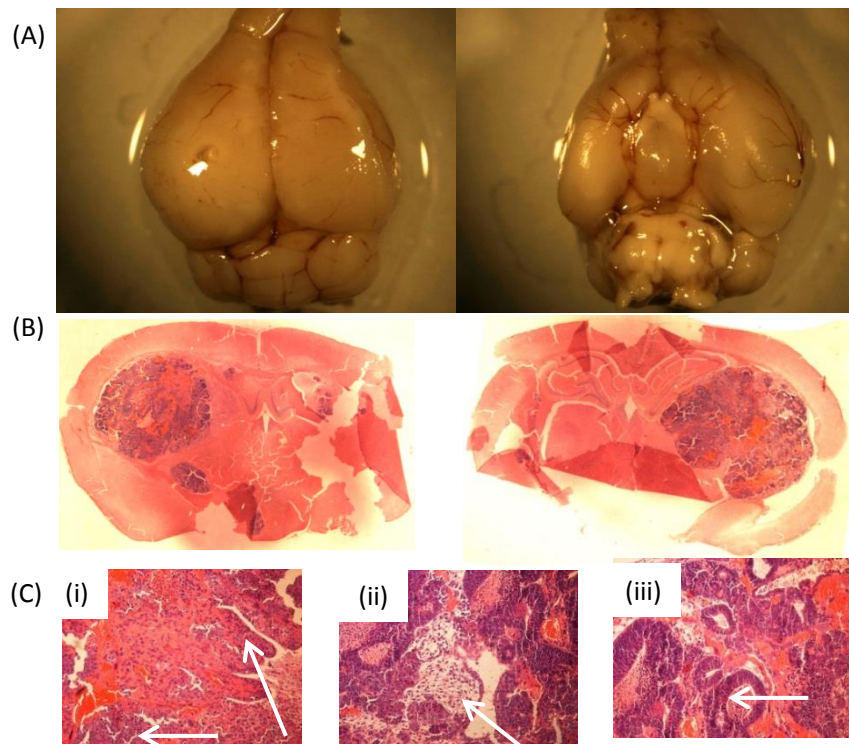


Figure 4.10. Histology of the lateral mouse, L3 (A) An example of an adult mouse brain injected with ES-Luc cells into a lateral region – L3. (B) Two sections of (A) with haematoxylin and eosin stain. (C) 40x magnification of regions of (B) that represent the three germ layers; endoderm (i), cartilage (ii), and rosettes characteristic of neural tissue (iii).

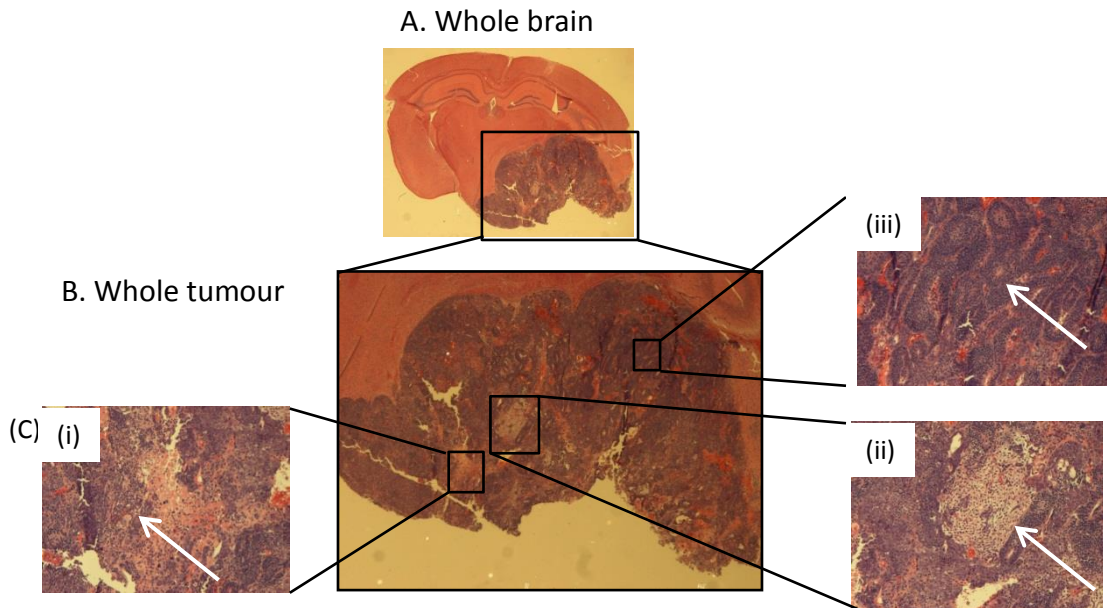


Figure 4.11. Histology of a teratoma in an adult mouse brain injected with ES-Luc cells. (A) A section of an adult mouse brain injected with ES-Luc cells that has formed a tumour. Stained with haematoxylin and eosin. (B) 10x magnification of only the tumour from (A). (C) Three sections of tumour magnified to 40x which represent the three germ layers: (i) endoderm; (ii) mesoderm such as cartilage; and (iii) neural rosettes for ectoderm.

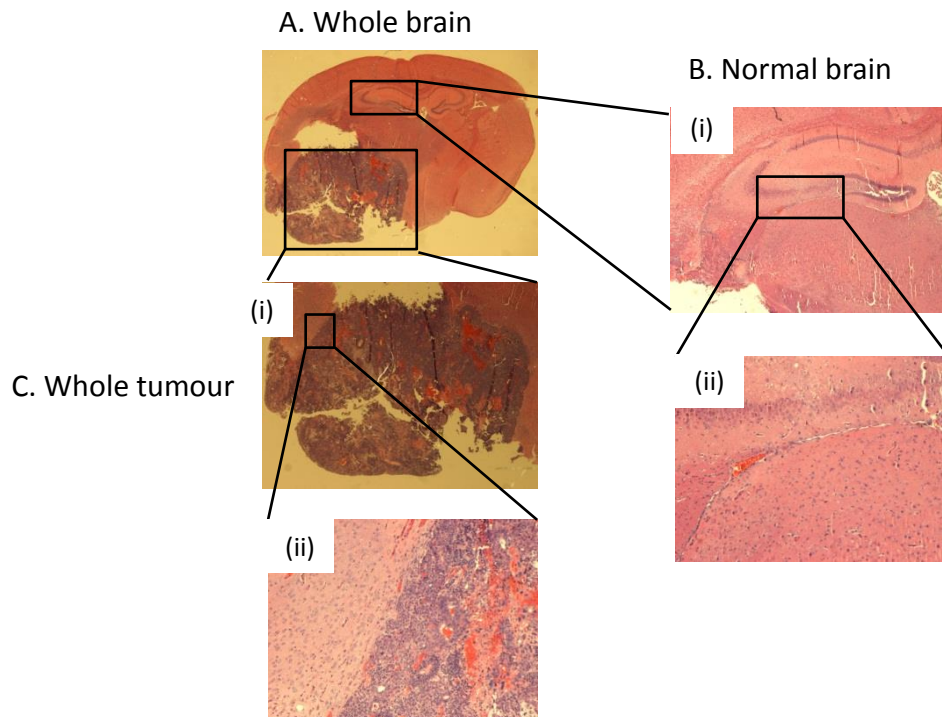


Figure 4.12. Histology of normal and tumour tissue in an adult mouse brain injected with ES-Luc cells. (A) A section of an adult mouse brain injected with ES-Luc cells that have developed into a tumour. Stained with haematoxylin and eosin. (B) An example of what normal brain looks like when magnified 10x (i) or 40x (ii). (C) The boundary of brain and tumour magnified at 10x (i) or 40x (ii). The normal brain is pink and aligned in a uniform fashion, and the tumour is blue with non-uniform structures.

Injection of approximately 5,000 ES-Luc cells into the ventral midline and lateral hemispheres

The previous experiments show no clear difference between teratoma formations in the midline compared to the lateral hemisphere. However, it may be possible that a high concentration of ES cells may have the capacity to form a microenvironment capable of supporting other ES cells. Considering the successful growth of histologically-confirmed teratomas from a large number of ES-Luc cells, we repeated the experiment with a lower number of cells.

Our primary objective was to test whether a biologically relevant number of cells had the capability of forming a teratoma in the lateral hemispheres. Therefore, we injected approximately 5,000 ES-Luc cells suspended in 5 μ l of PBS into either the midline or lateral region of SCID mice, and three mice per region were injected.

After only 2-3 days, all of the midline mice had to be terminated due to weight loss and irregular behaviour. After 6 weeks, one of the mice injected with ES-Luc cells into the lateral hemisphere was also terminated due to irregular behaviour. The final two mice in the lateral group were imaged for luminescence in either three-dimensions (Figure 4.13 A), or two-dimensions (Figure 4.13 B). Both scans showed signs of teratoma growth in the lateral regions so the remaining mice were terminated.

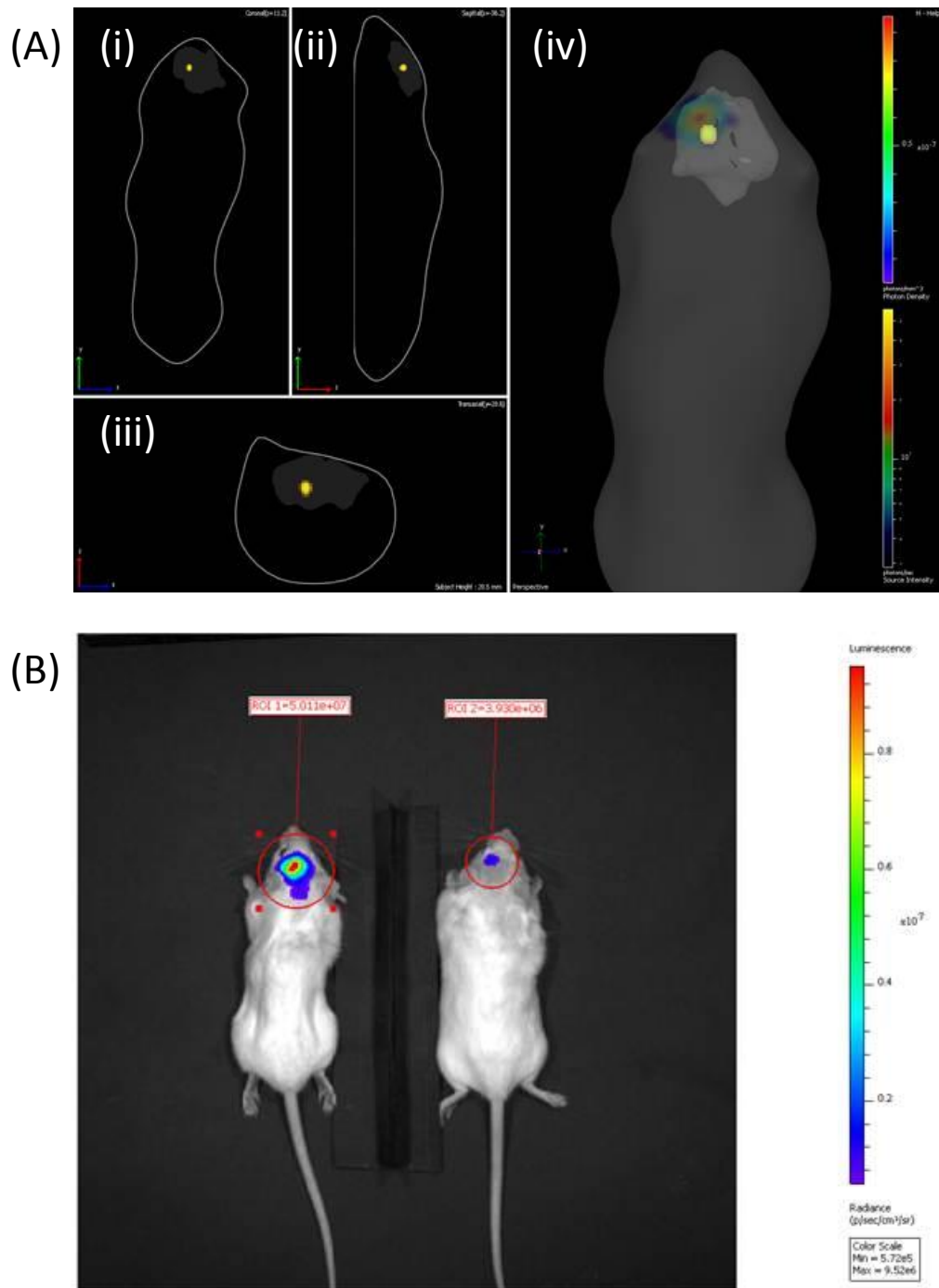


Figure 4.13. Detection of luminescence emitted from ES-Luc/teratoma cells. Two out of six mice were imaged for luminescence 7 weeks after injection of $\sim 5,000$ ES-Luc cells. ES-Luc cells were injected into the lateral hemispheres in both mice. Imaging was either three-dimensional (A) or two-dimensional (B). (A) Three planes of two-dimensional scanning (i-iii) are combined to form a three-dimensional image (iv). The rounded tumour can be clearly seen in the lateral region of the brain (iv).

The brains of all six mice were dissected, fixed, sectioned, and stained with haematoxylin and eosin. Since the mice of the midline group all died within a short time, there were no signs of tumour growth (Figure 4.14 A-C). Therefore, it was not possible to determine whether the cells in these locations would have grown.

All three mice injected with ES-Luc cells in the lateral region showed teratoma growth. One out of the three brains in this group only showed signs of a small teratoma, but appeared to have disseminated into a wider region (Figure 4.14 D i-iv). Comparatively, the other two brains in this group contained large teratomas (Figure 4.14 E-F). In summary, a small number of ES-Luc cells are capable of developing into large teratomas when transplanted into the lateral hemispheres of mice brains.

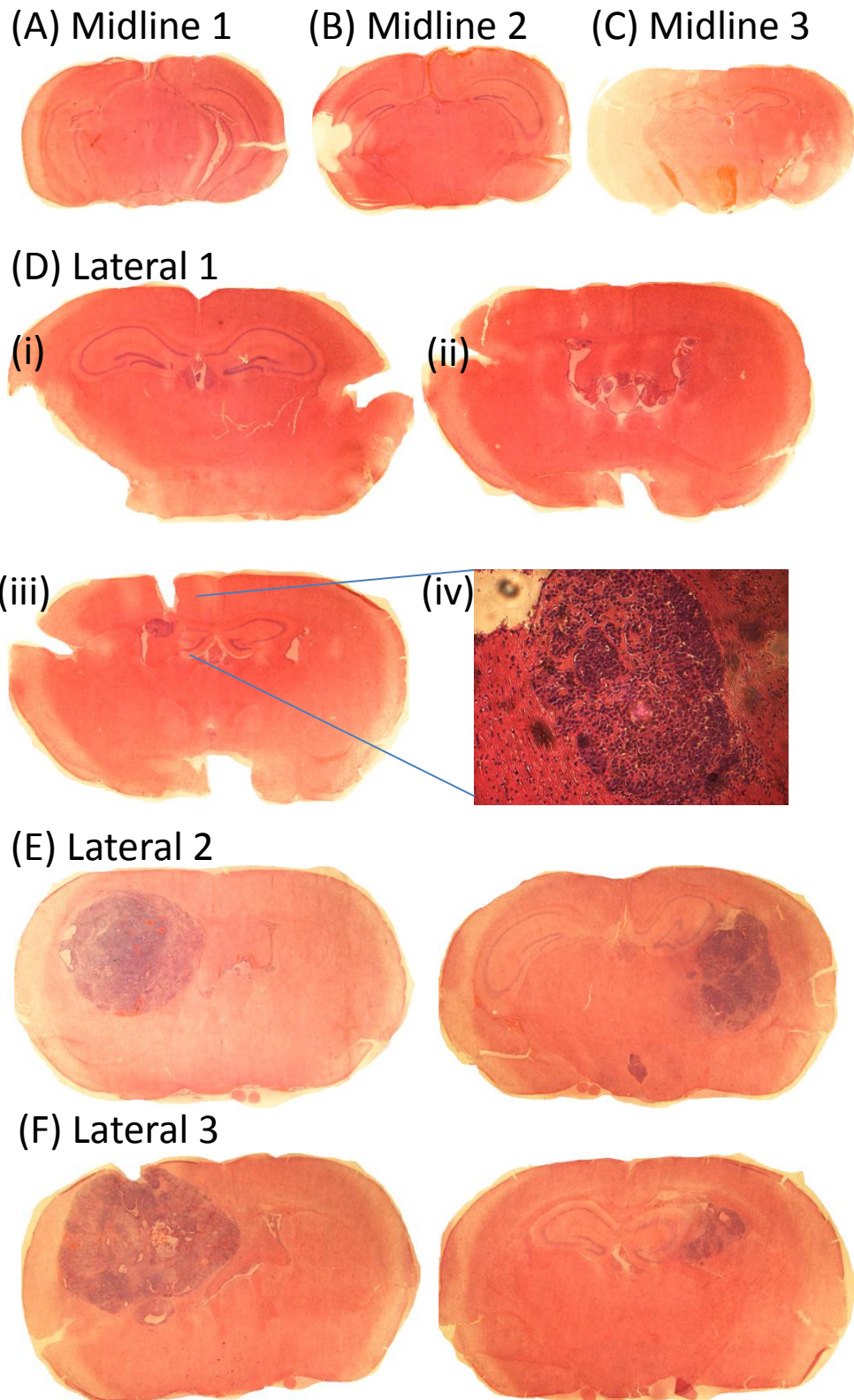


Figure 4.14. Teratoma formation in mice brains using low concentrations of ES-Luc cells. Approximately 5,000 ES-Luc cells were injected into either the midline of mice brains (A-C), or the lateral regions of the brain (D-F). (A-F) After termination of each of the mice injected with ES-Luc cells, the brains were removed, fixed, sectioned and stained for tumour growth. The midline brains were dissected after only 2-3 days due to poor health (A-C) but the lateral brains were left for 6-8 weeks (D-F). Each brain was sectioned at the site of injection and one slide from either side of the injection point is presented.

4.4 Discussion

The experiments described in this chapter tested whether teratomas could form in different regions of the brain. There were two questions to be answered by these experiments: firstly, was it possible for teratomas to form in the two different regions; and secondly, was there a difference in their growth rate of teratomas in these two regions.

I found that ES-Luc cells had the capacity to form teratomas in both regions of the brain that they were injected into. The tumours all increased in size very rapidly after injection into the brain, which was similar to the growth rates seen in other locations of the mouse body such as the kidney capsule. Therefore, there did not appear to be a significant protective environment in the lateral hemisphere to explain why teratomas are most frequently found in this region.

Approximately 100,000 cells were injected into the respective regions; however, there may be far fewer progenitors than 100,000 when these tumours arise in humans. ES-Luc cells have the potential to form their own collagen matrix, which may circumvent any differences in environment in the two different regions i.e. the ability of progenitor cells to result in tumours in these regions. Therefore, we tested both regions with a relatively low number of cells, and teratomas could still form in lateral locations.

One caveat was that the mice used were adult. Teratomas mainly form in the pre- or peri-natal age range, and the brain microenvironment is different between a developing embryo and an adult. From a practical perspective the issue of using adult mice is very difficult to resolve. The ideal solution would involve transplanting cells into embryos younger than E11.5. However, injecting cells accurately into an adult brain is challenging. Therefore, injecting cells into brains of embryos in utero that are much smaller than adults, as well as the embryos surviving to term and developing, is beyond our capability at present.

Overall, this caveat may be a minor issue. Teratomas have been found to arise in adults and are therefore not exclusive to the pre- or peri-natal age range.

While the aetiology of these tumours has been disputed, this experiment tested the microenvironment, and the non-midline environment did not appear to be protective against teratoma initiation and formation.

The second part of these experiments tested if there was a difference in the growth rate between teratoma formation in the midline compared to the lateral region. Unfortunately, the tumours proliferated rapidly so there was not enough time to track the growth rate over an extended period of time. Ideally the luminescence from each tumour would have been detected every two days until morbidity, or until the intensity of luminescence indicated that the tumour had grown beyond a certain size. This would have perhaps addressed whether there was a difference in the growth rate of progenitor cells. Technology at present is not sensitive enough to track the rate of growth accurately; however, there did not seem to be any substantial differences in the teratomas formed in the lateral regions.

If there was no growth advantage to the ventral midline, why have GCTs been more frequently reported to occur in the midline? In the pre- and peri-natal period, some parts of the brain may be more important for survival than others. Teratomas occurring in the lateral regions of the brain may be detrimental to development and are therefore not documented - since the pregnancy is terminated naturally or through clinical procedures. This speculation would be possible to test with a large cohort of autopsy reports for abortions but is beyond the scope of this project.

Is it likely that GCTs in lateral regions terminate pregnancy at an early stage? Perhaps it is more intuitive to think that the midline of the developing brain contains cells with a higher propensity, or a mechanism that increases the likelihood of developing a GCT. The next chapters will address these issues.

4.5 Conclusion

Overall, the strategy of injecting luminescent pluripotent cells (ES-Luc cells) into different regions of mouse brain has been informative. Mice that had been injected with ES-Luc cells developed into teratomas with no striking differences in growth, regardless of location. Taken together with other literature, it appears that non-germ-cell progenitors can form GCTs in either midline or lateral regions of the brain.

So why are certain CNS GCTs found only in particular locations? Why do germinomas appear to be confined to the midline? Why are teratomas diagnosed in the midline at a higher prevalence than those in the lateral regions? The next chapter will investigate the properties of the potential cell of origin for GCTs in the brain and suggest a hypothesis for tumour-growth bias.

Chapter 5 Neural stem cells and activation of OCT4

5.1 Introduction

The cell of origin for CNS GCTs is hypothesised by Teilum to be a mismigrating germ cell progenitor. Our hypothesis contradicts this, and we suggest that CNS GCTs arise from a brain-cell. Therefore, the experiments summarised in this chapter test the ability of a neural cell to form a GCT.

It has been known for many years that ES cells can initiate the formation of teratomas [192]. More recently, activation of only a single gene, Oct4, was shown to induce neural stem cells to become pluripotent, albeit at a low efficiency [81]. We hypothesise that neural stem cells either acquire Oct4 expression, or Oct4 is not silenced properly during embryogenesis (either delayed in silencing, or prevented from undergoing a single silencing mechanism altogether), and it is this activation of OCT4 that forms a pluripotent progenitor capable of forming a GCT.

Our hypothesis that neural progenitors form CNS GCTs by Oct4 expression presents several challenges. The first is the role of OCT4 *in vivo*; is Oct4 aberrantly expressed after it is silenced, or is there a lack of Oct4 silencing during the normal process, i.e. is Oct4 reactivated, or is Oct4 continually expressed?

The subtle difference between reactivation of Oct4, and continuous expression of Oct4, may change our hypothesis dramatically. If neural progenitors retain low levels of OCT4, this would require a different experimental design to a complete loss of Oct4 expression and reactivation. A loss of OCT4 is likely to cause progenitors to differentiate; however, if Oct4 expression was continued but low, it is much more likely that the progenitors have retained their pluripotent properties.

These two statements are integral in designing experiments to test this hypothesis because one of these mechanisms may not be sufficient to form a GCT. Therefore, both these possibilities need to be addressed.

Each subtype of GCT appears to have a different pattern of occurrence in the brain. Examining different regions of the brain at various time-points during embryogenesis would be too ambitious for the scope of this project. In light of this, it must be assumed that the progenitors are active and have a similar capability to form GCTs. Teratomas can apparently form anywhere in the brain; this would suggest that the progenitors are present in all regions of the brain, although there may be differences in the number of these cells. The differences between each class of tumour, especially germinomas compared with teratomas, will be discussed later.

5.2 Aims

The experiments in this chapter were designed to examine the role of OCT4 in GCT formation, and test the ability of OCT4 activation to induce a multipotent stem cell to form a teratoma *in vivo*. We had hoped to address this using three different approaches: induction of OCT4 *in vivo*, induction of OCT4 in brain tissue before transplanting into another mouse, and induction of OCT4 in a neural stem cell population before injecting into a mouse brain.

The original aim was to develop a transgenic mouse model in which OCT4 only becomes activated in specific cell types. The strategy behind these crosses was to use the Nestin promoter – a marker for neural lineage cells – to localise OCT4 activation to NSCs in the brain (Figure 5.1). With this strategy, it would have been possible to target other tissue locations in mice, but it would have reduced the major side-effects seen in mouse models that ubiquitously express Oct4. The first section of the results briefly describes an initial pilot trial of this strategy; however, this system proved unreliable, so the rest of this chapter

focusses on a mouse model that ubiquitously expressed Oct4 upon addition of doxycycline (Figure 5.2 A).

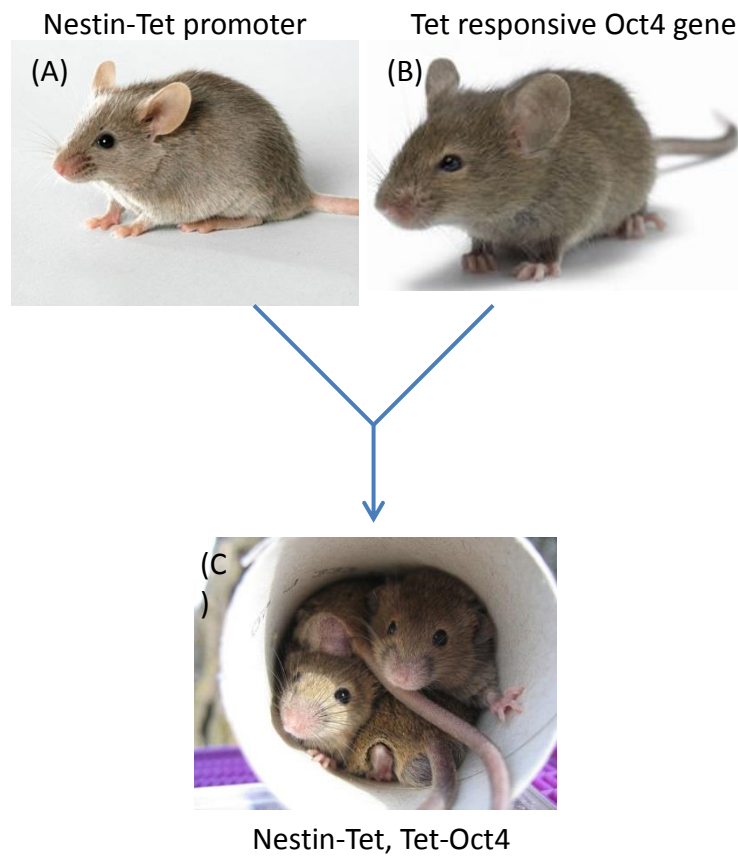


Figure 5.1. A breeding scheme showing the production of mice that express Oct4 in NESTIN-expressing cells upon doxycycline treatment. (A) Homozygous NESTIN-Tet mice were crossed with (B) homozygous rtTA-OCT4 mice to produce (C) mice capable of expressing Oct4 in cells that express NESTIN upon addition of doxycycline.

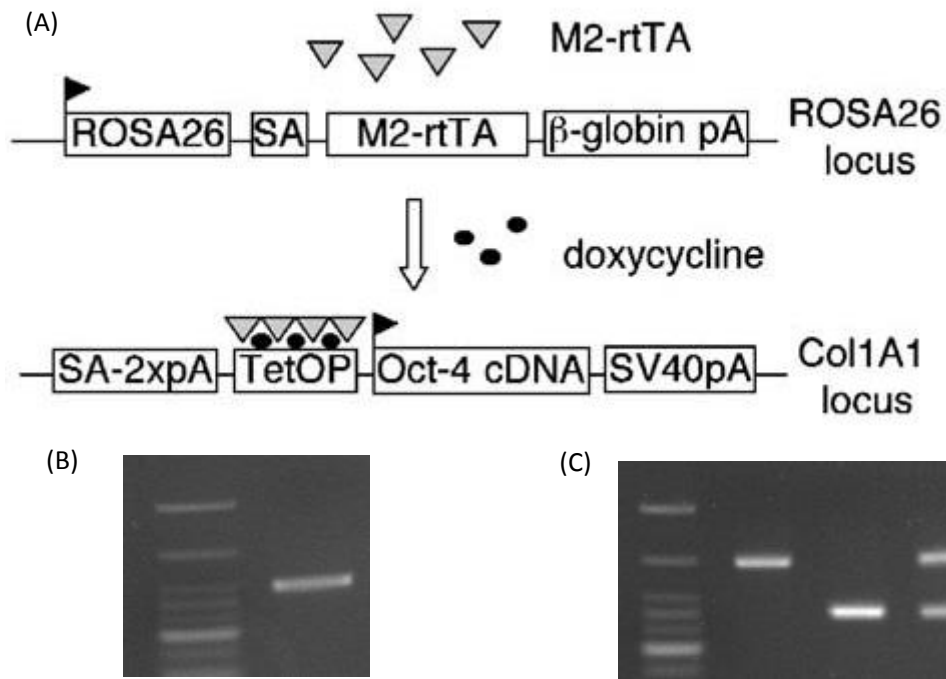


Figure 5.2. OCT4-inducible transgenic mice. (A) M2-rtTA (reverse transcription transactivator) is expressed by the Rosa26 promoter. The addition of doxycycline allows rtTA to bind to the TetOP (Tet-operon) in order to allow expression of Oct4 cDNA at the Col1A1 locus. The Rosa26 promoter is activated in all cells, so addition of doxycycline expresses rtTA, and therefore OCT4, throughout the body. (B and C) Each mouse was genotyped for the Rosa26-Tet, and Col1A1-Oct4 loci. This figure shows examples of tissue that is positive for Rosa26-Tet (A), and either homozygous, wild-type, or heterozygous for Col1A1-Oct4 (C – left to right).

The following experiments aimed to evaluate whether neural stem cells from the brain can form a teratoma, but there are limitations on how relevant these are *in vivo*. There is already an established OCT4-inducible mouse so I used this model to understand whether OCT4-induction can lead to the formation of a GCT (Figure 5.2).

In this particular experimental mouse model, doxycycline administration triggered ubiquitous Oct4 expression. However, Oct4 expression had not been clearly evaluated in the embryo. A robust evaluation of the OCT4-inducible system was therefore the first aim. This was followed by induction of OCT4 to determine the effect on development and survival to birth of embryos. Finally, the effect of OCT4 during embryogenesis on the long term survival and tumour formation on these mice was tested.

Since we were unsure of the exact cell type of origin, and it may be possible that the progenitors of GCTs are only present during a short window of development, we used two strategies as a preliminary step in order to focus on when and where these progenitors may be present. The first experiments tested whether a neural progenitor has the potential to form a GCT. The strategy uses either dissociated brain tissue or an isolated stem cell population.

The initial experiments required the isolation and characterisation of a potential progenitor population; neural stem cells (NSCs). We were unsure whether there was an abundance of cells with the potential to form a GCT in the brain; therefore, isolating and culturing a subpopulation allowed the number of progenitors to be increased.

Our plan was to activate OCT4 in NSCs and brain tissue, and test whether they had the potential to form a GCT. Injection of cells into the kidney capsule is an established method of testing pluripotency and whether a cell population has a tumour-forming capacity.

The first experiment evaluated the ability of brain tissue and NSCs to form tumours/teratomas when OCT4 was activated using our transgenic system. In

these experiments the cells were transplanted into in the kidney capsule of severe combined immune-deficient (SCID) mice, and were left to develop for 6 weeks. The potential of these cells to form teratomas in the brain was used to test the hypothesis that a brain cell can form a GCT.

5.3 Results

Three strategies test the ability of cells in the brain to form a type of germ cell tumour: testing whether a multipotent cell population found in the brain with OCT4 activation can form a GCT; transplanting portions of brain tissue induced with OCT4 into mice kidneys to examine teratoma formation; and inducing OCT4 *in vivo* during embryogenesis. All these experiments were carried out in parallel.

OCT4 activation localised to Nestin-expressing cells in a transgenic mouse model

Neural progenitors express Nestin, and according to our model, these are likely progenitors of CNS GCTs. We therefore set out to test this hypothesis by crossing two strains of mice: upon administration of doxycycline, the first strain expressed a transactivating protein (TA) in cells that already expressed Nestin; and the second strain responded to TA by activating OCT4. Therefore, OCT4 should have been activated in Nestin-expressing cells when doxycycline was added. This work was carried out in collaboration with Valerie Wilson at The University of Edinburgh.

Many rounds of breeding between Nestin-Tet promoter mice and mice carrying the Tet-responsive OCT4 gene (Figure 5.1) resulted in a strain that contained both the transgenes, confirmed by genotyping. Therefore, the ability of doxycycline to activate OCT4 needed to be tested. NSCs were cultured, along with controls from non-neural origin. Each of these samples was tested for OCT4

and *NANOG* activation using RT-PCR. The expected result was activation of OCT4 only in NSCs that had been in contact with doxycycline; however, in several cases even those NSCs that should not have been activated by doxycycline expressed Oct4 (data not shown).

In vivo activation of OCT4 by oral gavage also revealed an inconsistent result. OCT4 was being activated without the addition of doxycycline (data not shown).

These data showed that the system did not work as intended, so a different strategy was formulated. Instead of trying to isolate a restricted cell population using Nestin-localised expression, we changed to a mouse strain that ubiquitously expressed Oct4 when doxycycline was administered (summarised in Figure 5.2 A).

Establishing and maintaining a transgenic-mouse colony

This strategy examines whether OCT4 has the ability to trigger formation of a GCT when it is expressed during embryogenesis. As described in Chapter 1, Oct4 expression is silenced by around E11.5. Since GCTs are thought to originate from a progenitor cell that is activated in the first or second trimester, the ideal time window to test the effects of aberrant Oct4 expression is between E11.5 and birth.

Transgenic Rosa26-rtTA/Tet-OCT4 mice were bought from The Jackson Laboratory [193] and maintained by BMSU (QMC, Nottingham). The Rosa26 locus is expressed ubiquitously; therefore, all cells should express rtTA. The rtTA protein binds to the TetOP locus upon administration of doxycycline, which allows expression of Oct4 in all cells.

Homozygous, heterozygous, and wild-type mice from the colony were crossed. The genotype of these mice was confirmed by PCR. Figure 5.2 A shows the result of a typical genotyping PCR: two bands for a heterozygous genotype, and a single band of either 551bp for homozygous, or 331bp for wild-type. In this

case, wild-type is defined as the absence of the Tet-OCT4 gene inserted at the Col1a1 locus; however, these wild-type mice often possess the Rosa26-rtTA gene.

There were several rounds of mouse crosses and intermediate experiments which required genotyping (see Appendix I).

Isolation and characterisation of neural stem cells

According to our hypothesis, NSCs are a likely candidate for the progenitor cell for CNS GCTs. The first set of experiments tested the activation of OCT4 upon doxycycline addition, and validated NSCs. The first step was isolation and characterisation of NSCs.

NSCs, or 'neural-progenitor' cells, were isolated from different regions of mouse brain of different ages. Briefly, a small piece of mouse brain tissue was dissected from mice of various ages (E8.5 through to adult), and neural progenitors were cultured as neurospheres.

Neural progenitors could differentiate into both neuronal cells and glia, as tested by a differentiation assay followed by immunofluorescence of MAP2 and GFAP (Figure 5.3 B). Neural progenitors should have the capability to self-renew, and all regions/ages could serially form neurospheres from a single neural stem cell (Figure 5.3 C).

OCT4 should have been expressed upon treatment with doxycycline. Crucially, it was silent in all regions/ages when no doxycycline was added, but expressed when doxycycline was added (Figure 5.3 A). When NSCs were treated with doxycycline they continued to display NSC characteristics such as differentiation, and self-renewal (summarised in Figure 5.3 D).

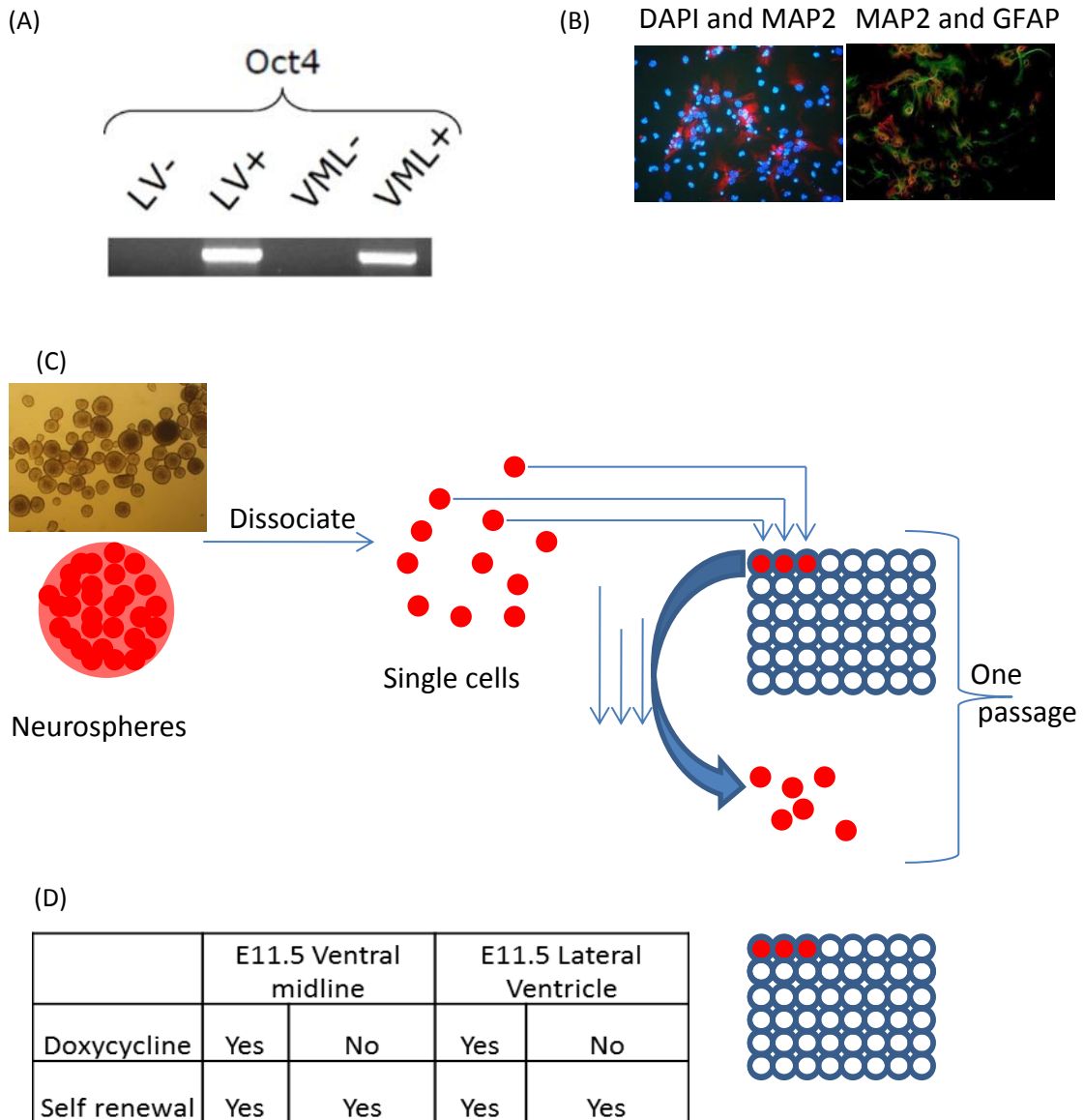


Figure 5.3. Validation of neural stem cell derived from Oct4 mice. (A) Polymerase chain reaction on cDNA synthesised from neural stem cells isolated from the ventral midline (VML) or lateral ventricular region (LV). Oct4 was only expressed in the presence of doxycycline. (B) After differentiation using retinoic acid, there was increased expression of MAP2 (a marker for neuronal cells) and GFAP (a marker for glial cells) in NSC populations that were either untreated, or treated with doxycycline. (C) A self-renewal assay; neurospheres were dissociated into single cells on Day 1; cell numbers were calculated to plate 0 or 1 cell into a well, and these were cultured for 2-5 days; a single well containing one neurosphere was dissociated and plated into wells at a concentration of 0 or 1 cell – this constituted one passage. This process was repeated until the neurospheres had been passaged three times, which confirmed NSC ability of self-renewal. (D) A summary of the properties of neurospheres cultured from the VML or LV of Oct4-inducible mice. Both regions are capable of being induced by Oct4, and self-renewal.

Time delay between doxycycline addition and OCT4 and *NANOG* activation

The induction of OCT4 in NSCs to a pluripotent state has already been tested using viral vectors. However, these methods took several weeks to form pluripotent cells and it was unclear whether the transduction process or the expression of Oct4 caused this delay. Therefore, the next set of experiments aimed to test the transgenic mouse system for the time between doxycycline addition and Oct4 expression. *Nanog* is a marker for pluripotency, or pluripotential ability, so this too was assessed. These experiments were carried out in parallel with other experiments in this chapter and informed the design of other tests.

The experimental plan to test the speed of Oct4 and *Nanog* expression was to add doxycycline, and assay NSCs by RT-PCR at certain time-points after this addition. Figure 5.4 A shows that Oct4 is expressed after only 2 hours, but *Nanog* requires between 24-48 hours to become active. By day 6, *Nanog* is expressed strongly indicating OCT4 activation leads to *NANOG* activation, as has been shown using other systems [194].

Time delay between removal of doxycycline and silencing of Oct4

Next, the removal of doxycycline, and the effect on Oct4 and *Nanog* expression was assessed. In this experiment NSCs were treated with doxycycline for 7 days (to ensure robust activation of both OCT4 and *NANOG*), then doxycycline was removed at '0 hours' and cells were analysed at various time-points. Oct4 is tightly regulated by the transgene and the message has a very short half-life because after only 2 hours there is no detectable transcript (Figure 5.4 B). *Nanog* is expressed at low levels in NSCs that do not express Oct4; therefore, it is difficult to determine when *Nanog* was no longer enhanced when using RT-PCR. However, Figure 5.4 B shows a gradual decline in intensity of signal

over 48 hours; hence, *in vitro* culturing of NSCs after 7 days of OCT4 activation does not result in irreversible expression of *Nanog*.

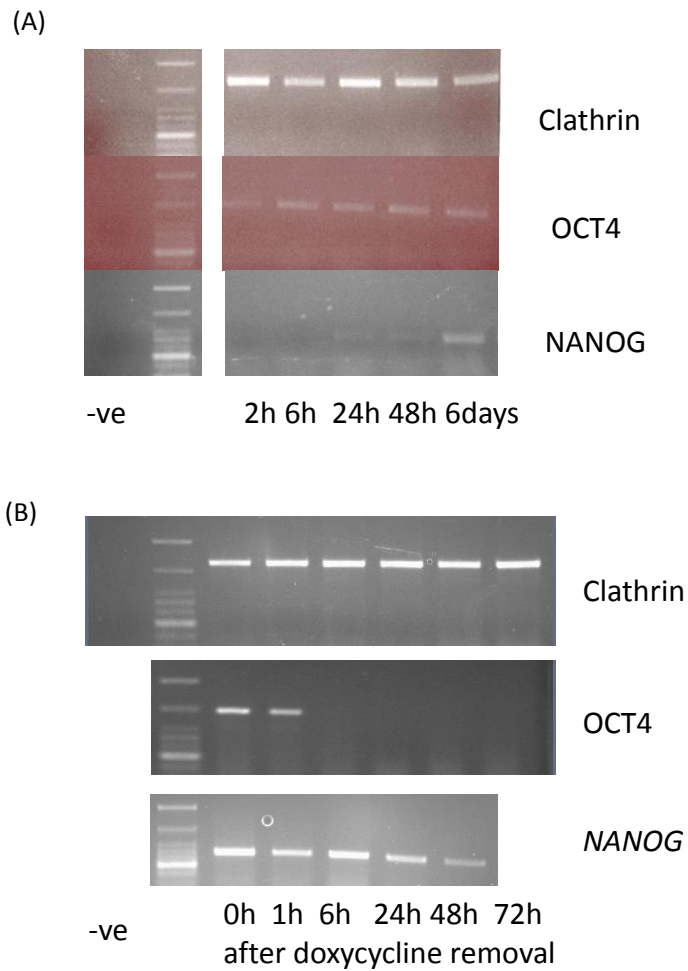


Figure 5.4. The effect of addition and removal of doxycycline on Oct4 and *Nanog* expression. (A) Doxycycline was added to neural stem cells cultured from postnatal day 4 Tet-Oct4 mice. The effects of doxycycline addition over time are shown by RTPCR. (A) clathrin loading control, (B) Oct4, (C) *Nanog*. Doxycycline was added and left for 10 days before being removed; at several timepoints after removal, RNA was taken for cDNA synthesis and RTPCR. (D) Clathrin, (E) Oct4, and (F) *Nanog*.

Activation of OCT4 in E8.5 ex-vivo brain tissue forms pluripotent colonies

The literature suggests that OCT4 induction in adult neural stem cells can activate a small number of cells to become pluripotent [81]. The strategy behind the experiments designed here aims at understanding the relationship between the cells in the brain and their ability to form a GCT. Our hypothesis is that CNS GCTs arise from cells from the brain, but it is not clear to which population the progenitor cell belongs. To understand how the stage of brain development of the cells might affect the ability to form a teratoma, the following strategy uses mixed brain cell types in order to determine if, and when, a brain cell could form a teratoma.

Transplantation of cells into the kidney capsule of a mouse is a useful assay to determine the potential of cells to form a teratoma. This assay shows at which ages of brain-cell populations can or cannot form teratomas.

However, there are limitations to this experiment. The kidney capsule does not have the same microenvironment as the brain. Both the local hormonal concentrations and physical interactions will be different, and these may be important factors in CNS GCT formation. As a specific example, glial cells often support the development of the brain and may be implicated in supporting tumour formation. The other major limitation was the age of mice; adult mice were used in this experiment but CNS GCTs most frequently occur by puberty.

In the first experiment, I examined mouse brain tissue of three different ages and their ability to form pluripotent cells when OCT4 was activated. This work was in collaboration with Dr. Valerie Wilson at the University of Edinburgh and was based on a protocol for culturing pluripotent epiblast stem cells. Figure 5.5 A shows the regions of brain removed from the mice before being cultured in EpiSC medium for 5 days in doxycycline to activate OCT4. These explants were assayed for OCT4 and *NANOG* expression by immunofluorescence. Figure 5.5 B shows that OCT4 and *NANOG* were activated at E11.5. However, at E13.5 *NANOG* was not present.

Interestingly, Oct4 expression was induced in cells from E13.5 but by post-natal day 7 (P7) it remained silent in tested cells. The Jackson Laboratory has documented that OCT4 protein is not found in the brain of postnatal mice treated with doxycycline so this result for P7 is consistent with these data.

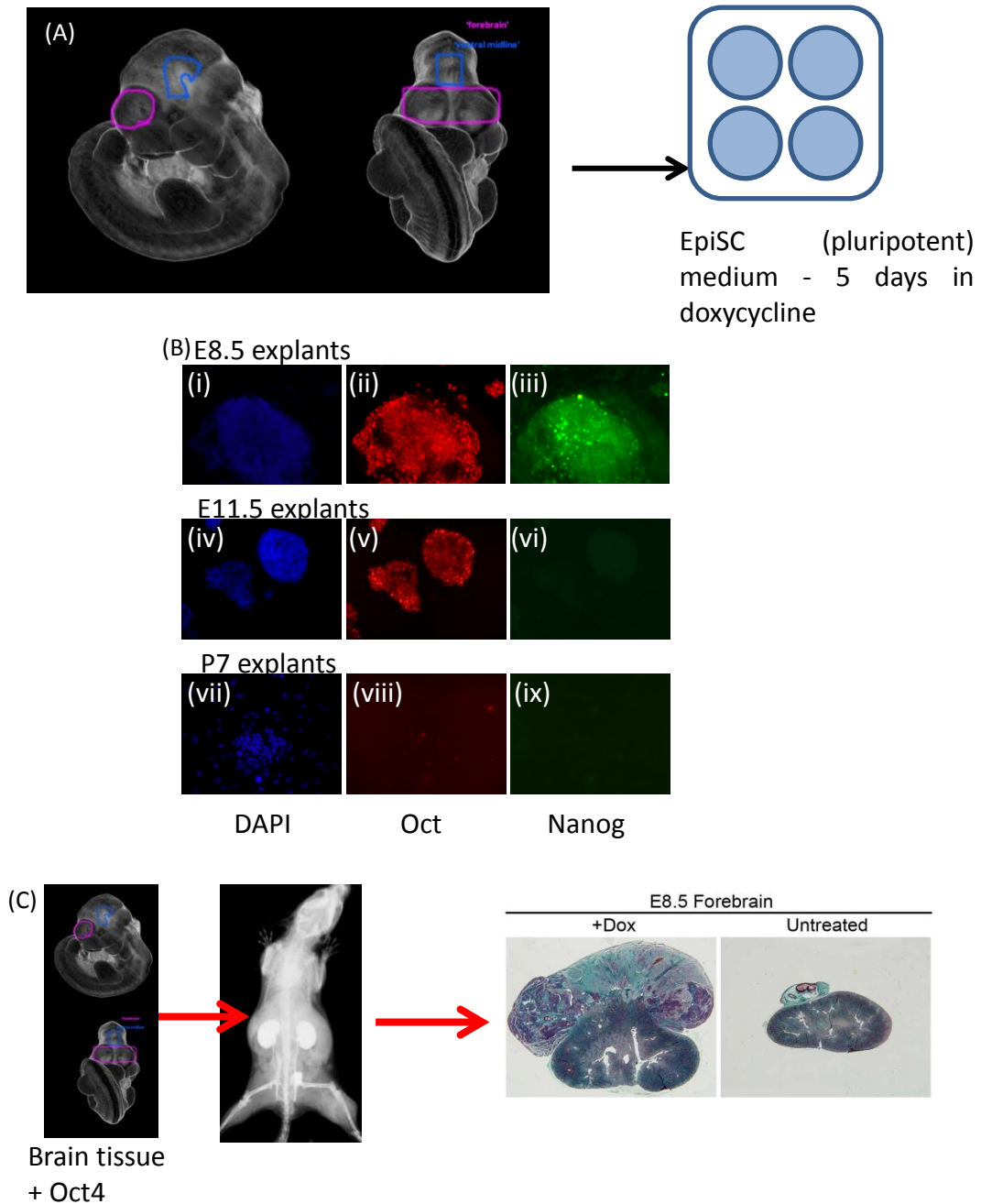


Figure 5.5. E8.5 brain tissue with activated OCT4 can form pluripotent cells and teratomas, but older tissue loses this ability. (A) A three-dimensional representation of the regions of mouse brain taken to test epiblast formation. Pink is forebrain, and blue is ventral midline. These regions were cultured in epiblast stem cell medium with doxycycline to activate Oct4. (B) Immunofluorescence for E8.5, E11.5 and P7 brain tissue using the procedure in (A). DAPI nuclear staining is illustrated in blue, OCT4 in red, and *NANOG* in green. E8.5 epiblasts express both OCT4 and *NANOG*, but E11.5 only express OCT4. By postnatal day 7, OCT4 is no longer expressed; however, this may be due to a transgene issue rather than a biological feature. (C) Brain tissue from E8.5 mice was cultured for 5 days in epiblast stem cell medium then transplanted into the kidney capsule of SCID mice. When Epiblast tissue was induced with OCT4 it formed a large teratocarcinoma, but without doxycycline no such tumour was found.

Activation of OCT4 triggers cells in E8.5 ex vivo brain tissue to form a teratoma in a mouse kidney

From the previous experiment, it appeared that Oct4 expression could activate *NANOG* expression at E8.5 and at E11.5, in agreement with published literature [195].

Our hypothesis predicts that activation of pluripotency may lead to the formation of a teratoma. Therefore, E8.5 was chosen as the developmental stage at which to test whether Oct4 expression could cause some cells to form a teratoma.

Figure 5.5 C is a schematic of the process to transplant EpiSC-cultured brain tissue into the kidney capsule. Whole forebrain tissue was dissected from E8.5 mouse embryos and directly transplanted into the kidney capsule of a SCID mouse. These SCID mice were treated with doxycycline by oral gavage, which activated OCT4 in only the transplanted cells. These tumours were left to develop for six weeks. The kidneys of mice treated with doxycycline or control mice with no treatment were dissected, wax embedded, and sectioned. Figure 5.5 C shows the large teratocarcinomas that formed in the kidneys of mice treated with doxycycline, but no growth was seen in controls.

During my time in Edinburgh (in collaboration with Valerie Wilson), forebrain tissue was isolated from E8.5 embryos and transplanted into the kidney capsule of SCID mice. Some of the host mice were treated with doxycycline to induce Oct4 expression and followed for several weeks. There was a clear distinction between the OCT4-activated and untreated kidneys; those mice treated with doxycycline formed large teratocarcinomas. This shows that aberrant expression of Oct4 in E8.5 ex-vivo brain tissue is capable of forming a germ cell tumour.

However, when this set of experiments was repeated several times in Nottingham, there were no signs of teratoma formation. There were several differences in the experiment in Nottingham. The main difference was the

preparation of tissue; in Nottingham, the tissue had to be dissociated before being injected into a kidney capsule, whereas in Edinburgh whole-forebrain was transplanted.

E8.5 is an early stage of development and it is unclear whether brain tissue from older mice would be able to form the same kind of tumours. However, since the positive result from collaboration in Edinburgh could not be repeated, it was not possible to assess which ages could form teratomas.

Induction of OCT4 in mouse embryos from E8.5-E10.5 causes minimal embryologic disruption

Oct4 is the only gene required to initiate neural stem cells to become pluripotent. Since the cell of origin for CNS GCTs is believed to be present in the first and second trimesters in humans, this equates to approximately E11.5 in mice. Therefore, we wanted to test whether activation of OCT4 *in vivo* before E11.5 would form a GCT.

The initial experiment tested the doxycycline-responsive system, and the effect of OCT4 on early embryogenesis. These were important to minimise the effect on animal welfare. Two female mice crossed with heterozygous males produced sets of embryos with a range of genotypes. The two females were given doxycycline by oral gavage each day from E8.5-E10.5 (Figure 5.6 A). When the mice reached E10.5 they were terminated, and the embryos were genotyped and assayed for expression of Oct4 by RTPCR (Figure 5.6 B). There appeared to be minimal disruption to the morphology of the E10.5 embryos when compared to controls (illustrated in Figure 5.2 C and D).

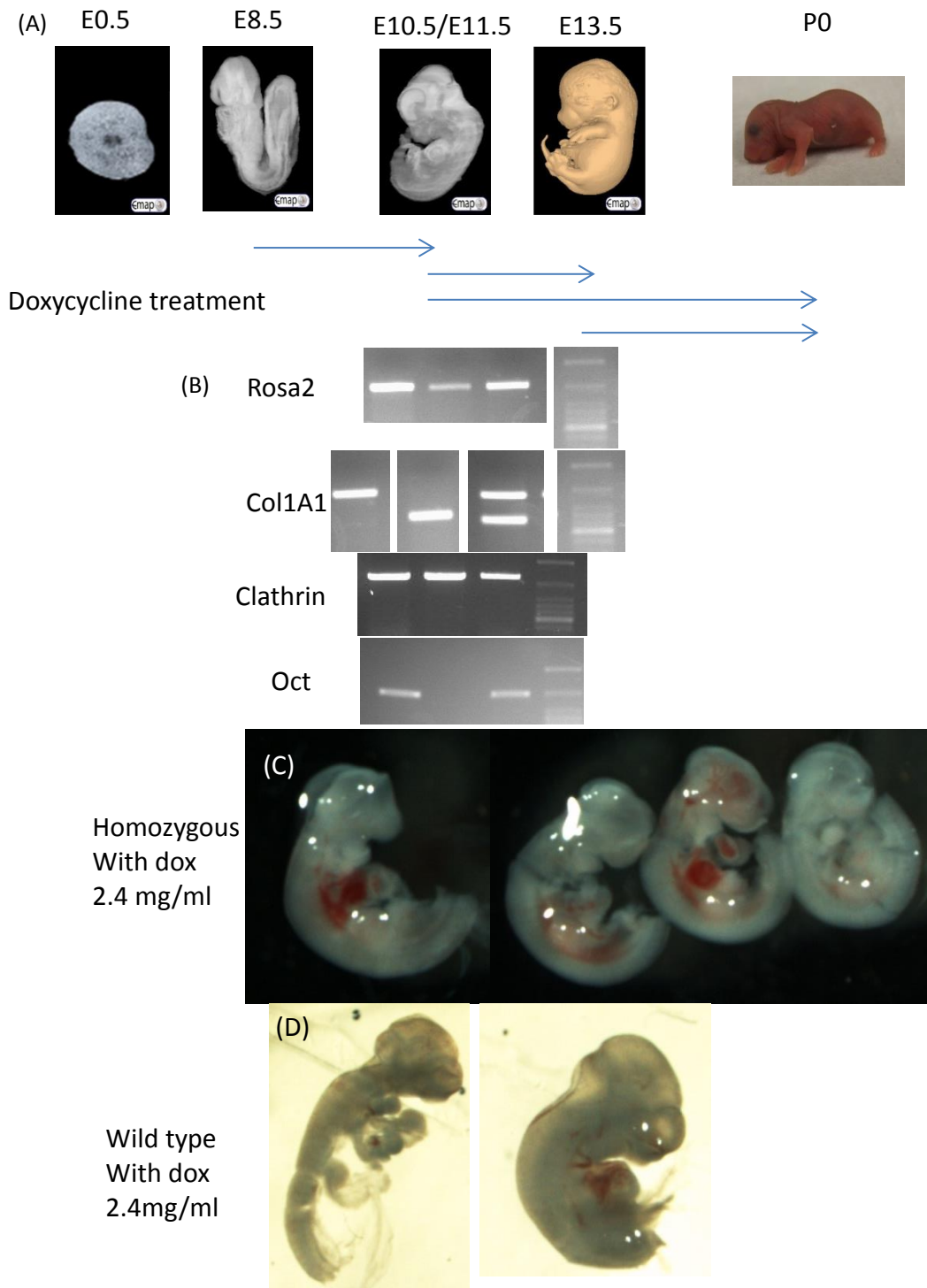


Figure 5.6. In vivo activation of OCT4 in mouse embryos. (A) Stages of embryo and length of time induced with doxycycline. Images of the embryonic stages of mice including E0.5, E8.5, E10.5/E11.5, E13.5 and a postnatal day 0 mouse. Oct4 was induced from varying embryonic ages for different lengths of time, mainly E8.5-E10.5, and E13.5 to birth. (B) Genotyping and RTPCR on brain tissue from doxycycline treated wild-type or homozygous mice. Genotyping was homozygous, wild-type, and heterozygous; and OCT4 was positive in the homozygous and heterozygous, but negative in the wild-type. (C and D) Induction of Oct4 from E8-10 embryos had minimal effect on embryogenesis. A pregnant female was treated by gavage with doxycycline (100 μ l of 2.4 mg/ml) on embryonic day 8 and 9 and the embryos were harvested on E10. (C) is a picture of 4 homozygous embryos; and (D) is a picture of two wild-type embryos. All embryos were severed at the cervical spine and had their tail removed for genotyping.

Induction of OCT4 in mouse embryos from E13.5 to birth causes minimal disruption to development

The experiments discussed above were designed to examine the effects of only a small time span of OCT4 induction; the next experiment tested the morphological effects over a longer period of time. Our overall objective was to induce OCT4 during an early age of embryogenesis and follow mice through to adulthood to see if they formed GCTs.

Pregnant mice were dosed with doxycycline from E13.5 until birth (Figure 5.6 A). The first female gave birth to her litter but did not feed or look after the pups. The pups were genotyped to confirm the presence of the Oct4 transgene, and the pup's brains were removed for analysis. All pups appeared to be normal (Figure 5.7 A) and were alive during the time between birth and termination. The brains from the pups had no distinct abnormalities, although this is difficult to confirm because dissection disrupted the fine detail (Figure 5.7 B and C). Analysis of these brains by RT-PCR showed that all of the pups expressed Oct4 compared with the wild-type control (Figure 5.7 D).

The fact that the mother left her pups unattended was an important problem because the long term aim of this experiment was to induce OCT4 during embryogenesis and determine if the pups formed tumours after several months of post-natal development. Only one pregnant mouse had been used to induce OCT4 in E13.5 embryos, so this experiment was repeated to determine if the problem was a result of the treatment.

The second pregnant mouse that was induced with OCT4 from E13.5 to birth also did not look after her pups. Genotyping confirmed that all of the pups carried both the Rosa26 and Col1a1 transgenes. However, this time there were some minor developmental defects. Figure 5.3 C is a photo of three pups and a very small deformed pup. It is unclear whether the deformity of this pup was caused by doxycycline and OCT4. A more consistent feature of Oct4 expression between E13.5 and birth was the reduced size of the limbs. In Figure 5.3 A, the

pups' limbs are longer and thinner than those in the repeat experiment. This suggests that Oct4 expression in other parts of the body is causing a morphological effect, and this phenomenon has been documented by The Jackson Laboratory. A second female dosed with doxycycline from E13.5-birth had a litter of several pups but proceeded to eat them – therefore, these data are not shown.

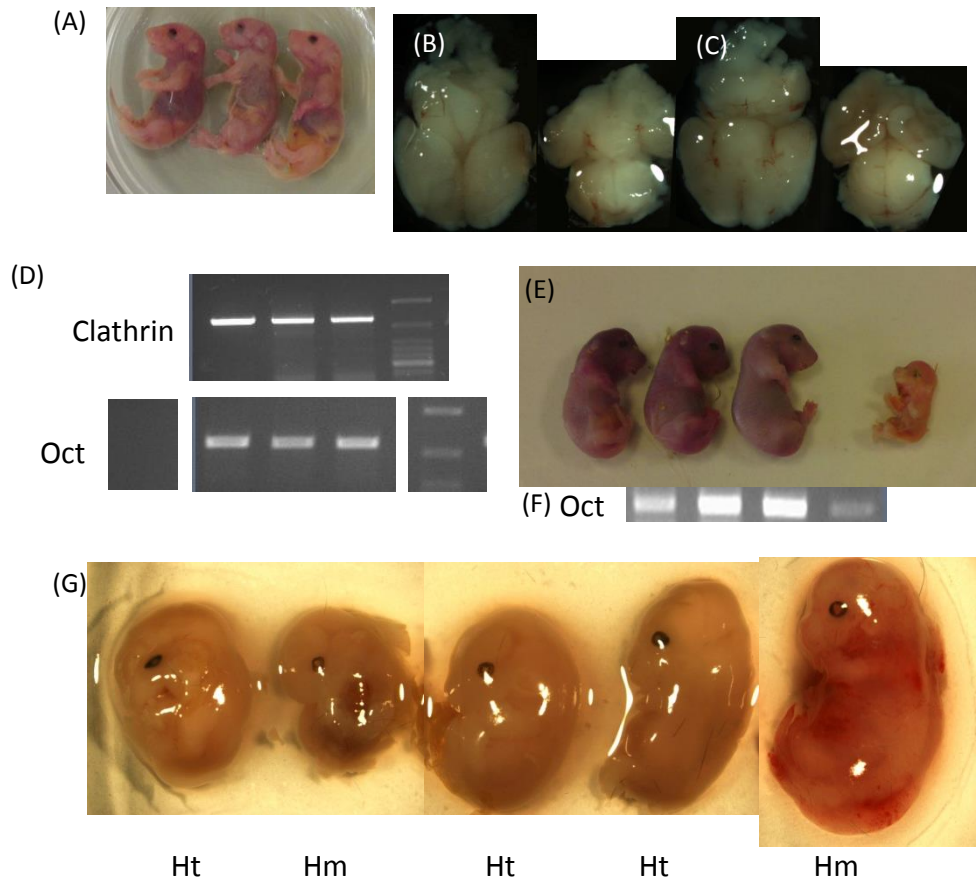


Figure 5.7. Induction of Oct4 from E13.5-birth has minor effects on embryogenesis.

(A) A pregnant mouse with E13.5 pups was treated by gavage with doxycycline (100 μ l of 2.4 mg/ml) every day until birth. At P1 all of the pups looked normal and were moving, but were terminated because the mother was not feeding them. (B and C) Two mouse brains were dissected and each was imaged from the dorsal and ventral view. Both of these brains looked normal, although there may have been subtle morphological differences. The dorsal view is pictured on the left, and the ventral image is on the right of each of the two brains. (D) Genotyping of the three mice in (A) confirmed the presence of the Oct4 transgene, and each mouse brain tested positive for Oct4. (E) A repeat of the E13.5-birth Oct4 induction experiment. The experiment in (A) was repeated and the pups were terminated at P0. These pups also looked fairly normal except for a shortening of the limbs, and deformation of a pup on the far right. (F) Genotyping confirmed that all the mice had Oct4 transgenes, and all expressed Oct4. The pup on the far right does not look like the others and may have been an anomaly. (G) Gavage was suggested to be a potential cause for the pups being left unfed by their mothers so doxycycline was changed to administration in the drinking water. The concentration was approximately 60mg/kg compared to gavage which was approximately 10mg/kg. The mother was terminated while the pups were E17.5 due to several morbidities. The uterus was dissected and the embryos revealed are pictured in (G). There was evidence of reabsorption in the uterus followed by the pups in this order. It is unclear whether this effect was caused by Oct4 or the absorption process. (<http://www.emouseatlas.org/emap/ema/home.html>).

In summary, in these experiments the mother was not looking after the pups. Nonetheless, the pups appeared to be able to survive pregnancy with minimal developmental disruption. It was suggested that gavage and scruffing (pulling the mice into position for gavage) may be causing stress to the pregnant mothers especially if they were treated until the day before birth. Therefore, we changed the protocol and administered doxycycline in the drinking water instead of gavage.

Homozygous mice were crossed with heterozygous mice to produce embryos that were all carrying the Oct4 transgene. The drinking water was supplemented with sucrose to ensure the mice drank it, and the concentration was calculated based on mice drinking 5ml of water. Unfortunately the mice became dehydrated and the pregnant female needed to be terminated at E17.5. The uterus was dissected and when the embryos (Figure 5.7 G) were analysed and all embryos were confirmed as either heterozygous or homozygous for the Oct4 transgene. There were some significant developmental defects in these embryos compared to the relatively normal pups in Figure 5.7 A and E. All the embryos had stunted growth and a deformed body. Pregnant females have been documented to “reabsorb” embryos if they are highly stressed so it was difficult to determine whether these results are part of the reabsorption process or a direct effect of doxycycline activation of OCT4.

Induction of OCT4 from E11.5-E14.5 causes spontaneous embryo reabsorption

In our ideal experiment, we would have treated E11.5 embryos with doxycycline because Oct4 is expressed but at low levels. Induction of OCT4 would therefore mimic a continuation of OCT4, and test whether this would form a GCT in the long-term.

There were four attempts to administer doxycycline by gavage beginning at E11.5; however, each time the pregnancy failed to reach term. It is sometimes difficult to confirm whether mice with E11.5 embryos are pregnant because the mother only shows strong signs of pregnancy between E13.5-E15.5. Therefore, all of the mice that had aborted pregnancy were dissected for evidence in the uterus, and each of the mice had been pregnant but appeared to have reabsorbed their embryos.

Induction of OCT4 from E13.5-E16.5 caused minimal effects on later development

The ideal situation to test whether OCT4 could cause CNS teratomas would have been induction of OCT4 from E11.5 through to birth. However, the data above suggested that using oral gavage was too stressful on pregnancy around E11.5, and towards birth. Therefore, the period of induction was limited to E13.5-E16.5. Information on the Jackson Laboratory's website suggests that this strain of mice should not be treated for more than 4-5 days because OCT4 activation can negatively affect the mother's health. Therefore, administration of doxycycline was limited to 4 days.

At the end of my project, a total of eight litters were born after being treated with doxycycline from E13.5-E16.5. These are now being monitored for changes in health, and perhaps brain tumour formation as they age.

5.4 Discussion

The experiments in this chapter tested the hypothesis that a CNS GCT could be formed from a brain cell. The three strategies examined this hypothesis in different ways to maximise the chance of forming a teratoma. Several studies have examined pluripotency, and in this section I will discuss how the experiments in this chapter have added to the literature.

The main aim of this chapter was to test whether a GCT forms when OCT4 is activated in brain cells *in vivo*. Pluripotency studies, such as that by Kim *et al.* (2009), examined induction of NSCs to a pluripotent state using overexpression of Oct4 by viral transduction [81]. Kim's use of viral transduction as an *in vitro* technique required cells to be cultured, which may have changed their properties. In comparison, our study used *in vivo* activation of OCT4, which had effects on development when activated during embryogenesis.

The OCT4 mouse model was validated for rapid activation of OCT4 in cultured NSC populations, and *in vivo*. GCTs often form during childhood, and are thought to arise in the first or second trimester. From a technical perspective, using a mouse model provides a practical method of rapidly activating OCT4 at a stage in development when GCTs are believed to arise.

OCT4 induction in mouse brain tissue and teratoma formation

The first important result is the ability of E8.5 forebrain to form teratocarcinomas when OCT4 is activated. This shows that when OCT4 is dysregulated and aberrantly expressed in a brain cell using our system it has the potential to induce the formation of a GCT. However, when the forebrain of an E8.5 embryo was dissociated and induced with doxycycline, in a repeat experiment, no teratomas formed. While this does not seem consistent, the role of the microenvironment may be important in understanding these results.

First, there is inevitable cell death when tissue is dissociated and resuspended in PBS. If there are only a few progenitors in an E8.5 forebrain, the chances of these surviving are limited by this dissociation.

Further, dissecting the forebrain and transplanting it directly into a kidney capsule maintains both intra- and intercellular structure. There are several supportive cell types within the brain, such as glial cells, which may be integral to maintaining the progenitors. This would explain why whole forebrain could form a teratocarcinoma but dissociated forebrain could not. While matrigel was not used during this experiment, it may be a useful addition in further experiments.

OCT4 induction in vivo

The *in vivo* experiments were informative, but had limitations. The conditions for doxycycline administration *in vivo* were optimised to balance maximum OCT4 activation with the greatest chance of survival for embryos. This period was from E13.5-E16.5, and these pups were looked after by their mothers.

A total of eight litters were born and are currently being kept for several months before termination and analysis. The formation of GCTs in the brains of these mice would be an indicator of two things: our hypothesis would be strengthened, and it would appear that reactivation of Oct4 after normal silencing is sufficient to form a GCT.

Conversely, would the lack of a CNS GCT disprove our hypothesis? Proponents for the hypothesis of a germ-cell or origin would argue that OCT4 is not sufficient to induce a GCT. However, since CNS GCTs are rare, it may be predictable that the conditions for GCT formation require more than just OCT4 activation.

The mechanism of OCT4 activation in our hypothesis may be intrinsic to why GCTs do not efficiently form in the brain. Our hypothesis suggests that disruption to the methylation of the Oct4 gene may be responsible for OCT4

activation. Disruption to just one gene seems implausible, and it may be more realistic that large sections of the genome lack methylation; for example, due to dysregulation of a DNA methyltransferase. A lack of methylation over large sections of DNA is likely to activate genes that are normally silenced, such as oncogenes, and these oncogenes may be crucial for the initiation of CNS GCTs. In summary, we suggest that lack of global methylation may be responsible for OCT4 activation, which subsequently activates accessory genes that synergise with pluripotency genes to form GCTs.

Our hypothesis here suggests that OCT4 is activated in a cell that has a hypomethylated genome, which may explain the lack of GCT formation in our experiments. In support of this hypothesis, the GCT subtypes associated with pluripotency, such as germinomas, often display distinctly lower levels of global methylation compared with the differentiated subtypes; for example, yolk-sac tumours. While we propose disruption to methylation as an initiating event, other factors may regulate the pathway the progenitor cells take. This may explain the differences between the progenitors proposed, which have low levels of methylation, and those that are methylated and differentiated (such as yolk sac tumours).

There were many factors to consider during the design of these experiments. One of the main difficulties was activating OCT4 at an early stage of embryogenesis. E8.5-E11.5 is an interesting period of development with regards to OCT4. During this E8.5-E11.5 period, endogenous levels of OCT4 are initially readily detectable but rapidly decrease. We originally set out to test whether GCTs would form after continuation or activation of OCT4. Since induction of OCT4 at E11.5 resulted in spontaneous termination of embryos, it was not possible to test whether continuation of OCT4 activation could initiate a GCT to form. Instead, we had to activate OCT4 at E13.5, which activates OCT4 in cells that do not express it.

It was unclear why doxycycline-treated mothers spontaneously reabsorbed their embryos. Stress due to the gavage procedure, or a direct effect

of OCT4 on the mother instead of the pups, may have been factors for reabsorption. The main argument would be that OCT4 caused abortion by disrupting embryo development, instead of the mother's ability to support them. If OCT4 causes abortion between the ages of E8.5-E13.5, the equivalent human patients would not reach maturity and form a GCT; however, aberrant expression of Oct4 probably only happens in one or a few cells in humans. These studies were in mice, and mouse development is very different to human development. Furthermore, the mothers themselves experienced activation of OCT4, which may have been the cause of these abortions. It should be noted that this is speculation, and this study could not confirm whether OCT4 can or cannot be a mechanism for GCT formation.

Our experiments attempted to induce pluripotency using activation of OCT4 *in vitro* and *in vivo*. We tested the potential for teratomas to form from an isolated stem cell population, brain tissue, or in a transgenic mouse model. Teratomas were successfully formed by inducing OCT4 in mouse forebrain tissue and transplanting the tissue into the kidney capsule. Further work will examine the effect OCT4 induction during embryogenesis has on the long-term health of our OCT4-transgenic mice.

Chapter 6: *KIT* and *ETV1* expression in the CNS as a mechanism for germinoma formation

6.1 Introduction

Germinomas in the CNS have been documented to mainly occur in the pineal and suprasellar regions. They are considered to be a homogeneous tumour and have been hypothesised to develop from undifferentiated carcinoma *in situ* (see Chapter 1). In this thesis I have so far examined alternative explanations and hypotheses for CNS GCT formation, and in this chapter I examine a specific mechanism for germinoma formation; the oncogenic potential of *ETV1* and *KIT* interaction.

Germinomas, seminomas, and dysgerminomas express high levels of *KIT*, in addition to possessing an activating mutation in the *KIT* coding sequence. The activating mutation in the *KIT* gene causes the *KIT* protein to be constitutively active i.e. it does not require the usual ligand (*STEEL*) for activation of its tyrosine kinase function. These two events may seem counter-intuitive; why would the protein need to be highly expressed as well as constitutively active? Several further questions follow on from this: is high expression of *KIT* without an activating mutation sufficient to form a germinoma from the cell of origin? Alternatively, would low expression of a mutated form of *KIT* be sufficient to signal downstream targets? First, we must understand the relationship between *KIT* and oncogenesis.

The study of certain gastric cancers has revealed that *KIT* and *ETV1* are sufficient to cause a cascade of events that eventually leads to a gastro-intestinal stromal tumour (GIST) [196]. *KIT* activates several proteins by a phosphorylation pathway, and one of those paths leads to the stabilisation of the transcription factor *ETV1* (Figure 6.1 A). *KIT* only stabilises *ETV1* and does not increase its expression.

Indeed, a key finding by Chi *et al.* 2010 was that the inhibition of ETV1 in cells that expressed a mutated form of KIT failed to induce tumour formations [196]. This shows that ETV1 is required for tumour formation in this setting. Equally, ETV1 overexpression was shown to have little effect on proliferation since it is the stabilisation of the protein that is important, not the amount of mRNA.

The cell of origin for gastro-intestinal stromal tumours (GIST) is a subset of interstitial cells of Cajal (ICC). The authors reported high expression of ETV1 in these cells, and showed that activation of the KIT pathway triggered the formation of cancer. Inhibition of KIT rapidly decreased the amount of ETV1 protein but did not change the level of ETV1 RNA, which supports the hypothesis that KIT stabilises ETV1 protein. Furthermore, overexpression of endogenous KIT without mutations did not have a significant effect on the stability of ETV1.

The increase in activated ETV1 by KIT was the most likely oncogenic mechanism because the cells where KIT activation occurred were those that already expressed ETV1. Since KIT is both mutated and overexpressed in almost all cases of germinoma, we concluded that ETV1 might also be essential to this process. This relationship is important because if ETV1 is required to form a germinoma it could be an important therapeutic target.

6.2 Hypothesis

Germinomas all express high levels of KIT (often carrying an activating mutation), which suggests that KIT is integral to germinoma formation. There are at least three potential explanations for this; KIT could initiate an oncogenic event in a cell in the brain and eventually trigger the formation of a germinoma; KIT is not involved in the initial oncogenic event but is required for a tumour to acquire a germinoma phenotype, as opposed to a different type of tumour; or germinomas are formed from mismigrating germ cells that already express high levels of KIT i.e. as Teilum's theory predicts. The latter has been discussed before so the first two suggestions will be the main focus of this chapter.

The majority of GCTs in the CNS, such as teratomas, develop in utero or shortly after. Comparatively, the earliest published case of CNS germinoma diagnosis was in a 5 year old patient [197], but germinomas more frequently occur around puberty [198]. Our hypothesis suggests that all GCTs arise from a brain cell that has become pluripotent; so what influences the development of a germinoma compared to a teratoma?

The germ-cell progenitor hypothesis states that these cells are simply misplaced germ cells and are encouraged to form germinomas during puberty due to high levels of hormonal activity. However, this chapter will examine the hypothesis that *ETV1* and *KIT* expression may play a role in the formation of germinomas from endogenous brain cells.

ETV1 has been documented to be required to form GISTs when *KIT* is expressed, so it seems plausible that if the same relationship applies to germinomas, *ETV1* should be expressed when *KIT*-positive germinomas occur [196]. *KIT* is known to stabilise *ETV1* protein through the RAS/RAF/MEK pathway. *KIT* is both mutated and expressed highly so this hypothesis also predicts that *KIT* might also be normally expressed in regions where germinomas form. Evidence that would support this hypothesis would be an overlap of these two genes in regions that would then support germinoma formation.

6.3 Aims

The main aim of these experiments was to evaluate the expression patterns of *Etv1* and *Kit* in the mouse brain in an unbiased way. Therefore, *in situ* hybridisation was used to detect regional expression of these genes. This required an RNA-probe specific and complementary to the RNA of either *Kit* or *Etv1*. The first aim was to design and test an RNA probe for both. These probes were then used to analyse expression in different ages and regions of mice brains.

6.4 Results

RNA-expression plasmid construction

Full-length *Kit* and *Etv1* cDNA were amplified by RT-PCR and ligated into the pcDNA3.1 vector (Figure 6.1 B). Subsequently, each cDNA (*Kit* and *Etv1*) was ligated into pBluescript for RNA probe synthesis. These plasmids were both verified by sequencing (Figure 6.1 C).

Kit and *Etv1* probes were synthesised from the respective pBluescript plasmid and tested for the ability to bind to complementary DNA. The plasmids that the probes were generated from were used to test this binding. (Figure 6.1 D). Plasmids were baked onto paper and tested by *in situ* hybridisation with the complementary probe; for example, anti-sense ETV1 probe on ETV1 plasmid. The colour solution was either left in development solution for 30 minutes or overnight, and an increased concentration of probe produced a more intense colour signal.

Next, the binding specificity was tested by hybridising a control probe onto each plasmid. Here, the *Kit* probe was tested on *Etv1* plasmid, and the *Etv1* probe was added to *Kit* plasmid. Figure 6.1 E shows that the *Etv1* probe produces a colour when bound to the *Etv1* plasmid, but not when attempted on the *Kit*

plasmid. This specificity was similar for the *Kit* probe, showing that the *Kit* probe was specific to *Kit* plasmid only. These data show that the probes produced were sensitive and specific enough to attempt an *in situ* hybridisation on mouse tissue.

Etv1 in situ hybridisation on E15.5 and adult mouse brains

Many attempts were made to optimise the *Etv1* and *Kit* probes (data not shown) before the successful attempts in Figure 6.2. The *Etv1* probe worked much better than the *Kit* probe so *Etv1* was the main focus of the *in situ* hybridisation experiment described. Expression of *Etv1* can be clearly seen in the E15.5 mouse head using an anti-sense probe (Figure 6.2 A and B). A blue signal is absent in the control section (Figure 6.2 C), which is hybridised with a sense probe. Although it is difficult to determine the exact regions of expression, it appears that there is strong staining in the medial and dorsal pallium which develops into the cortex, and widespread expression throughout other areas of the E15.5 brain.

In situ hybridisation using an anti-sense *Etv1* probe on adult mouse brain sections resulted in more distinct expression patterns (Figure 6.2 D and E) such as the cortex. This, compared to the sense-probe in Figure 6.2 G which did not show any staining for *Etv1*, suggests that the positive staining is specific.

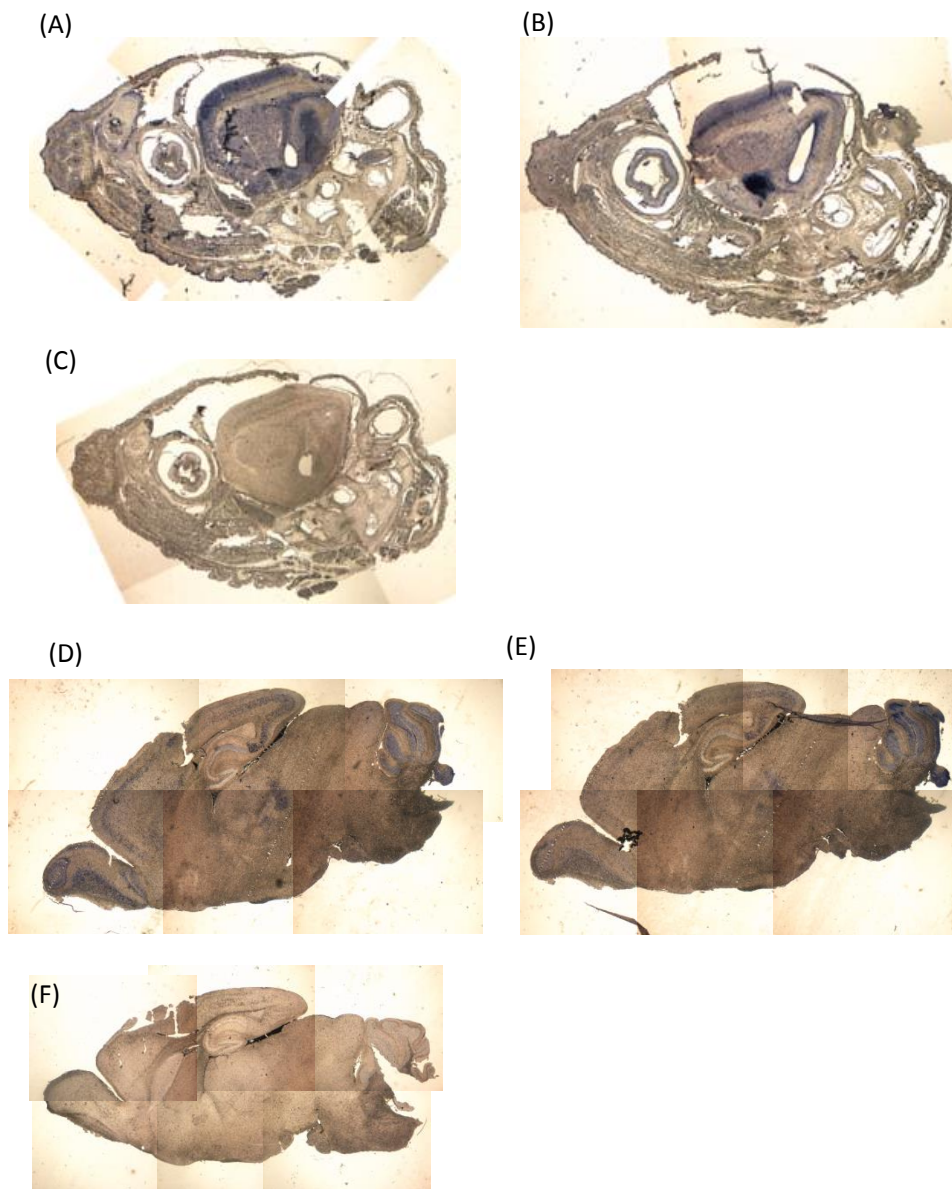


Figure 6.2. Optimisation of Etv1 probe on sagittal E15.5 embryos and adult mouse brain tissue (A-C) Sagittal sections of E15.5 embryo heads hybridised with either anti-sense (A-B) or sense control (C) probes for Etv1 *in situ* hybridisation. Etv1 positive staining is blue indicating expression, and normal tissue is brown. (D-F) Sagittal sections of an adult mouse brain hybridised with either anti-sense (D-E) or sense control (F) probes for Etv1 *in situ* hybridisation.

Etv1 in situ hybridisation on a postnatal day 7 mouse brain

Adult brains have different expression patterns of many genes, including *Etv1*, when compared with embryonic stages. However, sectioning embryonic stages is technically difficult and often does not show sufficient detail of where genes are expressed. With this in mind, a detailed analysis of a postnatal day 7 mouse was performed in order to gain a better understanding of developmental *Etv1* expression. Transverse sections were hybridised with the *Etv1* anti-sense probe; representative staining of sections are shown in (Figure 6.3 A-F). There are several regions of high expression such as the cortex which is consistent with the expression in the E15.5 stage and in adults. There is a lack of *Etv1* expression in the centre of the brain, especially in ventral sections. The only exception to this appears to be two small patches of expression in the dorso-medial thalamic nucleus.

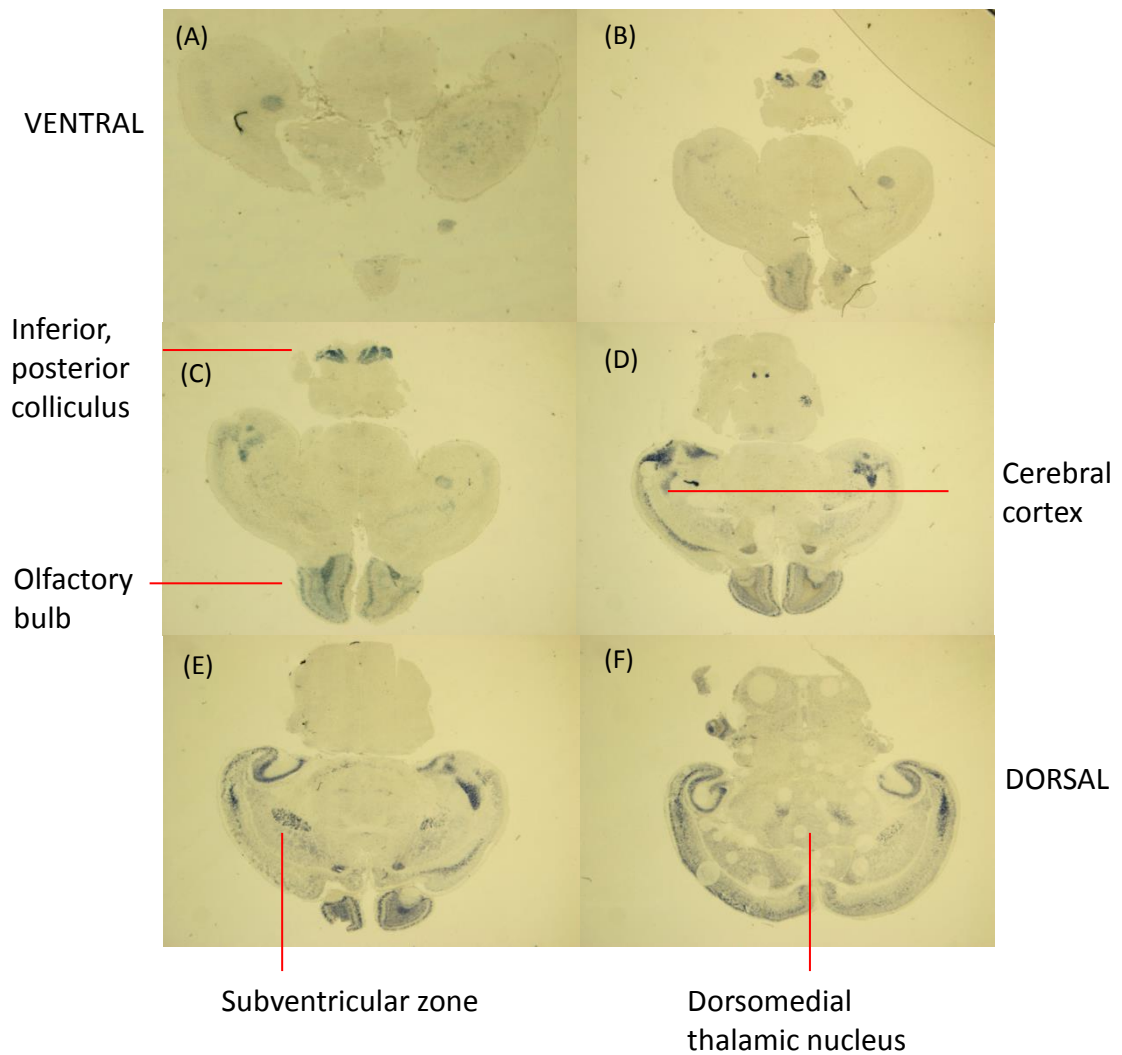


Figure 6.3. Postnatal day 7 mouse transverse sections of a brain hybridised with anti-sense Etv1 for in situ hybridisation. Etv1 positive staining is blue indicating expression, and normal tissue is beige. A-F are sections from ventral through to the dorsal. Several regions that have been stained are highlighted in red with the approximate anatomy labelled. (C) Two regions of the brain suggest the posterior colliculus. Olfactory staining is also present. (D) Staining in outer layers of the cerebral cortex, justified by the consistent staining in (E) and (F). (E) both subventricular zones appear to have staining, especially a single patch of strong staining anteriorly, which is consistent with (D). (F) two distinct patches suggest the dorsomedial thalamic nucleus. These structures are within the thalamus which is part of the diencephalon.

Allen Brain Atlas expression

At the end of 2012, the Allen Brain Atlas [199] updated their expression data on *Kit* and *Etv1*. Previously, the Allen Brain Atlas *in situ* hybridisation data was of poor quality; however the update increased the quality of these images. Figure 6.4 shows a comparison between the Allen Brain Atlas images and the data produced using my *Etv1* probes. There was distinct expression of *Etv1* in a layer of the cortex and cerebellum which was consistent with my results. In addition, there is a small patch of expression in the centre of the sagittal section which is shown on both the coronal and sagittal sections from the Allen Brain Atlas data. Since these figures were such high quality and consistent with my own previous attempts, further *in situ* hybridisations using the anti-sense *Etv1* probe on tissue of other ages were halted.

The Allen Brain Atlas update provided an opportunity to analyse the expression of *Etv1* and *Kit* in brain tissue of several different ages and from two different perspectives; sagittal and coronal. *Etv1* expression appeared to be localised to the same regions as previously mentioned i.e. a layer of the cortex, the granule layer of the cerebellum, and two small patches of expression in the thalamic region (Figure 6.4 A-F).

A brief look at the sections from the Allen Brain Atlas showed an ambiguous pattern around E13.5. This pattern needed to be validated so whole mount *in situ* hybridisation was used on E13.5 embryos with sense- and anti-sense probes (Figure 6.4 G and H). The sense probe (control) showed no staining, whereas the anti-sense probe for *Kit* showed a distinct staining pattern (Figure 6.4 H).

The *Etv1* anti-sense probe appeared to be reliable because in Figure 6.4 G it gave a distinct pattern of forelimb, hindlimb, and somites. This appeared to be specific binding because the rest of the forelimb was not stained and repeats showed that this pattern was consistent.

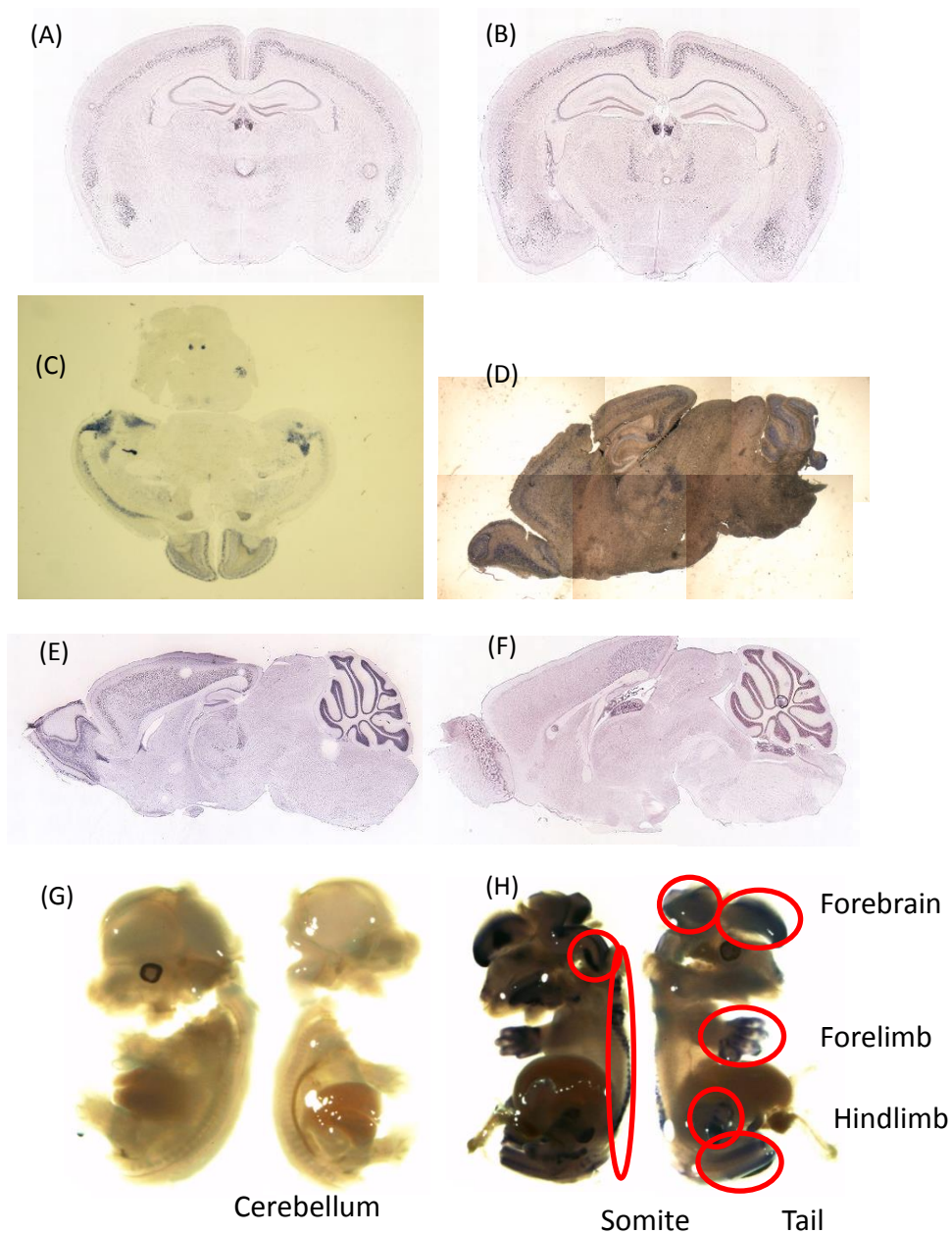


Figure 6.4. A comparison between sections of respective ages from the Allen Brain atlas compared to my results. Etv1 positive staining is blue indicating expression, and normal tissue is beige. (A-B) Coronal section showing a staining pattern of two regions of midline expression similar to (C). (D) Similar staining patterns to (E-F), notably the central expression, olfactory, and cortex. (G) Sense-probe whole mount *in situ* hybridisation on an E13.5 embryo compared to anti-sense probe (H). E13.5 embryos were cut in half through the sagittal plane. Staining appears to be in the cerebellum, forebrain, brainstem, somites, forelimb, hindlimb, and tail in (H). Staining in the extremities appears to be in the outer layers only instead of throughout, illustrated by staining for the hand. Figure 6.4 A, B, E and F are from Allen Brain Atlas, and all other *in situ* hybridisations used the Etv1 probe developed in previous figures.

Etv1 staining was also similar to the Allen Atlas (data not shown). These embryos were embedded in wax and sectioned but this was technically challenging and was not repeated (See Appendix II). While there was expression in the brain, the difficulties with embedding and sectioning meant that detailed analysis was not possible.

Due to the difficulties in sectioning young embryos, the Allen Brain Atlas was used to examine specific locations in the brain at several ages. The major limitation was a lack of repeats; sometimes there was only one view, for example sagittal.

Allen Brain Atlas sections showed four regions of dual *Kit/Etv1* expression: the medial habenula, periventricular thalamic nucleus, the medulla oblongata region, and the medullary spine. This section examines the first two of the four, and the last two are discussed shortly.

The medial habenula is part of the pineal stalk. Since we are more concerned with dual expression of *Kit/Etv1* correlating with germinoma formation, this region will either be described as the pineal or habenula region. Staining for *Etv1* is strong and discrete from stage E15.5 (Figure 6.6) to adulthood (Figures 6.7-6.11). Unfortunately there were no coronal sections for *Kit*, so it was not possible to verify expression of *Kit* in this region. Equally, it was not possible to exclude the possibility of *Kit* expression in this region – *Etv1* staining in the habenula is only visible using a coronal section and is not visible on a sagittal section.

The staining around the periventricular thalamic nucleus changes with age. This may be due to the slight differences in depth of section, which can appear different if only a thin layer of cells express the gene. For simplicity, this region will be termed the thalamic region. Staining in the thalamic region is consistent from E15.5 to adulthood for *Etv1* (Figure 6.5-6.11). Strong staining only appeared visible at P4 for *Kit* (Figure 6.8); however, upon higher magnification, *Kit* is expressed throughout the mouse brain. Specifically, *Kit* is strong in single cells, but these cells are not densely clustered together like *Etv1*. An example of this is

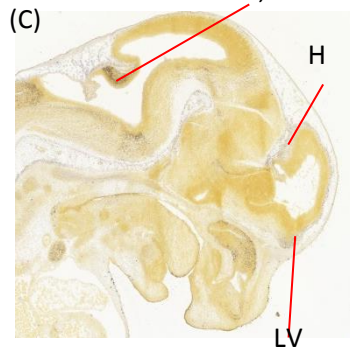
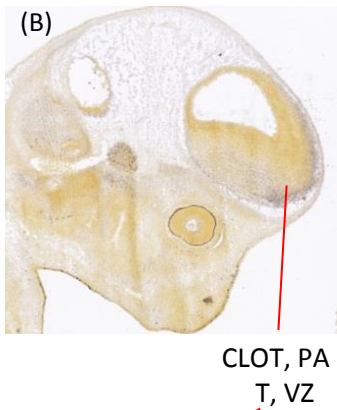
E18.5, where there are several denser patches of expression, but diffuse staining throughout the brain (Figure 6.7).

Embryos that were stained with *Etv1* and *Kit* showed expression in several regions at E13.5 (Figure 6.5 A-F), and midline regions by E15.5 (Figure 6.6 D-F), but the exact regions of expression were unclear. The medial habenula (Figure 6.6 D), periventricular thalamic nucleus region (Figure 6.6 E), and corpus callosum (Figure 6.6 F) were all implicated as regions where *Etv1* was expressed in these embryonic ages. There were no coronal sections stained for *Kit* at E15.5.

In summary, *Etv1* and *Kit* expression overlapped in the pineal stalk, the suprasellar region, and cortex over several ages of development and into adulthood in mice. Other regions of the mouse brain expressed only *Kit*, such as the cerebellum.

Figure 6.5. E13.5

Kit



Etv1

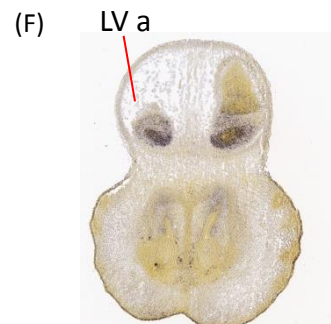
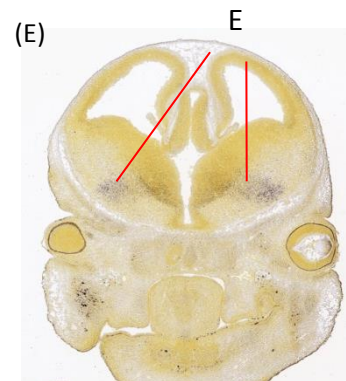
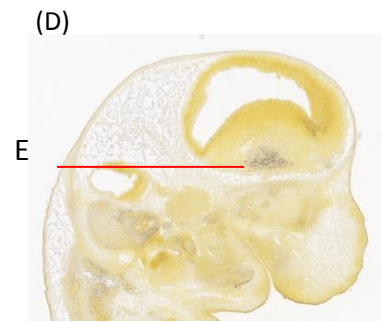


Figure 6.5-6.23. In situ hybridisation using a Kit or Etv1 anti-sense probe on various ages and views of mouse brain taken from the Allen Brain atlas or EMAGE database. Background is pale blue or brown, and positive staining is dark blue. Some areas appear dark blue due to the density of cells in that area such as the cerebellum. When producing Figures 6.5-6.23, all regions of colour development were labelled according to the Allen Brain Atlas. Each colour signal was verified by magnification to confirm that the colour signal was within the cells of the tissue, and not solid colour, which can suggest non-specific staining. Confirmed regions of expression are indicated by a red line and a code. The code refers to a region of the brain found in the abbreviations section. Kit staining is weak and found in almost all regions at E18.5 and beyond but only regions of intense staining are indicated as positive. Only select regions are highlighted in these figures; all regions with positive staining can be found in Appendix II.

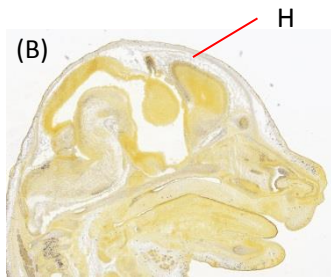
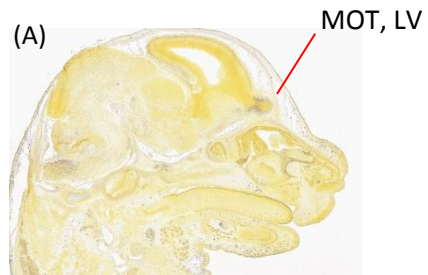
Figure 6.5-6.11. All regions that show positive staining have been identified except those in the medulla or hindbrain regions. Kit is expressed in the cerebellum at E18.5 (Figure 6.7 A and B), P4 (Figure 6.8 A and B), P14 (Figure 6.9 A and B), P28 (Figure 6.10 A and B), and P56 (Figure 6.11 A and B). Sections hybridised with Etv1 probe did not show staining in the cerebellum at any age (Figure 6.7-6.11). There are low levels of Kit expression throughout the brain when magnified, but Etv1 appears to be distinct to specific regions.

There were several midline regions that showed overlap of the expression of both genes. The two most striking regions were the thalamic nuclei and habenula. These two regions are comparable to the hypothalamic region and the pineal region respectively. The thalamic nuclei appeared to express Etv1 and Kit genes at E18.5 (Figure 6.7 C), P4 (Figure 6.8 A-D), P14 (Figure 6.9 C), P28 (Figure 6.10 C-E), and P56 (Figure 6.11 D). There was sparse expression of Kit when examining specific regions as mentioned above.

The habenula or pineal stalk is a very small region but for Etv1 it was clearly seen at E15.5 (Figure 6.6 D), E18.5 (Figure 6.7 E), P4 (Figure 6.8 F), P14 (Figure 6.9 E), P28 (Figure 6.10 F), and P56 (Figure 6.11 G). The habenula was not seen on sagittal section of Etv1 but were clear when using coronal sections. Unfortunately, since there were only sagittal sections for Kit expression, which may have meant that expression was present in small areas, such as the habenula, but sagittal sections were not as reliable as coronal sections in this instance.

Figure 6.6. E15.5

Kit



Etv1

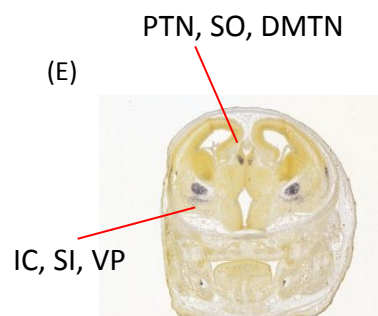
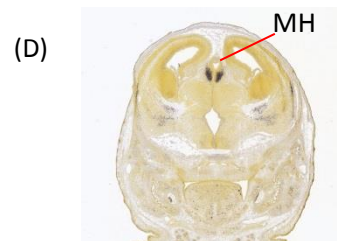
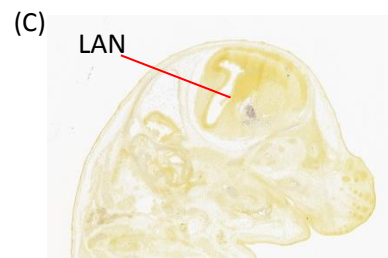
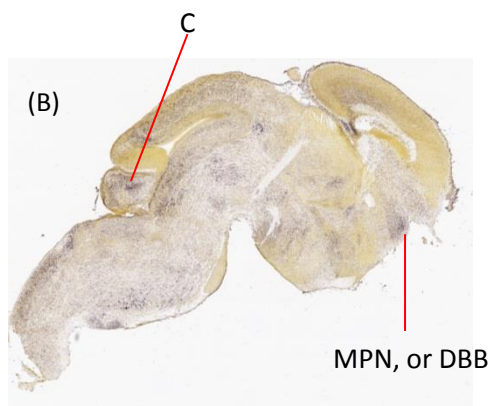
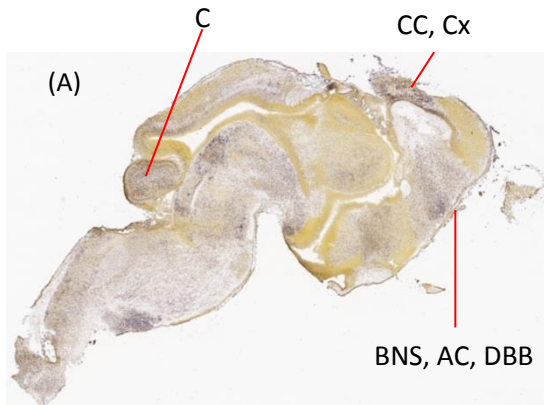


Figure 6.7. E18.5

Kit



Etv1

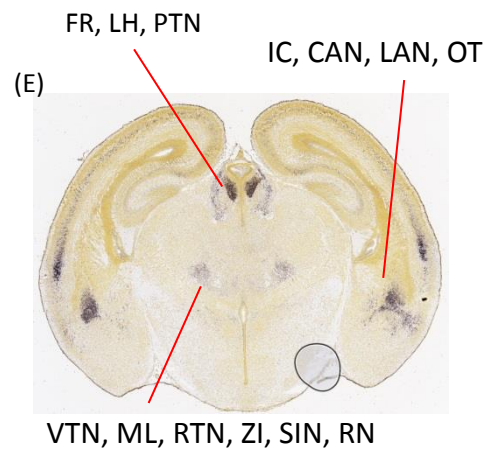
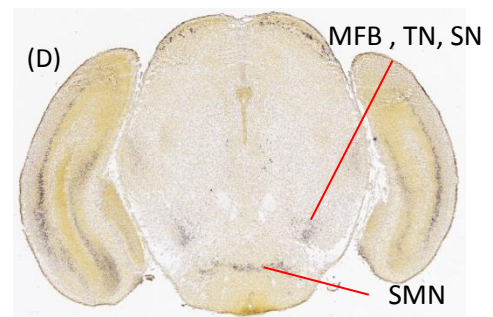
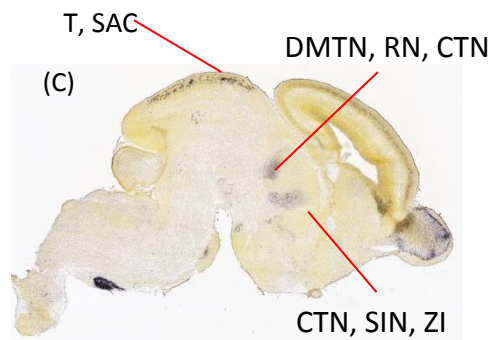
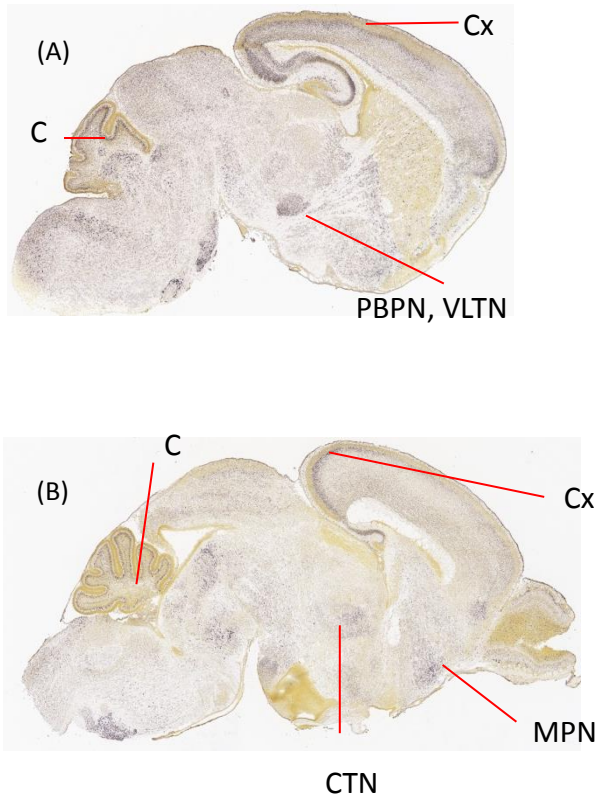


Figure 6.8. P4

Kit



Etv1

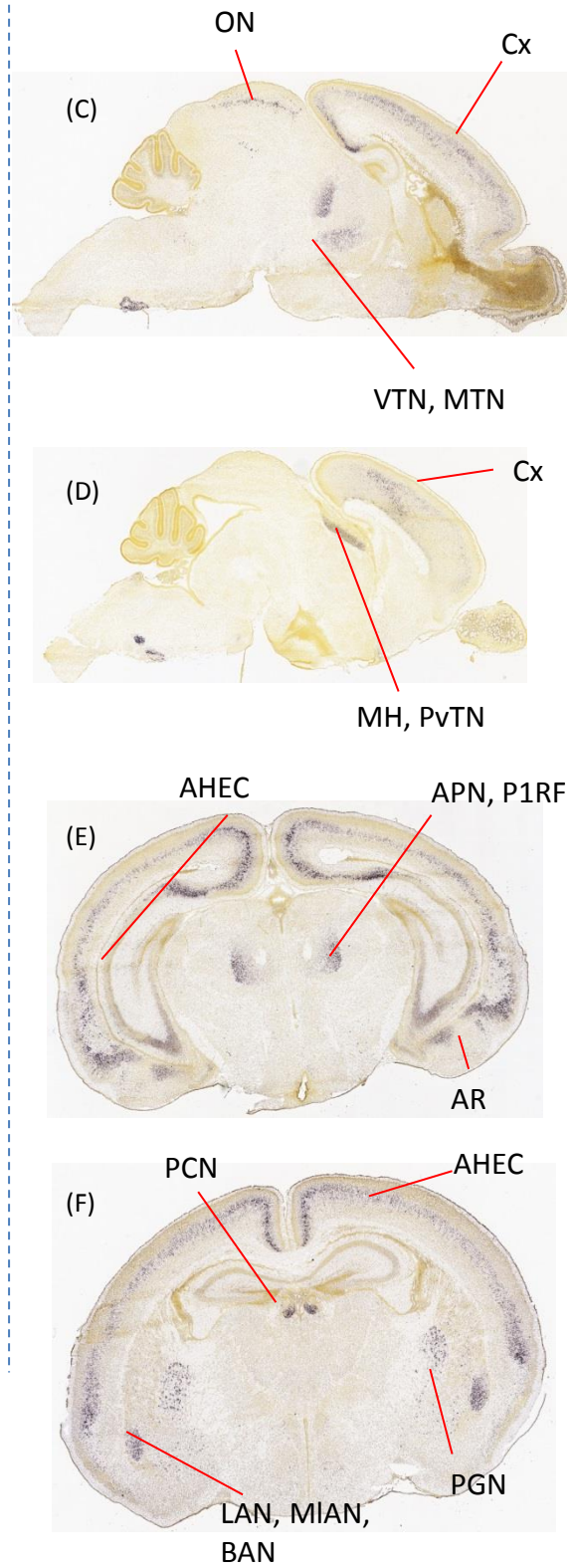
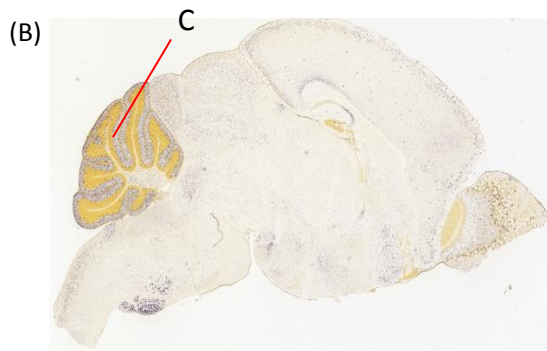
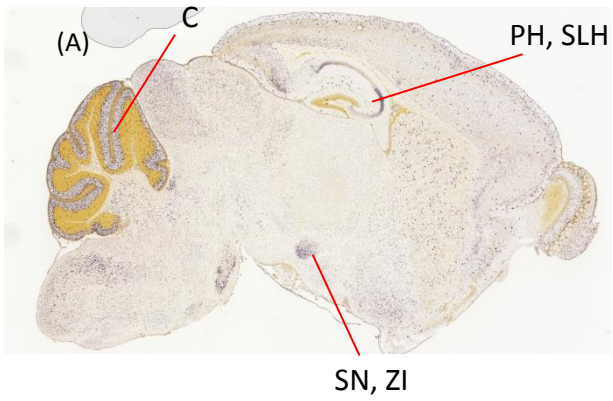


Figure 6.9. P14

Kit



Etv1

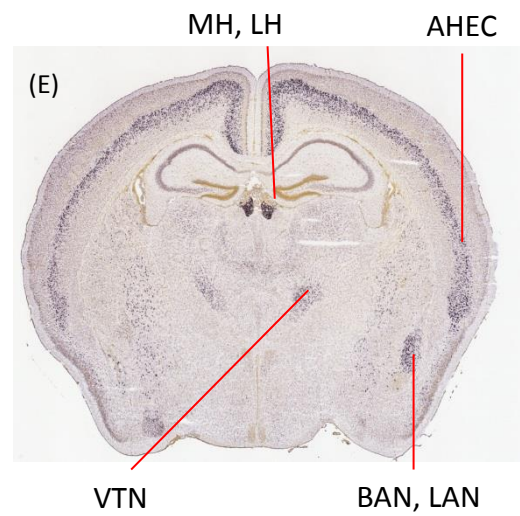
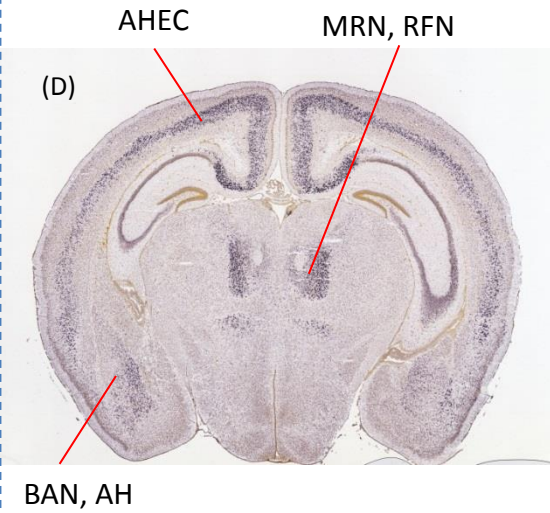
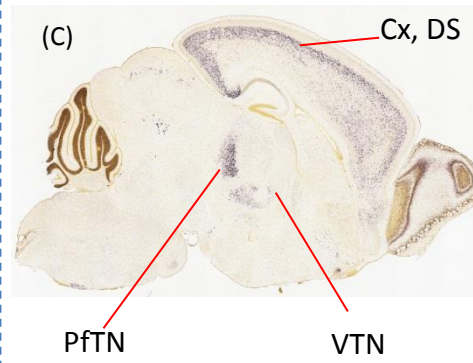
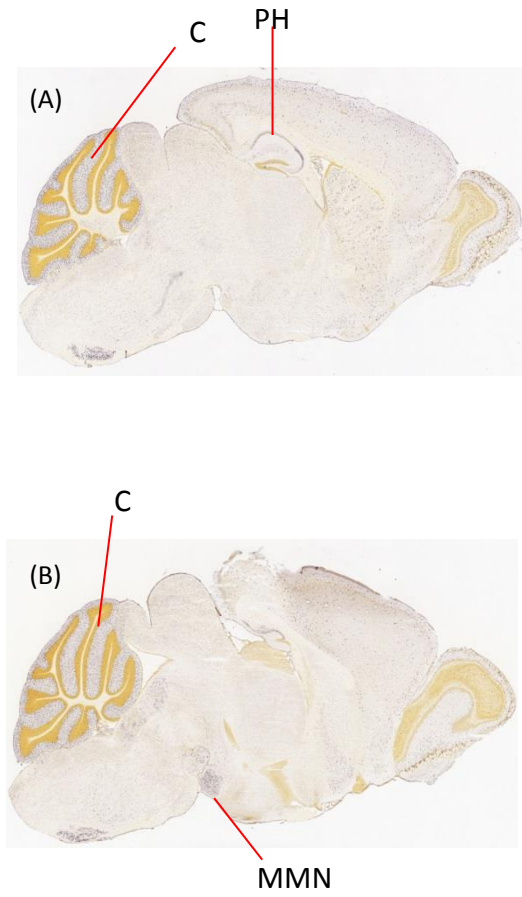


Figure 6.10. P28

Kit



Etv1

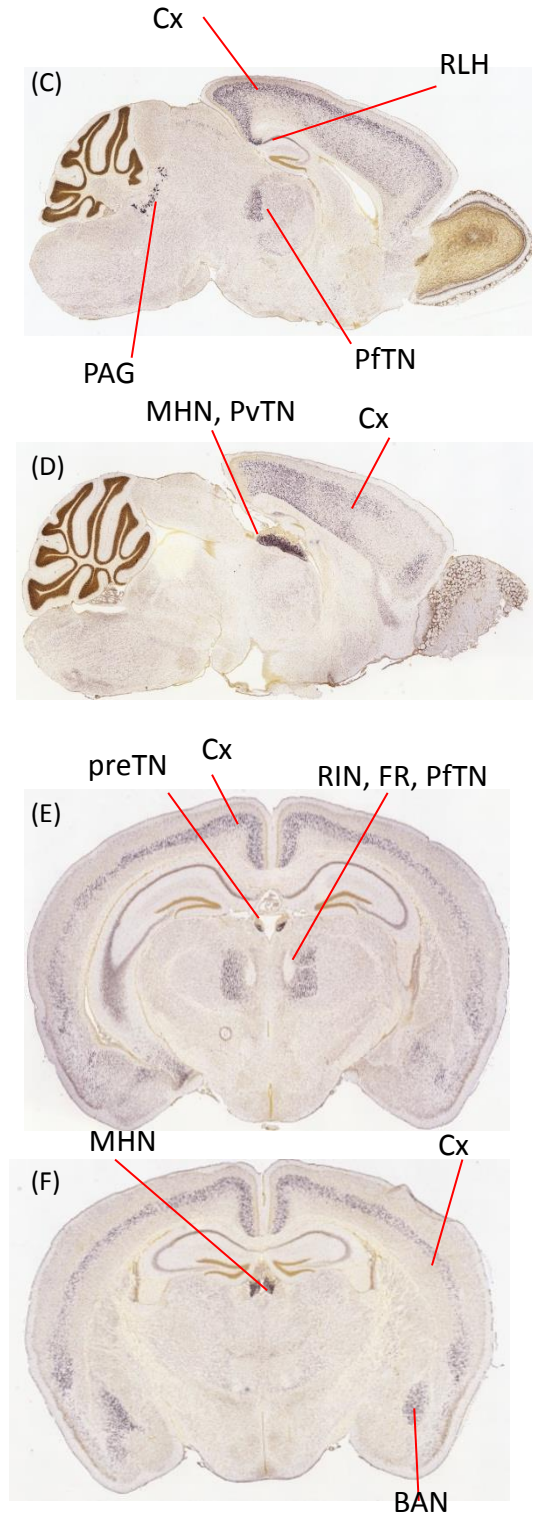
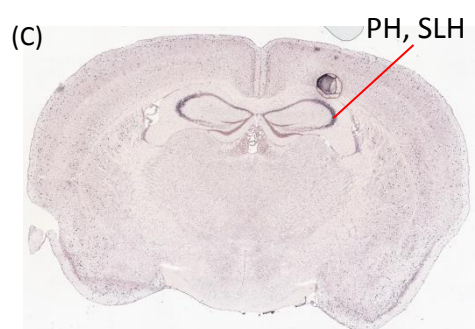


Figure 6.11. P56

Kit



Etv1

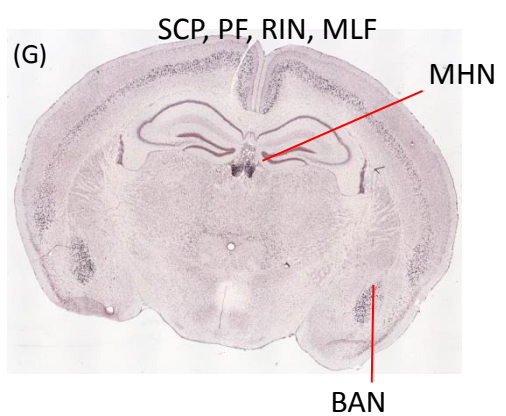
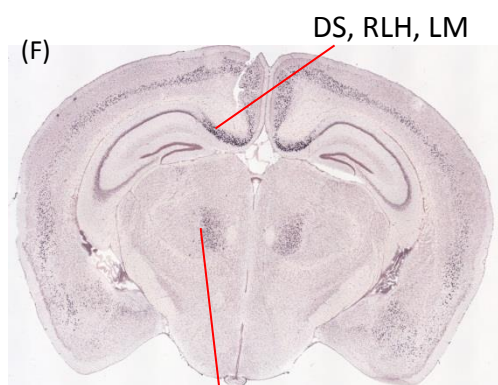
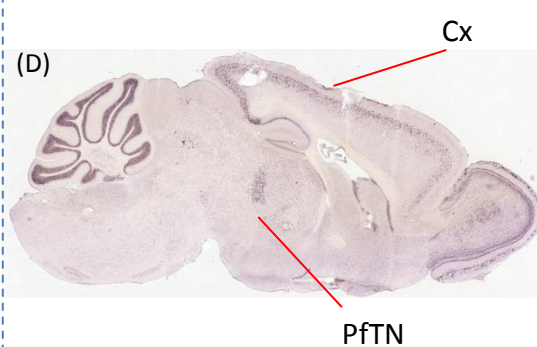


Figure 6.12. E9.5

Kit

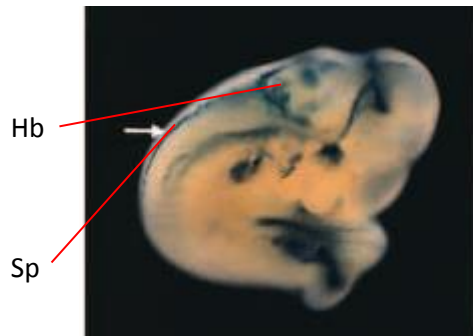


Figure 6.13. E10.5

Kit

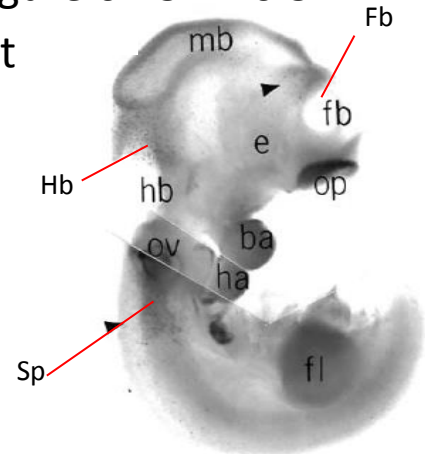
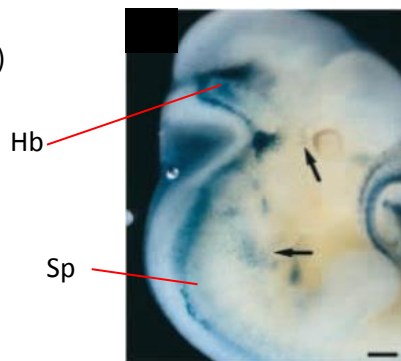


Figure 6.14. E11.5

Kit

(A)



(B)

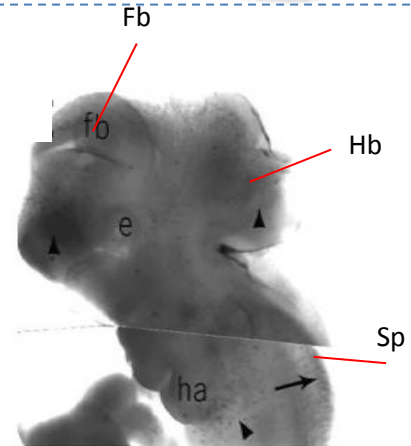


Figure 6.15. E10.5

Etv1

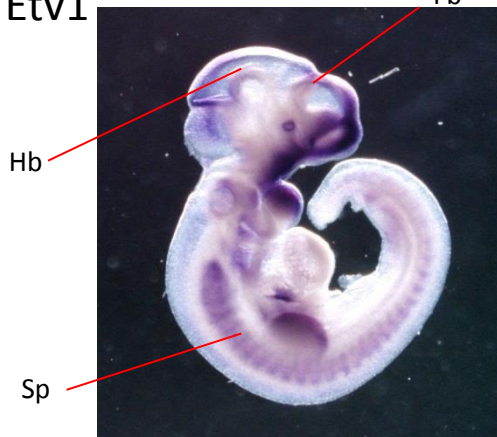


Figure 6.16. E14.5

Etv1

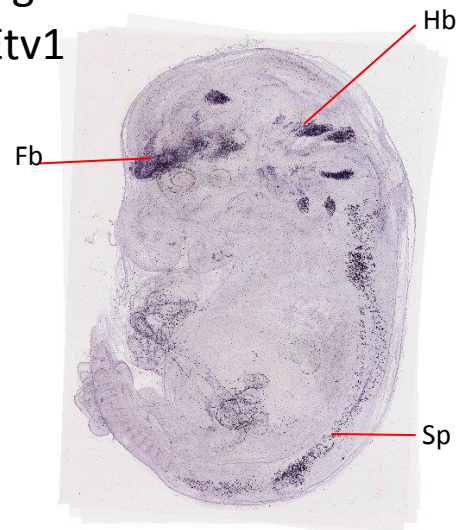


Figure 6.12-6.16. In situ hybridisation on whole-mount or whole-embryo sections for Kit and Etv1. See Figure 6.5 for further details. The exact locations of expression for ages between E9.5-E11.5 are unclear but there is expression of both Kit and Etv1 in the hindbrain, forebrain, and spine (Figure 6.12-6.15). A more specific expression pattern for Etv1 is evident at E14.5 with clear expression in the hindbrain, forebrain, and spine (Figure 6.16). Figure 6.12 and Figure 6.14 A are taken from Bernex et al, 1996 [200]. Figure 6.13 and Figure 6.14 B are taken from Wehrle-Haller, 1995 [201]. Figure 6.15 and Figure 6.16 are taken from www.emouseatlas.org

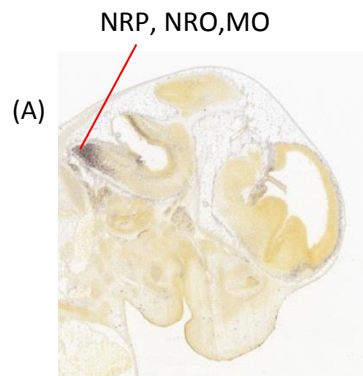
Kit and Etv1 expression in the medulla oblongata and medullary spine region

While analysing the Allen Brain Atlas sections for expression, both *Kit* and *Etv1* were seen in the hindbrain region at several ages (Figure 6.17-6.23).

The pons region had a consistent expression pattern when using the *Kit* probe (Figure 6.20 A and 6.21 A). This region did not produce a colour signal when hybridised with *Etv1* probe; however, this specific region may have been overlooked due to the sections being thin and only a few were stained. Equally, *Kit* was only expressed around these two ages, and was not found later.

Figure 6.17. E13.5

Kit



Etv1

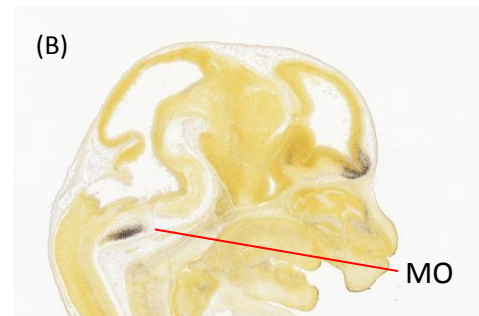


Figure 6.17-6.23. All positive staining in the spine, hindbrain or medulla oblongata regions are indicated. See Figure 6.5 for further details. All ages from E13.5 to adult expressed both Etv1 and Kit near the medulla oblongata (Figure 6.17 – 6.23). Beyond P4, expression appears to become weaker but both Kit and Etv1 are expressed in a few cells at P56 in the medulla oblongata region (Figure 6.23 C and D).

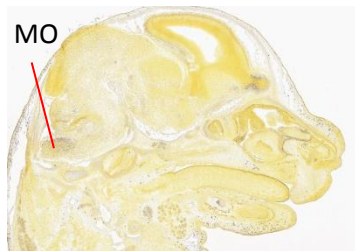
In addition to the overlap of expression of Etv1 and Kit in the medulla oblongata region, both Kit and Etv1 were expressed in the spine at E15.5 (Figure 6.18 A and C). Ages beyond E15.5 were either unclear or unavailable.

Figure 6.18. E15.5

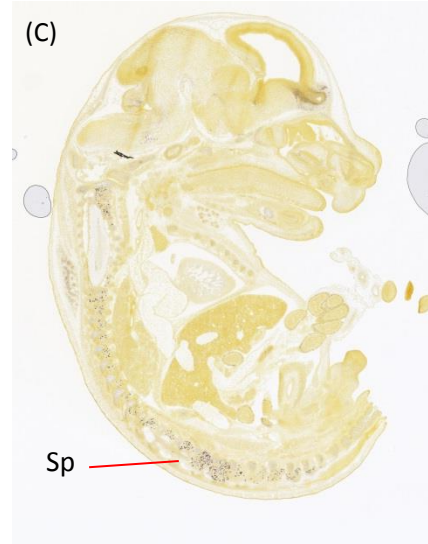
Kit



(B)



Etv1



(D)

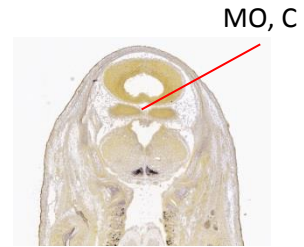
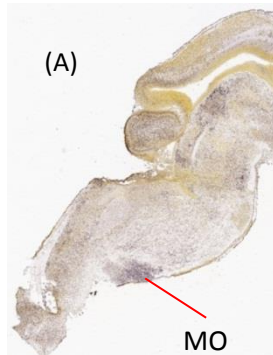


Figure 6.19. E18.5

Kit



Etv1

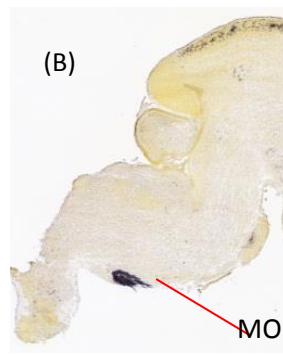
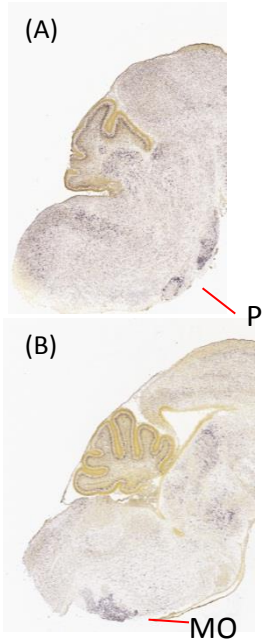


Figure 6.20. P4

Kit



Etv1

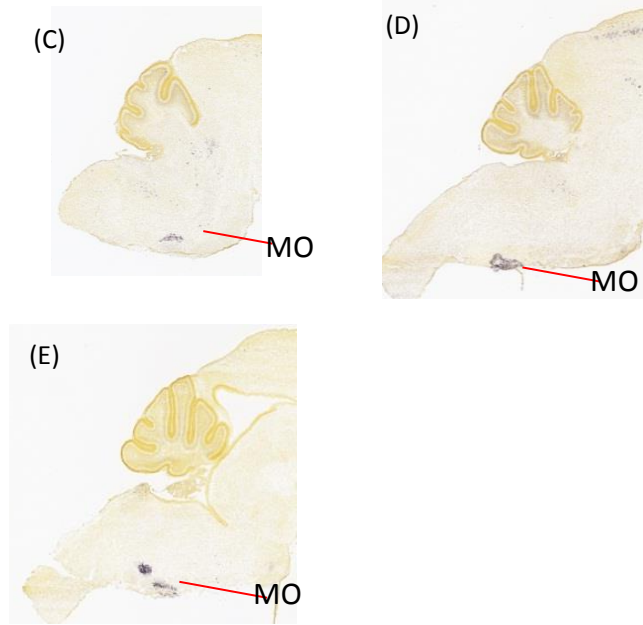
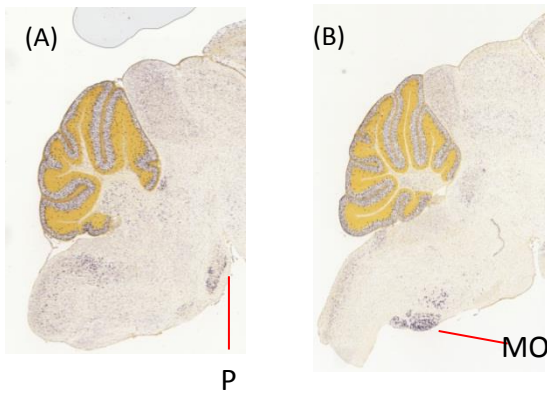


Figure 6.21. P14

Kit



Etv1



Figure 6.22. P28

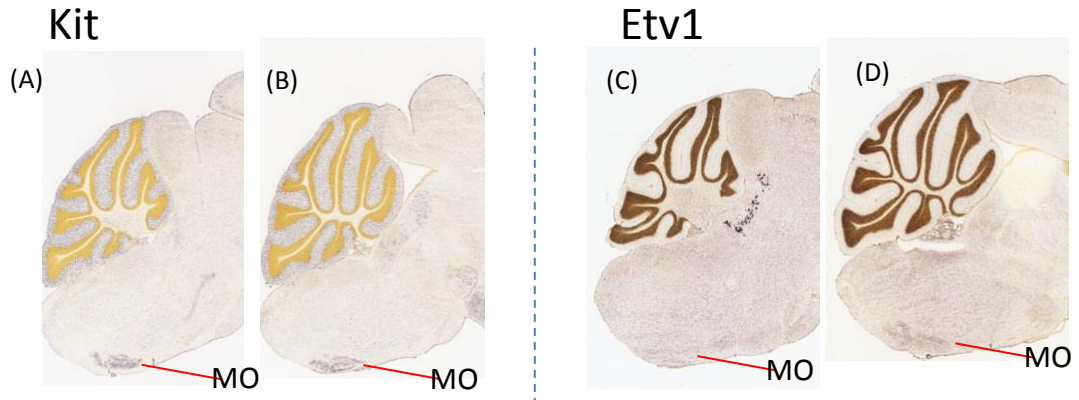
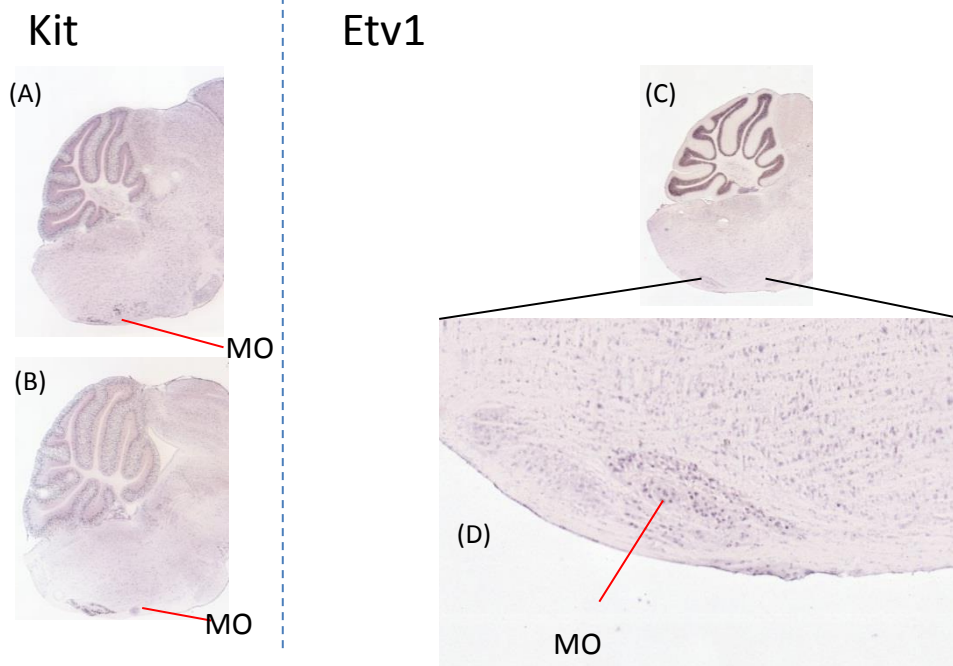


Figure 6.23. P56



Germinomas can occur in the medulla oblongata and medullary spine region

Germinomas are commonly found in pineal and suprasellar regions, and dual *Kit/Etv1* expression was also present in these regions. After discovering overlapping expression of *Kit* and *Etv1* in these regions, the next question was whether germinomas in human patients are restricted only to regions of dual *Kit/Etv1* expression or whether germinomas are seen in all regions of dual *Kit/Etv1* expression.

The medulla oblongata and medullary spine regions showed dual *Kit/Etv1* expression and our hypothesis predicts this region should also be the site of germinoma formation. Therefore, a thorough literature search of germinomas in human patients was carried out. This search subsequently identified the medulla oblongata and spinal regions as a third and fourth region for germinoma formation.

All identified clinical cases of germinomas occurring in these two sites published between 1990-2013 are included in Table 6.1. Equally, all the images that could be accessed are collated in Figure 6.24 and 6.25. The images in Figure 6.24 show germinomas in almost identical regions: attached to the medulla oblongata in the midline of the brain. Germinomas in the medulla oblongata region occurred in a wide age-range from 12-40 years old.

The images of germinomas occurring in the medullary spine show that these tumours do not arise consistently in a specific location (Figure 6.25). Germinomas appeared to be able to occur along the entire length of the spine, and had a wide age-range from 5-39 years old.

There was no obvious bias towards male or female cases. The ratios of male to female were 3:5 for germinomas in the medulla oblongata region, and 13:9 for the medullary spine. While the ratios appear to change from a subtle female bias to a male bias, this may be due to the small number of cases.

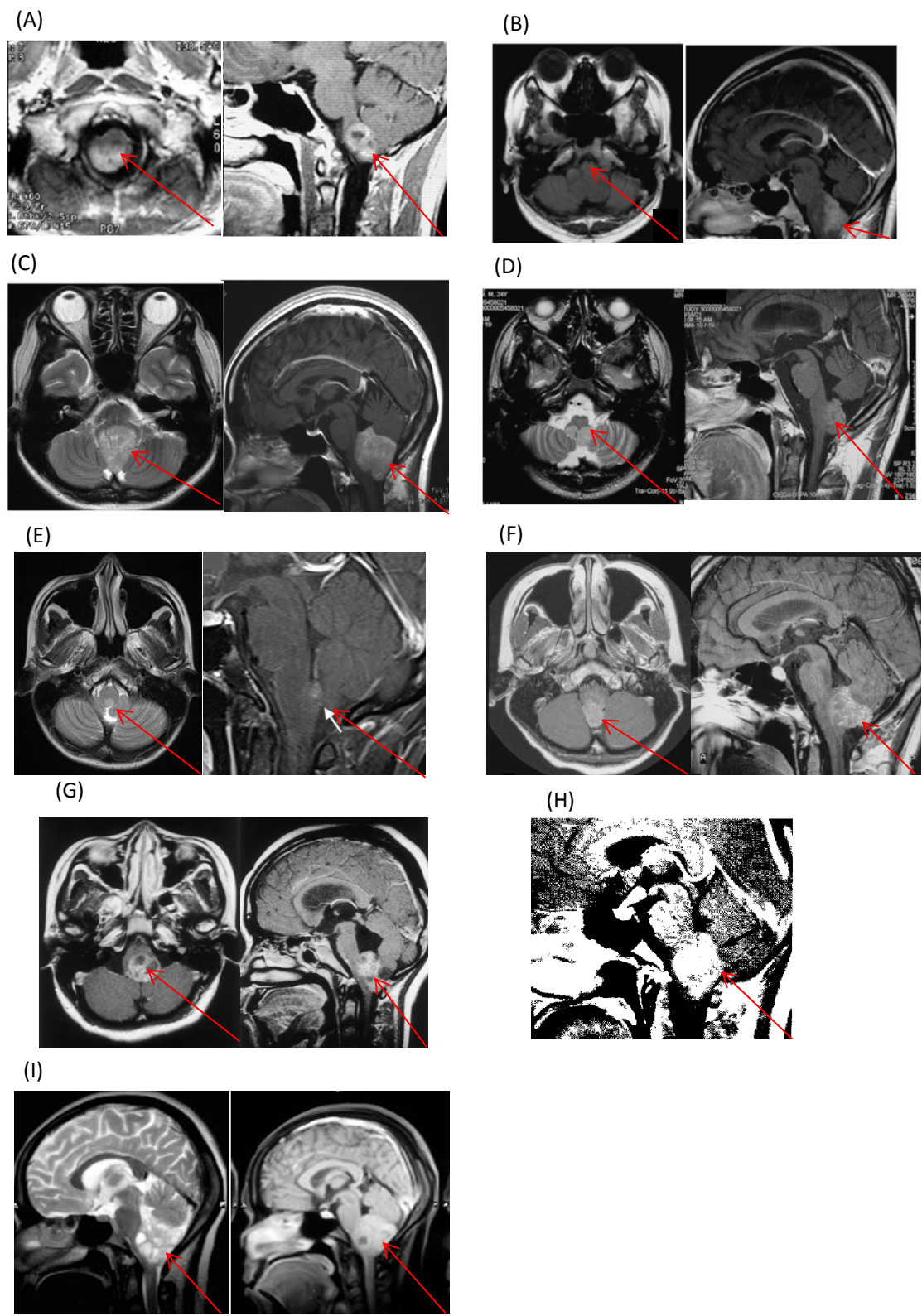


Figure 6.24. Images from either a transverse or sagittal view of a germinoma in the medulla oblongata region. Red arrows indicate the tumour mass. Each scan is from a different patient with a different age and gender: (A) 28 year old man [202], (B) 27 year old woman [203], (C) 30 year old woman [204], (D) 24 year old man [204], (E) 31 year old woman [205], (F) 18 year old woman [206], (G) 16 year old girl [207], (H) 30 year old woman [208], and (I) 24 year old woman.

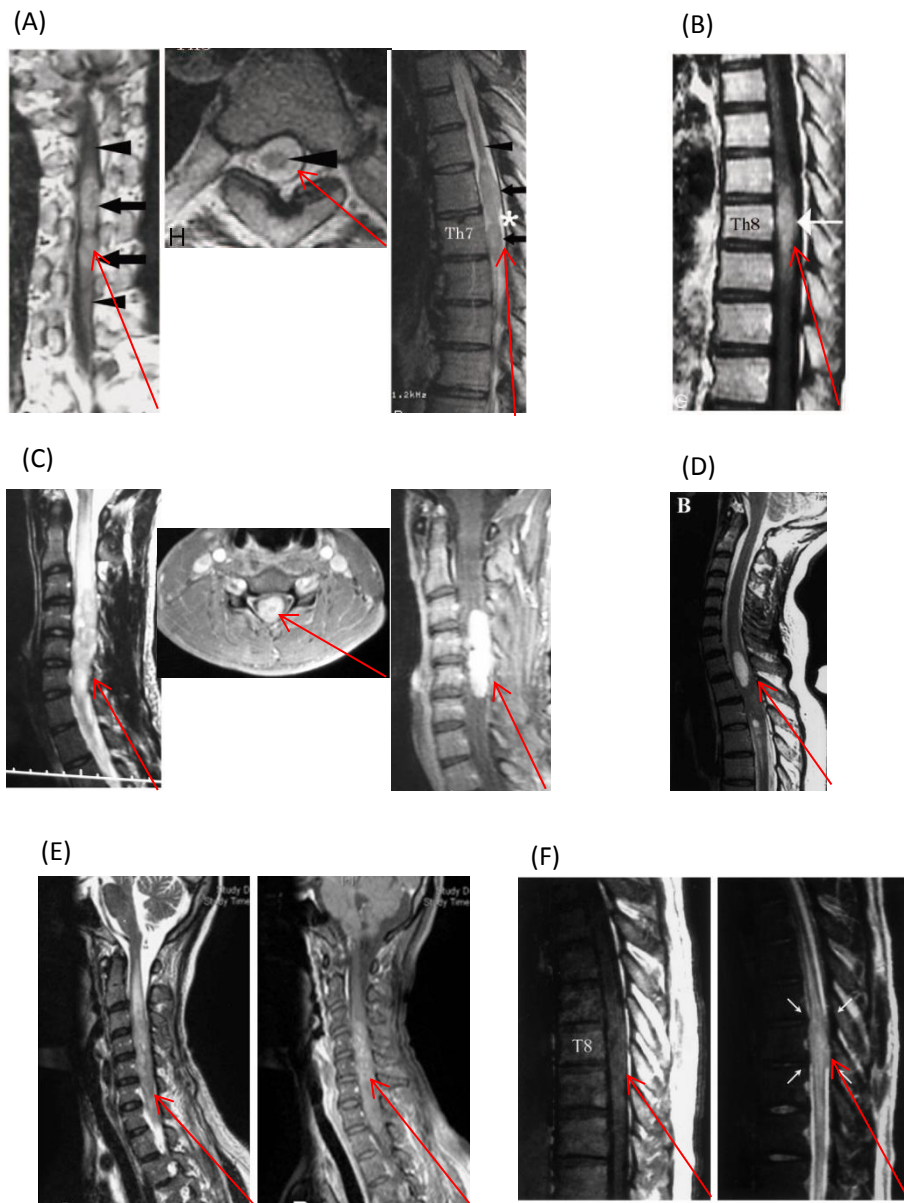


Figure 6.25. Sagittal or transverse images of germinomas in the spine. Red arrows indicate the tumour mass. The region of the spine, age, and gender are described: (A) T6-T7 germinoma in a 35 year old man [209], (B) T7-T9 in a 27 year old man [209], (C) C3-C6 in an 18 year old man [210], (D) T1-T3 in a 33 year old woman [211], (E) C2-T1 in a 39 year old woman [212], and (F) T7-T9 in a 33 year old man [213].

Germinoma location	Age of patient	Gender	Reference
Medulla oblongata	24	Male	[204]
Medulla oblongata	28	Male	[202]
Medulla oblongata	19	Male	[204]
Medulla oblongata	33	Male	[204]
Medulla oblongata	17	Male	[203]
Medulla oblongata	12	Male	[203]
Medulla oblongata	14	Female	[214]
Medulla oblongata	40	Female	[204]
Medulla oblongata	27	Female	[203]
Medulla oblongata	16	Female	[207]
Medulla oblongata	31	Female	[205]
Medulla oblongata	18	Female	[206]
Medulla oblongata	32	Female	[214]
Medulla oblongata	24	Female	[215]
Medulla oblongata	30	Female	[204]
Medulla oblongata	30	Female	[208]
Medullary spine	28	Male	[216]
Medullary spine	33	Male	[213]
Medullary spine	35	Male	[209]
Medullary spine	27	Male	[209]
Medullary spine	18	Male	[210]
Medullary spine	5	Male	[210]
Medullary spine	31	Male	[210]
Medullary spine	24	Male	[210]
Medullary spine	24	Male	[210]
Medullary spine	29	Male	[210]
Medullary spine	33	Male	[210]
Medullary spine	7	Male	[210]
Medullary spine	18	Male	[210]
Medullary spine	32	Female	[210]
Medullary spine	34	Female	[210]
Medullary spine	16	Female	[210]
Medullary spine	31	Female	[210]
Medullary spine	34	Female	[210]
Medullary spine	33	Female	[211]
Medullary spine	39	Female	[212]
Medullary spine	16	Female	[217]
Medullary spine	34	Female	[217]

Table 6.1 Germinomas in the medulla oblongata or medullary spine. Six male and ten female cases of germinoma have been recorded as occurring in the medulla oblongata region. Thirteen male and nine female cases of germinoma have been recorded as occurring in the medullary spine. Each of these categories is organised by male first and female second. All cases between 1990-2013 were included.

6.5. Discussion:

Germinomas in the brain express high levels of KIT and the *KIT* gene is frequently mutated. Research into GISTs has shown that a mutated form of KIT interacts with and stabilises ETV1 which results in an oncogenic event. Since germinomas are known to have high levels of KIT expression, this set of experiments investigated the normal expression levels of *Kit* and *Etv1* in mice of several ages.

Overlap of Kit and Etv1 expression correlates with germinoma formation

The hypothesis at the beginning of this experiment predicted an overlap of expression of *KIT* and *ETV1* in the regions where germinomas normally occur in the brain: the suprasellar and pineal regions. In fact, the data suggest a much more complex pattern of expression.

As predicted, *Kit* and *Etv1* expression was detected in the thalamic nuclei, and in the pineal region at all ages for both genes. There were some regions which could have benefited from a more detailed analysis, such as the pineal or habenula region for *Kit* using a coronal section. The pineal or habenula region had very strong staining, but the surrounding regions lacked expression. Therefore, *Kit* and *Etv1* expression provides evidence in support of the proposed mechanism because the pineal region is the most common region for germinomas to occur.

The only other region that showed consistent overlap was the medulla oblongata and hindbrain area. This hindbrain region showed strong expression of both *Etv1* and *Kit* in samples of all ages. Indeed, the spine also showed some overlap of expression but a full description of this was limited by the images because only sections up to E15.5 showed the spinal cord. Although germinomas are generally discussed as being associated with only two locations, the pineal and suprasellar regions, a thorough search of the literature revealed that germinomas also occur in both the spine and near the medulla oblongata.

Although very rare, the MRI or CT images have shown a consistency in the locations of these tumours in the medulla oblongata. Germinomas were found at locations throughout the spine which is also consistent with this hypothesis because both *Kit* and *Etv1* are expressed along the length of the spine.

This revelation requires further explanation of the evidence; why do germinomas occur much more frequently in the pineal and suprasellar regions if the same mechanism may be present in the medulla oblongata and spine? I propose that the abundance of growth factors in these respective regions might be an integral part of germinoma establishment. We know that seminomas in the testis respond to high levels of growth hormones during puberty which explains their prevalence around this time. Germinomas diagnosed in regions of hormonal centres, such as the pineal and suprasellar regions, presumably have much greater growth hormone levels than those in the spine or medulla region. The more posterior regions of the CNS may obtain a sufficient amount of stimulus over time to form but this is longer than the others in the diencephalon. This has been evidenced by medulla oblongata and spinal germinomas occurring at a later stage of development, in patients between 5-40 years old (median of 25.5 and 30 respectively) (Table 6.1).

Expression of only *Etv1* or *Kit* does not correlate with germinoma formation

Those opposing the above hypothesis would perhaps question why there is expression of one or both of these genes in locations where germinomas are not known to normally occur - the cerebellum is one such example. *Kit* was expressed in the same layer of the cerebellum in all ages examined. However, *Etv1* was not strongly expressed in this region. Since ETV1 was required for KIT-driven oncogenesis in the GIST study [196], it appeared that the lack of germinoma formation in the cerebellum strengthens the argument that both KIT and ETV1 are required for an oncogenic event.

Kit and Etv1 as part of the brain-cell hypothesis

So far in this chapter, I have proposed that germinomas have arisen from cells that already expressed both *KIT* and *ETV1* and acquired a mutation in the *KIT* gene, which caused an oncogenic event. To understand how this integrates into the initiation of GCTs as a class of tumours, it is important to discuss when germinomas and teratomas develop in humans.

Germinomas in the pineal or suprasellar regions have a peak incidence around puberty between 6-30 years old (Figure 1.2 C). On the other hand, teratomas have a peak incidence around birth. This difference in peak incidence would suggest a difference in either the cell of origin or the environment the cells are in.

We know that germinomas and teratomas have been diagnosed together in tumours, and Chapter 1 and 3 argue that all CNS GCTs have a common cell type of origin. Therefore, the environment of CNS GCTs is most likely to be the cause of the differences between peak incidences.

My hypothesis here is that the cells in those regions with an overlap of *ETV1* or *KIT* have the potential to initiate germinomas. One difficult question regarding our hypothesis is in the different regions in which germinomas occur in. Germinomas in the spine or medulla oblongata appear to form much later than those that arise in the pineal or suprasellar regions. Using our hypothesis that hormones influence growth, regions outside of the pineal and suprasellar region may receive much lower concentrations than near centres of hormonal activity. Comparatively, those progenitor cells in the pineal or suprasellar regions may require a lower threshold of growth hormones to drive oncogenesis.

GCTs may share KIT activation of ETV1 as a common mechanism regardless of location

ETV1 and *KIT* are strongly expressed in the testis, ovary, brain, and to some extent the spine [218-221]. This observation is evidence that the mechanism for germinoma formation could be similar regardless of location. I propose that a single activating mutation in the *KIT* gene is an oncogenic mechanism to transform cells in various locations into germinomas.

Our hypothesis suggests that a *KIT* mutation in a pluripotent cell leads to germinoma formation. I believe that *ETV1* is expressed in the progenitors of germinomas, and contributes to the formation of germinomas. Germinomas appear to be limited to regions where there is dual *ETV1/KIT* expression. Our hypothesis would therefore predict that the brain regions in which germinomas do not occur lack *ETV1* expression. This is supported by the close correlation of dual expression to germinoma formation.

Most *KIT* mutations are localised to a D816V point mutation. While several other mutations have been found, there are some germinomas/seminomas that express *KIT* but do not appear to have a point mutation in any of the known sites. Most germinomas have been assessed for *KIT* mutations only in specific 'hotspots'. Sakuma *et al.* 2004 examined five hotspots in *KIT*, and found gain-of-function mutations in approximately 25% of germinomas (total of 16 examined) [23]. Unfortunately, no studies (to our knowledge) have sequenced the entire *KIT* gene, especially in those germinomas that do not carry mutations in hotspots.

Another example is the Kuno *et al.* 2012 paper, which describes a seminoma without a *KIT* mutation [222]. Although only four exons were examined, the authors concluded there was a lack of gain-of-function mutations; however, according to our hypothesis, other mutations within *KIT* may have been present at locations outside of the amplified regions assessed.

Research into GCTs with *KIT* mutations does not at present compare to research on other cancers driven by *KIT*, such as melanoma and leukaemia [223,

224]. Carvajal *et al.* 2011 examined the mutations in *KIT* for melanomas in many more than five exons, and Wang *et al.* 2005 sequenced the coding regions of the *KIT* gene in over 100 leukaemias. These other studies in non-germinoma cases show that mutations outside of the five regions often cited as *KIT* hotspots can also cause gain-of-function.

One interesting experiment would be to sequence the entire *KIT* gene in tumour samples that do not appear to have mutations, but do express *KIT*. This sequence would be examined for mutations, and these could be tested *in vitro* for an activating function. My hypothesis would be that *KIT* is particularly prone to mutations that change the conformation of the protein, which in turn relinquishes the need for an activating ligand.

I propose that the activation of *KIT* signals the stabilisation of *ETV1*, and subsequently transforms a cell into a GCT. This theory suggests that *ETV1* may be activated by other proteins in the *KIT-ETV1* pathway; for example *RAS* and *RAF*. In the case of germinomas that do not possess *KIT* mutations, other genes within the *KIT-ETV1* pathway should be examined for activating mutations.

Clinical cases support KIT activation of ETV1 as a mechanism for GCT formation

A clinical case published by Aker *et al.* [225] describes the occurrence of a pineal germinoma with multiple melanocytic nevi. *KIT* is associated with melanocytic lesions [226], so this rare occurrence of two cancers appears to have an oncogenic mechanism of *KIT* activation. The patient in this case apparently had no GCTs in other locations, which suggests that the activation of *KIT* is not linked to progenitor germ-cell migration. If *KIT* was linked to progenitor germ-cell migration, we would expect multiple GCTs along the route of migration towards the brain.

This point is controversial but is supported by other data. Proponents of the germ-cell progenitor hypothesis may suggest that germinomas in several locations of the brain are due to the presence of two germ cells. However, Da

Silva *et al.* 2009 reported a case of three germinomas in a single patient [227]. It seems unlikely that three germ cells mismigrated and became lodged in the brain without forming a GCT anywhere else in the body – especially since we know germ-cell progenitors transplanted into extra-gonadal locations form GCTs.

KIT and ETV1 appear to be integral to germinoma formation or maintenance. Since radiotherapy can cause long-term damage to patients, clinical research has begun to focus on pathway-targeted medicine. Imatinib is a tyrosine-kinase inhibitor used to treat GISTs. GISTs have a similar underlying *KIT* mutation as either the initiating or driving oncogenic event. Imatinib has been tested for germinoma treatment but the lack of penetration of the drug through tissue is an issue. Dasatinib also targets KIT but unlike Imatinib has a greater penetrance profile i.e. it can reach tumour cells away from major vasculature. While Dasatinib is the most recent drug tested as a pathway-targeted treatment, other therapies are likely to target specific pathways of cancer. Therefore, understanding the mechanisms and oncogenic events that initiate and drive GCTs is integral to both treating the disease and limiting the long-term sequelae.

6.6 Conclusion

The hypothesis before investigating *Kit* and *Etv1* expression in the brain was that a *KIT* mutation stabilises ETV1 and leads to a germinoma. There is much work to be done in order to validate this theory, but there is evidence that *Etv1* is already expressed in a region where germinomas normally occur. This clearly needs to be validated at a functional level, and further *in situ* hybridisation on younger embryos would be useful.

Chapter 7: Discussion

7.1. Introduction

The findings presented in this thesis challenge the hypothesis that migrating germ-cell progenitors are the cell of origin for CNS GCTs. Advances in our understanding of pluripotency-induction strengthen our opposing hypothesis that CNS GCTs arise from brain cells, instead of germ-cells. This final chapter discusses the arguments against the germ-cell model; the evidence in support of our brain-cell model; how clinical observations can be explained by our model, and further work needed to validate our hypothesis.

CNS GCT subtypes have a lineage relationship

A proposed model for the various histological subtypes of GCT is that they represent stages in a progression starting with carcinoma *in situ* (CIS), also called intratubular germ cell neoplasia unclassified (IGCNU). The germinomatous and embryonal carcinoma (EC) forms are believed to arise from CIS. The more differentiated teratoma, choriocarcinoma and yolk sac tumour forms are proposed to then arise from the EC, by so-called 'activation of pluripotency'[228]. Two observations support this model. Firstly, GCTs are often found to be of mixed histology, with some containing 4 histological subtypes [152, 229]. This is true of all GCT sites, including the brain [153, 158].

Secondly, there are well-documented examples for each subtype of a GCT reappearing as a different subtype following resection (Chapter 3). This is common for sacrococcygeal tumours, which recur as YSTs [230, 231]. In particular, several studies have reported recurrence of a germinoma following resection of an intracranial teratoma. This implies that the cells of these tumours can give rise to different histological subtypes and therefore share a common cellular lineage. Consequently, if activation of Oct4 expression could cause an NSC to initiate growth as a teratoma, such a tumour could then convert to any one of the other GCT histological subtypes by the time it was diagnosed.

In summary, all GCT subtypes appear to have a common cell type of origin, regardless of the progenitor hypothesised to form them. Therefore, both our and the PGC hypotheses must explain the mechanism behind each subtype of GCT developing in the brain.

Challenges for the germ-cell progenitor hypothesis

This thesis argues that a cell population in the brain has the potential to develop into CNS GCTs. The arguments against the hypothesis of a germ-cell origin for CNS GCTs have been laid out in Chapter 1 and 3; but will be briefly revisited later.

There are several unanswered questions regarding the mechanism suggested for germ-cell progenitors. There are inconsistencies regarding when genetic aberrations occur in the 'mis-migrating progenitors'. Chromosomal abnormalities such as chromosome 12p duplications or *KIT* mutations are proposed as a mechanism for mis-migration; but why do some CNS GCTs lack these mutations? How have CNS GCTs with few mutations by-passed the apoptotic pathway designed to eliminate germ-cell progenitors?

If we are to consider the germ-cell hypothesis, there are a number of questions that must be answered. The principal questions revolve around *in vivo* data: when germ-cell progenitors are unshackled from their migratory control mechanism in experimental models, why are these progenitors never detected in the brain? Indeed, even if there are technical issues with tracking these cells, why do the progenitors never form CNS GCTs in these models?

7.1.1 Hypothesis

GCTs that arise in the gonads have similar chromosomal aberrations, histology, and protein markers to CNS GCTs. Proponents of the germ-cell origin hypothesis believe the similarity between GCTs in these locations is evidence of a common cell of origin, but I propose the parallels are due to a common

pathogenesis. Germ-cell progenitors are pluripotent, and the induction of pluripotent cells from brain cells would perhaps be equivalent to the germ-cell progenitors in the testis; the cell of origin may be different, but the resulting tumours the same. Therefore, the similarity in genetic aberrations may indicate similar driving mechanisms from a pluripotent cell to a GCT.

The germ-cell progenitor hypothesis simply describes differentiation of a PGC in an extragonadal location. Our hypothesis requires the activation of OCT4, which is an extra oncogenic event. Since CNS GCTs have a lower incidence than those in gonadal locations, the extra oncogenic event required would explain why GCTs are less likely to occur in the brain.

Our hypothesis proposes aberrant OCT4 activation in a multipotential cell to be an initiating event in CNS GCTs pathogenesis. The Oct4 is controlled by methylation, so disruption to DNA methylation may explain the expression of Oct4. In fact, a lack of methylation is observed in some subtypes of CNS GCTs, especially those that express Oct4 [90]. Chromosomal duplications, such as an extra X or 12p, may provide an alternative method of activating OCT4 and is discussed later.

The differences between GCT subtypes may be explained by additional mutations in genes such as *KIT* for germinomas. On the other hand, teratomas and yolk sac tumours appear to be the consequence of differentiation of pluripotent cells; for example when embryonic stem cells are transplanted into SCID mice. It is therefore more likely that these tumours are the result of differentiation of pluripotent cells in a developing environment (Figure 7.1). We propose a testable hypothesis for CNS GCTs initiation and progression that has been examined in this thesis.

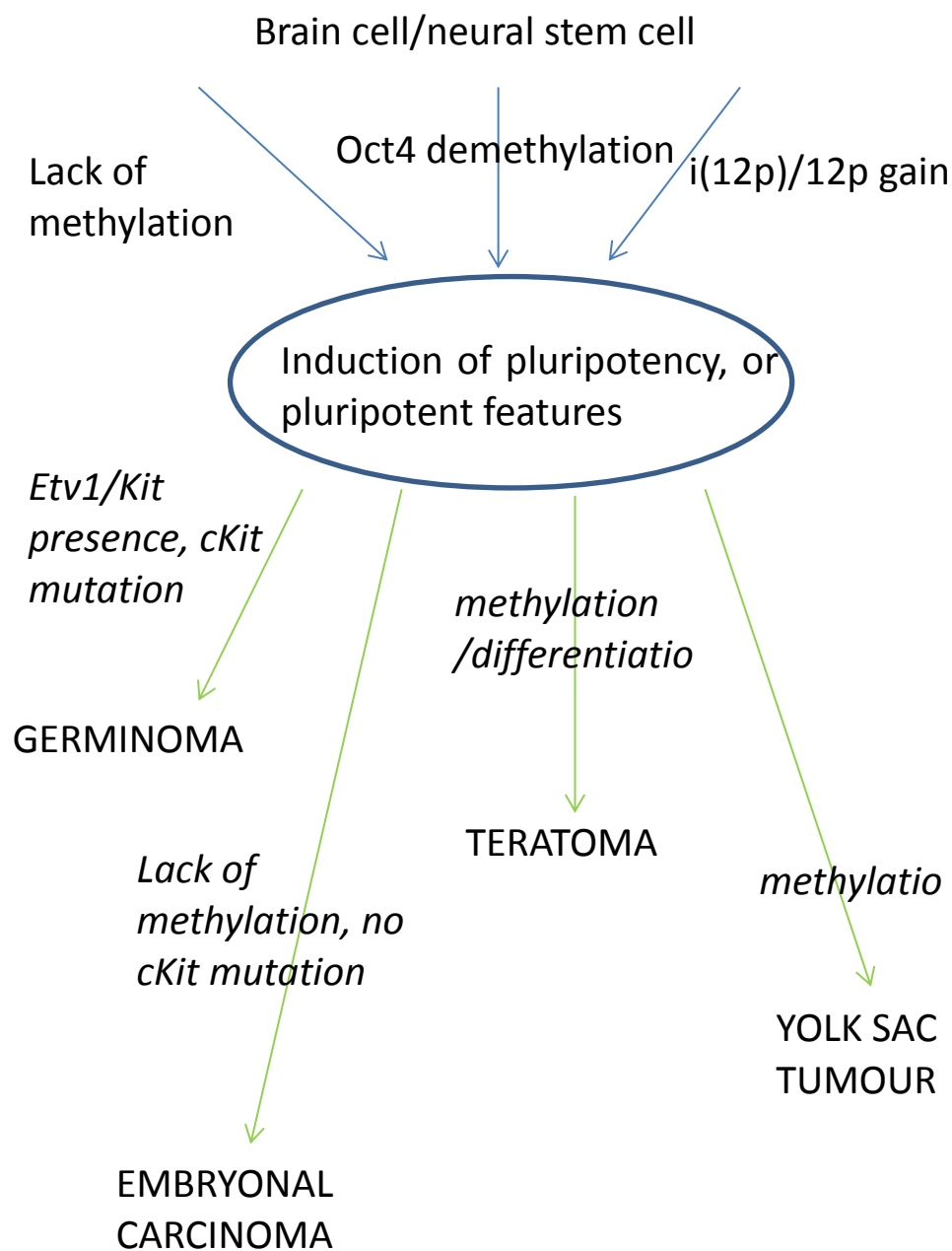


Figure 7.1. A schematic of the potential mechanisms involved in forming different subtypes of GCT from a brain cell. The hypothesis begins with a brain cell that can gain pluripotent features through one (or a combination) of three mechanisms – lack of methylation to silence Oct4, demethylation (i.e. activation of OCT4), and/or i(12p)/12p gain. Once induced to a pluripotent state, each of the different subtypes may be influenced by the mechanisms proposed: a KIT mutation in the case of germinomas; maintenance of pluripotency for embryonal carcinomas; and methylation and differentiation for teratomas and yolk sac tumours.

Plasticity and the incidence of CNS GCTs in children

Our hypothesis is compatible with the observation that CNS GCTs occur in the early years of life. Neural progenitors begin as radial glia and the capacity to differentiate into multiple lineages becomes increasingly restricted during development. Our hypothesis does not have sufficient evidence to identify a specific population of neural progenitors but the ages at which GCTs are diagnosed (Chapter 3) suggests that a progenitor for CNS GCTs is present in the brain between the first and second trimester.

The cells in the CNS undergo various DNA methylation changes during the early stages of embryonic or fetal development, and are therefore vulnerable to aberrant expression of genes controlled by methylation; for example, retinoblastomas (a tumour that occurs in the eye) can be initiated when only a single gene – Rb – is aberrantly methylated [232]. A lack of methylation of the Oct4 promoter is a reasonable mechanism for OCT4 ‘activation’ – or more accurately, lack of silencing.

7.1.2 CNS GCTs are not restricted to the midline

GCTs are in the midline and PGCs migrate in the midline

My literature review showed that CNS GCTs are not restricted to the midline, which challenges the ‘midline migratory path’ of germ-cell progenitors. If CNS GCTs have a germ-cell progenitor, but are not restricted to the midline, how would they migrate to these regions? If they can migrate to any region of the body, why are GCTs not seen in a much wider range of sites? These observations are more consistent with a small group of local cells of origin that are only found in very restricted locations.

There are several characterised genetic aberrations and clinical markers for GCTs. The germ-cell hypothesis proposes that markers such as KIT and OCT4 are linked to germ-cell progenitors and mis-migration. However, since both are seen in NSCs in the same situations, we propose that these same markers are activated or maintained aberrantly in brain tissue and are the driving forces

behind local neoplasia, instead of mis-migration.

CNS GCTs are classified as a single group and can form in any region of the brain, but some subtypes have a more defined area of occurrence. Teratomas form in almost any region of the brain, but germinomas are restricted to the midline. Germinomas are the most common type of CNS GCT so this pattern explains the widely-held belief that CNS GCTs occur in the midline.

Germinomas, or seminomas, are very similar to undifferentiated carcinoma *in situ* [31]. Pluripotent or undifferentiated cells often require a specific combination of factors to maintain pluripotency, which may explain why germinomas are restricted to the midline. Based on the restricted pattern of germinomas in the midline, I would predict that the midline is rich in extracellular signals concerned with maintaining pluripotency rather than tumour initiation. The potential for germinomas to form in lateral regions could be tested in the same way as teratomas in Chapter 4 – by stereotaxic injection of a seminoma/germinoma cell line into the midline and lateral regions. If my hypothesis is correct, germinomas would form, and be maintained in the midline, but in lateral regions germinomas may struggle to grow or differentiate into one of the other CNS GCT subtypes.

GCTs occur in locations other than the CNS and gonads

The germ-cell hypothesis provides a logical explanation for GCTs that occur in locations such as the peritoneum; however, could a similar alternative hypothesis also explain these tumours? Our hypothesis relies on the induction of pluripotency through the activation of all four Yamanaka factors. In the case of CNS GCTs we propose that OCT4 is activated to induce pluripotency, but there may be other cell types that lack a different factor.

While it is beyond the scope of this thesis, our hypothesis may be relevant for other extragonadal GCTs. Briefly, pluripotent progenitors have been identified in other non-gonadal locations, such as the sacrococcygeal region. Wilson *et al.* (2002 and 2007) suggest that axial progenitors have the potential to

form tumours from pluripotent cells [99, 100]. Aberrant differentiation of these axial progenitors would have the potential to form teratomas. Furthermore, these progenitors are present during embryogenesis but decrease rapidly post-natally, which correlates with the peak incidence of sacrococcygeal teratomas around birth but few found later in development.

7.1.3 The role of methylation in CNS GCTs

Do progenitors for CNS GCTs lack imprinting?

One of the arguments in favour of a germ-cell progenitor as the cell of origin for CNS GCTs is the lack of imprinting. However, in Chapter 1 highlighted the presence of neural progenitors that also lack imprinting of genes such as SNRPN [57].

Many CNS GCTs appear to lack imprinting but it is unclear whether there is larger heterogeneity of imprinting patterns in different regions of CNS GCTs. Schneider *et al.* (2001) confirmed that the majority of CNS GCT cells lack imprinting [37], which suggests that the progenitor cell for CNS GCTs lacks imprinting; however, this does not mean that the cell of origin was a germ-cell progenitor.

Loss of imprinting (LOI) is an established oncogenic mechanism. LOI for IGF2, for example, is implicated in Wilm's tumour, kidney, leukaemia, colorectal cancer, lung adenocarcinoma, oesophageal cancer, and meningiomas (a type of brain tumour) [37]. LOI is also present in hepatoblastoma and laryngeal squamous cell carcinoma [37]. More importantly, LOI is observed in rhabdomyosarcoma, a tumour very similar to teratomas; gliomas, a type of brain tumour; and Ewing's sarcoma, a tumour discussed further in this chapter.

LOI provides a selective advantage to form cancers and is common among both CNS and non-CNS cancers. Therefore, there is potential for this mechanism to be an initiating event in CNS GCTs, or even gonadal GCTs. LOI affects a wide range of genes including MYCN and RASSF1A, both of which are associated with cancer. These two genes will be discussed again later as part of a

specific CNS GCT-initiating mechanism. In summary, LOI could be a mechanism to initiate CNS GCTs from a brain cell. A lack of imprinting in CNS GCTs does not, therefore, imply an origin from PGCs.

The methylation status of CNS GCTs poses a 'chicken and egg' situation with regards to progenitor cells. Did a methylation defect cause activation of OCT4, or did pluripotency-activation reduce the levels of methylation? NANOG, which can be activated by OCT4 and is generally expressed in germinomas, has an important role in regulating TET1 and TET2, and TET proteins control DNA methylation [233, 234]. This perhaps explains the lack of methylation in CNS GCT subtypes such as germinomas, but it is not possible to confirm whether NANOG first demethylates Oct4, or OCT4 first activates Nanog.

In summary, there are several key arguments used to support the germ-cell hypothesis, which we believe can be explained by our brain-cell hypothesis.

The last part of this thesis describes clinical features, and their relationship to our brain-cell hypothesis.

7.2. Chemoresistance and OCT4

OCT4 is implicated in cancer formation or progression in several cancers; for example, melanoma [235]. Dedifferentiation is cited as the mechanism for OCT4 to contribute to oncogenesis. Different subtypes of CNS GCT respond differently to chemotherapy and radiotherapy, as reviewed in Chapter 1. Chemoresistance is attributed to the loss of OCT4 in some studies [236], but Quinn *et al.* correlated the loss of OCT4 in prostate cancer cell lines with decreased chemoresistance [237]. These observations appear contradictory and highlight the complex relationship between OCT4 and cancer.

The role of Oct4 as an oncogene is different from, for example, P53. OCT4 is controlled by several factors, which may explain the differences in chemotherapy resistance when using OCT4 as a marker i.e. some of the factors involved in regulating OCT4 may not be present in certain cases. Therefore, a more suitable model may be to correlate pluripotency with chemoresistance,

instead of using Oct4 expression alone as a marker. But why might loss of pluripotency correlate with chemoresistance?

Several mechanisms have been examined to explain why pluripotency might correlate with chemoresistance. Repair mechanisms and the immune system are two of the most studied areas to explain chemoresistance. A reduced repair mechanism is a logical hypothesis because a cell that has lowered this ability should be more sensitive to chemotherapy; however, there does not appear to be a significant correlation in CNS GCTs; specifically, expression of DNA repair genes did not correlate to response to cisplatin [48].

Korkola *et al.* 2006 prefer to correlate chemotherapy resistance with the immune system. The presence of an 'immune signature', mainly in pluripotent CNS GCTs, correlates with a good prognosis; but a lack of 'immune signature' correlates with a bad prognosis. This immune signature is characterised by expression of a range of genes associated with IgG, B cell, and T cell genes. Increases in differentiation, especially neural differentiation, also correlate with a poorer prognosis [48]. The mechanism behind this correlation is unknown but it is tempting to suggest an inability for the body to recognise differentiated cells, which would explain the lack of immune response and poorer prognosis.

In fact, Korkola *et al.* are not the only group to suggest that immune response correlates with prognosis in GCTs. Wang *et al.* correlated chromosomal changes, and lack of immune response with poorer prognosis [16]. Further work in this area may reveal genes that can sensitise cancer cells.

The 'immune signature' hypothesis appears to be compatible with the association between pluripotent features and sensitivity to chemotherapy. This hypothesis would also be a logical correlation because chemotherapy may debulk the tumour and the immune system would target remaining cells.

Although pluripotent cells appear to have an 'immune signature' this does not necessarily mean that it is the pluripotent state is the reason behind resistance. Overexpression of pluripotent genes, or testing chemotherapy on

pluripotent cells compared to differentiated ones would perhaps elucidate the true correlation.

7.3. 12p and pluripotency

The gain of the 12p or i(12p) chromosome is suggested to be a marker of germ-cell origin; but could i(12p) instead be responsible for induction or maintenance of pluripotency in a brain cell? Our hypothesis would be strengthened if there was evidence that i(12p) influenced a brain cell to become a CNS GCT.

The first observation is that ES cells undergo the same gain of i(12p) after long-term passage. This i(12p) gain in ES cells is suggested to confer a selective advantage for proliferation of undifferentiated cells [238].

Analysis of the genes on 12p reveals a cluster of stem cell-associated genes around 12p13. Importantly, STELLAR, GDF3, and NANOG are all within this cluster. NANOG is already known to maintain pluripotency and regulate OCT4. Since pluripotency is regulated in a complex manner by several factors, the combination of genes on 12p could be the initiating event for a brain cell to become pluripotent – or at least gain pluripotent features. Indeed, downregulation of these genes causes differentiation of male GCTs [236].

There is even evidence of 12p gain occurring in CNS tumours such as glial tumours [239], myofibroblastic sarcoma [240], and parenchymal tumours of the pineal region [51]. The role of 12p gain is unknown in these tumours but shows that tumours arising from brain cells can contain 12p gain.

There are several reasons it is important to understand 12p gain in CNS GCTs. First, 12p gain may be a mechanism to either induce or maintain pluripotency, which strengthens our hypothesis. Our hypothesis may not change the way CNS GCTs are clinically treated but if the mechanism of forming a CNS GCT is different to a gonadal GCT we can compare the role of 12p gain in order to understand the effect on pluripotency.

7.4. The KIT-ETV1 axis

My model suggests that the KIT-ETV1 axis triggers germinoma formation. The expression of ETV1 and stabilisation by KIT/RAS/RAF/MEK activation is an axis that is found in many cancers and is highly redundant.

The KIT-ETV1 axis can be split into two parts: the stabilisation of ETV1 by KIT; or the aberrant activation of ETV1 target genes. The mechanism for these two stages is different in each cancer, but the outcome is the same – transcription of the ETV1 downstream targets.

The KIT/RAS/RAF/MEK pathway is commonly activated in a range of cancers [241-243]. The mechanism is often point mutation; for example, in the case of *KIT*, a single mutation relieves the KIT receptor from its need for a ligand and the tyrosine kinase function of KIT becomes constitutively active. Gain-of-function point mutations in *KIT* have been found in several types of cancer including gastro-intestinal stromal tumours [196], melanomas [223], and leukaemias [224]. The most common mutation site is D816V, but there are several other sites of mutation that relinquish the need for a ligand [23]. Indeed, KIT is not the only protein to be mutated in this pathway: mutation of RAS, RAF, and MEK are all documented to have roles in cancer formation or progression [241-243].

I propose that the activation of the KIT/RAS/RAF/MEK pathway is necessary, but not sufficient to form a tumour. The end of this pathway activates MEK, which stabilises and increases protein levels of ETV1 [196]. In order for MEK to do this, ETV1 must already be expressed; therefore, I propose that ETV1 is already expressed (as in the case of GISTs), or is aberrantly expressed.

There are a number of methods of activating ETV1, other than stabilisation of the protein: fusion proteins [244], chromosomal gains, and endogenous expression are all common, with each mechanism seen in a different type of cancer.

Imprinting and the KIT-ETV1 axis

Loss of imprinting is commonly found in CNS GCTs and may activate the KIT-ETV1 axis. An analysis of imprinted genes revealed MYCN and RASSF1A as imprinted genes – both of which are strongly associated with cancer. RASSF1A is especially relevant because it is a downstream target of KIT in the KIT/RAS/RAF/MEK pathway. It would be interesting to test the activation of RASSF1A in a brain cell expressing endogenous ETV1 *in vitro* or *in vivo* to determine whether ETV1 target genes would be activated. If the coding region of *KIT* was sequenced in all germinomas, I would predict that RAS mutations would be activated instead of KIT as a redundant mechanism to activate ETV1.

The KIT-ETV1 axis and germinoma incidence

An important biological question needs to be addressed in order to qualify the KIT-ETV1 hypothesis: why do teratomas occur around birth and germinomas occur much later? Both teratomas and germinomas are classified as CNS GCTs but they have different age ranges for peak incidence.

Between these ages, the biological environment changes dramatically from being plastic during development, to being largely differentiated and in a low-proliferative state in adulthood. I hypothesise that in the brain, a cell retains or acquires pluripotent features, and becomes the cell of origin for all CNS GCTs. Figure 7.2 presents teratomas as the result of proliferation and differentiation in an environment where there are many proliferative and pluripotent signals. These signals decrease over time causing differentiation and the decrease of teratoma peak incidence.

Germinomas present a different pathogenesis but a similar cell of origin. The expression of pluripotent genes may confer several pluripotent features, but lack the proliferative drive. I propose these OCT4-expressing cells remain quiescent or non-proliferative until puberty, when hormones and growth factors that influence the proliferation rate appear. Cells that have acquired a *KIT*

mutation stimulate the KIT/RAS/RAF/MEK pathway, in a cell that already expresses ETV1 (in regions such as the pineal and suprasellar regions), which responds by proliferating - similar to gonadal GCTs [37].

This hypothesis is still biologically relevant to germinomas that occur in non-traditional regions such as in the spine and medulla oblongata regions. I propose that the pathogenesis is the same, and the increased age of peak incidence is due to the weaker hormonal influence. The pineal and suprasellar region have higher concentrations of growth factors and hormones than hind-brain regions. Therefore, it is plausible that those regions further from hormonal centres require more time to grow under conditions with reduced proliferative support.

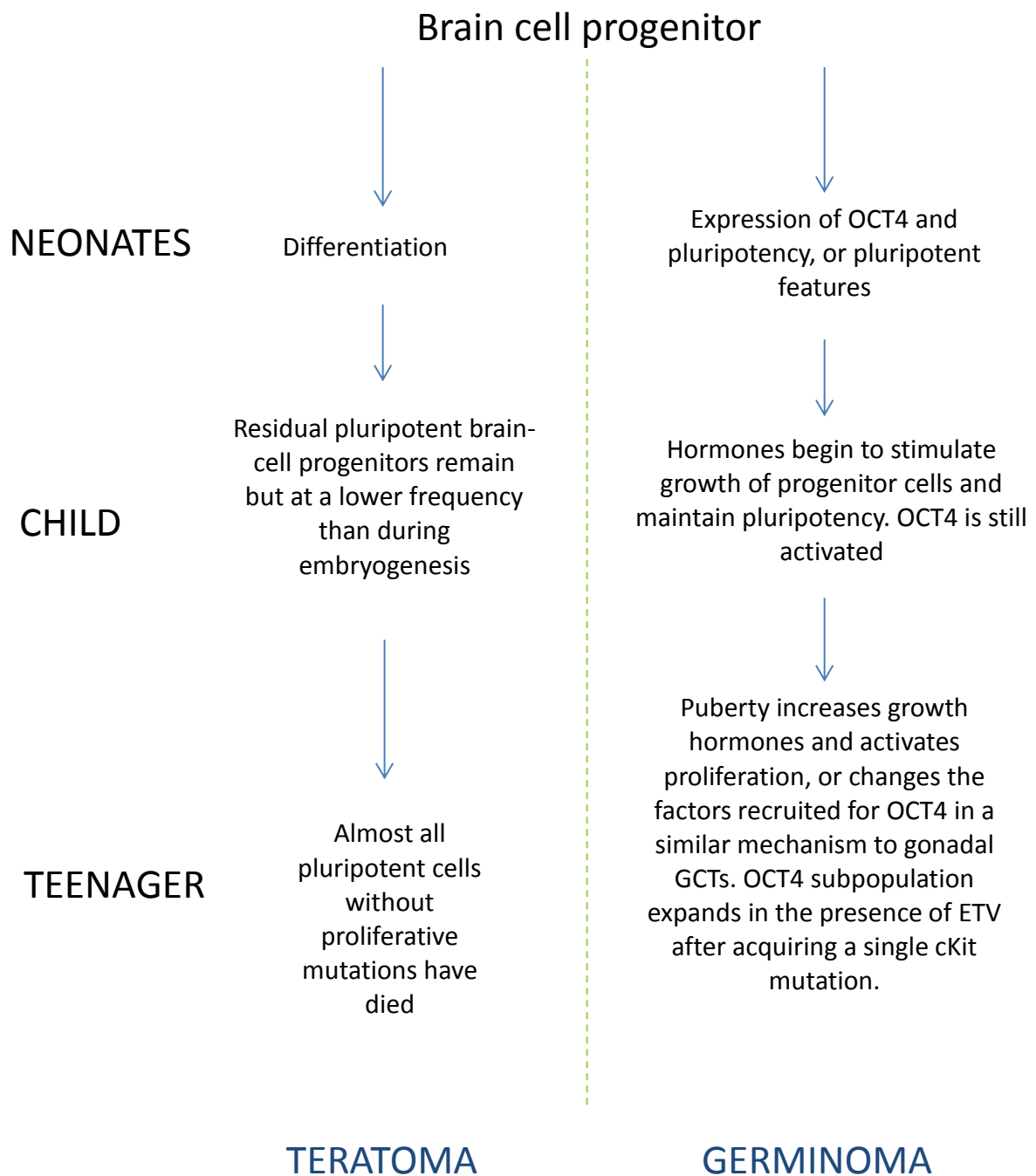


Figure 7.2. The proposed differences between teratoma and germinoma formation over development. All intracranial GCT are proposed to develop from a brain-cell with OCT4 activated. Those without mutations undergo differentiation during embryogenesis and form teratomas by birth. Germinomas are proposed to either be cells that had pluripotent features but were not recognised by the immune system, or had acquired mutations to drive oncogenesis. The mutations in germinoma progenitors, - such as those found in KIT - enable the lesion to respond to factors released during puberty by proliferating.

7.5. Factors influencing CNS GCT incidence

The incidence of CNS GCTs changes significantly depending on geographical location, CNS location, age, gender, and with the presence of Klinefelter syndrome. In this section I will focus on the role of geographical location and Klinefelter syndrome on CNS GCT incidence.

Geographical variation in the incidence of CNS GCTs

Chapter 1 highlights the differences in CNS GCT incidence between the countries in the East and the West. Studies using exome sequencing have highlighted a significant correlation between Eastern populations with a certain group of alleles linked to an increased incidence of CNS GCTs. Importantly, a higher incidence of CNS GCTs was recorded in people who expressed these genes but had moved from the East to the West. This strengthens the hypothesis that these genes are responsible for an increased incidence of CNS GCTs. Further, this data set was independently corroborated by another group doing a similar study. Because this work is unpublished, it is not possible to discuss the group of genes specifically (3rd International CNS Germ Cell Tumour Symposium, Cambridge, 2013 - Koichi Ichimura, Ching Lau, and Keita Terashima).

Little is known about the group of genes in question and their mechanism of activation, normal expression, or targets. However, they are expressed in certain types of cancer, and are implicated in epigenetics. The discovery of these genes is an exciting advance in understanding CNS GCT pathogenesis and elucidating the mechanism of these genes on cancer formation may help to determine the origin of CNS GCTs.

The relationship between Klinefelter syndrome and CNS GCTs

Klinefelter syndrome is a disease caused by an additional X chromosome and correlates with higher CNS GCT formation. While Klinefelter syndrome

increases the incidence of CNS GCTs there is no significant correlation for gonadal GCTs. This suggests a mechanism that is specific to a CNS GCT progenitor in the brain rather than tumours derived from PGCs in general.

Testing our hypothesis for a brain-cell of origin for CNS GCTs is essential to understanding the risk factors involved in initiating these tumours. The extra X chromosome in Klinefelter syndrome provides an obvious mechanism for forming CNS GCTs according to our hypothesis – the stabilisation of endogenous ETV1. Both A-RAF and E-RAS are located on the X chromosome and our hypothesis would be that they could activate MEK, which in turn stabilises ETV1 protein for transcription of ETV1 target genes.

7.6. Conclusion

In this thesis I have investigated the hypothesis that CNS GCTs arise from a brain cell. Literature searches showed that teratomas could grow in all regions of the brain, and an *in vivo* study confirmed that large teratomas could form in the lateral regions of the brain. Neural stem cells were examined as a potential cell of origin for CNS GCTs using *in vitro* and *in vivo* techniques. Finally, the overlap of ETV1 and KIT was proposed as a mechanism for germinoma formation in the CNS. I have established a testable mechanism for how a brain cell is activated to a pluripotent state and forms one of several subtypes of CNS GCT.

Several areas of our hypothesis require further work, such as the role of 12p and the KIT-ETV1 axis. CNS GCTs can be particularly sensitive to radiotherapy and chemotherapy, while subtypes such as yolk-sac tumours are difficult to treat. Indeed, understanding the pathogenesis of CNS GCTs may reveal the mechanism that confers this resistance/sensitivity [245].

Acceptance of our brain-cell hypothesis and a strong understanding of the pathogenesis of CNS GCTs will help us to develop more appropriate models. No transgenic model has yet managed to replicate extragonadal GCTs, making it difficult to study these tumours. Further work is required to fully understand the

networks involved in CNS GCT progression in order to develop therapies that cause fewer long-term sequelae than at present.

References

1. Available from: <http://universe-review.ca/R10-33-anatomy.htm>.
2. Oosterhuis, J.W., et al., *Why human extragonadal germ cell tumours occur in the midline of the body: old concepts, new perspectives*. *Int J Androl*, 2007. **30**(4): p. 256-63; discussion 263-4.
3. Packer, R.J., B.H. Cohen, and K. Cooney, *Intracranial germ cell tumors*. *Oncologist*, 2000. **5**(4): p. 312-20.
4. Damjanov, I. and P.W. Andrews, *The terminology of teratocarcinomas and teratomas*. *Nat Biotechnol*, 2007. **25**(11): p. 1212; discussion 1212.
5. Frazier, A.L., C. Weldon, and J. Amatruda, *Fetal and neonatal germ cell tumors*. *Semin Fetal Neonatal Med*, 2012. **17**(4): p. 222-30.
6. Vasdev, N., A. Moon, and A.C. Thorpe, *Classification, epidemiology and therapies for testicular germ cell tumours*. *Int J Dev Biol*, 2013. **57**(2-3-4): p. 133-139.
7. Isaacs, H., Jr., *Perinatal (fetal and neonatal) germ cell tumors*. *J Pediatr Surg*, 2004. **39**(7): p. 1003-13.
8. Wakai, S., T. Arai, and M. Nagai, *Congenital brain tumors*. *Surg Neurol*, 1984. **21**(6): p. 597-609.
9. Schlembach, D., et al., *Fetal intracranial tumors detected by ultrasound: a report of two cases and review of the literature*. *Ultrasound Obstet Gynecol*, 1999. **14**(6): p. 407-18.
10. Arora, R.S., et al., *Comparative incidence patterns and trends of gonadal and extragonadal germ cell tumors in England, 1979 to 2003*. *Cancer*, 2012. **118**(17): p. 4290-7.
11. Travis, L.B., et al., *Second cancers among 40,576 testicular cancer patients: focus on long-term survivors*. *J Natl Cancer Inst*, 2005. **97**(18): p. 1354-65.
12. van den Belt-Dusebout, A.W., et al., *Treatment-specific risks of second malignancies and cardiovascular disease in 5-year survivors of testicular cancer*. *J Clin Oncol*, 2007. **25**(28): p. 4370-8.
13. Kleihues, P., P.C. Burger, and B.W. Scheithauer, *The new WHO classification of brain tumours*. *Brain Pathol*, 1993. **3**(3): p. 255-68.
14. Kochi, M., et al., *Successful treatment of intracranial nongerminomatous malignant germ cell tumors by administering neoadjuvant chemotherapy and radiotherapy before excision of residual tumors*. *J Neurosurg*, 2003. **99**(1): p. 106-14.
15. Louis, D.N. and C. International Agency for Research on, *WHO classification of tumours of the central nervous system*. 4th ed. World Health Organization classification of tumours 2007, Lyon: International Agency for Research on Cancer. 309 p.
16. Wang, H.W., et al., *Pediatric primary central nervous system germ cell tumors of different prognosis groups show characteristic miRNome traits and chromosome copy number variations*. *BMC Genomics*, 2010. **11**: p. 132.
17. Keene, D., et al., *Epidemiological survey of central nervous system germ cell tumors in Canadian children*. *J Neurooncol*, 2007. **82**(3): p. 289-95.
18. McCarthy, B.J., et al., *Primary CNS germ cell tumors in Japan and the United States: an analysis of 4 tumor registries*. *Neuro Oncol*, 2012. **14**(9): p. 1194-200.
19. Arora, R.S., et al., *Comparative incidence patterns and trends of gonadal and extragonadal germ cell tumors in England, 1979 to 2003*. *Cancer*.

20. Villano, J.L., et al., *Descriptive epidemiology of central nervous system germ cell tumors: nonpineal analysis*. Neuro Oncol, 2010. **12**(3): p. 257-64.
21. Maconochie, N., et al., *Risk factors for first trimester miscarriage--results from a UK-population-based case-control study*. BJOG, 2007. **114**(2): p. 170-86.
22. Teilum, G., *Classification of endodermal sinus tumour (mesoblastoma vitellinum) and so-called "embryonal carcinoma" of the ovary*. Acta Pathol Microbiol Scand, 1965. **64**(4): p. 407-29.
23. Sakuma, Y., et al., *c-kit gene mutations in intracranial germinomas*. Cancer Sci, 2004. **95**(9): p. 716-20.
24. Scotting, P.J., *Are cranial germ cell tumours really tumours of germ cells?* Neuropathol Appl Neurobiol, 2006. **32**(6): p. 569-74.
25. BNOS, *Rare Brain and CNS Tumours Guidelines*, 2011, British Neuro-Oncology Society.
26. Anderson, R., et al., *The onset of germ cell migration in the mouse embryo*. Mech Dev, 2000. **91**(1-2): p. 61-8.
27. Sato, K., H. Takeuchi, and T. Kubota, *Pathology of intracranial germ cell tumors*. Prog Neurol Surg, 2009. **23**: p. 59-75.
28. Chaganti, R.S. and J. Houldsworth, *Genetics and biology of adult human male germ cell tumors*. Cancer Res, 2000. **60**(6): p. 1475-82.
29. Schwartz, D., et al., *p53 controls low DNA damage-dependent premeiotic checkpoint and facilitates DNA repair during spermatogenesis*. Cell Growth Differ, 1999. **10**(10): p. 665-75.
30. Schneider, D.T., et al., *Molecular genetic analysis of central nervous system germ cell tumors with comparative genomic hybridization*. Mod Pathol, 2006. **19**(6): p. 864-73.
31. Skakkebaek, N.E., et al., *Germ cell cancer and disorders of spermatogenesis: an environmental connection?* APMIS, 1998. **106**(1): p. 3-11; discussion 12.
32. Runyan, C., et al., *Steel factor controls midline cell death of primordial germ cells and is essential for their normal proliferation and migration*. Development, 2006. **133**(24): p. 4861-9.
33. Wylie, C., *Germ cells*. Cell, 1999. **96**(2): p. 165-74.
34. Wakhlu, A., et al., *Sacrococcygeal teratoma*. Pediatr Surg Int, 2002. **18**(5-6): p. 384-7.
35. Iwagaki, H., et al., *Extragenital sacrococcygeal seminoma--a case report*. Jpn J Surg, 1990. **20**(2): p. 225-8.
36. Schmidt, B., et al., *Sacrococcygeal teratoma: clinical course and prognosis with a special view to long-term functional results*. Pediatr Surg Int, 1999. **15**(8): p. 573-6.
37. Schneider, D.T., et al., *Multipoint imprinting analysis indicates a common precursor cell for gonadal and nongonadal pediatric germ cell tumors*. Cancer Res, 2001. **61**(19): p. 7268-76.
38. Cook, M.S., et al., *Regulation of male germ cell cycle arrest and differentiation by DND1 is modulated by genetic background*. Development, 2011. **138**(1): p. 23-32.
39. Runyan, C., et al., *The distribution and behavior of extragenital primordial germ cells in Bax mutant mice suggest a novel origin for sacrococcygeal germ cell tumors*. Int J Dev Biol, 2008. **52**(4): p. 333-44.
40. Cusack, M. and P.J. Scotting, *DNA methylation in germ cell tumour aetiology: current understanding and outstanding questions*. Reproduction, 2013.
41. Daxinger, L. and E. Whitelaw, *Understanding transgenerational epigenetic inheritance via the gametes in mammals*. Nat Rev Genet, 2012. **13**(3): p. 153-62.

42. Gregg, C., et al., *High-resolution analysis of parent-of-origin allelic expression in the mouse brain*. *Science*, 2010. **329**(5992): p. 643-8.
43. Gregg, C., et al., *Sex-specific parent-of-origin allelic expression in the mouse brain*. *Science*, 2010. **329**(5992): p. 682-5.
44. Jelinic, P. and P. Shaw, *Loss of imprinting and cancer*. *J Pathol*, 2007. **211**(3): p. 261-8.
45. Bussey, K.J., et al., *SNRPN methylation patterns in germ cell tumors as a reflection of primordial germ cell development*. *Genes Chromosomes Cancer*, 2001. **32**(4): p. 342-52.
46. Looijenga, L.H., et al., *Chromosomes and expression in human testicular germ-cell tumors: insight into their cell of origin and pathogenesis*. *Ann N Y Acad Sci*, 2007. **1120**: p. 187-214.
47. Bussey, K.J., et al., *Chromosome abnormalities of eighty-one pediatric germ cell tumors: sex-, age-, site-, and histopathology-related differences--a Children's Cancer Group study*. *Genes Chromosomes Cancer*, 1999. **25**(2): p. 134-46.
48. Korkola, J.E., et al., *Molecular events in germ cell tumours: linking chromosome-12 gain, acquisition of pluripotency and response to cisplatin*. *BJU Int*, 2009. **104**(9 Pt B): p. 1334-8.
49. Ottesen, A.M., et al., *High-resolution comparative genomic hybridization detects extra chromosome arm 12p material in most cases of carcinoma in situ adjacent to overt germ cell tumors, but not before the invasive tumor development*. *Genes Chromosomes Cancer*, 2003. **38**(2): p. 117-25.
50. Smith, A.A., et al., *Intracranial germ cell tumors: a single institution experience and review of the literature*. *J Neurooncol*, 2004. **68**(2): p. 153-9.
51. Rickert, C.H., et al., *Comparative genomic hybridization in pineal germ cell tumors*. *J Neuropathol Exp Neurol*, 2000. **59**(9): p. 815-21.
52. Lemos, J.A., J. Barbieri-Neto, and C. Casartelli, *Primary intracranial germ cell tumors without an isochromosome 12p*. *Cancer Genet Cytogenet*, 1998. **100**(2): p. 124-8.
53. Shen, V., et al., *Absence of isochromosome 12p in a pineal region malignant germ cell tumor*. *Cancer Genet Cytogenet*, 1990. **50**(1): p. 153-60.
54. de Bruin, T.W., et al., *Isochromosome 12p-positive pineal germ cell tumor*. *Cancer Res*, 1994. **54**(6): p. 1542-4.
55. Casalone, R., et al., *Cerebral germ cell tumor and XXY karyotype*. *Cancer Genet Cytogenet*, 1994. **74**(1): p. 25-9.
56. Gilbertson, R.J., *Mapping cancer origins*. *Cell*, 2011. **145**(1): p. 25-9.
57. Lee, S.H., et al., *Variable methylation of the imprinted gene, SNRPN, supports a relationship between intracranial germ cell tumours and neural stem cells*. *J Neurooncol*, 2010. **101**(3): p. 419-28.
58. Uyeno, S., et al., *IGF2 but not H19 shows loss of imprinting in human glioma*. *Cancer Res*, 1996. **56**(23): p. 5356-9.
59. Wang, X. and J. Dai, *Concise review: isoforms of OCT4 contribute to the confusing diversity in stem cell biology*. *Stem Cells*. **28**(5): p. 885-93.
60. Papamichos, S.I., *An Alu exonization event allowing for the generation of a novel OCT4 isoform*. *Gene*, 2013. **512**(1): p. 175-7.
61. Pan, G.J., et al., *Stem cell pluripotency and transcription factor Oct4*. *Cell Res*, 2002. **12**(5-6): p. 321-9.
62. Zhang, Z., et al., *Post-translational modification of POU domain transcription factor Oct-4 by SUMO-1*. *FASEB J*, 2007. **21**(12): p. 3042-51.
63. Minucci, S., et al., *Retinoic acid-mediated down-regulation of Oct3/4 coincides with the loss of promoter occupancy in vivo*. *EMBO J*, 1996. **15**(4): p. 888-99.

64. Lee, S.H., et al., *Dynamic methylation and expression of Oct4 in early neural stem cells*. J Anat, 2010. **217**(3): p. 203-13.
65. Christman, J.K., *5-Azacytidine and 5-aza-2'-deoxycytidine as inhibitors of DNA methylation: mechanistic studies and their implications for cancer therapy*. Oncogene, 2002. **21**(35): p. 5483-95.
66. Deb-Rinker, P., et al., *Sequential DNA methylation of the Nanog and Oct-4 upstream regions in human NT2 cells during neuronal differentiation*. J Biol Chem, 2005. **280**(8): p. 6257-60.
67. Blom, H.J., *Folic acid, methylation and neural tube closure in humans*. Birth Defects Res A Clin Mol Teratol, 2009. **85**(4): p. 295-302.
68. De Wals, P., et al., *Reduction in neural-tube defects after folic acid fortification in Canada*. N Engl J Med, 2007. **357**(2): p. 135-42.
69. Freberg, C.T., et al., *Epigenetic reprogramming of OCT4 and NANOG regulatory regions by embryonal carcinoma cell extract*. Mol Biol Cell, 2007. **18**(5): p. 1543-53.
70. Gu, P., et al., *Differential recruitment of methylated CpG binding domains by the orphan receptor GCNF initiates the repression and silencing of Oct4 expression*. Mol Cell Biol, 2006. **26**(24): p. 9471-83.
71. Akamatsu, W., et al., *Suppression of Oct4 by germ cell nuclear factor restricts pluripotency and promotes neural stem cell development in the early neural lineage*. J Neurosci, 2009. **29**(7): p. 2113-24.
72. Pardo, M., et al., *An expanded Oct4 interaction network: implications for stem cell biology, development, and disease*. Cell Stem Cell, 2010. **6**(4): p. 382-95.
73. Liang, J., et al., *Nanog and Oct4 associate with unique transcriptional repression complexes in embryonic stem cells*. Nat Cell Biol, 2008. **10**(6): p. 731-9.
74. Webster, D.M., et al., *O-GlcNAc modifications regulate cell survival and epiboly during zebrafish development*. BMC Dev Biol, 2009. **9**: p. 28.
75. Takahashi, K. and S. Yamanaka, *Induction of pluripotent stem cells from mouse embryonic and adult fibroblast cultures by defined factors*. Cell, 2006. **126**(4): p. 663-76.
76. Sternecker, J., S. Hoing, and H.R. Scholer, *Concise review: Oct4 and more: the reprogramming expressway*. Stem Cells, 2012. **30**(1): p. 15-21.
77. Kim, J., et al., *Direct reprogramming of mouse fibroblasts to neural progenitors*. Proc Natl Acad Sci U S A, 2011. **108**(19): p. 7838-43.
78. Loh, Y.H., et al., *The Oct4 and Nanog transcription network regulates pluripotency in mouse embryonic stem cells*. Nat Genet, 2006. **38**(4): p. 431-40.
79. Pan, G., et al., *A negative feedback loop of transcription factors that controls stem cell pluripotency and self-renewal*. FASEB J, 2006. **20**(10): p. 1730-2.
80. Chew, J.L., et al., *Reciprocal transcriptional regulation of Pou5f1 and Sox2 via the Oct4/Sox2 complex in embryonic stem cells*. Mol Cell Biol, 2005. **25**(14): p. 6031-46.
81. Kim, J.B., et al., *Direct reprogramming of human neural stem cells by OCT4*. Nature, 2009. **461**(7264): p. 649-3.
82. Greenow, K. and A.R. Clarke, *Controlling the stem cell compartment and regeneration in vivo: the role of pluripotency pathways*. Physiol Rev, 2012. **92**(1): p. 75-99.
83. Zhang, H.J., et al., *Oct4 is epigenetically regulated by methylation in normal placenta and gestational trophoblastic disease*. Placenta, 2008. **29**(6): p. 549-54.
84. Rajasingh, J., et al., *Improvement of cardiac function in mouse myocardial infarction after transplantation of epigenetically-modified bone marrow progenitor cells*. PLoS One. **6**(7): p. e22550.

85. Lim, M.L., et al., *A novel, efficient method to derive bovine and mouse embryonic stem cells with in vivo differentiation potential by treatment with 5-azacytidine*. *Theriogenology*, **76**(1): p. 133-42.
86. Ezeh, U.I., et al., *Human embryonic stem cell genes OCT4, NANOG, STELLAR, and GDF3 are expressed in both seminoma and breast carcinoma*. *Cancer*, 2005. **104**(10): p. 2255-65.
87. Hoei-Hansen, C.E., et al., *New evidence for the origin of intracranial germ cell tumours from primordial germ cells: expression of pluripotency and cell differentiation markers*. *J Pathol*, 2006. **209**(1): p. 25-33.
88. Palmer, R.D., et al., *Pediatric malignant germ cell tumors show characteristic transcriptome profiles*. *Cancer Res*, 2008. **68**(11): p. 4239-47.
89. Brait, M., et al., *DNA methylation profiles delineate epigenetic heterogeneity in seminoma and non-seminoma*. *Br J Cancer*, 2011. **106**(2): p. 414-23.
90. Jeyapalan, J.N., et al., *Methylator phenotype of malignant germ cell tumours in children identifies strong candidates for chemotherapy resistance*. *Br J Cancer*, 2011. **105**(4): p. 575-85.
91. Scotting, P.J., D.A. Walker, and G. Perilongo, *Childhood solid tumours: a developmental disorder*. *Nat Rev Cancer*, 2005. **5**(6): p. 481-8.
92. Anderton, J.A., et al., *Global analysis of the medulloblastoma epigenome identifies disease-subgroup-specific inactivation of COL1A2*. *Neuro Oncol*, 2008. **10**(6): p. 981-94.
93. Laffaire, J., et al., *Methylation profiling identifies 2 groups of gliomas according to their tumorigenesis*. *Neuro Oncol*, 2010. **13**(1): p. 84-98.
94. Rogers, H.A., et al., *Supratentorial and spinal pediatric ependymomas display a hypermethylated phenotype which includes the loss of tumor suppressor genes involved in the control of cell growth and death*. *Acta Neuropathol*, 2011. **123**(5): p. 711-25.
95. Hori, N., et al., *Induction of DNA demethylation depending on two sets of Sox2 and adjacent Oct3/4 binding sites (Sox-Oct motifs) within the mouse H19/insulin-like growth factor 2 (Igf2) imprinted control region*. *J Biol Chem*, 2012. **287**(52): p. 44006-16.
96. Satge, D., et al., *Aspects of intracranial and spinal tumors in patients with Down syndrome and report of a rapidly progressing Grade 2 astrocytoma*. *Cancer*, 2001. **91**(8): p. 1458-66.
97. Hasle, H., et al., *Cancer incidence in men with Klinefelter syndrome*. *Br J Cancer*, 1995. **71**(2): p. 416-20.
98. Queipo, G., et al., *Intracranial germ cell tumors: association with Klinefelter syndrome and sex chromosome aneuploidies*. *Cytogenet Genome Res*, 2008. **121**(3-4): p. 211-4.
99. Cambray, N. and V. Wilson, *Two distinct sources for a population of maturing axial progenitors*. *Development*, 2007. **134**(15): p. 2829-40.
100. Cambray, N. and V. Wilson, *Axial progenitors with extensive potency are localised to the mouse chordoneural hinge*. *Development*, 2002. **129**(20): p. 4855-66.
101. Horton, D. and D.W. Pilling, *Early antenatal ultrasound diagnosis of fetal intracranial teratoma*. *Br J Radiol*, 1997. **70**(840): p. 1299-301.
102. Saada, J., et al., *Early second-trimester diagnosis of intracranial teratoma*. *Ultrasound Obstet Gynecol*, 2009. **33**(1): p. 109-11.
103. Beschorner, R., et al., *Mature cerebellar teratoma in adulthood*. *Neuropathology*, 2009. **29**(2): p. 176-80.

104. Lee, D. and Y.L. Suh, *Histologically confirmed intracranial germ cell tumors; an analysis of 62 patients in a single institute*. *Virchows Arch*, 2010. **457**(3): p. 347-57.
105. Kim, S.M., et al., *Congenital cerebellar mixed germ cell tumor presenting with hemorrhage in a newborn*. *Korean J Radiol*, 2008. **9 Suppl**: p. S26-9.
106. Utsuki, S., et al., *Malignant transformation of intracranial mature teratoma to yolk sac tumor after late relapse. Case report*. *J Neurosurg*, 2007. **106**(6): p. 1067-9.
107. Shaffrey, M.E., et al., *Maturation of intracranial immature teratomas. Report of two cases*. *J Neurosurg*, 1996. **85**(4): p. 672-6.
108. Dal Cin, P., et al., *Immature teratoma of the pineal gland with isochromosome 12p*. *Acta Neuropathol*, 1998. **95**(1): p. 107-10.
109. Yamashita, N., et al., *Immature teratoma producing alpha-fetoprotein without components of yolk sac tumor in the pineal region*. *Childs Nerv Syst*, 1997. **13**(4): p. 225-8.
110. Kim, C.Y., et al., *Intracranial growing teratoma syndrome: clinical characteristics and treatment strategy*. *J Neurooncol*, 2011. **101**(1): p. 109-15.
111. Naudin ten Cate, L., et al., *Intracranial teratoma with multiple fetuses: pre- and post-natal appearance*. *Hum Pathol*, 1995. **26**(7): p. 804-7.
112. Lipman, S.P., et al., *Fetal intracranial teratoma: US diagnosis of three cases and a review of the literature*. *Radiology*, 1985. **157**(2): p. 491-4.
113. Chiu, C.D., et al., *Gamma knife radiosurgery for intracranial mature teratoma--long-term results and review of literature*. *Surg Neurol*, 2006. **65**(4): p. 343-51.
114. Ogawa, K., et al., *Treatment and prognosis of patients with intracranial nongerminomatous malignant germ cell tumors: a multiinstitutional retrospective analysis of 41 patients*. *Cancer*, 2003. **98**(2): p. 369-76.
115. Lee, Y.H., et al., *Treatment and outcomes of primary intracranial teratoma*. *Childs Nerv Syst*, 2009. **25**(12): p. 1581-7.
116. Sandow, B.A., et al., *Best cases from the AFIP: congenital intracranial teratoma*. *Radiographics*, 2004. **24**(4): p. 1165-70.
117. Kitanaka, C., et al., *Precocious puberty in a girl with an hCG-secreting suprasellar immature teratoma. Case report*. *J Neurosurg*, 1994. **81**(4): p. 601-4.
118. Rickert, C.H., et al., *Congenital immature teratoma of the fetal brain*. *Childs Nerv Syst*, 1997. **13**(10): p. 556-9.
119. Poremba, C., et al., *Immature teratomas of different origin carried by a pregnant mother and her fetus*. *Diagn Mol Pathol*, 1993. **2**(2): p. 131-6.
120. Uysal, A., et al., *Prenatal diagnosis of a fetal intracranial tumor*. *Arch Gynecol Obstet*, 2005. **272**(1): p. 87-9.
121. Longano, A. and R. Conyers, *Medulloblastoma arising from intracranial immature teratoma*. *Pathology*, 2010. **42**(1): p. 102-4.
122. Chien, Y.H., et al., *Congenital intracranial teratoma*. *Pediatr Neurol*, 2000. **22**(1): p. 72-4.
123. Sesenna, E., et al., *Huge orbital teratoma with intracranial extension: a case report*. *J Pediatr Surg*, 2010. **45**(5): p. e27-31.
124. Erman, T., et al., *Congenital intracranial immature teratoma of the lateral ventricle: a case report and review of the literature*. *Neurol Res*, 2005. **27**(1): p. 53-6.
125. Pikus, H.J., B. Holmes, and R.E. Harbaugh, *Teratoma of the cavernous sinus: case report*. *Neurosurgery*, 1995. **36**(5): p. 1020-3.
126. Sinha, V.D., S.R. Dharker, and C.L. Pandey, *Congenital intracranial teratoma of the lateral ventricle*. *Neurol India*, 2001. **49**(2): p. 170-3.

127. Aibe, M., T. Hirano, and I. Takeshita, [*Teratoma in the cerebellar hemisphere of an infant*]. No To Hattatsu, 2001. **33**(1): p. 45-8.
128. Yang, J.C. and J.S. Huang, *Third ventricle immature teratoma: a case report*. Kaohsiung J Med Sci, 2004. **20**(4): p. 192-7.
129. Selcuki, M., et al., *Mature teratoma of the lateral ventricle: report of two cases*. Acta Neurochir (Wien), 1998. **140**(2): p. 171-4.
130. El-Gaidi, M.A. and E.M. Eissa, *Infantile intracranial neoplasms: characteristics and surgical outcomes of a contemporary series of 21 cases in an Egyptian referral center*. Pediatr Neurosurg, 2010. **46**(4): p. 272-82.
131. Chan, L.W., et al., *Foetal intracranial teratoma: choosing the best time and mode of delivery*. Hong Kong Med J, 2007. **13**(4): p. 323-6.
132. Jaing, T.H., et al., *Intracranial germ cell tumors: a retrospective study of 44 children*. Pediatr Neurol, 2002. **26**(5): p. 369-73.
133. Canan, A., et al., *Neonatal intracranial teratoma*. Brain Dev, 2000. **22**(5): p. 340-2.
134. Im, S.H., et al., *Congenital intracranial teratoma: prenatal diagnosis and postnatal successful resection*. Med Pediatr Oncol, 2003. **40**(1): p. 57-61.
135. Pinto, V., et al., *Prenatal sonographic imaging of an immature intracranial teratoma*. Fetal Diagn Ther, 1999. **14**(4): p. 220-2.
136. Peng, S.S., et al., *Ultrafast fetal MR images of intracranial teratoma*. J Comput Assist Tomogr, 1999. **23**(2): p. 318-9.
137. Sherer, D.M., et al., *Prenatal ultrasonographic diagnosis of intracranial teratoma and massive craniomegaly with associated high-output cardiac failure*. Am J Obstet Gynecol, 1993. **168**(1 Pt 1): p. 97-9.
138. Ulreich, S., A. Hanieh, and M.E. Furness, *Positive outcome of fetal intracranial teratoma*. J Ultrasound Med, 1993. **12**(3): p. 163-5.
139. Kuller, J.A., et al., *Unusual presentations of fetal teratoma*. J Perinatol, 1991. **11**(3): p. 294-6.
140. Dolkart, L.A., R.J. Balcom, and G. Eisinger, *Intracranial teratoma: prolonged neonatal survival after prenatal diagnosis*. Am J Obstet Gynecol, 1990. **162**(3): p. 768-9.
141. Coulibaly, O., et al., *Mature posterior fossa teratoma mimicking infratentorial meningioma: a case report*. Neurochirurgie, 2012. **58**(1): p. 40-3.
142. Smirniotopoulos, J.G., E.J. Rushing, and H. Mena, *Pineal region masses: differential diagnosis*. Radiographics, 1992. **12**(3): p. 577-96.
143. Sugimoto, K., I. Nakahara, and M. Nishikawa, *Bilateral metachronous germinoma of the basal ganglia occurring long after total removal of a mature pineal teratoma: case report*. Neurosurgery, 2002. **50**(3): p. 613-6; discussion 616-7.
144. Ikeda, J., et al., *Metachronous neurohypophyseal germinoma occurring 8 years after total resection of pineal mature teratoma*. Surg Neurol, 1998. **49**(2): p. 205-8; discussion 208-9.
145. Janzarik, W.G., et al., *Occurrence of a germinoma 22 years after resection of a mature cerebral teratoma*. J Neurooncol, 2008. **88**(2): p. 217-9.
146. Mao, Q., et al., *Germinoma occurring 2 years after total resection of an intracranial epidermoid cyst in the pineal region*. J Neurooncol, 2012. **106**(2): p. 437-9.
147. Czirjak, S., et al., *Third ventricle germinoma after total removal of intrasellar teratoma. Case report*. J Neurosurg, 1992. **77**(4): p. 643-7.
148. Gilcrease, M.Z., M.L. Brandt, and E.P. Hawkins, *Yolk sac tumor identified at autopsy after surgical excision of immature sacrococcygeal teratoma*. J Pediatr Surg, 1995. **30**(6): p. 875-7.

149. Kamoshima, Y., et al., *Metachronous mature teratoma in the corpus callosum occurring 12 years after a pineal germinoma*. J Neurosurg, 2008. **109**(1): p. 126-9.
150. Benesch, M., et al., *Mediastinal yolk sac tumor ten years after treatment of intracranial germinoma*. Medical and Pediatric Oncology, 2003. **40**(1): p. 54-56.
151. Bi, W.L., S.I. Bannykh, and J. Baehring, *The growing teratoma syndrome after subtotal resection of an intracranial nongerminomatous germ cell tumor in an adult: case report*. Neurosurgery, 2005. **56**(1): p. 188.
152. Taccagni, G.L., et al., *Mixed germ cell tumour of the mediastinum (seminoma, embryonal carcinoma, choriocarcinoma and teratoma). Light and electron microscopic cytology and histological investigation*. Pathol Res Pract, 1989. **185**(4): p. 506-10; discussion 511-3.
153. Akahira, J., et al., *Ovarian mixed germ cell tumor composed of dysgerminoma, endodermal sinus tumor, choriocarcinoma and mature teratoma in a 44-year-old woman: case report and literature review*. Pathol Int, 1998. **48**(6): p. 471-4.
154. Mosharafa, A.A., et al., *Histology in mixed germ cell tumors. Is there a favorite pairing?* J Urol, 2004. **171**(4): p. 1471-3.
155. Ho, D.M. and H.C. Liu, *Primary intracranial germ cell tumor. Pathologic study of 51 patients*. Cancer, 1992. **70**(6): p. 1577-84.
156. Shokry, A., et al., *Primary intracranial germ-cell tumors. A clinicopathological study of 14 cases*. J Neurosurg, 1985. **62**(6): p. 826-30.
157. Kuriu, A., et al., *Fourth ventricular mixed germ cell tumor demonstrating adipose tissue in a young adult*. Jpn J Radiol, 2010. **28**(2): p. 166-8.
158. Bohara, M., et al., *Pineal mixed germ cell tumor with a synchronous sellar lesion in the sixth decade*. Brain Tumor Pathol, 2011. **28**(2): p. 163-6.
159. Kim, J.P., B.J. Park, and Y.J. Lim, *A primary intrasellar mixed germ cell tumor with suprasellar extension*. Childs Nerv Syst, 2011. **27**(7): p. 1161-4.
160. Koh, E.J., et al., *Mixed germ cell tumor of the midbrain. Case Report*. J Neurosurg Pediatr, 2009. **4**(2): p. 137-42.
161. Wildenberg, L.E., et al., *Sellar and suprasellar mixed germ cell tumor mimicking a pituitary adenoma*. Pituitary, 2011. **14**(4): p. 345-50.
162. Cunliffe, C.H., et al., *Synchronous mixed germ cell tumor of the pineal gland and suprasellar region with a predominant angiomatous component: a diagnostic challenge*. J Neurooncol, 2009. **93**(2): p. 269-74.
163. Makidono, A., et al., *Metachronous gliomas following cranial irradiation for mixed germ cell tumors*. Childs Nerv Syst, 2009. **25**(6): p. 713-8.
164. Ichikawa, T., et al., *Mixed germ cell tumor and hemangioblastoma in the cerebellum: report of a rare coexistence*. Brain Tumor Pathol, 2011. **28**(3): p. 279-84.
165. Allan, R.W., C.B. Algood, and M. Shih Ie, *Metastatic epithelioid trophoblastic tumor in a male patient with mixed germ-cell tumor of the testis*. Am J Surg Pathol, 2009. **33**(12): p. 1902-5.
166. Kim, E., et al., *Primary malignant teratoma with a primitive neuroectodermal tumor component in thyroid gland: a case report*. J Korean Med Sci, 2007. **22**(3): p. 568-71.
167. Chen, P.Y., et al., *Malignant ganglioneuroma arising from mediastinal mixed germ cell tumor*. J Chin Med Assoc, 2007. **70**(2): p. 76-9.
168. Pelosi, G., et al., *Differentiating neuroblastoma arising in mediastinal germ cell tumour*. Histopathology, 2008. **53**(3): p. 350-2.
169. Contreras, A.L., et al., *Mediastinal germ cell tumors with an angiosarcomatous component: a report of 12 cases*. Hum Pathol, 2010. **41**(6): p. 832-7.

170. Miller, R.R., K. Champagne, and R.C. Murray, *Primary pulmonary germ cell tumor with blastomatous differentiation*. Chest, 1994. **106**(5): p. 1595-6.
171. Marusic, Z., et al., *Papillary renal cell-like carcinoma in a retroperitoneal teratoma*. Pathol Int, 2010. **60**(8): p. 581-5.
172. Xu, A.M., et al., *Primary mixed germ cell tumor of the liver with sarcomatous components*. World J Gastroenterol, 2010. **16**(5): p. 652-6.
173. Petricek, C.M., *Colonic adenocarcinoma metastasizing as a germ cell neoplasm: a case report and review of the literature*. Arch Pathol Lab Med, 2001. **125**(4): p. 558-61.
174. Jung, C.K., et al., *Oligodendroglioma arising in a sacrococcygeal immature teratoma*. J Korean Med Sci, 2002. **17**(3): p. 426-8.
175. Busse, C., et al., *Sacrococcygeal immature teratoma with malignant ependymoma component*. Pediatr Blood Cancer, 2009. **53**(4): p. 680-1.
176. Lovric, E., et al., *An unusual mixed germ cell tumor of the testis consisting of rhabdomyosarcoma, mature teratoma and yolk sac tumor*. Asian J Androl, 2010. **12**(3): p. 451-2.
177. Idrees, M.T., et al., *Clonal evidence for the progression of a testicular germ cell tumor to angiosarcoma*. Hum Pathol, 2010. **41**(1): p. 139-44.
178. Lavalley, L.T., et al., *A unique case of a sarcoma arising in a testicular non-seminomatous mixed germ cell tumour with a predominant yolk sac component*. Can Urol Assoc J, 2011. **5**(5): p. E81-3.
179. Serrano-Olmo, J., et al., *Neuroblastoma as a prominent component of a mixed germ cell tumor of testis*. Cancer, 1993. **72**(11): p. 3271-6.
180. Emerson, R.E., et al., *Nephroblastoma arising in a germ cell tumor of testicular origin*. Am J Surg Pathol, 2004. **28**(5): p. 687-92.
181. Allen, E.A., P.C. Burger, and J.I. Epstein, *Microcystic meningioma arising in a mixed germ cell tumor of the testis: a case report*. Am J Surg Pathol, 1999. **23**(9): p. 1131-5.
182. Bel Haj Salah, M., et al., *[Mixed germ cell tumor of the ovary with rhabdomyosarcomatous component. A case report]*. Ann Pathol, 2010. **30**(5): p. 394-7.
183. Echevarria, M.E., J. Fangusaro, and S. Goldman, *Pediatric central nervous system germ cell tumors: a review*. Oncologist, 2008. **13**(6): p. 690-9.
184. Swartling, F.J., et al., *Distinct Neural Stem Cell Populations Give Rise to Disparate Brain Tumors in Response to N-MYC*. Cancer Cell, 2012. **21**(5): p. 601-13.
185. Kum, J.B., et al., *Molecular genetic evidence supporting the origin of somatic-type malignancy and teratoma from the same progenitor cell*. Am J Surg Pathol, 2012. **36**(12): p. 1849-56.
186. Lustig, M., et al., *Nr-CAM expression in the developing mouse nervous system: ventral midline structures, specific fiber tracts, and neuropilar regions*. J Comp Neurol, 2001. **434**(1): p. 13-28.
187. Runko, E., C. Wideman, and Z. Kaprielian, *Cloning and expression of VEMA: a novel ventral midline antigen in the rat CNS*. Mol Cell Neurosci, 1999. **14**(6): p. 428-43.
188. Hemberger, M., et al., *H19 and Igf2 are expressed and differentially imprinted in neuroectoderm-derived cells in the mouse brain*. Dev Genes Evol, 1998. **208**(7): p. 393-402.
189. Hentze, H., et al., *Teratoma formation by human embryonic stem cells: evaluation of essential parameters for future safety studies*. Stem Cell Res, 2009. **2**(3): p. 198-210.

190. Paxinos, K.F.a.G., *Mouse Brain in Stereotaxic Coordinates*. Third edition ed: Academic press.
191. Dorr, A., J.G. Sled, and N. Kabani, *Three-dimensional cerebral vasculature of the CBA mouse brain: a magnetic resonance imaging and micro computed tomography study*. *Neuroimage*, 2007. **35**(4): p. 1409-23.
192. Yamanaka, S., *A fresh look at iPS cells*. *Cell*, 2009. **137**(1): p. 13-7.
193. Jackson Laboratories. Available from: <http://jaxmice.jax.org/strain/006911.html>.
194. Rodda, D.J., et al., *Transcriptional regulation of nanog by OCT4 and SOX2*. *J Biol Chem*, 2005. **280**(26): p. 24731-7.
195. Navarro, P., et al., *OCT4/SOX2-independent Nanog autorepression modulates heterogeneous Nanog gene expression in mouse ES cells*. *EMBO J*, 2012. **31**(24): p. 4547-62.
196. Chi, P., et al., *ETV1 is a lineage survival factor that cooperates with KIT in gastrointestinal stromal tumours*. *Nature*, 2010. **467**(7317): p. 849-53.
197. Hu, Y.W., et al., *Salvage treatment for recurrent intracranial germinoma after reduced-volume radiotherapy: a single-institution experience and review of the literature*. *Int J Radiat Oncol Biol Phys*, 2012. **84**(3): p. 639-47.
198. Thakkar, J.P., L. Chew, and J.L. Villano, *Primary CNS germ cell tumors: current epidemiology and update on treatment*. *Med Oncol*, 2013. **30**(2): p. 496.
199. *Allen Brain Atlas*. Available from: <http://mouse.brain-map.org/>.
200. Bernex, F., et al., *Spatial and temporal patterns of c-kit-expressing cells in WlacZ/+ and WlacZ/WlacZ mouse embryos*. *Development*, 1996. **122**(10): p. 3023-33.
201. Wehrle-Haller, B. and J.A. Weston, *Soluble and cell-bound forms of steel factor activity play distinct roles in melanocyte precursor dispersal and survival on the lateral neural crest migration pathway*. *Development*, 1995. **121**(3): p. 731-42.
202. Shuto, T., et al., *Primary medulla oblongata germinoma in a male patient*. *J Clin Neurosci*, 2012. **19**(5): p. 769-71.
203. Yasuhara, T., et al., *Primary germinoma in the medulla oblongata - case report*. *Neurol Med Chir (Tokyo)*, 2011. **51**(4): p. 326-9.
204. Akimoto, J., et al., *Primary medulla oblongata germinoma--an unusual posterior fossa tumors in young adults*. *J Clin Neurosci*, 2009. **16**(5): p. 705-8.
205. Nakatsuka, S., et al., *Primary extragonadal germinoma of the medulla oblongata*. *Int J Surg Pathol*, 2012. **20**(3): p. 276-9.
206. Nakajima, H., et al., *Primary intracranial germinoma in the medulla oblongata*. *Surg Neurol*, 2000. **53**(5): p. 448-51.
207. Yen, P.S., et al., *Primary medulla oblongata germinoma: a case report and review of the literature*. *J Neurooncol*, 2003. **62**(3): p. 339-42.
208. Tashiro, T., et al., *Primary intracranial germinoma involving the medulla oblongata--case report*. *Neurol Med Chir (Tokyo)*, 1993. **33**(4): p. 251-4.
209. Nakata, Y., A. Yagishita, and N. Arai, *Two patients with intraspinal germinoma associated with Klinefelter syndrome: case report and review of the literature*. *AJNR Am J Neuroradiol*, 2006. **27**(6): p. 1204-10.
210. Huang, J.H., et al., *Intramedullary cervical spine germinoma: case report*. *Neurosurgery*, 2004. **55**(6): p. 1432.
211. Watanabe, A., et al., *Intramedullary spinal cord germinoma expresses the protooncogene c-kit*. *Acta Neurochir (Wien)*, 2005. **147**(3): p. 303-8; discussion 308.
212. Yang, K.Y., et al., *Concurrent chemoradiotherapy for primary cervical spinal cord germinoma*. *J Clin Neurosci*, 2009. **16**(1): p. 115-8.

213. Hata, M., et al., *Intramedullary spinal cord germinoma: case report and review of the literature*. *Radiology*, 2002. **223**(2): p. 379-83.
214. Sugiyama, K., et al., *Germinoma of the medulla oblongata--case report*. *Neurol Med Chir (Tokyo)*, 1994. **34**(5): p. 291-4.
215. Neelima, R., et al., *Germinoma of medulla*. *Neurol India*, 2010. **58**(5): p. 768-70.
216. Hanakita, S., et al., *Intramedullary recurrence of germinoma in the spinal cord 15 years after complete remission of a pineal lesion*. *J Neurosurg Spine*, 2012. **16**(5): p. 513-5.
217. Aoyama, T., et al., *Intramedullary spinal cord germinoma--2 case reports*. *Surg Neurol*, 2007. **67**(2): p. 177-83; discussion 183.
218. Unni, S.K., et al., *Stage-specific localization and expression of c-kit in the adult human testis*. *J Histochem Cytochem*, 2009. **57**(9): p. 861-9.
219. Robinson, L.L., et al., *Germ cell specific expression of c-kit in the human fetal gonad*. *Mol Hum Reprod*, 2001. **7**(9): p. 845-52.
220. Prabhu, S.M., et al., *Expression of c-Kit receptor mRNA and protein in the developing, adult and irradiated rodent testis*. *Reproduction*, 2006. **131**(3): p. 489-99.
221. Monte, D., et al., *Molecular characterization of the ets-related human transcription factor ER81*. *Oncogene*, 1995. **11**(4): p. 771-9.
222. Kuno, T., et al., *Extragenital seminoma presenting as a large mass in the pelvic cavity without c-kit-activating mutations*. *Jpn J Clin Oncol*, 2012. **42**(7): p. 650-3.
223. Carvajal, R.D., et al., *KIT as a therapeutic target in metastatic melanoma*. *JAMA*, 2011. **305**(22): p. 2327-34.
224. Wang, Y.Y., et al., *AML1-ETO and C-KIT mutation/overexpression in t(8;21) leukemia: implication in stepwise leukemogenesis and response to Gleevec*. *Proc Natl Acad Sci U S A*, 2005. **102**(4): p. 1104-9.
225. Aker, F.V., et al., *Pineal germinoma associated with multiple congenital melanocytic nevi: a unique presentation*. *Neuropathology*, 2005. **25**(4): p. 336-40.
226. Pilloni, L., et al., *The usefulness of c-Kit in the immunohistochemical assessment of melanocytic lesions*. *Eur J Histochem*, 2011. **55**(2): p. e20.
227. da Silva, J.C., et al., *Multiple midline intracranial germinoma managed by neuroendoscopy*. *Arq Neuropsiquiatr*, 2009. **67**(1): p. 125-6.
228. Looijenga, L.H., *Human testicular (non)seminomatous germ cell tumours: the clinical implications of recent pathobiological insights*. *J Pathol*, 2009. **218**(2): p. 146-62.
229. Krag Jacobsen, G., et al., *Testicular germ cell tumours in Denmark 1976-1980. Pathology of 1058 consecutive cases*. *Acta Radiol Oncol*, 1984. **23**(4): p. 239-47.
230. Rescorla, F.J., et al., *Long-term outcome for infants and children with sacrococcygeal teratoma: a report from the Childrens Cancer Group*. *J Pediatr Surg*, 1998. **33**(2): p. 171-6.
231. Swamy, R., N. Embleton, and J. Hale, *Sacrococcygeal teratoma over two decades: birth prevalence, prenatal diagnosis and clinical outcomes*. *Prenat Diagn*, 2008. **28**(11): p. 1048-51.
232. Zhang, J., et al., *A novel retinoblastoma therapy from genomic and epigenetic analyses*. *Nature*, 2012. **481**(7381): p. 329-34.
233. Ito, S., et al., *Role of Tet proteins in 5mC to 5hmC conversion, ES-cell self-renewal and inner cell mass specification*. *Nature*, 2010. **466**(7310): p. 1129-33.
234. Costa, Y., et al., *NANOG-dependent function of TET1 and TET2 in establishment of pluripotency*. *Nature*, 2013. **495**(7441): p. 370-4.

235. Kumar, S.M., et al., *Acquired cancer stem cell phenotypes through Oct4-mediated dedifferentiation*. *Oncogene*, 2012. **31**(47): p. 4898-911.
236. Korkola, J.E., et al., *Down-regulation of stem cell genes, including those in a 200-kb gene cluster at 12p13.31, is associated with in vivo differentiation of human male germ cell tumors*. *Cancer Res*, 2006. **66**(2): p. 820-7.
237. Quinn, S.C., et al., *Attributes of researchers and their strategies to recruit minority populations: results of a national survey*. *Contemp Clin Trials*, 2012. **33**(6): p. 1231-7.
238. Draper, J.S., et al., *Recurrent gain of chromosomes 17q and 12 in cultured human embryonic stem cells*. *Nat Biotechnol*, 2004. **22**(1): p. 53-4.
239. Bayani, J., A. Pandita, and J.A. Squire, *Molecular cytogenetic analysis in the study of brain tumors: findings and applications*. *Neurosurg Focus*, 2005. **19**(5): p. E1.
240. Meng, G.Z., et al., *Myofibroblastic sarcoma vs nodular fasciitis: a comparative study of chromosomal imbalances*. *Am J Clin Pathol*, 2009. **131**(5): p. 701-9.
241. Prior, I.A., P.D. Lewis, and C. Mattos, *A comprehensive survey of Ras mutations in cancer*. *Cancer Res*, 2012. **72**(10): p. 2457-67.
242. Dhillon, A.S. and W. Kolch, *Oncogenic B-Raf mutations: crystal clear at last*. *Cancer Cell*, 2004. **5**(4): p. 303-4.
243. Emery, C.M., et al., *MEK1 mutations confer resistance to MEK and B-RAF inhibition*. *Proc Natl Acad Sci U S A*, 2009. **106**(48): p. 20411-6.
244. Thompson, A.D., et al., *Divergent Ewing's sarcoma EWS/ETS fusions confer a common tumorigenic phenotype on NIH3T3 cells*. *Oncogene*, 1999. **18**(40): p. 5506-13.
245. Houldsworth, J., et al., *Expression profiling of lineage differentiation in pluripotential human embryonal carcinoma cells*. *Cell Growth Differ*, 2002. **13**(6): p. 257-64.

Appendix I – Genotyping transgenic mice

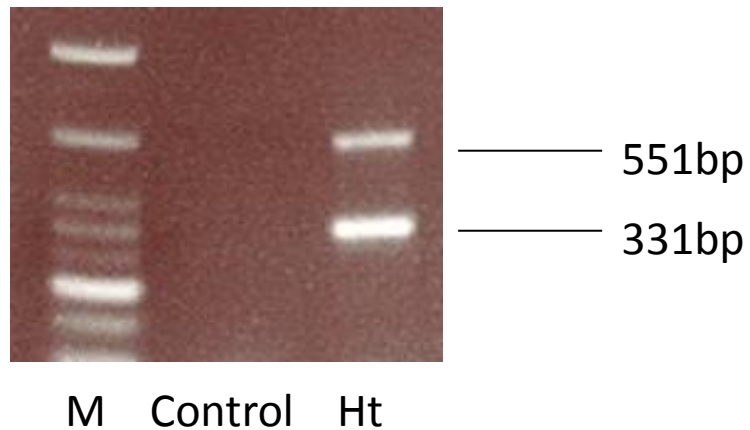


Figure I.1 Col1a1-Oct4 genotyping. All three primers (Common, wild-type, and mutant) were used to amplify heterogenous mouse DNA. The upper 551bp band indicates presence of the mutant allele, and the 331bp band represents the wild-type allele. Homozygous mutant or wild-type genotypes are a single band of either the upper or lower band respectively.

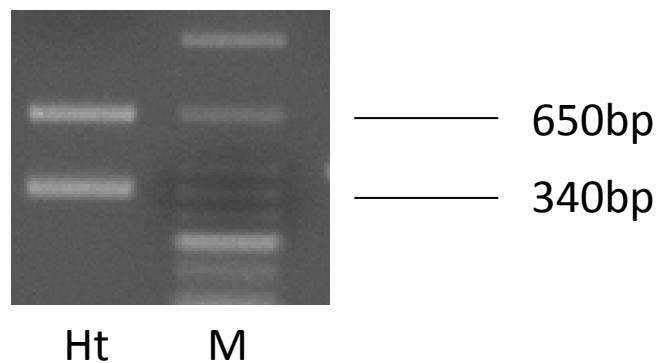


Figure I.2 Rosa genotyping. All three primers (Common, wild-type, and mutant) were used to amplify heterogenous mouse DNA. The upper 650bp band indicates presence of the mutant allele, and the 340bp band represents the wild-type allele. Homozygous mutant or wild-type genotypes are a single band of either the upper or lower band respectively.

Pedigree number	Genotype						
11883	Ht	15502	Ht	25562	Ht	32874	Hm
11930	Ht	15503	Ht	25563	Hm	32875	Ht
11931	Hm	19185	Hm	25564	Hm	32876	Hm
11932	Ht	19186	Wt	25565	Ht	32877	Ht
11933	Hm	19187	Ht	25566	Ht	32878	Hm
11934	Hm	19188	Wt	25567	Ht	32879	Hm
11935	Ht	19189	Hm	26199	Hm	32031	Hm
11936	Ht	19190	Hm	26200	Hm	32032	Ht
11937	Ht	19393	Hm	27340	Ht	32033	Ht
14422	Ht	19394	Hm	27341	Ht	34524	Ht
14423	Wt	22015	Wt	27342	Ht	32528	Hm
14424	Wt	22016	Wt	27343	Wt	32529	Ht
14267	Hm	22017	Ht	27344	Ht	32530	Hm
14268	Ht	22018	Ht	27345	Wt	32522	Hm
14269	Hm	22019	Hm	27346	Hm	33500	Ht
14270	Ht	22020	Wt	30228	Hm	33599	Ht
14271	Ht	22021	Wt	30229	Ht	33600	Ht
14420	Wt	22655	Hm	30230	Ht	33601	Hm
14421	Wt	22656	Hm	30231	Ht	33824	Ht
14422	Ht	22657	Hm	30232	Ht	33825	Wt
14423	Wt	22658	Hm	30233	Hm	33826	Ht
14424	Wt	22659	Hm	28732	Ht	34530	Hm
15094	Ht	22660	Hm	28959	Wt	36040	Hm
15095	Ht	23928	Wt	28964	Hm	36050	Ht
15096	Hm	23929	Ht	28965	Hm	36061	Hm
15499	Ht	23930	Hm	28966	Hm	36065	Ht
15500	Hm	23931	Hm	28967	Hm	38408	Hm
15501	Hm	23932	Ht	28968	Hm	38409	Hm
		25561	Ht	32030	Ht	38410	Ht

Table I.1. Genotyping for transgenic mice. Each mouse was tagged with a pedigree number to track the genotype and mating data. The genotypes for each mouse are shown next to the corresponding number

Appendix II - *in situ* hybridisations

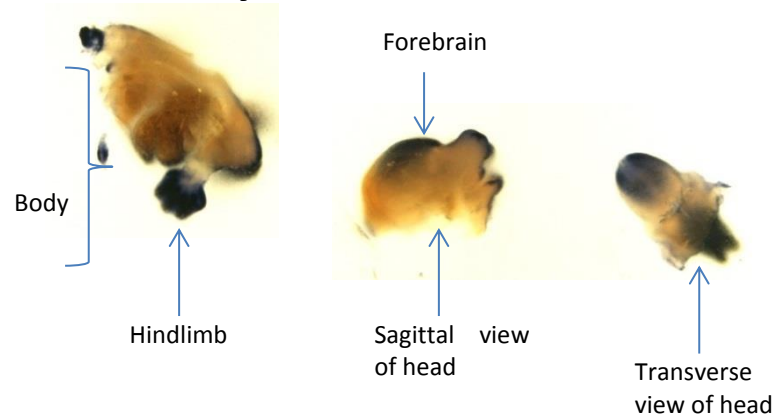


Figure II.1. Wax sectioning of an E13.5 embryo after whole-mount *in situ* hybridisation using an ETV1 probe. The whole-mount *in situ* hybridisation quality is low, and did not increase the ability to distinguish specific areas of staining compared to whole-mount without wax sectioning. .

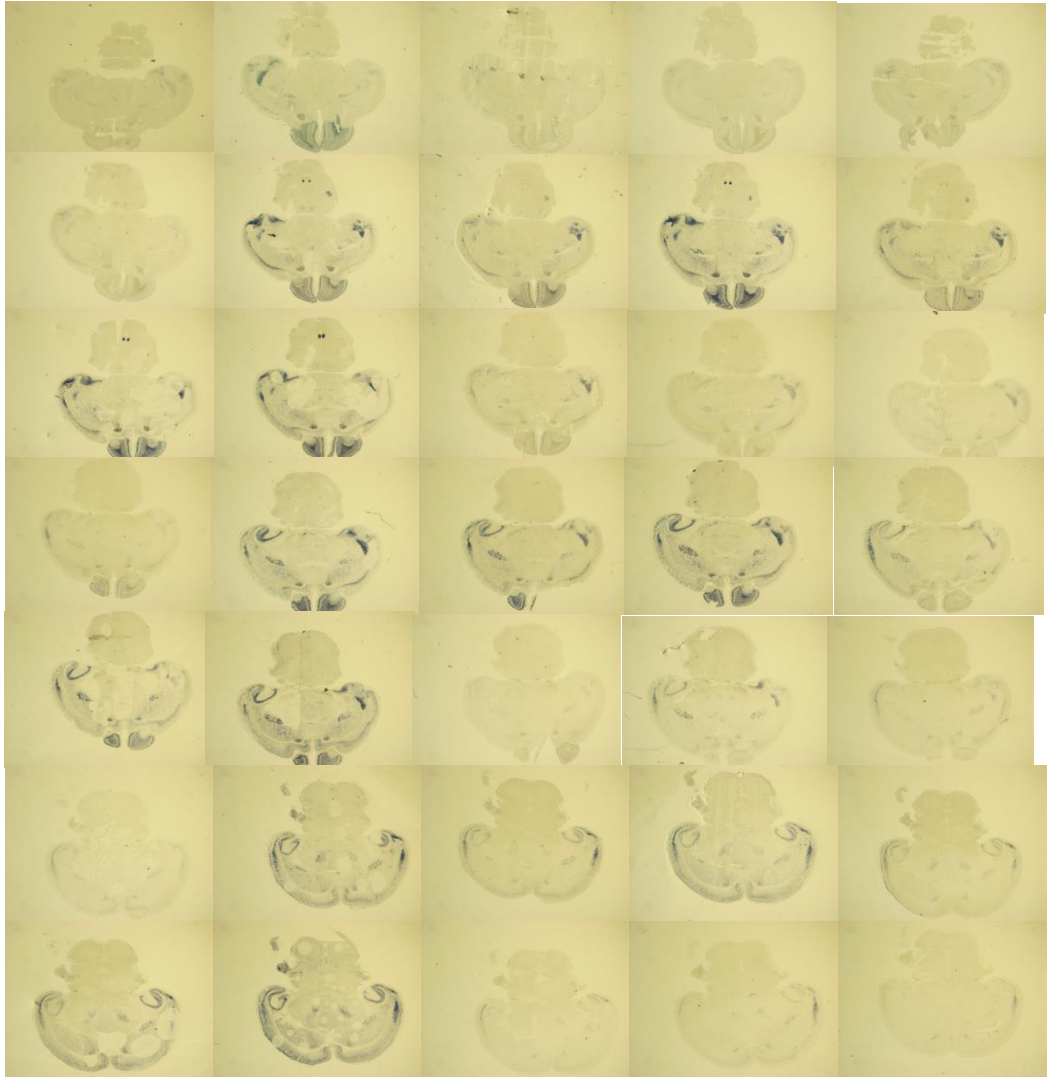
Ventral section 1 \longrightarrow Section 5



Section 25

Figure II.2. Wax sectioning of a postnatal day 7 mouse brain after *in situ* hybridisation using an ETV1 anti-sense probe. ETV1 positive staining is purple indicating expression, and normal tissue is beige. The images are shown beginning from a transverse ventral section on the top left (section 1) to the top right (section 5), and ending with a transverse section towards the dorsal side of the brain at the bottom right (section 25).

Ventral



Dorsal

Figure II.3-II.18. Allen Brain Atlas *in situ* hybridisation using a KIT or ETV1 probe on a mouse embryo. Positive staining is purple indicating expression, and normal tissue is beige. All images are taken from the Allen Mouse Brain Atlas. Three-dimensional images showing regions of expression from four planes are above two-dimensional images when available. Figure II.3-II.10 show expression of *Etv1*, and Figure II.11-II.18 use a *Kit* probe.

ETV images

Figure II.3. E11.5

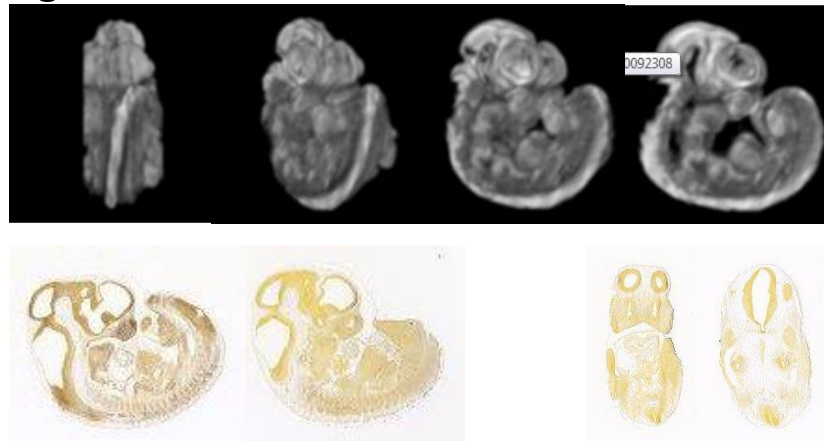


Figure II.4. E13.5

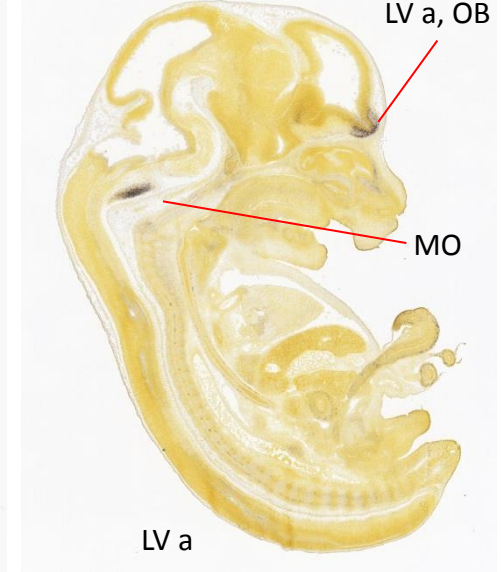
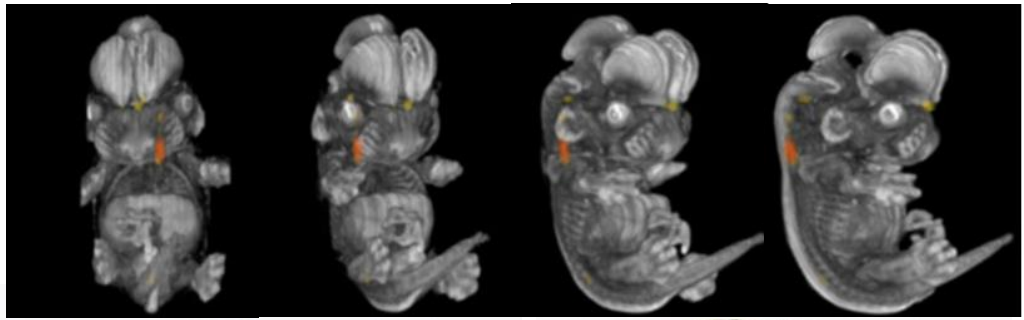
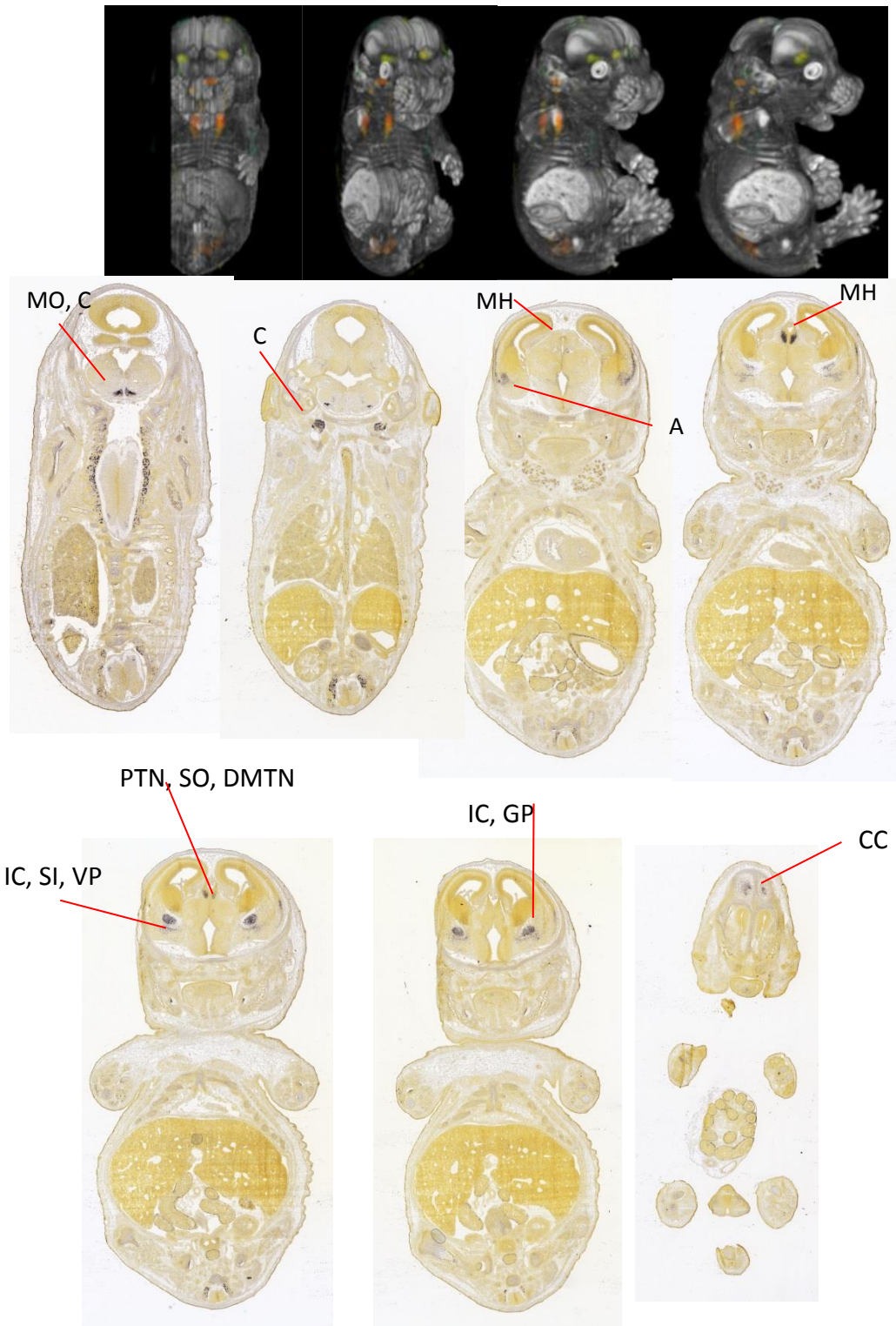


Figure II.5. E15.5



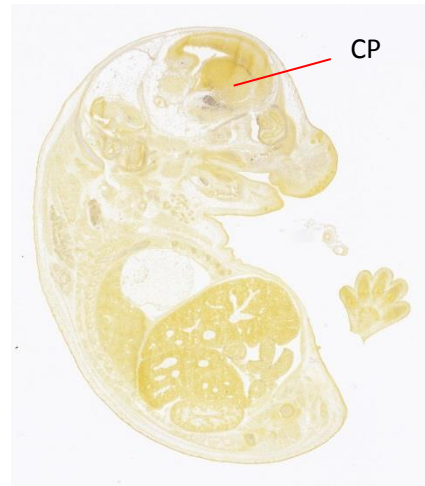


Figure II.6. E18.5

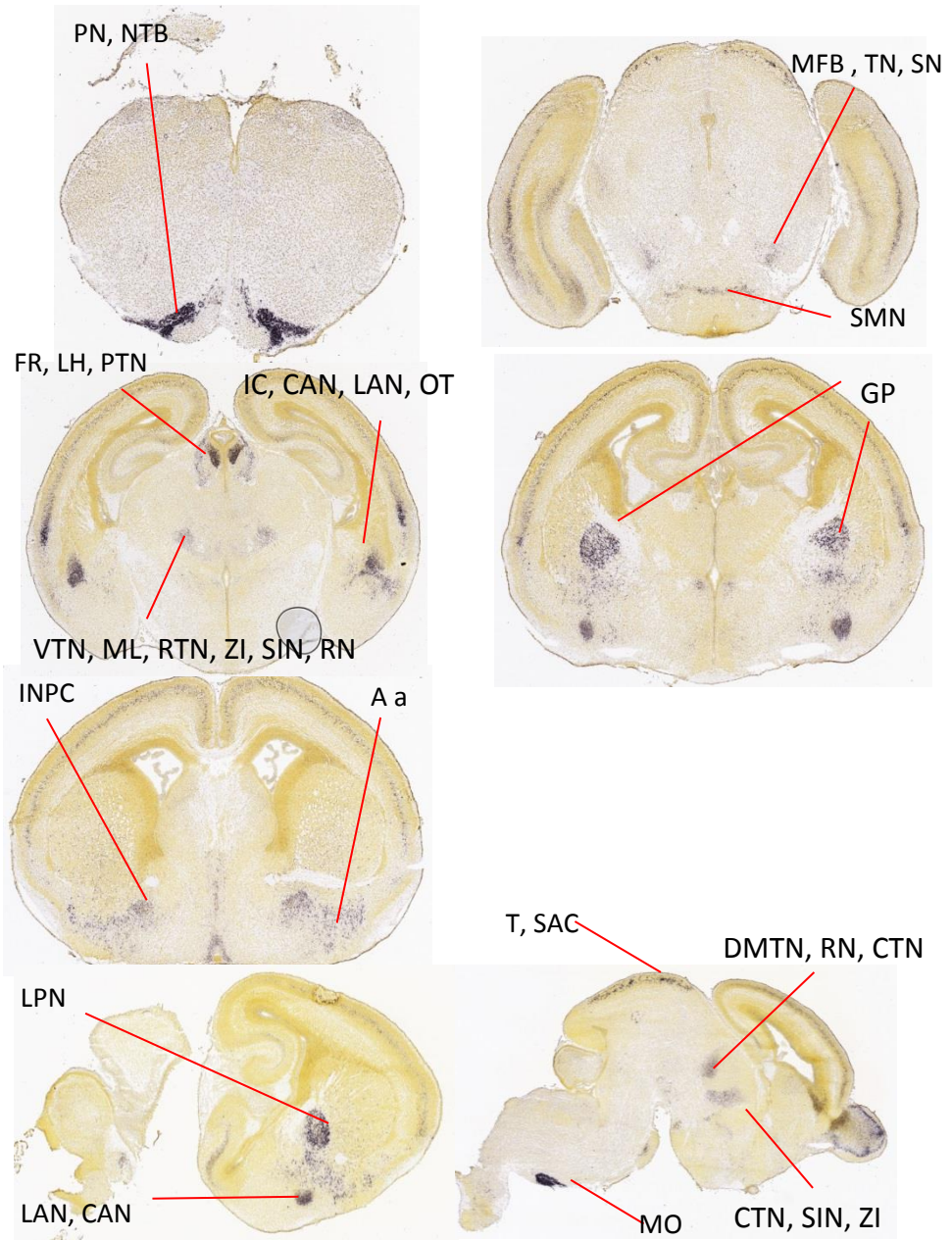
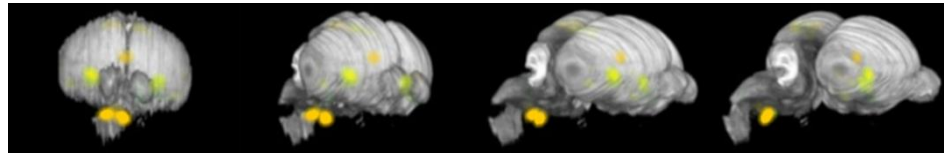


Figure II.7. P4

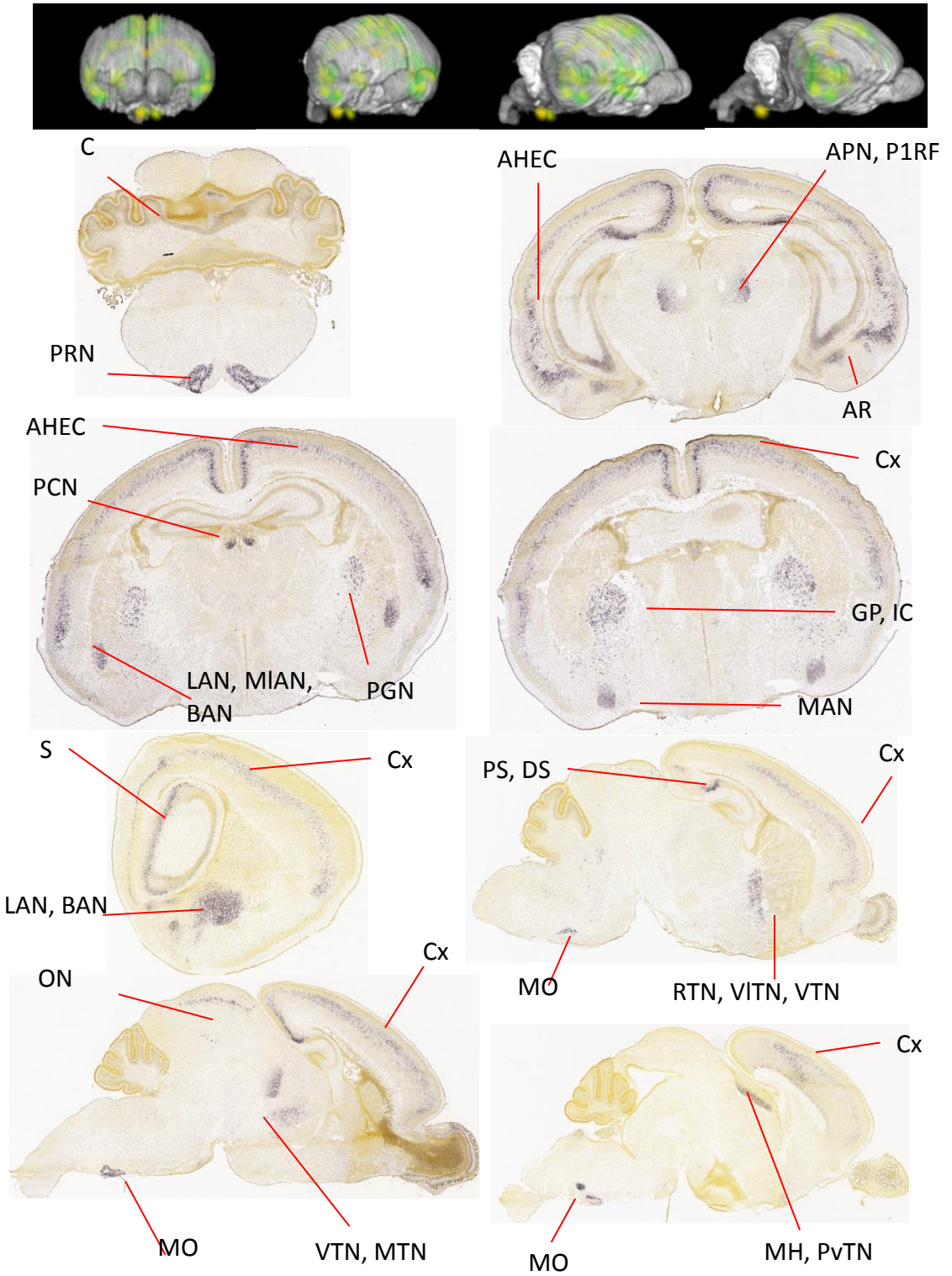


Figure II.8. P14

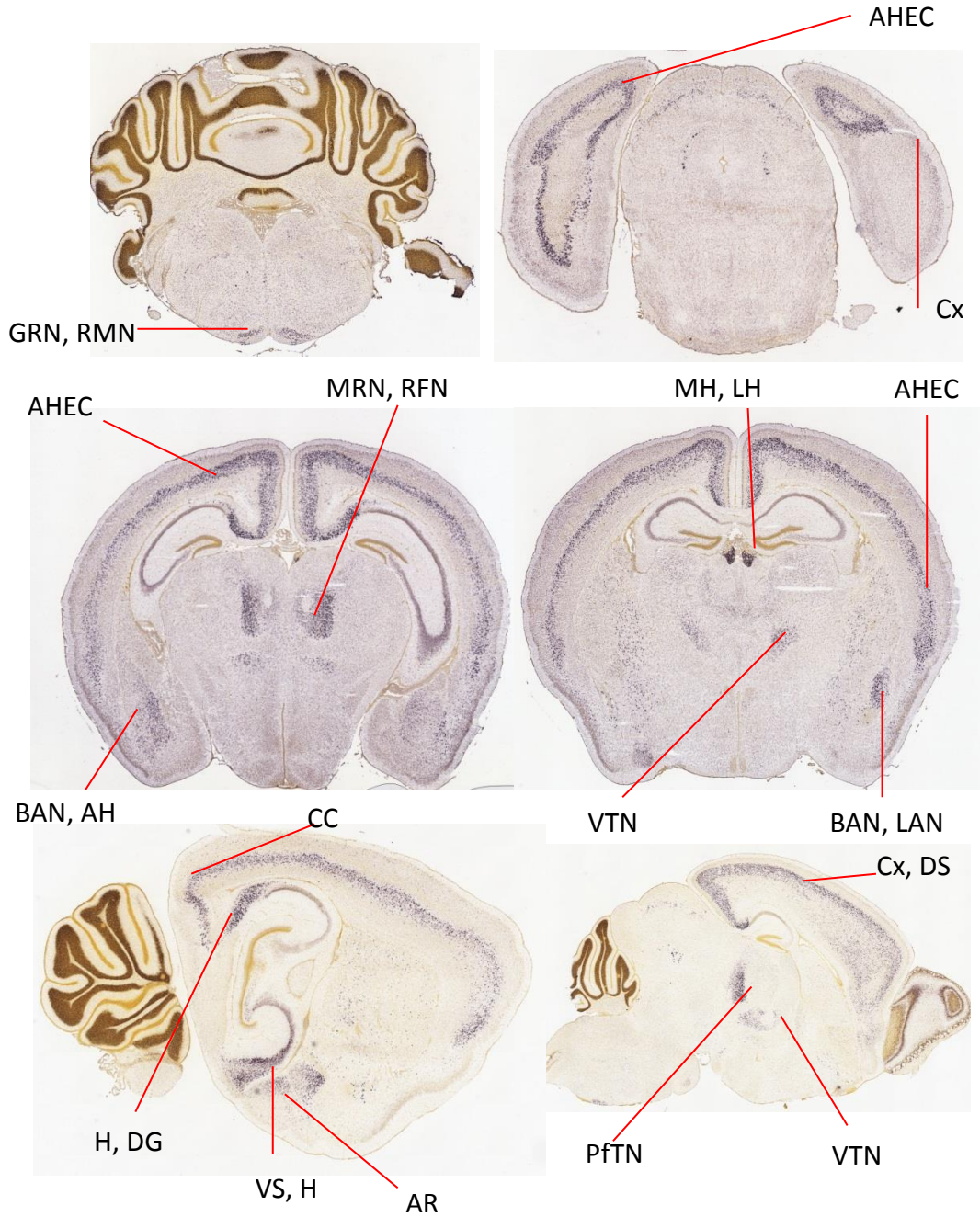
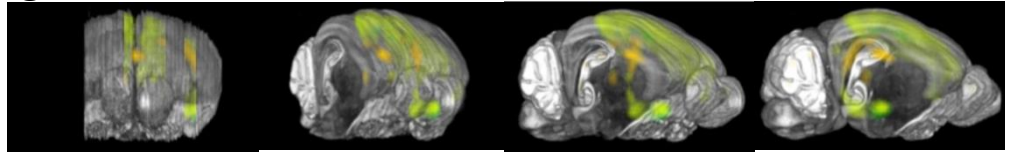


Figure II.9. P28

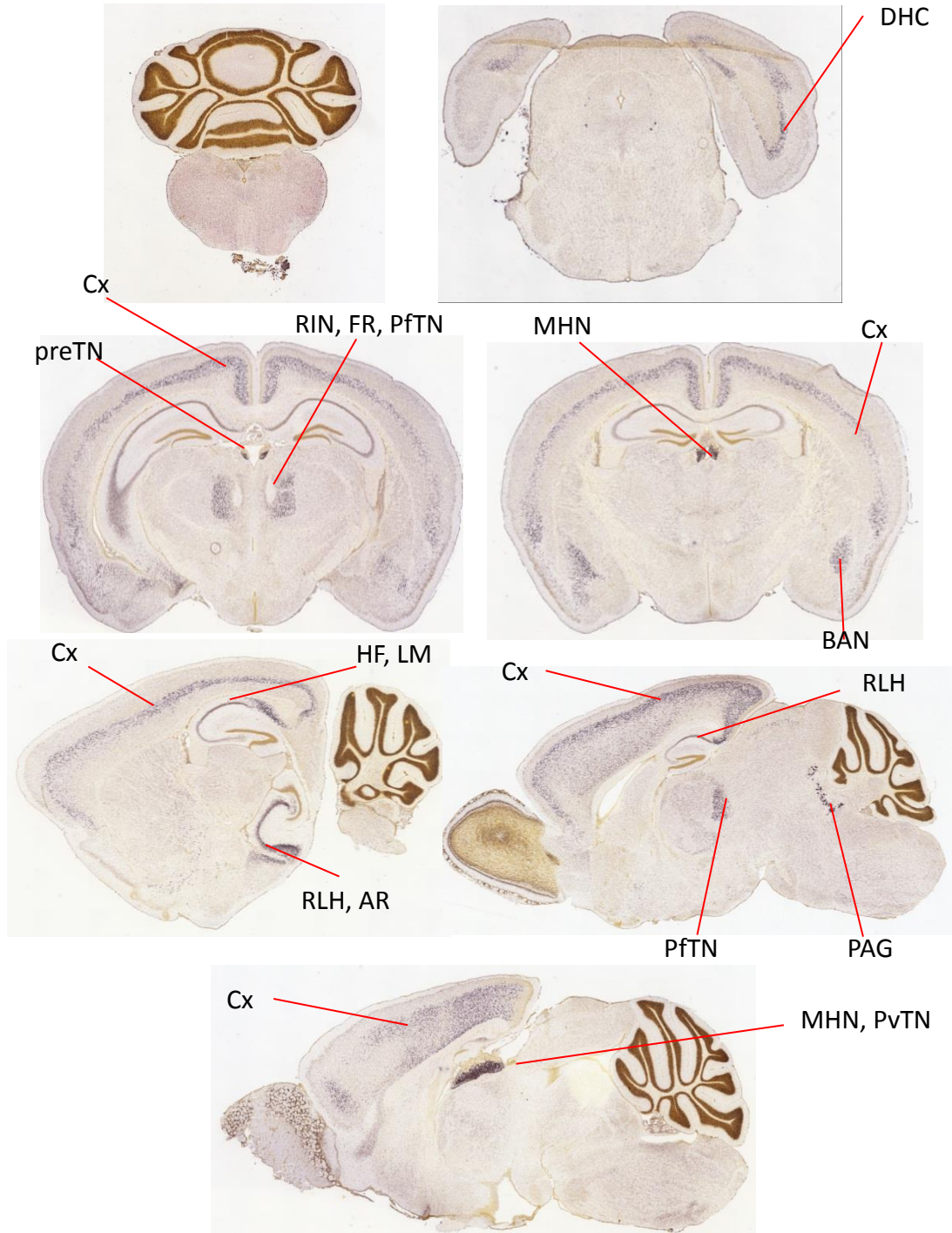
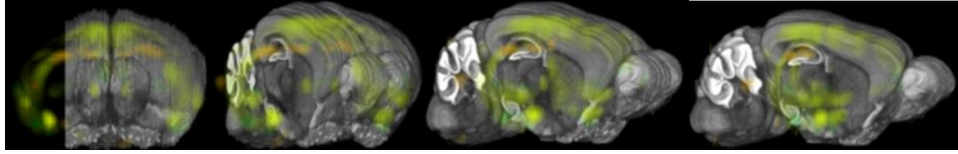
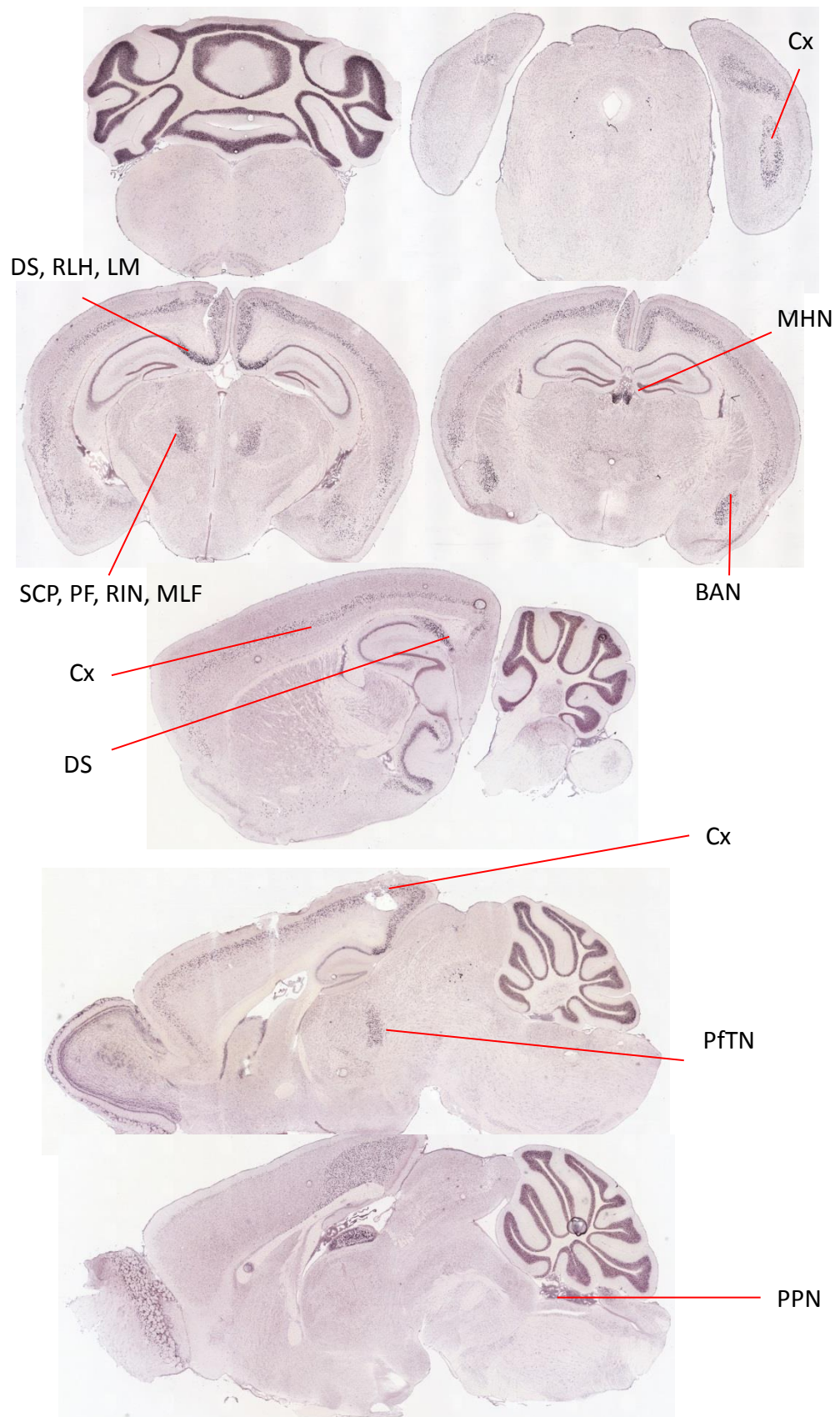


Figure II.10. P56



Kit images

Figure II.11. E11.5

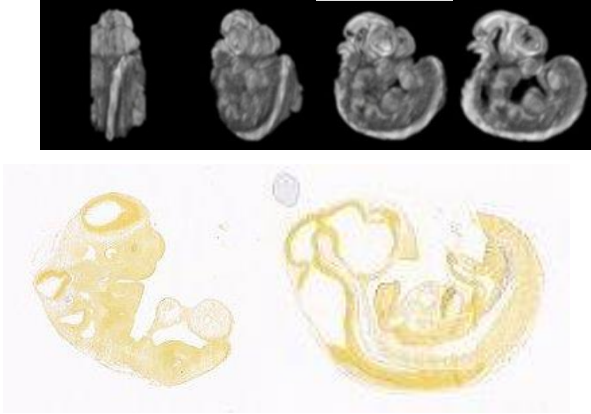


Figure II.12. E13.5

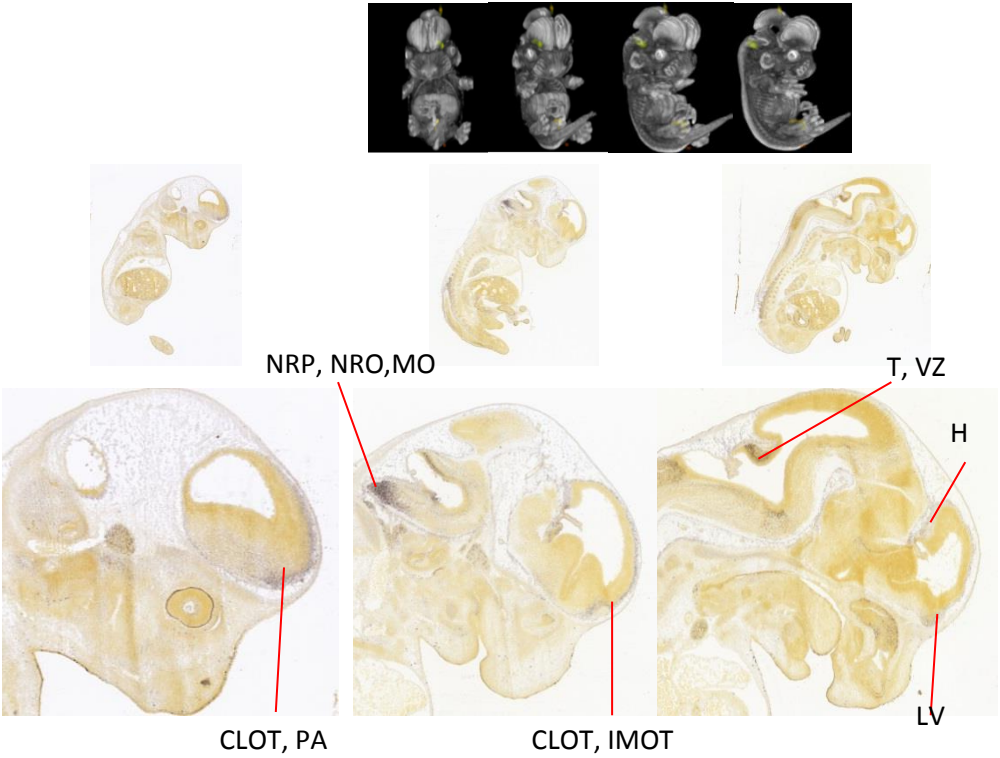


Figure II.13. E15.5

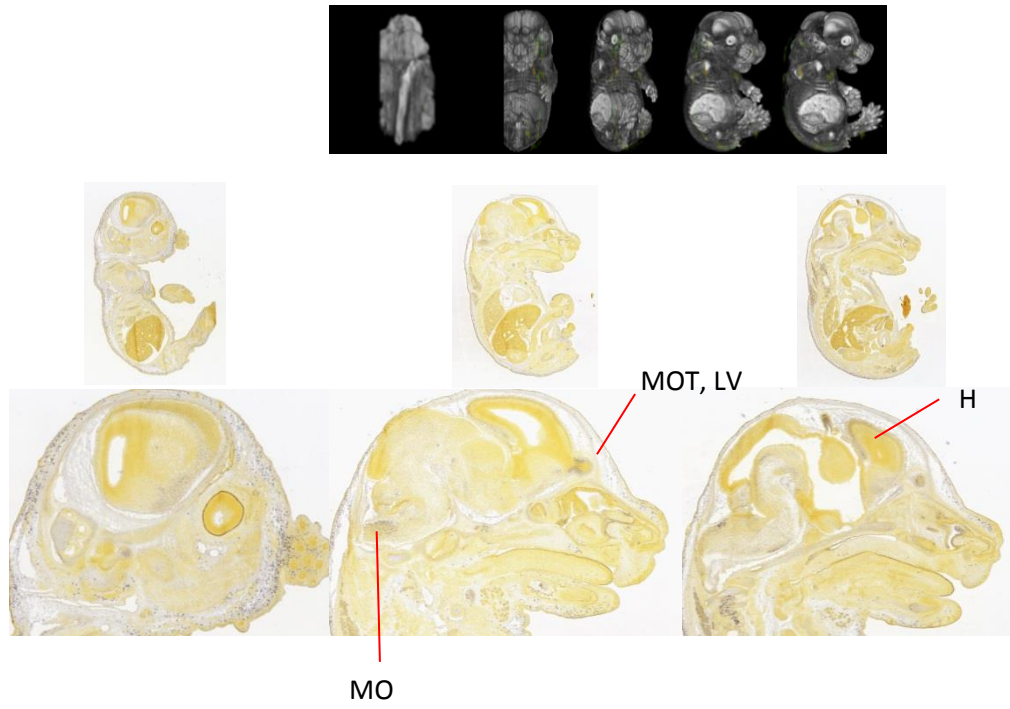


Figure II.14. E18.5

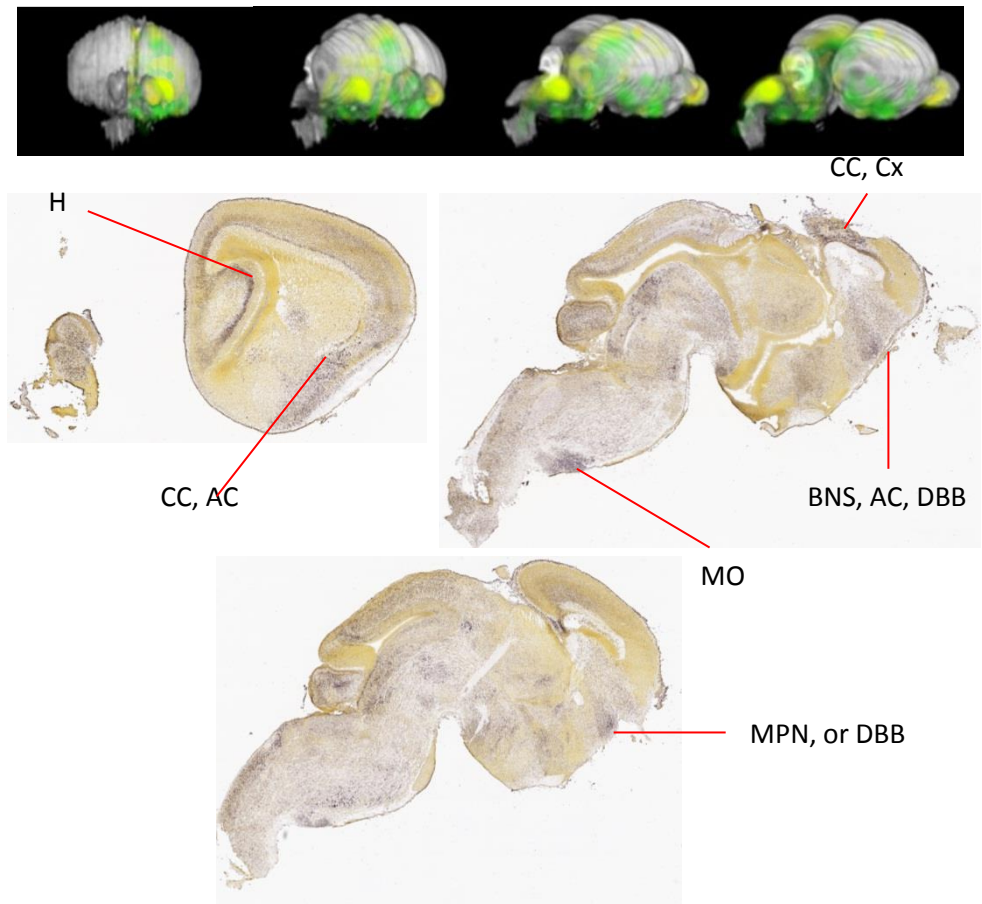


Figure II.15. P4

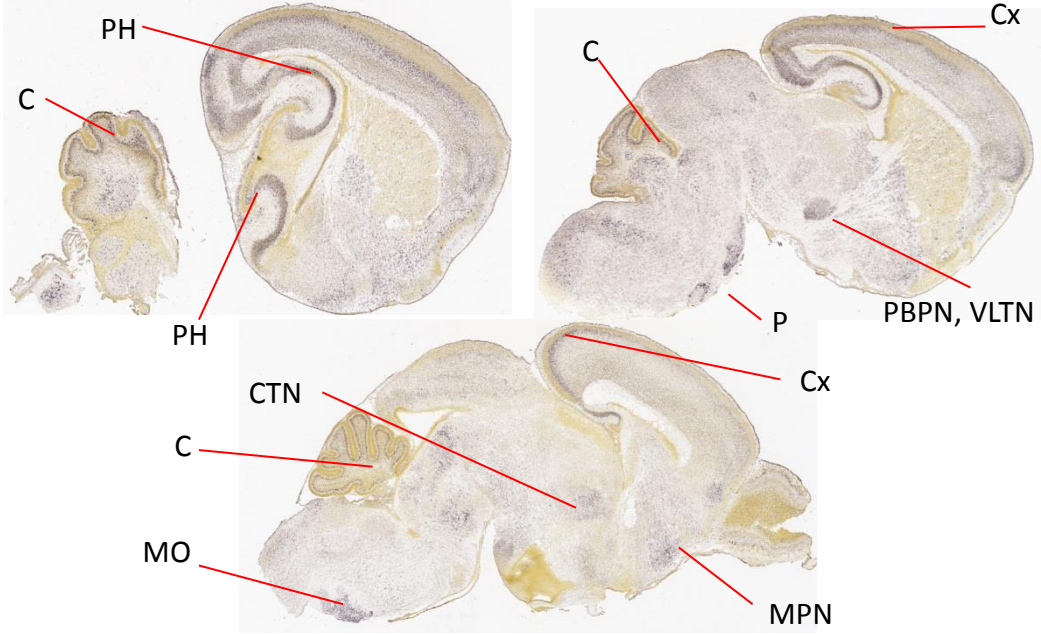
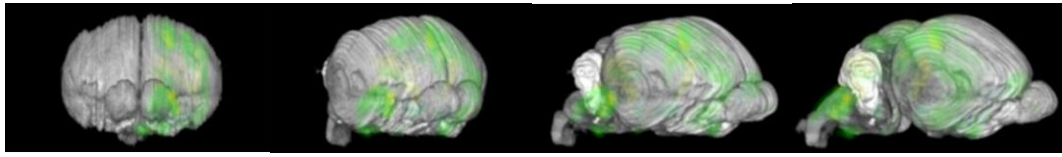


Figure II.16. P14

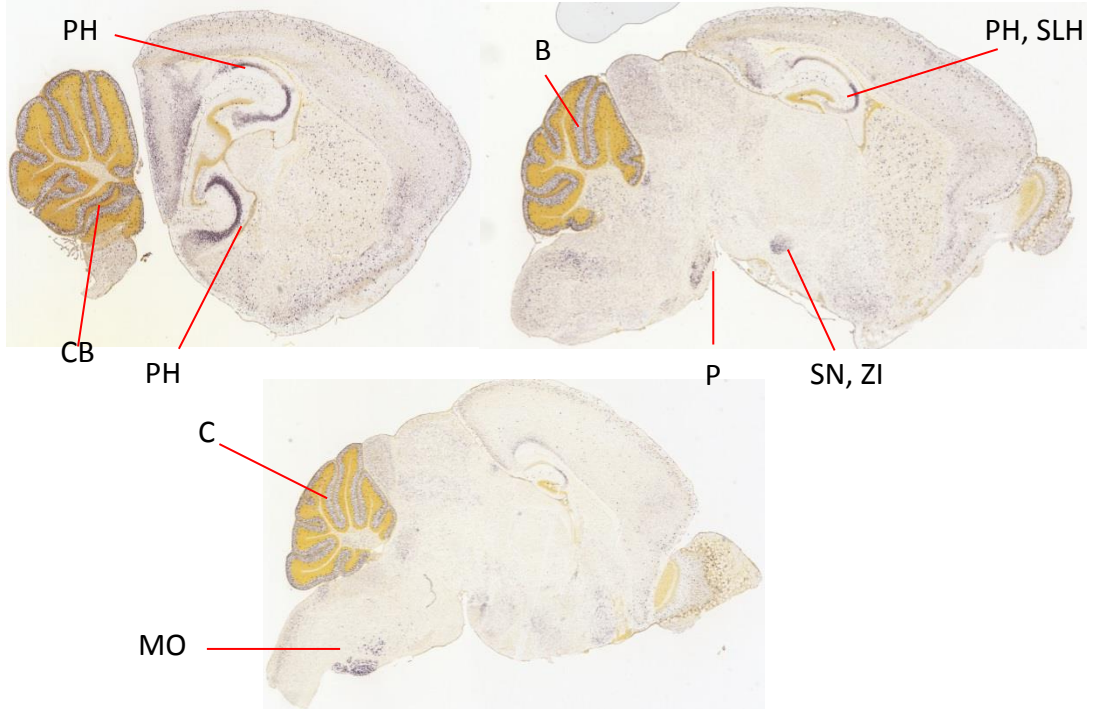
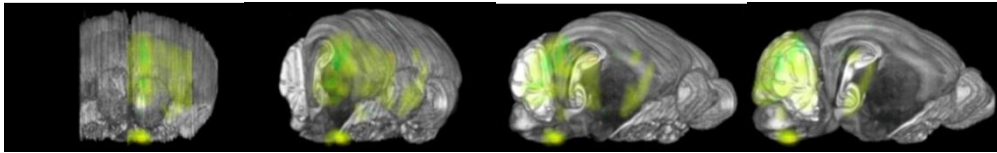


Figure II.17. P28

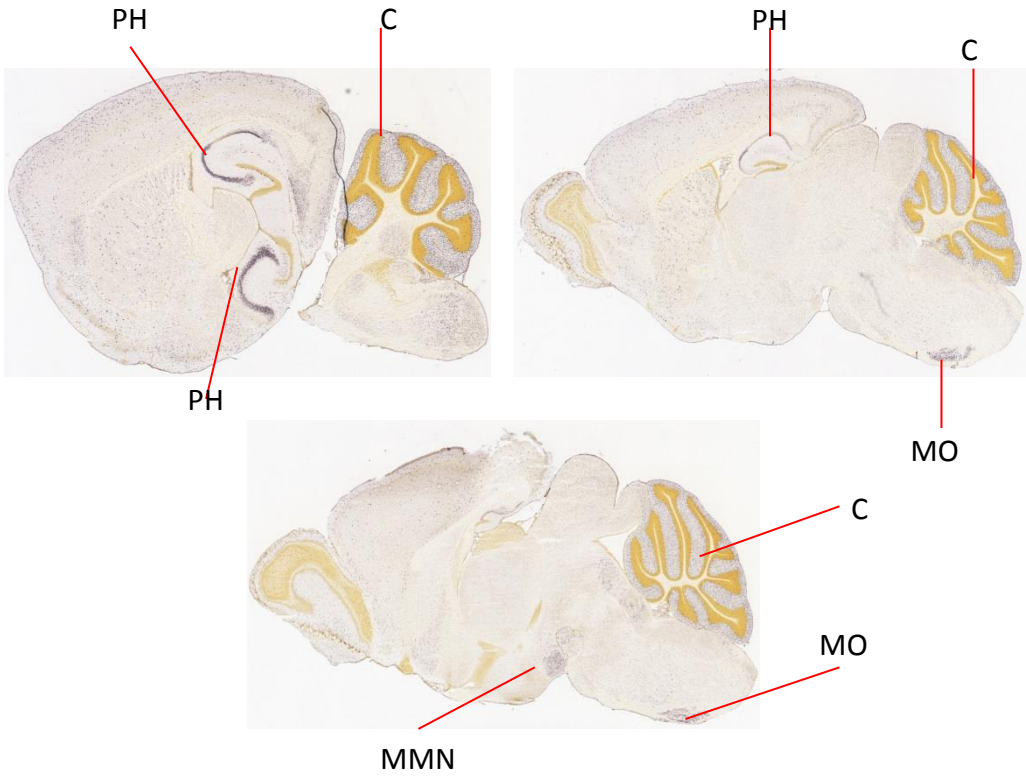
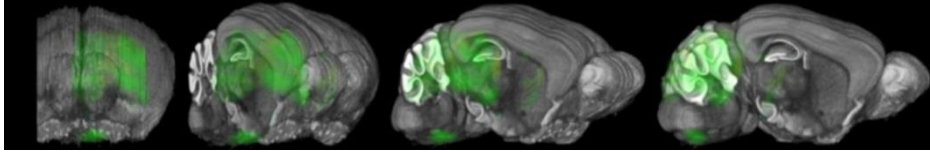
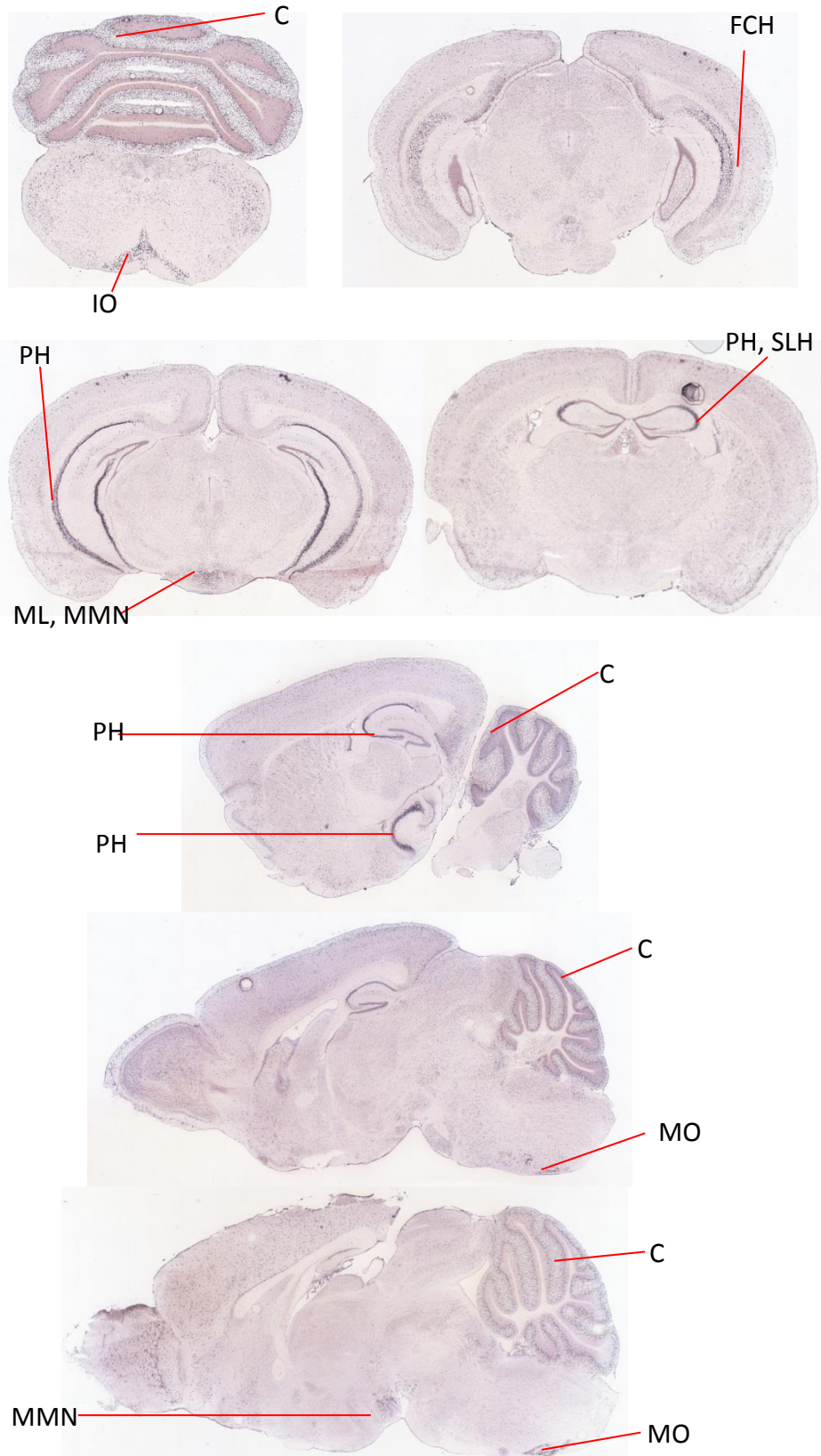


Figure II.18. P56



Appendix III - Publications arising from this thesis